Online Detection and Removal of Eye Blink Artifacts from Electroencephalogram

Ashvaany Egambaram

UBFC
UNIVERSITÉ
BOURGOGNE FRANCHE-COMTÉ

UNIVERSITÉ DE BOURGOGNE

THÈSE DE DOCTORAT DE L'ÉTABLISSEMENT UNIVERSITÉ BOURGOGNE FRANCHE-COMTÉ

PRÉPARÉE À L'UNIVERSITÉ DE BOURGOGNE

École doctorale n°37

Sciences Pour l'Ingénieur et Microtechniques

Doctorat d'Informatique

par

ASHVAANY EGAMBARAM

DÉTECTION ET ÉLIMINATION EN LIGNE DU BLINK DES YEUX ARTEFACTS DE L'ÉLECTROENCEPHALOGRAMME

Thèse présentée et soutenue à Le Creusot, le 10 juin 2020

Composition du Jury :

CHRISTOPHE DUCOTTET	Professeur à l'Université de Saint-Etienne	Président
VRABIE VALERIU	Professeur à l'Université de Reims	Rapporteur
DESIRE SIDIBE	Professeur à l'Université d'Evry Val d'Essonne	Rapporteur
OLIVIER LALIGANT	Professeur à l'Université Bourgogne	Examinateur
CHRISTOPHE STOLZ	Professeur à l'Université Bourgogne	Directeur de thèse
ERIC FAUVET	Maître de conférences à l'Université Bourgogne	Codirecteur de thèse
NASREEN BADRUDDIN	Associate Professor à l'Universiti Teknologi PETRONAS	Invité

N° | X | X | X |

école doctorale **sciences pour l'ingénieur et microtechniques**

Titre : DÉTECTION ET ÉLIMINATION EN LIGNE DU BLINK DES YEUX ARTEFACTS DE L'ÉLECTROENCEPHALOGRAMME

Mots-clés : décomposition modale empirique, Électroencéphalogramme, analyse par corrélation canonique, clignement de l'oeil

Résumé :

Parmi les artefacts contaminant les signaux d'électroencéphalogramme (EEG) les plus importants sont les clins d'oeuil qui pourraient potentiellement conduire à une mauvaise interprétation du signal EEG. La détection et la suppression en ligne des artefacts de clignement des yeux des signaux EEG sont essentielles dans des applications telles que les interfaces cerveau-ordinateur (BCI), le neurofeedback et la surveillance de l'épilepsie. Dans cette thèse, des algorithmes qui combinent la détection non supervisée des artefacts de clignement des yeux (eADA) avec une décomposition en mode empirique améliorée (FastEMD) et une analyse de corrélation canonique (CCA) sont proposés, sous le nom de FastEMD-CCA^2 et FastCCA, pour identifier automatiquement les artefacts de clignement des yeux et les supprimer en temps réel. Les algorithmes FastEMD-CCA^2 et FastCCA sont comparés à la méthode FORCe. La précision, la sensibilité, la spécificité et le taux d'erreur moyens de suppression des artefacts de FastEMD-CCA^2 sont respectivement de 97,9%, 97,65%, 99,22% et 2,1%, validés sur un ensemble de données Hitachi. Pour ces mêmes critères nous obtenons avec FastCCA une moyenne de 99,47%, 99,44%, 99,74% et 0,53% validés également sur l'ensemble de données Hitachi. Les algorithmes FastEMD-CCA^2 et FastCCA sont développés et mis en œuvre dans le langage de programmation C ++ pour étudier la vitesse de traitement qu'ils pourraient atteindre en cas d'implémentation embarquée. L'analyse a montré que FastEMD-CCA^2 et FastCCA ont pris respectivement environ 10,7 et 12,7 millisecondes, en moyenne, pour traiter un segment d'EEG de 1 seconde. Cela en fait une solution réalisable pour les applications nécessitant la suppression en temps réel des clins d'oeuil dans les signaux EEG.

Title: DÉTECTION ET ÉLIMINATION EN LIGNE DU BLINK DES YEUX ARTEFACTS DE L'ÉLECTROENCEPHALOGRAMME

Keywords: Empirical Mode Decomposition, Electroencephalogram, Canonical Correlation Analysis, Eyeblink Artifacts

Abstract:

The most prominent type of artifact contaminating electroencephalogram (EEG) signals are the eyeblink (EB) artifacts, which could potentially lead to misinterpretation of the EEG signal. Online detection and removal of eyeblink artifacts from EEG signals are essential in applications such a Brain-Computer Interfaces (BCI), neurofeedback and epilepsy diagnosis. In this thesis, algorithms that combine unsupervised eyeblink artifact detection (eADA) with enhanced Empirical Mode Decomposition (FastEMD) and Canonical Correlation Analysis (CCA) are proposed, i.e. FastEMD-CCA^2 and FastCCA, to automatically identify eyeblink artifacts and remove them in an online setting. FastEMD-CCA^2 and FastCCA have outperformed one of the existing state-of-the-art methods, FORCe. The average artifact removal accuracy, sensitivity, specificity and error rate of FastEMD-CCA^2 is 97.9%, 97.65%, 99.22%, and 2.1% respectively, validated on a Hitachi dataset with 60 EEG signals, consisting more than 5600 eyeblink artifacts. FastCCA achieved an average of 99.47%, 99.44%, 99.74% and 0.53% artifact removal accuracy, sensitivity, specificity and error rate respectively, validated on the Hitachi dataset too. FastEMD-CCA^2 and FastCCA algorithms are developed and implemented in the C++ programming language to investigate the processing speed these algorithms could achieve in a different medium. Analysis has shown that FastEMD-CCA^2 and FastCCA took about 10.7 and 12.7 milliseconds respectively, on average to clean a 1-second length of EEG segment. This makes them a feasible solution for applications requiring online removal of eyeblink artifacts from EEG signals.

UBFC UNIVERSITÉ BOURGOGNE FRANCHE-COMTÉ
Université Bourgogne Franche-Comté
32, avenue de l'Observatoire
25000 Besançon, France

REMERCIEMENTS

This thesis is a result of a research work, whereby I have been accompanied and fostered by many. It is a pleasant moment that now I have the opportunity to express my gratitude to all of them.

Firstly I thank God for His blessing that I am finally able to complete my research and thesis. Secondly, I would like to thank my supervisor, Dr Nasreen badruddin. She has always been a good advisor, provided proper guidance and delivered valuable feedback on the progress of my research, despite her busy schedule. Her consistent support, advices, views, comments and discussion have led to completion of this thesis successfully.

I would also like to sincerely appreciate my co-supervisors, Dr. Vijanth S Asirvadam, Dr. Eric Fauvet, Dr. Christophe Stolz and my field supervisor, Dr. Tahamina Begum. They have been very helpful throughout the journey of completing this research work and thesis successfully.

In particular, I would also like to extend my sincere thanks to all my colleagues and others that have assisted me in various occasions.

Last but not least, I am thankful to my family and friends for being supportive all the time.

Thank you for being there.

SOMMAIRE

1 Introduction 1

1.1 Motivation . . . 1
1.2 Problem Statement . . . 3
1.3 Research Questions . . . 3
1.4 Hypothesis . . . 4
1.5 Research Objectives . . . 4
1.6 Scope of Study . . . 4
1.7 Contribution of the Research . . . 5
1.8 Organization of Thesis . . . 5

2 Existing Eyeblink Artifact Detection and Removal Methods from Electroencephalogram 7

2.1 Background . . . 7
2.2 Related Work on Artifact Detection . . . 8
2.3 Commonly Available Artifact Removal Techniques . . . 9
2.3.1 Regression . . . 9
2.3.2 Blind Source Separation . . . 9
2.3.2.1 Independent Component Analysis . . . 10
2.3.2.2 Principal Component Analysis . . . 10
2.3.2.3 Canonical Correlation Analysis . . . 10
2.3.3 Wavelet Transform . . . 11
2.3.4 Empirical Mode Decomposition . . . 12
2.3.5 Hybrid Techniques . . . 13
2.3.5.1 ICA with Regression . . . 13
2.3.5.2 Wavelet with BSS . . . 14
2.3.5.3 Wavelet with EMD . . . 14
2.3.5.4 Statistical features with BSS/WT . . . 15
2.3.5.5 EMD/EEMD with BSS/PCA . . . 15
2.3.5.6 Adaptive Filters with Neural Networks/WT . . . 15

2.3.5.7 Support Vector Machine with WT/BSS 16
2.3.6 Online Artifact Removal Techniques 17
2.3.6.1 Wavelet Neural Network 17
2.3.6.2 FORCe 17
2.3.6.3 Real-time Source-mapping Toolbox 18
2.4 Discussion 19
2.4.1 Significance of Eyeblink Artifacts in EEG-based Applications 19
2.4.1.1 Epileptic Seizure Detection 19
2.4.1.2 Other EEG-based Applications 20
2.4.2 The Need of Online Eyeblink Arifact Elimination in EEG Based Applications 21
2.4.3 Gap Analysis 22
2.5 Summary 22

3 Preliminary Investigation 25

3.1 Overview of Classical Empirical Mode Decomposition 25
3.2 Eyeblink Artifact Interpretation from EMD 28
3.3 Envelope Interpolation Techniques in EMD 28
3.3.1 Piecewise Cubic Spline Interpolation 28
3.3.2 Use of Alternative Interpolation Techniques in EMD 29
3.3.2.1 Piecewise Cubic Hermite Spline Interpolation 29
3.3.2.2 Proposed Piecewise Akima Spline Interpolation 29
3.3.3 Simulation of Synthetic Signals 30
3.3.4 Performance Analysis on Interpolation Techniques in EMD with Synthetic Signals 31
3.4 Overview of Canonical Correlation Analysis 32
3.5 Eyeblink Artifact Correction with CCA 34
3.6 Estimation of Weighted De-mixing Matrices in CCA 34
3.6.1 Conventional Approach : Eigen Decomposition 34
3.6.2 Alternative Approaches to Estimate Weighted De-mixing Matrices . 35
3.6.2.1 Singular Value Decomposition 36
3.6.2.2 QR Decomposition and Singular Value Decomposition . . 36
3.6.3 Implementation of CCA in Artifact Removal 37
3.6.3.1 Artifactual Component Elimination from EEG Signal 37
3.6.3.2 Reconstruction of Clean EEG Signal 39

3.6.4 Performance Analysis on Decomposition Techniques in CCA with Real EEG Signals . . . 40
3.7 Preliminary Results and Discussion . . . 41
3.7.1 Comparison of Envelope Interpolation Techniques in EMD for Eyeblink Aryifact Removal . . . 41
3.7.2 Comparison of Decomposition Techniques in CCA for Eyeblink Aryifact Removal . . . 44
3.8 Summary . . . 46

4 Proposed Techniques and Methodology 47
4.1 EEG Recording/Simulation and Analysis . . . 47
4.1.1 Synthetic Signals . . . 47
4.1.2 Real Signals . . . 48
4.1.2.1 Hitachi Dataset . . . 48
4.1.2.2 Public Dataset (INV-SK) . . . 49
4.2 Proposed Eyeblink Artifact Detection Algorithm (eADA) . . . 49
4.2.1 Determination of EEG Segments with Eyeblink Artifacts . . . 49
4.2.2 Automatic Thresholding to Identify Eyeblink Artifact Components . . . 50
4.2.2.1 Classification of EEG potentials and Eyeblink Artifact Components . . . 51
4.3 Proposed FastEMD-CCA^2 for Eyeblink Artifact Removal . . . 55
4.3.1 Proposed Modification to Classical EMD : Modified EMD (FastEMD) 55
4.3.1.1 Envelope Interpolation in FastEMD . . . 56
4.3.1.2 Stopping Criterion and Fixed Number of IMFs in FastEMD 56
4.3.1.3 IMF Selection Through CCA for Eyeblink Template Extraction . . . 57
4.3.2 Eyeblink Artifact Elimination . . . 60
4.3.2.1 Optimal Use of FastEMD with CCA for Online Applications 60
4.3.2.2 Application of Windowed CCA for Eyeblink Artifact Removal 61
4.4 Proposed FastCCA for Eyeblink Artifact Removal . . . 64
4.5 Performance Analysis . . . 66
4.5.1 Eyeblink Artifact Detection . . . 66
4.5.1.1 eADA vs Fixed Thresholds . . . 66
4.5.2 Eyeblink Artifact Removal . . . 67
4.5.2.1 FastEMD-CCA^2 vs FastCCA vs Wavelet Transform . . . 67
4.5.2.2 FastEMD-CCA^2 vs FastCCA vs Conventional EMD-CCA . 69
4.5.2.3 FastEMD-CCA^2 vs FastCCA vs FORCe . . . 70

4.6 Summary 72

5 Results and Discussion 73

5.1 Eyeblink Artifact Detection Algorithm 73

5.1.1 Welch ANOVA Results 74

5.2 Eyeblink Artifact Removal Algorithms 76

5.2.1 Comparison between FastEMD-CCA^2, FastCCA and Wavelet Transform 76

5.2.2 Comparison between FastEMD-CCA^2, FastCCA and Conventional EMD-CCA 79

5.2.3 Comparison between FORCe, FastEMD-CCA^2 and FastCCA 83

5.2.3.1 Welch ANOVA Results for Hitachi Dataset 92

5.2.3.2 Welch ANOVA Results for INV-SK Dataset 94

5.3 Summary 95

6 Implementation of FastEMD-CCA^2 and FastCCA in C++ 99

6.1 Implementation Strategies for Online Artifact Removal 99

6.2 Performance Evaluation 100

6.2.1 Offline Evaluation 100

6.2.2 Online Evaluation 101

6.3 Results and Discussion 102

6.3.1 Offline Analysis Results through Visual Inspection 102

6.3.1.1 Discussion 109

6.3.2 Offline Analysis Results through Quantitative Evaluation 109

6.3.2.1 Time Domain Analysis 109

6.3.2.2 Frequency Domain Analysis 110

6.3.2.3 Discussion 111

6.3.3 Online Analysis Results 113

6.4 Summary 113

7 Conclusion and Future Directions 115

7.1 Conclusion 115

7.2 Limitations 116

7.3 Future Work 116

I Annexes **139**

A Individual EEG Results of Chapter 6 **141**

B List of Publications **161**

1

INTRODUCTION

1.1/ MOTIVATION

The human brain communicates or transmits information to other parts of the body through signals sent via brain cells, called neurons. A synapse is a junction between brain cells. Information is being transferred across the synapse in the form of neurotransmitters, where electrical potentials are generated during this cerebral activity. This cerebral activity can be acquired as brain signals through a non-invasive modality, the electroencephalogram (EEG) [1], resulting in an electrical signal which is termed as EEG signal. EEG signals are usually recorded from multiple locations of the scalp using electrodes placed at predetermined points. The International Federations and Societies for Electroencephalography and Clinical Neurophysiology has recommended the 10-20 electrode placement [2], which consists of 19 active electrodes and 2 reference electrodes. Fig. 1.1 shows the positions of EEG electrodes following the 10-20 system.

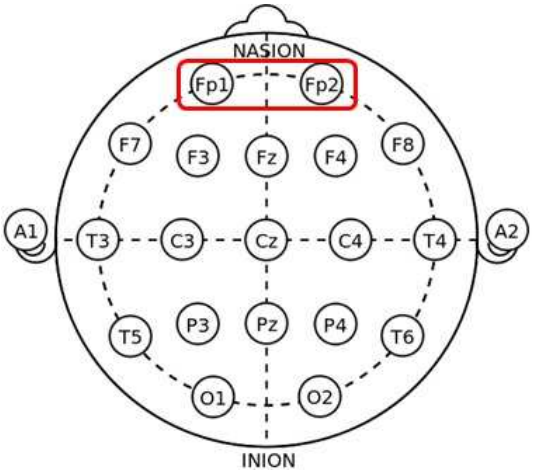

FIGURE 1.1 – 10-20 Electrodes Placement

The EEG signal's amplitude measured on the scalp usually lies between 10 to 100uV [3]. Basically, there are five types of brain rhythms that range from low to high frequencies. They are the delta waves, theta waves, alpha waves, beta waves and gamma waves. The delta wave which ranges from (0.5-4 Hz) are primarily associated with deep sleep. The theta waves are found between (4-7.5 Hz), which indicates a state of consciousness slips towards drowsiness. The alpha wave ranges between (8-13 Hz), common in humans

in a relaxed state which has been thought to indicate a relaxed plus awareness state without any attention or concentration. The beta waves between (14-30 Hz) are found in normal adults during active thinking, active attention, focus on the outside world, or solving concrete problems, while the gamma waves (>30 Hz) are of very low amplitudes, rarely found in the human brain [3]. EEG is one of the most preferred modalities in online applications due to its non-invasive nature, for instance, in epileptic seizure detection, in real-time detection of fatigue or drowsiness in drivers and brain-computer interfaces (BCI).

However, EEG signals are highly susceptible to contamination from artifacts, which causes deviation in the signal of interest. Artifacts are undesired information which appear in the signal of interest, but not related to neural activity. These artifacts are physiological signals that originate from various activities from other parts of the body. The most common types of artifacts contaminating EEG signals are the cardiac artifact, the muscle artifact and the eyeblink artifact, originating from the heartbeat, muscle movement, eyeball movement and eye blinking. The most trivial artifact superimposing the EEG signal is the cardiac artifacts, mainly generated by the electrical activity of the heart, which are repetitive and are of regular pattern. The influence of cardiac artifact on the scalp is typically low with low amplitude. The muscle artifacts are produced by muscle movement and muscle contraction during EEG recording. The pattern or trend of muscle artifacts is random and purely dependent on the degree of muscle contraction. Eyeblink artifacts appear as spikes with amplitudes of typically around 10 times greater than the actual brain potentials, noticeable in the delta wave range and can last up to 200ms to 400ms [2, 3]. The eyeblink potential propagates and spreads out to all EEG electrodes but in various conduction volume-higher conduction near the frontal and parietal regions while the conduction in the occipital region is very low. The Fp1 and Fp2 electrode positions, which are closest to the eyes and highlighted in Fig. 1.1, can be used to capture the eyeblink artifacts. Each of the artifact signals can be recorded separately near the artifact originating regions, using reference electrodes. The cardiac activity can be recorded with Electrocardiogram (ECG) electrodes, the muscle activity can be recorded with Electromyogram (EMG) electrodes and the eyeblink activity can be recorded with Electrooculogram (EOG) electrodes. In most of the available artifact removal algorithms, the use of a reference channel is preferred, because it can serve as a piece of trusted complementary information to identify the locations of cardiac, muscle and eyeblink artifacts in EEG signals [4]. Out of all the artifacts, the eyeblink artifact is the most prominent in EEG signals as blinking the eyes is inevitable and it produces relatively large electrical potentials around the eyes.

The superimposition of eyeblink artifacts with EEG signals could potentially lead to inaccurate EEG interpretation. This issue is particularly relevant in the medical field where EEG signals are widely used as a diagnostic tool, thus failing to recognize and remove eyeblink artifacts may affect clinical decisions. Therefore, eyeblink artifact identification and removal in EEG signal processing is the first and most crucial step. This thesis presents algorithms, i.e. FastEMD-CCA^2 and FastCCA, which can automatically detect and remove eyeblink artifacts in real-time.

1.2/ Problem Statement

Since applications such as Brain-computer Interface (BCI), neurofeedback and epilepsy seizure detection units require online EEG signal processing, artifact detection and removal algorithms should be capable of online processing too. Important criteria an online eyeblink artifact detection and removal algorithm should possess are listed below :

- Accurate and sensitive in identifying and removing eyeblink artifacts.
- Artifact-free EEG segments of an EEG signal are preserved after artifact correction is performed.
- The processing speed should be insignificant, making it feasible for online applications.

However, existing eyeblink artifact detection and removal algorithms do not comply with the above criteria. They :

- Depend on a separate reference eyeblink activity recording via Electrooculogram (EOG) to identify the eyeblink artifact events
- Depend on constant thresholds or constant features to make a binary decision to recognize if an EEG segment contains an eyeblink artifact
- Cause loss of significant neural information in the artifact-free EEG segments during eyeblink artifact correction
- Are computationally inefficient and slow, as the algorithms are applied to the entire EEG signal for eyeblink artifact correction during real-time recording and analysis.

Hence, existing artifact removal algorithms are not favourable for applications requiring online detection and removal of eyeblink artifacts.

1.3/ Research Questions

Through literature survey, algorithms based on Empirical Mode Decomposition (EMD) and Canonical Correlation Analysis (CCA) can be useful for online applications if eyeblink artifact detection is made automatic and the computational complexity of the algorithms is reduced. This has lead to the following questions which will be addressed in this research :

i. How can the eyeblink artifacts be automatically identified without reference electrodes or an expert's advice ?

ii. How can algorithms based on EMD and CCA developed and adapted for online removal of eyeblink artifacts, which can be utilized for online applications ?

iii. How well do the proposed algorithms perform in identifying and removing eyeblink artifacts from EEG signals in real-time compared to conventional methods ?

iv. How well do the proposed algorithms could retain neural information in artifact-free EEG segments after eyeblink artifact correction is performed ?

1.4/ HYPOTHESIS

Based on the above research questions, it is hypothesized that the following solutions would be able to produce suitable online eyeblink artifact removal algorithms.

- Develop an unsupervised and automatic eyeblink artifact detection algorithm with adaptive threshold levels for eyeblink artifact components classification.
- Process the multi-channel EEG signals in blocks/windows, and apply eyeblink artifact correction only on windows that are identified with eyeblink artifacts, which can prevent loss of neural information on artifact-free EEG segments.
- Speed up the entire eyeblink artifact removal algorithm by processing multi-channel EEG signals in blocks, rather than removing eyeblink artifacts from an entire EEG signal.

1.5/ RESEARCH OBJECTIVES

The main objectives of the research are :

- To develop an unsupervised eyeblink detection algorithm with the help of adaptive threshold values to identify eyeblink artifact components.
- Modify the use of existing EMD and CCA techniques to remove eyeblink artifacts from multi-channel EEG signals effectively, with an acceptable processing time delay (real-time processing of a system is estimated between 6 to 20 milliseconds) for online applications.
- To investigate the performance of the proposed algorithms in C++ programming language in terms of processing time, if they are feasible for online implementation.

1.6/ SCOPE OF STUDY

This research explores a suitable algorithm to identify eyeblink artifacts that are contaminating the EEG signals without any manual supervision, with an automated varying threshold value. The eyeblink artifacts are detected to assist in the subsequent artifact removal process. For this purpose, the algorithm is evaluated on MATLAB using an EEG dataset collected from Hitachi.

The decomposition and blind source separation techniques, specifically the EMD and CCA techniques, are modified and investigated for their ability to remove the identified eyeblink artifacts effectively, with the aim to help online removal of eyeblink artifacts feasible. The proposed algorithms to remove eyeblink artifacts from EEG signals are designed from the modified EMD and CCA. The investigation and evaluation of the proposed algorithms are conducted on the EEG dataset of Hitachi. Apart from that, a publicly available EEG dataset that contains involuntary eyeblinks were used to evaluate the consistency of performance of the proposed algorithms. All investigation and evaluation are performed offline in MATLAB.

The proposed algorithms are then developed and investigated in the C++ programming language. The primary purpose is to investigate the computation time or the processing

speed the proposed algorithms, FastEMD-CCA^2 and FastCCA could achieve, in line to support an online application, while being able to retain the neural information on the artifact-free EEG segments. The Hitachi EEG dataset is used for this investigation.

1.7/ Contribution of the Research

- Developed a novel unsupervised eyeblink artifact detection (eADA) algorithm which identifies the locations of eyeblink artifacts correctly. Since the eyeblink artifact locations are correctly detected, the artifact-free EEG segments remain undistorted after artifact elimination is performed.
- Developed FastEMD-CCA^2 and FastCCA algorithms that have achieved instantaneous eyeblink artifact elimination with acceptable processing time, while being able to retain artifact-free EEG segments undistorted effectively, thus making them suitable algorithms for online applications.

1.8/ Organization of Thesis

In Chapter 2, commonly available eyeblink artifact removal techniques or algorithms that were proposed and evaluated by other researchers are reviewed. Additionally, studies that addressed online detection and removal of artifacts are reviewed. Critical analysis of these techniques and algorithms are discussed, as well as the motivation to develop the proposed algorithms.

Chapter 3 discusses the necessary theoretical background of Empirical Mode Decomposition (EMD), followed by discussion on the use of an alternative interpolation technique within EMD. The performance of an alternative interpolation technique in EMD to extract out the eyeblink artifact template is evaluated on synthetically contaminated signals. Then, the chapter presents the background and mathematical derivation of Canonical Correlation Analysis (CCA). Three different matrix decomposition techniques that can be used to estimate the de-mixing matrices in CCA are discussed as well. Then, the implementation of CCA to eliminate artifactual components from EEG segments and reconstruction of clean EEG segments are illustrated. Finally, the performance of the three matrix decomposition techniques within CCA is evaluated for their ability to properly decompose a matrix, consequently producing a reliable EEG reconstruction.

In Chapter 4, the proposed algorithms and the methodologies are presented. First, a novel unsupervised eyeblink artifact detection algorithm based on adaptive threshold determination is proposed to assist subsequent eyeblink artifact elimination step. Next, various modifications to the classical EMD algorithm to resolve the processing time inefficiency of the algorithm are illustrated and discussed. It also elaborates on the method to classify IMFs of EMD with the help of CCA, whether they belong to EEG or the eyeblink artifact. The modified version of the EMD is then combined with the unsupervised artifact detection algorithm and CCA to form the proposed eyeblink artifact detection and removal algorithm, FastEMD-CCA^2. Third, an algorithm that combines the unsupervised artifact detection algorithm and CCA, FastCCA is proposed to remove eyeblink artifacts from EEG signals for online applications.

The validation results of FastEMD-CCA^2 and FastCCA algorithms on synthetic and real

EEG signals are provided in Chapter 5. The algorithms are evaluated for the computation time they take in identifying and removing eyeblink artifacts on real EEG signals, and for their effectiveness in identifying and removing eyeblink artifacts.

In Chapter 6, implementation and assessment of the proposed algorithms in C++ is described. These algorithms are developed and implemented in C++ programming language to investigate the feasibility of the algorithms in removing eyeblink artifacts in an online manner. So these two proposed algorithms are compared and critically analyzed for their performance in effectively identifying and removing eyeblink artifacts online, both in MATLAB computing environment and C++ programming language. Finally, conclusion and future work are discussed in Chapter 7.

2

Existing Eyeblink Artifact Detection and Removal Methods from Electroencephalogram

This chapter presents commonly available techniques that have been used for the removal of artifacts from EEG by other researchers, mostly on eyeblink artifact removal, along with their pros and cons. The impact of eyeblink artifacts in EEG based applications is discussed as well. Then, analysis on available techniques is conducted before stating the motivation to develop online artifact detection and removal algorithms.

2.1/ Background

EEG signals have been extensively used in the medical field for diagnosing epilepsy, sleep disorders, coma, encephalopathy, brain injury and brain death [5–12]. EEG signals are also utilized for research purposes in neuroscience, cognitive science, cognitive psychology, neurolinguistics and psychophysiology [13–15]. Although EEG signals play a vital role in many research and medical fields, they are often contaminated by various artifacts. Some of the most common artifacts that contaminate the EEG signals are eyeblink activity, cardiac activity and muscle activity, as stated in Chapter 1. The artifacts may sometimes superimpose with the EEG signal, which is then considered as a pure EEG signal. This can mislead a practical application, such as the brain-computer interface (BCI) [16]. It may also sometimes imitate cognitive behaviour ; therefore, it could cause misinterpretation and diagnosis of sleep disorders and Alzheimer's disease [17], etc. Therefore, artifact detection and removal is an imperative preprocessing step for any EEG-based application.

For this purpose, various eyeblink artifact removal algorithms are developed to date. They include algorithms of which are capable of manual, semi-automated, fully-automated artifact elimination, either from single-channel EEG or multichannel EEG. The manual eyeblink artifact rejection method is one of the most commonly used techniques, where eyeblink artifact regions are identified through manual inspection by experts, and these segments are discarded. This method can cause a significant loss of information as the EEG segments being removed may contain useful neurological information. Alternatively, many semi-automatic and fully-automatic eyeblink artifact removal algorithms were developed to replace manual eyeblink artifact rejection method, which were discussed and

reviewed in [4, 18–22]. In addition to the existing automatic artifact removal algorithms, techniques addressing and implementing online removal of eyeblink artifacts are essential [20]. This is particularly relevant in BCI research for proper BCI output device controllability and generating distinct feedback signals in neurofeedback. The subsequent sections and subsections elaborate existing eyeblink artifact detection and removal techniques and algorithms.

2.2/ Related Work on Artifact Detection

Many methods were developed in the past to automate identification or detection of eyeblink artifacts in the EEG signal. One of the easiest and preferred way for eyeblink artifact recognition is by merely using an amplitude threshold [23]. This method determines if an eyeblink artifact is present in an EEG segment if the amplitude in the segment exceeds a predetermined amplitude threshold. In most EEG-based applications, this method is preferred due to its straightforwardness. However, eyeblink artifact detection through an amplitude threshold may not be suitable in applications that require high detection accuracy [24]. This method can also be useful when there is an abundance of EEG data available, thus discarding required EEG segments or retaining unwanted EEG segments may not cause any critical issue to the EEG signal analysis [25]. However, the amplitude of eyeblink artifacts may vary depending on the blinking strength of an individual; hence this method may not identify eyeblink artifacts from an individual who exhibits gentle blinks, which may have lower amplitudes than the threshold value. Moreover, this method struggles when the blinking duration of an individual varies [26].

The other common technique of detecting eyeblink artifacts is through feature-based identification, where the presence of eyeblink artifacts in EEG segments is determined by extracting certain features. Some of the common features used are kurtosis, maximum absolute value, entropy-based features and second-order difference [23, 25, 27, 28]. As a general rule, these artifact detection features require a certain threshold value to classify or make a binary decision whether or not an EEG segment is contaminated by eyeblink artifacts. As elaborated earlier for the amplitude threshold, applying a fixed threshold value for the features discussed may lead to detection errors due to individual variance in blinking pattern and blinking strength. As a result, the threshold values may need to be tailored for every individual, making the technique impractical in online applications.

Recently, WD Chang et al. [29] have proposed a method that combines digital filters and a rule-based decision system. This method may not be useful for applications that require online processing of EEG data because it depends on the proper selection of threshold value for every EEG dataset. The same authors have proposed an automatic approach in [30] so that their existing method could support real-time eyeblink artifact detection. They have combined the digital filters with an automatic thresholding algorithm proposed by Kim et al. [31]. However, the proposed method may not correctly adjust its threshold in extreme conditions, such as when there is more than one eye blink in every second of the EEG signal.

2.3/ Commonly Available Artifact Removal Techniques

2.3.1/ Regression

Regression-based methods [32–34] perform a regression or correlation test between the signal to be processed and a reference signal. For example, the EOG signal can be used as the reference signal to be compared with the EEG signal. The segment of the EEG signal that highly correlates with the EOG is then assumed to be related to the eyeblink artifacts and thus removed. However, since EOG also contains some EEG components due to the close proximity of EOG electrodes to the frontal region of the brain, artifact removal via regression methods may also remove essential EEG data. Also, a reference electrode is obligatory in regression-based methods, which may cause discomfort to patients when there is an extra pair of electrodes placed around the eyes, especially for longer EEG recordings.

2.3.2/ Blind Source Separation

In the late 1990s, Blind Source Separation (BSS) methods are investigated to estimate the underlying clean EEG signal from a contaminated EEG signal [35–37]. The fundamental goal of a BSS technique is to segregate source signals from a set of mixed signals. Isolation of the source signals from the mixed signals are performed without any priori knowledge about the signals or the way they are mixed together. Conceptually, BSS assumes the contaminated or the mixed signals are the combination of clean EEG sources and artifacts, blended together with a mixing formula. Thus in EEG's artifact correction, BSS attempts to isolate EEG sources and artifacts apart, with an unmixing formula. Mathematically, a contaminated multichannel EEG signal can be represented as $\mathbf{X}$, which is a result of linear mixing of sources, $\mathbf{S}$, where sources comprise EEG sources and artifactual components :

$$\mathbf{X} = \mathbf{WS} \tag{2.1}$$

The mixing of sources relies on the weighted mixing matrix, $\mathbf{W}$. The source signals can then be estimated by projecting the weighted de-mixing matrix, $\mathbf{A}$ onto the contaminated EEG signal :

$$\begin{aligned} \mathbf{A} &= \mathbf{W}^{-1} \\ \mathbf{S} &= \mathbf{AX} \end{aligned} \tag{2.2}$$

As stated earlier, the source signals consist of EEG sources and artifactual components. Therefore, eliminating the artifactual components would yield artifact-free sources which can be used to reconstruct a clean EEG signal. Among well-known BSS methods that have been used to tackle eyeblink artifact removal from EEG signals are Independent Component Analysis (ICA), Principal Component Analysis (PCA) and Canonical Correlation Analysis (CCA).

2.3.2.1/ Independent Component Analysis

Independent component analysis (ICA) is a BSS technique that produces independent components (ICs), out of a multichannel EEG signal [38]. ICs acquired are identified to be distinct and independent, provided that the temporal information of recorded multichannel data are maximally independent with one another [39]. Therefore, ICA appears to be ideal in separating artifactual ICs from EEG sources, assuming artifactual components and EEG sources are entirely independent. In EEG's preprocessing step, variations of ICA are used to remove artifacts [40–46]. Although ICA performs well in artifact removal from EEG, it is not automatic as one has to manually identify and select the artifact related ICs for correction [47]. Manual selection of ICs is not practical in applications requiring real-time processing and it may also result in incorrect IC selection [47]. Many automatic approaches have been proposed and studied to automate IC selection through statistical analysis or feature classification that is able to classify an IC as artifactual [48–50]. Most of these approaches prioritize automation on the selection of artifact related ICs to remove them, but not many have focused on how well these techniques are preserving the underlying EEG signal after artifact removal [51]. Furthermore, ICA based algorithms are not suitable in online applications as it introduces higher computational complexity [4].

2.3.2.2/ Principal Component Analysis

Principal component analysis (PCA) is a statistical technique that groups multichannel EEG observations into linearly uncorrelated variables. This is accomplished by applying the orthogonal transformation to find the largest variance in the EEG observations, thus transforming them into linearly uncorrelated variables, called principal components (PCs). Each PC should be orthogonal and should exhibit the highest variance possible with its predecessor [52]. Thus, the most prominent PC will have the largest possible variance. With this concept, PCA is applied to EEG signals to obtain the largest variance in these signals, which returns the major components representing eyeblink activity. Once the principal components representing artifacts are removed, a clean EEG signal can be reconstructed through an inverse computation. PCA was first used by P.Berg et al. [53] for eyeblink artifact removal. Thereafter, PCA has been used in various studies and evaluation to remove artifacts from EEG and FMRI [54–57]. PCA is also used for comparison purposes in removing artifacts from EEG signals in [45, 58, 59]. These papers clearly point out that ICA performs better than PCA in EEG artifact removal ; therefore, a concrete opinion on PCA's performance in artifact removal can't be provided. Apart from this, Lagerlund et al. [60] have outlined limitations of PCA, whereby it is not able to completely separate some artifacts from the raw EEG signal in the event that both artifacts and EEG signals are of comparable amplitudes.

2.3.2.3/ Canonical Correlation Analysis

Canonical Correlation Analysis (CCA) is a BSS method that yields canonical components by maximizing the temporal correlation within an epoch. The most pertinent artifactual canonical components, usually the first row of the canonical components, are forced to become zero in order for it to behave non-artifactual. The artifact-free canonical components are then projected back to reconstruct an EEG segment that is clean from artifacts.

CCA was initially proposed in [61] by Hotelling. In EEG artifact removal, CCA was employed in several works to remove muscle and ocular artifacts. CCA is implemented by De Clercq et al. [62] to remove muscle artifacts from the EEG signal, followed by Hallez et al. [63]. Other studies that have successfully implemented CCA proven that CCA outperforms ICA in EEG artifact removal are [64–66]. Table 2.1 lists some of the published artifact removal studies using ICA, PCA and CCA.

TABLE 2.1 – Studies on BSS Algorithms to Remove Artifacts

Study	Year	Method	Artifact
Berg and Sherg [53]	1991	PCA	eyeblink
Makeig et al. [38]	1996	ICA	eyeblink
Jung et al. [67]	1997	ICA	eyeblink
Vigario et al. [46]	1997	ICA	eyeblink
Jung et al. [68]	2000	ICA	eyeblink
Jung et al. [45]	2000	ICA	eyeblink
Vigon et al. [59]	2002	PCA	eyeblink
Casarotto et al. [69]	2004	PCA	eyeblink
Joyce et al. [70]	2004	ICA	eyeblink
Dorffner et al. [71]	2005	ICA	eyeblink
Li et al. [44]	2006	ICA	eyeblink
Liu et al. [72]	2006	PCA	eyeblink
Teixeiraa et al. [73]	2006	PCA	eyeblink
Clercq et al. [62]	2006	CCA	muscle
Hallez et al. [63]	2006	CCA	eyeblink
Frank et al. [74]	2007	ICA	eyeblink
Delorme et al. [42]	2007	ICA	eyeblink
Mammone et al. [75]	2008	ICA	eyeblink
Hoffmann et al. [41]	2008	ICA	eyeblink
Viola et al. [50]	2009	ICA	eyeblink
Gao et al. [65]	2010	CCA	muscle
Mennes et al. [40]	2010	ICA	eyeblink
Vos et al. [64]	2010	CCA	muscle
Feng et al. [76]	2010	ICA	eyeblink
Winkler et al. [49]	2011	ICA	eyeblink
Zhang et al. [77]	2012	CCA	eyeblink
Chaumon et al. [47]	2015	ICA	eyeblink
Raduntz et al. [48]	2015	ICA	eyeblink
Turnip et al. [58]	2015	PCA	eyeblink
Somer et al. [78]	2016	CCA	eyeblink
Pontifex et al. [51]	2017	ICA	eyeblink

2.3.3/ WAVELET TRANSFORM

Wavelet transform (WT) is a technique that decomposes an EEG signal into time-frequency representations. This is obtained by convolving the EEG signal with the mother wavelet [79]. Fundamentally, WT decomposes a signal into detail and approximation coefficients. The detail coefficients are high-frequency components, while the approximation coefficients are lower frequency components. Thus setting a threshold on the approximation coefficients could isolate out the artifactual components, and a clean EEG signal can be reconstructed thenafter [79]. Wavelet has been extensively used for eyeblink artifact removal in EEG by [79–82]. However, WT depends on choosing a suitable decomposition

mother wavelet. The mother wavelet is a function comprising sine and cosine waves, thus most often it will not characterize or adapt to a non-linear EEG signal, which may produce decomposition errors [82]. It has to be emphasized here that WT removes artifacts only from a single-channel EEG signal. Furthermore, selecting an inappropriate mother wavelet could lead to inaccuracy in reconstructing artifact-free EEG signals. The accuracy of WT is also sensitive to the selection of thresholding function, where selecting an inappropriate threshold could have an effect on preserving or discarding the neural information in an EEG signal.

2.3.4/ Empirical Mode Decomposition

Empirical Mode Decomposition (EMD) is an algorithm that decomposes a raw signal into several oscillating trends in a recursive manner through a repetitive interpolation and subtraction process, producing highly oscillating and low oscillating decomposed trends. These decomposed trends are called Intrinsic Mode Functions, IMFs. Each IMF extracted out from the original signal is a slower oscillating trend compared to its predecessor. Adding up all IMFs and the remaining residual signal obtained from the decomposition would reconstruct the original signal as in Eq.(2.3) :

$$X(t) = \sum_{i=1}^{n-1} x_i(t) + R_n(t) \tag{2.3}$$

where $X(t)$ is the raw EEG signal, $x_i(t)$ are i number of IMFs, and $R_n(t)$ is the residual trend, which is monotonous.

In [83–89], EMD has been proven effective in removing artifacts. Despite the fact that it can effectively remove artifacts from the EEG signals compared to other techniques, the algorithm is relatively slow. This is because EMD keeps on repeating until the final residual trend becomes a monotonic function. Hence, the conventional EMD algorithm is not computationally efficient in removing artifacts from EEG signals. Apart from this, this algorithm is also susceptible to mode mixing issue, where the decomposed IMFs may have overlapping EEG and artifact oscillations. To overcome this issue, the ensemble EMD (EEMD) was developed, which is based on a noise assisted decomposition to sift out IMFs [90].

A study by Dora et al. [91] proposed an enhanced version of the EMD technique, called the Variational Mode Decomposition (VMD) to suppress ocular artifacts (OA). The proposed algorithm identifies the ocular artifacts with the help of modified multiscale sample entropy (mMSE). Then VMD is applied to obtain band limited IMFs (BLIMFs), to ease the identification of OA related IMFs which are high in amplitude and low in frequency. The estimated OA is then regressed with a contaminated EEG signal to obtain a clean EEG signal. Although the proposed algorithm has shown an improved performance in comparison with conventional EMD and EEMD algorithms, the computational complexity of VMD is increased significantly, interpreted in terms of the execution time of the algorithm to decompose a 10s EEG segment (VMD-57.14s, EMD-0.55s and EEMD-148.125s). Hence, VMD may not be a good choice for applications that requires online eyeblink artifact elimination. Table 2.2 lists some of the published artifact removal studies using WT and EMD.

TABLE 2.2 – Studies Based on WT and EMD to Remove Artifacts

Study	Year	Method	Artifact
Zikov et al. [92]	2002	Wavelet	eyeblink
Krishnaveni et al. [82]	2006	Wavelet	eyeblink
Iyer et al. [93]	2007	Wavelet	eyeblink
Looney et al. [89]	2008	EMD	eyeblink
Molla et al. [88]	2010	EMD	eyeblink
Yong et al. [94]	2012	Wavelet	eyeblink
Molla et al. [85]	2012	EMD	eyeblink
Safieddinw et al. [86]	2012	EMD	eyeblink
Shahbakthi et al. [87]	2012	EMD	eyeblink
Seeeney et al. [90]	2013	EEMD	eyeblink
Looney et al. [84]	2014	EMD	eyeblink
Patel et al. [83]	2016	EMD	eyeblink
Khatun et al. [80]	2016	Wavelet	eyeblink
Guarascio et al. [95]	2017	EEMD	eyeblink
Chavez et al. [79]	2018	Wavelet	eyeblink
Dora et al. [91]	2019	VMD	eyeblink

2.3.5/ HYBRID TECHNIQUES

Researchers have studied various hybrid techniques to detect and remove eyeblink artifacts from EEG signals, which may be useful for online applications. The impression behind developing hybrid techniques or algorithms is to make use of the different beneficial properties possessed by several individual techniques in correcting artifacts. Therefore, researchers combine the advantageous features of several techniques to produce effective artifact removal algorithms and evaluate the performance of these algorithms. Some of these techniques are discussed in the following subsections.

2.3.5.1/ ICA WITH REGRESSION

In the combination of regression and ICA, regression is performed between the ICs produced by ICA and the EOG signal. Klados et al. [96] used ICs obtained through ICA undergoes regression with the EOG signal to remove the ocular artifacts, maintaining the underlying neural signal. EOG-like artifacts are removed and projected back to get the clean EEG signal. However, this algorithm requires dedicated EOG reference electrodes to identify the ICs related to ocular artifacts. Moreover, there is no automatic selection of ICs is performed, where all the ICs have to undergo regression with the EOG signal. This can cause loss of neural information in cases when non-artifactual ICs exhibit artifact-like properties. In [19], Mannan et al. proposed an automatic ocular related IC identification. First, ICs from ICA are classified into neural and ocular ICs, based on features with certain threshold level such as composite multiscale entropy and kurtosis. Secondly, the ocular ICs are subjected to an additional level of threshold filtering, where any ocular IC that exceeds a certain threshold of median absolute deviation is removed. Then, regression is performed between the remaining ocular ICs and EOG signal to remove the artifactual components further. Finally, the neural ICs and the ocular artifact removed ICs are combined together to reconstruct the clean EEG signal. The authors have evaluated the performance of their proposed algorithm in removing ocular over ICA, regression analysis,

wavelet-ICA (wICA), and regression-ICA (REGICA). The analysis showed an improved performance in terms of means square error(2.05, 86% lesser error than ICA, 59% lesser error than REGICA) and mean absolute error (lowest MAE in beta band-0.0022, highest MAE in Delta band-0.1087). One distinct disadvantage of the algorithm is that it depends on EOG signals to remove the ocular artifacts.

2.3.5.2/ WAVELET WITH BSS

BSS techniques and WT are extensively combined together in artifact removal studies. Akthar et al. [97, 98] have used the spatially constrained ICA (SCICA), with wavelets. First SCICA is applied to extract artifactual ICs, then WT is applied to these ICs to remove the remaining neural information. Once artifact-only ICs are obtained, these ICs are projected back and subtracted from the original EEG signal to get an EEG signal that is free from artifacts. Quantitative measures have have indicated an improved performance over wICA in terms of normalized mean squared error and mutual information on artifact-free segments. However, this approach requires prior information to initialize the SCICA, thus considered as semi-automatic and may not be suitable for online applications. Mowla et al. in [99] performed similar artifact rejection as in [97], but the authors used CCA for muscle artifact removal and second-order blind identification (SOBI) for ocular artifact removal instead of SCICA. To automate the IC selection process in ICA, Al-Qazzaz et al. [100] proposed an automatic ICA technique combined with WT (AICA-WT). In this algorithm, ICs estimated by ICA are subjected to an automated artifactual IC identification step through features such as the skewness, sample entropy and kurtosis. WT is then applied on these ICs for de-noising ; thus, a clean signal is obtained. On the other hand, Mammone et al. [101] suggested an algorithm based on automatic Wavelet Independent Component Analysis (AWICA). WT is applied on the EEG signal, producing wavelet coefficients which are then subjected to automatic artifactual selection trough kurtosis and Renyi's entropy. These coefficients are then passed through ICA for another layer of artifact rejection by eliminating artifactual ICs. Finally, the inverse of ICA and the inverse of WT is performed to reconstruct a clean EEG signal. AWICA has outperformed wICA in term of RMSE (AWICA-0.1, wICA-0.17) and the correlation (AWICA-0.8, wICA-0.22) between the artifact-free EEG segment and reconstructed EEG segment, while removing the eyeblink artifacts. Zhao et al. [102] proposed the wavelet enhanced CCA (wCCA), where CCA is applied on the contaminated EEG signal to get the canonical components. The most prominent canonical component vector representing the artifact is subjected to WT to separate out the neural information, and the artifact-only components are removed. The algorithms have shown an improved performance in removing ocular artifacts over CCA, ICA and wICA, in terms of signal-to-artifact ratio (wCCA-23.6 at posterior, wICA-2.16 at anterior). However, this result is obtained on semi-simulated data, and no quantitative results on real EEG signals were provided.

2.3.5.3/ WAVELET WITH EMD

Bono et al. [103, 104] has conducted a comparison study between Wavelet Packet Transform with Empirical Mode Decomposition (WPTEMD), and Wavelet Packet Transform with ICA (WPTICA). The main concept of these two algorithms is first to apply WPT on a contaminated EEG signal. The energy of the wavelet coefficients on every branch is calculated for each channel. A common wavelet branch that captures the most energy is categorized

to hold the artifact's effect, thus selected and eliminated. The cleaned WPT-signal is fed to either ICA or EMD for further artifact suppression. The authors have concluded that WPTEMD outperformed WPTICA in removing eyeblink artifacts, in terms of Root Mean Squared Error and Artifact to Signal Ratio.

2.3.5.4/ Statistical features with BSS/WT

Some of the researchers have combined statistical methods with a BSS or WT. Mahajan et al. [105] automatically identify the eyeblink artifacts with modified multiscale sample entropy (mMSE) and Kurtosis features. Identified eyeblink artifacts are then denoised through a bi-orthogonal WT. Cinar et al. [106] have used the outlier detection method with ICA (OD-ICA). In this algorithm, ICA is first applied on the contaminated EEG signal to get a set of ICs. Then the outlier detection algorithm utilized the Chauvenet criterion, the Peiree's criterion and an adjusted box plot to determine if an IC is artifactual. Identified artifactual ICs are then removed to construct a clean EEG signal.

2.3.5.5/ EMD/EEMD with BSS/PCA

Sweeney et al. [90, 107] used EEMD with CCA (EEMD-CCA) for single-channel artifact correction, where CCA is applied on the IMFs obtained through EEMD. Artifactual canonical components are removed to reconstruct a clean EEG signal from a single channel . Mumtaz et al.[108] has proposed the use of EMD to decompose a single channel contaminated EEG signal into multiple IMFs. IMFs that characterize the artifact are summed together to form an eyeblink artifact template. Then CCA is applied on the multichannel contaminated EEG signal along with the artifact template obtained previously. Finally, the algorithm eliminates artifactual canonical components and reconstructs a clean multichannel EEG signal. Patel et al. [109] have suggested an approach based on PCA application on the IMFs obtained through EEMD to remove eyeblink artifacts. The artifactual PCs are removed and a clean single-channel signal is reconstructed. Chen et al. [110] used the EEMD and multiset CCA (MCCA) for single-channel muscle artifact correction. EEMD is applied on a contaminated EEG signal to get a set of IMFs. MCCA is then applied on the IMFs, artifact components are made to zero followed by clean EEG signal reconstruction. This technique is not suitable for online artifact removal as it removes artifacts only from single-channel EEG. In 2018, Chen et al. [111] used multivariate EMD with ICA to remove muscle artifacts from multi-channel EEG instead of single-channel artifact correction. Multivariate EMD (MEMD) is a method of applying EMD on a contaminated multi-channel EEG signal to get a set of IMFs. Obtained IMFs are subjected to CCA for artifact removal.

2.3.5.6/ Adaptive Filters with Neural Networks/WT

Jafarifarmand et al. [112] make use of the neural network with an adaptive filter. Adaptive noise cancellation (ANC) is a method that compares a contaminated EEG signal with an artifact reference such as EOG, thus producing an artifactual signal. The artifactual signal then acts as feedback to an adaptive filter, which is subtracted from the contaminated signal to produces a clean EEG signal. Zhao et al. [113] proposed an algorithm that used WT with adaptive predictive filtering (WT-APF). First, WT is applied on a contaminated

EEG signal, then an adaptive autoregressive model for prediction is used on the artifactual coefficients of WT, thus removing the artifacts.

2.3.5.7/ Support Vector Machine with WT/BSS

Soker et al. [114] proposed the use of support vector machine (SVM) on the ICs of a contaminated EEG signal produced by ICA, to classify artifactual and non-artifactual ICs accordingly. Sai et al. [115] used SVM on the components obtained through WT and ICA (WT-ICA), where contaminated EEG signal is subjected to ICA to get ICs, which are then subjected to WT. The artifactual wavelet coefficients obtained through WT is identified with a pre-trained SVM and removed. Lawhern et al. [116] used the Autoregressive (AR) model for artifact feature selection, followed by an SVM classifier for training purposes in detecting the artifacts. Some of the hybrid techniques are listed in Table 2.3.

TABLE 2.3 – Studies Based on Hybrid Techniques to Remove Artifacts

Study	Year	Method	Artifact
Shoker et al. [114]	2005	ICA-SVM	eyeblink
Halder et al. [117]	2007	ICA-SVM	eyeblink
Akhtar et al. [98]	2009	SCICA-WT	eyeblink
Ghandeharion et al. [118]	2010	ICA-WT	eyeblink
Lindsen et al. [119]	2010	ICA-EMD	eyeblink
Chan et al. [120]	2010	AF-ICA	eyeblink
Raghavendra et al. [121]	2011	CCA-WT	eyeblink
Klados et al. [96]	2011	AF-ICA	eyeblink
Zhao et al. [102]	2011	WT-CCA	eyeblink
Guerrero et al. [122]	2012	AF-ICA	eyeblink
Mommone et al. [101]	2012	ICA-WT	eyeblink
Akhtar et al. [97]	2012	SCICA-WT	eyeblink
Sweeney et al. [107]	2012	EEMD-CCA	eyeblink
Lawhern et al. [116]	2012	Autoregressive-SVM	eyeblink
Jafarifarmand et al. [112]	2013	AF-NN	eyeblink
Peng et al. [123]	2013	AF-WT	eyeblink
Sweeney et al. [90]	2013	EEMD-CCA	eyeblink
Soomro et al. [108]	2013	EMD-CCA	eyeblink
Zhao et al. [113]	2014	WT-AF	eyeblink
Chen et al. [110]	2014	EEMD-CCA	muscle
Mahajan et al. [105]	2015	Statistical-WT	eyeblink
Mingai et al. [124]	2015	ICA-WT	eyeblink
Gao et al. [125]	2015	ICA-EMD	eyeblink
Mowla et al. [99]	2015	CCA-WT	eyeblink
Zeng et al. [126]	2015	EEMD-ICA	eyeblink
Wang et al. [127]	2015	ICA-EMD	eyeblink
Mannan et al. [19]	2016	ICA-AF	eyeblink
Bono et al. [103]	2016	WT-ICA/EMD	eyeblink
Kanoga et al. [128]	2016	ICA-WT	eyeblink
Patel et al. [109]	2016	EMD-PCA	eyeblink
Jafarifarmand et al. [129]	2017	ICA-AF	eyeblink
Patel et al. [130]	2017	EMD-Regression	eyeblink
Al-Qazzaz et al. [100]	2017	ICA-WT	eyeblink
Cinar et al. [106]	2017	Statistical-ICA	eyeblink
Vijayasankar et al. [131]	2018	EMD-WT	eyeblink
Chen et al. [111]	2018	EMD-ICA	muscle
Sai et al. [115]	2018	ICA-WT-SVM	eyeblink
Issa et al. [132]	2019	ICA-WT	eyeblink

2.3.6/ Online Artifact Removal Techniques

Some of the most related works which may be viable for online applications are discussed in the following subsections and summarized in Table 2.4.

2.3.6.1/ Wavelet Neural Network

Nguyen et al. [133] have reported their work on ocular artifact removal by combining WT and Artificial Neural Network (ANN) and naming their technique Wavelet Neural Network (WNN). Initially, the neural network is trained to classify artifacts using a separate artifact/EOG recording and non-artifacts with simulated EEG signals. Once the network is trained, contaminated EEG signals are subjected to WT to obtain wavelet coefficients, which are then passed to the ANN classifier for artifact identification and correction. Corrected wavelet coefficients are then reconstructed to get a clean version of the EEG signal. The authors have mentioned that this algorithm is computationally efficient; therefore, it may be a reliable solution for real-time artifact removal. Though it is computationally efficient, this algorithm requires an additional artifact/EOG recording to train the ANN classifier, which may add up some time delay for its implementation in real-time. Moreover, the algorithm is only capable of removing artifacts from a single-channel EEG signal, which is not practical for a real-world application.

2.3.6.2/ FORCe

Daly et al. [134] have developed a software plugin GUI, called the Fully Online and Automated Artifact Removal for Brain-Computer Interfacing (FORCe). This plugin works based on the combination of WT, ICA and thresholding. It is designed to perform in an automated online environment and to remove several types of artifacts, such as the eyeblink artifacts, cardiac artifacts and muscle artifacts. First, WT is applied to a 1-second epoch on every channel of an EEG signal. The resulting approximation coefficients attained through WT are subjected to ICA to get a set of independent components, ICs. Next, the artifactual ICs are identified through several threshold criteria, where ICs exceeding certain threshold values are classified as eyeblink and cardiac artifacts, and thus removed. The inverse of ICA on the remaining non-artifactual ICs is performed to estimate a set of cleaned approximation coefficients. Then, soft thresholding is applied on resulting approximation coefficients from ICA and detail coefficients acquired through wavelet to suppress/remove muscle artifacts. Finally, the algorithm produces EEG epochs that are free of artifacts.

While the algorithm is able to remove eyeblink, cardiac and muscle artifacts online, the algorithm relies completely on manually pre-determined thresholds to classify if an IC is artifactual. Furthermore, the selection of thresholds was based on the analysis performed only on the EEG signals of two participants. Since artifact patterns or characteristics may vary for every individual, manually adjusted and pre-determined thresholds based on signals of two participants may not be suitable to detect and remove artifactual ICs of a wider range of EEG datasets. The authors have also stated that the running time of the algorithm would linearly increase with an increasing number of channels. So, this would add up some time delay to its implementation in online operations, especially in applications requiring additional number of channels, for example, in seizure detection

units to localize epileptic foci.

2.3.6.3/ Real-time Source-mapping Toolbox

Most recently, Tonachini et al. in [135] have developed an online automatic artifact rejection (REST), toolbox using artifact subspace reconstruction (ASR), PCA, online recursive ICA (ORICA) and an IC classifier. ASR is an automated, variance-based algorithm, that learns the statistical properties of an artifact-free EEG segment. Once the learning is complete, PCA is applied to transform contaminated EEG segments into PCs, which are then compared with the learnt data. PCs that are exceeding initially calibrated/learnt data are removed, where transient and large-amplitude artifacts get removed in this stage. Remaining PCs are re-projected back to acquire a partially cleaned EEG segment. Next, ORICA is performed on partially cleaned EEG segments from PCA, which produces a set of ICs. These ICs are categorized into eye movement ICs and non-eye movement ICs using an altered version of the EyeCatch classifier. The classification is done by getting the correlation value of the ICs with the IC scalp maps contained in the library of EyeCatch. ICs that exceed a fixed correlation value is removed and a clean EEG segment is reconstructed.

Though the authors have stated that this algorithm operates in an online setting to remove eyeblink, cardiac and muscle artifacts, they have clearly mentioned that ASR had negligible effect on the removal of eyeblink artifacts. On the other hand, the time it took for ORICA to converge well enough on the blink-related IC for the artifact to be removed is 26 seconds, which is too long for an online algorithm. Additionally, the authors have pointed out that the altered version of EyeCatch classifier has introduced some instability to the correlation values used in classifying the artifactual ICs. Hence, an online implementation is certainly intolerable with the significant amount of time consumed by ORICA to identify an eyeblink artifact related IC, and the instability introduced by the EyeCatch classifier. Thus, it is concluded that this algorithm may not be suitable to eliminate eyeblink artifacts in an online manner, although it can effectively remove cardiac and muscle artifacts.

TABLE 2.4 – Related Work on Online Artifact Removal

Related Work	Techniques	Findings/Limitations
Wavelet Neural Network (WNN)	WT + Artificial Neural Network	Authors have clearly mentioned that this algorithm requires an additional artifact/EOG recording to train the ANN classifier, which may add up some time delay for its implementation in real time, and it removes artifacts only from a single-channel EEG
Fully Online and Automated Artifact Removal for Brain-Computer Interfacing (FORCe)	ICA + WT + Thresholding	Runs in MATLAB and is stated can be used forreal-time BCI applications. FORCe able to remove artifacts from multi EEG channels
Real-time Source Mapping Toolbox (REST)	ASR + PCA + ORICA + IC classifier (EyeCatch)	Had negligible effect on eyeblink artifact removal, instability of the EyeCatch classifier and ORICA requires about 26 seconds to converge well on a blink-related IC

2.4/ DISCUSSION

2.4.1/ SIGNIFICANCE OF EYEBLINK ARTIFACTS IN EEG-BASED APPLICATIONS

Eyeblink artifacts pose a significant effect on the analysis and results of many EEG applications. The impact of eyeblink artifacts on some of the applications is discussed in this section.

2.4.1.1/ EPILEPTIC SEIZURE DETECTION

Epilepsy is a neurological disorder of the brain which causes seizures. According to a study, an estimate of 150000 epilepsy cases is diagnosed yearly in the US (http ://www.ninds .nih.gov/). One of the most common ways of diagnosing epilepsy is through seizure detection using EEG signals. Whenever an epileptic patient develops a seizure, a disruption of the electrical communication between neurons will occur, which might endanger his life. Hence, developing automatic seizure detection is crucial. There are several numbers of researches carried out to date for epileptic seizure detection. Yash

et al. [136] and Alotaiby et al. [137] have reviewed most of the existing seizure detection algorithms. They include seizure detection and prediction through time-domain, frequency-domain, Wavelet Transform, Singular Value Decomposition, Principal Component Analysis, Independent Component Analysis, discrete Fourier transform, Hilbert transform, Gabor transform, rational transform and Empirical Mode Decomposition. Recent techniques utilize convolutional neural network [138, 139], pyramidal one-dimensional convolutional neural network [140], local binary pattern feature extraction [141] and cross-bispectrum of EEG signal [142] in detecting epileptic seizures.

The latest direction in seizure detection is to perform real-time epileptic seizure detection. Real-time seizure detection is necessary because patients suffering from epilepsy can be treated without any time delay if their seizures are detected or predicted in real-time. It is apparent that only very few studies been proposed on real-time epileptic seizure detection. One of the issues in real-time seizure detection algorithms is how the eyeblink artifacts can be identified and removed in real-time. Eyeblink artifacts often lead to misinterpretation of artifactual segments as an epileptiform activity. Epileptiform refers to waves and spikes that may be associated with epilepsy. Eyeblink artifacts that are misinterpreted as the epileptiform activity may result in incorrect medication and treatment of epilepsy patients [143]. Acar et al. [144] have stated that artifacts originating from eye blinks and eye movements often undermine efforts to localize epileptic segments from the EEG signal of an epilepsy patient.

Studies that are addressing real-time epileptic seizure detection techniques can be found in [145–149]. Hanosh et al. [145] used Passive Infrared Sensors (PIR) for real-time epileptic seizure detection during sleep. In this study, identifying and removing eyeblink artifacts are not applicable as the study focused on seizure detection during sleep, where no eye blinking activity occurs during this stage. Forooghifar et al. [146] have proposed the use of a multi-parametric machine learning technique for real-time epileptic seizure detection. The authors have mentioned that their proposed technique was not evaluated with the presence of intense physical activities and artifacts, so the performance of the seizure may degrade in the presence of such artifacts. Hosseini et al. [147] used the Random Subspace Ensemble Learning. In this study, it was found that artifacts cause feature extraction and classification prone to errors during automatic seizure detection. Vidyaratne et al. [148] suggested a real-time seizure detection based on harmonic wavelet packet transform (HWPT) and fractal dimension (FD). This study has also mentioned that EEG artifacts may cause false seizure detection. The most recent study on real-time epileptic seizure detection was proposed by Mansouri et al. [149] based on a network model of the brain and a distance metric based on the spectral profiles of EEG signals. In this study and analysis, the authors have found that the proposed method revealed poor performance on some of the signals due to an excessive level of artifacts.

It is, therefore, crucial to remove eyeblink artifacts from EEG signals in real-time for proper seizure detection and prediction in real-time epileptic seizure detection units.

2.4.1.2/ Other EEG-based Applications

In brain-computer interface (BCI) devices, eyeblink artifacts are considered as the most significant and apparent type of artifact [150, 151]. If not correctly identified and removed, eyeblink artifacts may be accidentally used as a source that could mislead classification and the controllability of the BCI device. This scenario could lead to a drop in the BCI sys-

tem's performance during real-time applications. For this reason, BCIs related to severe motor disabilities are in demand for accurate eyeblink artifact recognition and elimination during online operations, which will make the BCI device more robust [152].

In neurofeedback, eyeblink artifacts are considered more problematic if not identified and removed. Since the frequency of eyeblink artifacts often overlaps with those used for neurofeedback training, the eyeblink artifacts could potentially manipulate the feedback signal, which may strongly influence and invalidate the learning outcome [153]. Another study by Sherlin et al. in [154] stated that eyeblink artifacts are possibly misinterpreted, causing incorrect learning process. Therefore, the authors have strongly suggested that a real-time eyeblink artifact detection and removal is required to avoid "artifact-driven" feedback.

In research related to Alzheimer's disease, EEG recording during the eyes open state is not preferred mainly due to contamination from eyeblink artifacts, and artifact avoidance is impractical. Whenever EEG signals are recorded during the eyes open state, excessive eyeblink artifacts are present, thus artifact-free segments have to be patched together to obtain sufficient duration of EEG signal for analysis. However, patching EEG segments together produces discontinuous neural information, which may introduce incorrect interpretation on the analysis of Alzheimer's EEG signal [17]. In research related to cognitive development, researchers prefer EEG portions associated with the cognitive process of interest to be free of eyeblink artifacts so that the data analysis is meaningful [155]. It is, therefore, mandatory to remove eyeblink artifacts from EEG signals for proper EEG signal interpretation in any EEG-based application.

2.4.2/ The Need of Online Eyeblink Arifact Elimination in EEG Based Applications

In clinical monitoring such as epileptic seizure detection units, neurofeedback and the BCI, where EEG signals are analyzed and manipulated as they are being recorded, an online artifact removal solution is required [20]. Various EEG based applications like BCI, neurofeedback and epileptic seizure detection systems rely on the availability of instructions from the brain, which should be received instantly, and real-time operation of the devices. It is imperative that these EEG-based systems are workable while the users are performing their daily tasks or during a real-time monitoring, which means they should operate in an online manner. However, researches and studies conducted thus far are most often conducted in laboratory settings. Thus, the evolution of the applications from the laboratory to real-life environments is essential. The online processing of a system refers to operations of the desired application in acquiring EEG signal, process and produces output instructions to be executed during the experiment itself with acceptable time delay. Therefore, it is mandatory for any algorithm that deals with BCI, neurofeedback and epilepsy detection units perform EEG acquisition, artifact correction, feature extraction and classification online. For reliable analysis of EEG signals, it is therefore essential that eyeblink artifacts are correctly identified and removed. Useful EEG instructions can be fed to BCI or neurofeedback applications only if eyeblink artifacts contaminating the EEG signals are correctly identified and removed. Although automatic eyeblink artifact removal algorithms are available, it has to be noted that studies addressing and implementing online removal of eyeblink artifacts are essential.

2.4.3/ Gap Analysis

Since applications such as BCI, neurofeedback and epileptic seizure detection require online signal processing, artifact removal methods and algorithms should be capable of online processing. Hence, to cater for online eyeblink artifact removal, the methods or algorithm should satisfy a few criteria. The most important requirement is that the algorithm should be fully automatic without any expert's intervention. Secondly, online applications should avoid utilizing additional electrodes around the artifact originating regions, such as EOG, as it may cause discomfort and inconvenience to the subject during long-term EEG recordings. Third, it is advisable that the algorithm used for online applications do not rely on eyeblink activity recording for training purposes, as they will add a significant amount of time delay to the entire algorithm. Next, a multi-channel online eyeblink artifact removal algorithms are preferred instead of single-channel artifact removal, as applications like BCI and epilepsy detection require the availability of multi-channel cleaned EEG data. Finally, online implementation requires the artifact removal algorithm to have minimal computational complexity so that the algorithm doesn't introduce unacceptable time delay to the entire application.

All the techniques elaborated and discussed in section 2.3 are among the most commonly available techniques in EEG's artifact removal. An analysis is conducted on these techniques to decide whether or not they can be used to remove eyeblink artifacts online, which can be employed in EEG-based applications. Table 2.5 lists out existing techniques and their viability for real-time eyeblink artifact correction.

From the analysis of the existing eyeblink artifact removal techniques, the following observations are made. Regression-based techniques can perform automatic eyeblink artifact removal in the presence of a reference signal, hence may not be suitable for online applications. On the other hand, ICA, CCA and PCA-based techniques can be used for online applications, provided these techniques are combined with an automatic artifact identification and if the computational complexity is low. So among these 3 techniques, CCA, which is with low computational complexity, can be considered as a solution for online eyeblink artifact removal if the artifact identification is made automatic. Wavelet-based techniques met 4 out of the 5 criteria listed for an online eyeblink artifact removal approach, however, it could only remove artifacts from a single-channel EEG. EMD-based techniques also remove eyeblink artifacts from a single-channel EEG, but when combined with BSS techniques, it could perform multi-channel artifact removal. However, EMD-based techniques are computationally costly, preventing it from being used for online applications. All the hybrid techniques are also computationally complex, and some of them requires training of the algorithms which may not be suitable for applications requiring online removal of eyeblink artifacts. It can be concluded that a feasible online artifact removal algorithm can be developed if artifact identification in CCA is made automatic and the computational complexity of statistical features-BSS, EMD/EEMD-BSS/PCA algorithms are reduced, without the need for training.

2.5/ Summary

Contamination from eyeblink artifacts in EEG signals is inevitable, which could pose an impact on the desired EEG application. To this extent, many studies have been conducted and various methods are developed to identify and remove eyeblink artifacts from

EEG signals. However, studies and work to deal with online removal of eyeblink artifacts remain an attractive research area. Every online artifact removal technique discussed in this chapter depends on either a dedicated artifact reference recording or some kind of training data that records artifacts separately for training purposes, which may add some time delay to the techniques in online applications. There are still many issues in making artifact removal algorithms truly real-time, reliable and practical. It has to be concluded that studies addressing real-time processing and removal of eyeblink artifacts from EEG signals are crucial.

Through literature survey, an algorithm that combines EMD and CCA in [108], is shown to outperform the other commonly available artifact removal techniques in terms of artifact removal accuracy, when evaluated on EEG signals added with synthetically generated eyeblink artifacts. Despite the fact that it can accurately remove artifacts from the EEG signals compared to other techniques, the algorithm is relatively slow due to its iterative nature, making it computationally complex. As discussed earlier, if the artifact identification is made automatic and if the computational complexity of the EMD-CCA algorithm is reduced, the algorithm can be a feasible solution for online applications. The next chapter provides an overview of EMD and CCA before discussing how these techniques can be modified to make them faster for online applications.

TABLE 2.5 – Criteria of Existing Techniques

Method	Automatic	Additional Reference	Training	Artifact Removal	Computational Complexity	Online ?
Expectation	***Yes***	***No***	***No***	***Multi-channel***	***Low***	***Yes***
Regression	Yes	Yes	No	Multi-channel	Low	No
BSS						
ICA	No	No	No	Multi-channel	High	No
PCA	No	No	No	Multi-channel	High	No
CCA	No	No	No	Multi-channel	Low	No
Decomposition						
Wavelet	Yes	No	No	Single-channel	Low	No
EMD	No	No	No	Single-channel	High	No
Hybrid						
ICA-Regression	Yes	Yes	No	Multi-channel	High	No
Wavelet-BSS	Yes	No	No	Single-channel	High	No
Wavelet-EMD	Yes	No	No	Single-channel	High	No
Statistical features-Wavelet/BSS	Yes	No	No	Multi-channel	High	No
EMD/EEMD-BSS/PCA	Yes	No	No	Multi-channel	High	No
Adaptive filters-Neural Network/WT	Yes	Yes	Yes	Single-channel	High	No
SVM-WT/BSS	Yes	No	Yes	Multi-channel	High	No

3

PRELIMINARY INVESTIGATION

This chapter discusses the implementation of Empirical Mode Decomposition (EMD) with different interpolation techniques and Canonical Correlation Analysis (CCA) with different matrix decomposition techniques, with the aim to help online eyeblink artifact removal feasible. The Cubic Spline Interpolation (CSI) technique is the most commonly used technique in classical EMD for envelope construction [156]. In this chapter, EMD with Cubic Hermite Spline Interpolation (CHSI) and the Akima Spline Interpolation (ASI) techniques will be evaluated for their performance and efficiency in removing eyeblink artifacts, compared to the conventional CSI technique. For CCA, three decomposition techniques, i.e. Eigen decomposition, Singular Value Decomposition (SVD) and QR decomposition with SVD are assessed in terms of their ability to decompose a multi-channel EEG segment efficiently. Eyeblink artifact elimination and reconstruction of clean EEG segments with CCA are illustrated as well.

3.1/ OVERVIEW OF CLASSICAL EMPIRICAL MODE DECOMPOSITION

Empirical Mode Decomposition (EMD) is an algorithm that decomposes a signal into multiple oscillating components. The algorithm reiterates itself until it can isolate the highest oscillating component that remains in a signal. This is achieved through a process called ”sifting”, where it continually sifts out a local high oscillating trend called the intrinsic mode functions (IMF). Each IMF should satisfy the following criteria as illustrated in [156] :

- contains equal number of extrema and zero crossings, or differ at most by one
- envelopes of the IMF are symmetric with respect to zero

In sifting, the signal of interest is first subjected to extrema search, where all the relative maximum and minimum points are identified and saved. Then, interpolation is performed to connect all the maximum points, thus forming an upper envelope. Similarly, all minimum points are interpolated together to form the lower envelope. Next, the upper and lower envelopes are averaged out to get a mean trend. Finally, the mean trend is subtracted from the signal, resulting in a residual signal. This residual signal will be saved as an IMF if it satisfies the IMF properties, otherwise sifting is continued on the residual signal. The sifting process is repeated multiple times until multiple IMFs are obtained. In general, EMD is performed to decompose a signal, $X(t)$, into multiple IMFs, $x_i(t)$ and a single residual component, $R_n(t)$, which is monotonous through the sifting process, as in Eq. (3.1) :

$$X(t) = \sum_{i=1}^{n-1} x_i(t) + R_n(t) \tag{3.1}$$

The detailed sifting process in classical EMD in extracting out the IMFs are described below :

a. EMD is first fed with an input signal, $z(t)$ which is also the signal of interest, $X(t)$.

$$z(t) = X(t) \tag{3.2}$$

b. All relative extrema points in the input signal are identified and interpolated, constructing upper and lower envelopes by connecting maximum and minimum points through Cubic spline interpolation.

c. The upper and lower envelopes are then averaged to get a mean trend, $m(t)$, which is then subtracted from the input signal, $z(t)$, producing an output signal,$y_j(t)$:

$$y_j(t) = z(t) - m(t) \tag{3.3}$$

d. The algorithm checks if the output trend, $y_j(t)$ satisfies the IMF criteria as stated in this section.

e. Steps b., c. and d. are repeated until the IMF criteria are satisfied. If the IMF criteria are not met, then the current output signal, $y_j(t)$ is re-injected into the algorithm as a new input signal :

$$z(t) = y_j(t) \tag{3.4}$$

f. Once the IMF criteria are satisfied, the algorithm assumes the current trend, $y_j(t)$ as the first IMF output, $x_1(t)$:

$$x_1(t) = y_j(t) \tag{3.5}$$

g. The steps mentioned above are repeated recursively on the residual signal $R_1(t)$, where :

$$R_1(t) = X(t) - x_1(t) \tag{3.6}$$

Each successful sifting loop produces the i-th IMF of the algorithm, $x_i(t)$. The recursive sifting discontinues after the algorithm extracts out $n-1$ IMFs, the instance where the residual signal, $R_n(t)$ becomes a monotonic trend. $R_n(t)$ is the residue from the original EEG data after $n-1$ IMFs have been extracted, while $x_i(t)$ is the i-th IMF of the algorithm. Fig. 3.1 shows the flow chart of EMD. The algorithm is relatively slow because it reiterates itself until the final residual becomes a monotonic function.

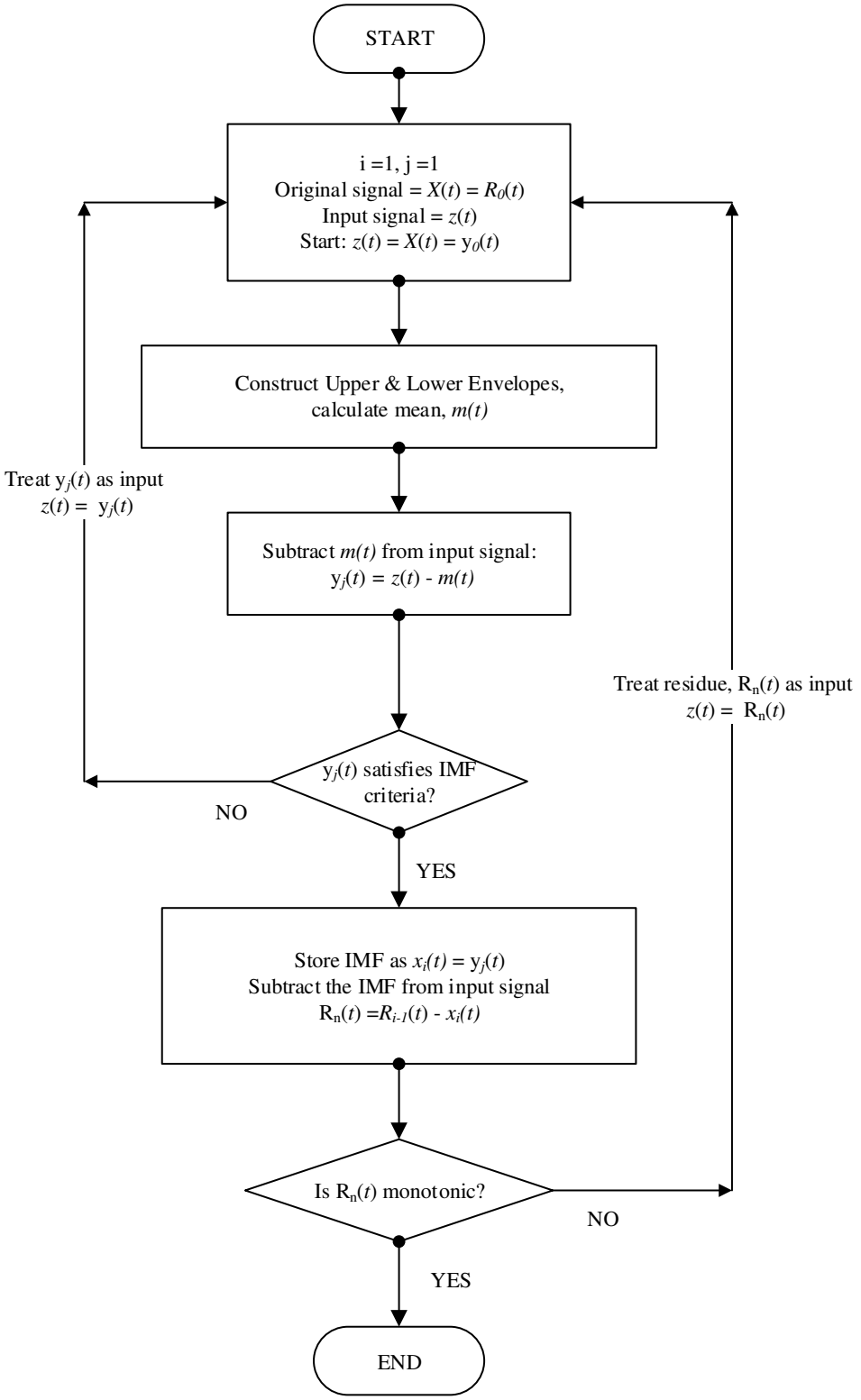

FIGURE 3.1 – Flowchart of Classical EMD Algorithm

3.2/ Eyeblink Artifact Interpretation from EMD

The idea of isolating out the eyeblink artifact from the EEG signal by applying EMD is suggested by Flandrin et al. in [157]. As elaborated above, the signal of interest is decomposed into several IMFs and a residue. It extracts out the highly oscillating signal that remains in the signal. Each IMF is a slower oscillating trend compared to the one extracted in the previous iteration. The original signal can be reconstructed by adding up all IMFs and the final residual signal. The EEG signal, which is the highly oscillating trend with low amplitudes, will be captured in the first few IMFs of the decomposition. The eye blink artifact, which is the slowly varying trend with a higher amplitude, is expected to be captured by higher IMF trends and by the final residual trend. Hence, partial reconstruction of the higher IMFs and the final residual function obtained from decomposition would yield the eyeblink artifact trend.

3.3/ Envelope Interpolation Techniques in EMD

An overview of the cubic spline interpolation is discussed in the next subsection. The following subsection discusses alternative interpolation techniques that can be used in EMD.

3.3.1/ Piecewise Cubic Spline Interpolation

Cubic Spline Interpolation (CSI) uses a second-order derivative function at every data point to ensure continuity and minimum curvature for smoothness of the curve as elaborated below.

i. In cubic spline interpolation, a 3rd-degree polynomial function is constructed between two data points ($[x_{i-1}, y_{i-1}]$ $[x_i, y_i]$), represented by a cubic polynomial function.

ii. The function to the left of point $[x_i, y_i]$ is indicated as $f_i(x_i)$ at point x_i. Similarly, the function to the right of point $[x_i, y_i]$ is indicated as $f_{i+1}(x_i)$ at point x_i. These segments are connected together, thus satisfying :

$$f_i(x_i) = f_{i+1}(x_i) \tag{3.7}$$

iii. In order for the segments to become continuous at every joint, the curve segments should have the same slope where they join, which could be achieved by equating the first derivative of two adjacent functions. This enforces continuity as the slopes match where the curves join, i.e.

$$f_i^{'}(x_i) = f_{i+1}^{'}(x_i) \tag{3.8}$$

iv. To guarantee that the curves have minimal curvature for smoothness at the joint, the second derivatives of the functions are forced to be equal :

$$f_i^{''}(x_i) = f_{i+1}^{''}(x_i) \tag{3.9}$$

3.3.2/ Use of Alternative Interpolation Techniques in EMD

The impact of alternative interpolation techniques instead of CSI in EMD has not been adequately evaluated. Rilling et al. [158] have suggested that CSI is preferred over linear interpolation, which tends to increase the required number of sifting iterations and "over-decompose" signals by spreading out their components over adjacent modes. In [159], Hawley et al. used the trigonometric interpolation instead of CSI. They have suggested that trigonometric interpolation is useful from an analytical point of view, but computationally it is much more expensive than CSI. On the other hand, Chen et al. in [160] approached the B-spline interpolation to fit combined extrema before obtaining the local mean. In [161], Kopsinis et al. used the Hermite spline interpolation. All these alternative interpolation techniques have shown initial encouraging results, however, they are either in the development stage or need further development.

3.3.2.1/ Piecewise Cubic Hermite Spline Interpolation

The Cubic Hermite Spline Interpolation (CHSI) as proposed in [161] is investigated, and the computation efficiency is evaluated as compared to CSI. Each segment in the CHSI is also constructed by a cubic polynomial function. The proposed CHSI sacrifices curve smoothness to prevent overshoots. This is achieved by eliminating the equivalent second-order derivative at every point and substituting it with a specified first-order derivative, which is the tangent to the segments at point $[x_i, y_i]$:

$$f_i^{'}(x_i) = f_{i+1}^{'}(x_i) = f'(x_i) \tag{3.10}$$

3.3.2.2/ Proposed Piecewise Akima Spline Interpolation

Akima Spline Interpolation (ASI) is first developed by Hiroshi Akima in the late 1960s [162]. Similar to the CSI and CHSI, each spline segment of ASI is constructed by a cubic polynomial function from point $[x_i, y_i]$ to point $[x_{i+1}, y_{i+1}]$. The main concept of this technique is calculating the slope $f'(x_i)$ at point x_i which depends on the two immediate predecessors of $x_i's$, $([x_{i-1}, y_{i-1}][x_{i-2}, y_{i-2}])$, and the two immediate successors of $x_i's$, $([x_{i+1}, y_{i+1}][x_{i+2}, y_{i+2}])$ as shown in Fig. 3.2.

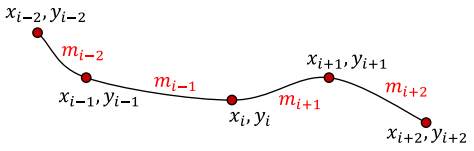

FIGURE 3.2 – Slope computation at point $[x_i, y_i]$

The slope $f'(x_i)$ at x_i is calculated by :

$$f^{'}(x_i) = \frac{\mid m_{i+2} - m_{i+1} \mid (m_{i-1}) + \mid m_{i-1} - m_{i-2} \mid (m_{i+1})}{\mid m_{i+2} - m_{i+1} \mid + \mid m_{i-1} - m_{i-2} \mid} \tag{3.11}$$

where,

$$m_{i-2} = \frac{y_{i-1} - y_{i-2}}{x_{i-1} - x_{i-2}} \tag{3.12}$$

The slopes of ASI are determined based only on the slopes of adjacent segments as elaborated before. This minimizes the necessity to solve large system equations, which in turn, reduces the computation time.

3.3.3/ Simulation of Synthetic Signals

A synthetically generated EEG signal through autoregressive (AR) model for a duration of 10 seconds (2560 EEG sample points at a sampling frequency of 256 Hz) can be represented using the equation below as proposed in [163] :

$$Y(t) = 1.5084y(t-1) - 0.1587y(t-2) - 0.3109y(t-3) - 0.0510y(t-4) + w(t) \tag{3.13}$$

The eyeblink artifact can be generated through exponential function :

$$Z(t) = 100e^{-(10t-4.5)^2} - 75e^{-(10t-7.5)^2} + 50e^{-(10t-20.5)^2} \tag{3.14}$$

Signals simulated using Eq. (3.13) and (3.14) shown in Fig. 3.3(a) and 3.3(b) respectively can then be added together to obtain a contaminated EEG signal, $X(t)$ as shown in Fig. 3.3(c) :

$$X(t) = Y(t) + Z(t) \tag{3.15}$$

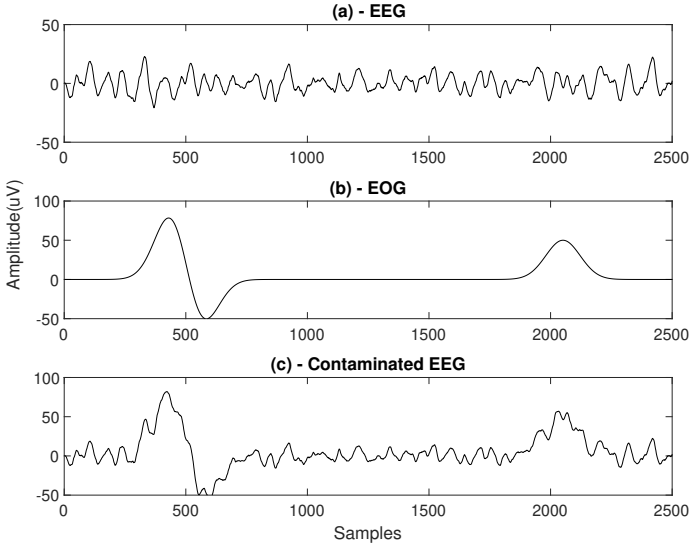

FIGURE 3.3 – (a) Synthetically Generated EEG Signal, (b) Synthetically Generated Eyeblink signal, (c) Mixed EEG and Eyeblink Signal

3.3.4/ Performance Analysis on Interpolation Techniques in EMD with Synthetic Signals

This section aims to evaluate the performance of three different interpolation techniques in terms of Root Mean Square Error (RMSE), Percentage Root Means Square Difference (PRD), Signal to Noise Ratio (SNR), correlation coefficient and the total computation time. The three interpolation techniques that will be evaluated for its performance in EMD are CSI, CHSI and ASI.

To evaluate the decomposition accuracy of EMD via CSI, CHSI and ASI techniques in extracting out the eyeblink artifact, RMSE is calculated. RMSE is calculated by finding the difference between the original eyeblink artifact and the extracted eyeblink artifact, in which the extracted eyeblink artifact can be obtained through partial reconstruction of higher IMFs and the final residual trend acquired from EMD decomposition. In Eq. (3.16), $Z(t)$ refers to the original eyeblink artifact generated from Eq. (3.14), and the $x_{\text{end}}(t)$ and $R_n(t)$ correspond to the IMF and residue which belong to eyeblink artifact, respectively. RMSE closer to zero indicates the extracted eyeblink artifact via EMD is more precise and closer to the original eyeblink artifact.

$$RMSE = \sqrt{\frac{\sum(Z(t) - (x_{\text{end}}(t) + R_n(t)))^2}{n}} \tag{3.16}$$

The percentage root means square difference (PRD), measures the distortion percentage between the original EEG signal and the reconstructed EEG signal. After decomposition via EMD, partially reconstructing the lower IMFs will produce the clean EEG signal, denoted as $Y_{\text{out}}(t)$ in Eq. (3.17). The $Y(t)$ in Eq. (3.17) represents the original EEG signal simulated through Eq. (3.13). A higher PRD value signifies that the reconstructed EEG signal has a higher distortion compared to the original EEG signal.

$$PRD = 100 * \sqrt{\frac{\sum(Y_{\text{out}}(t) - Y(t))^2}{(Y_{\text{out}}(t) * Y(t))}} \tag{3.17}$$

Correlation coefficient is a measurement that quantifies the similarity between two data vectors, in this case, between the simulated EEG signal and the corrected EEG signal after decomposition :

$$\text{Correlation Coefficient} = \frac{C_{Y(t),Y_{\text{out}}(t)}}{\sigma_{Y(t)} * \sigma_{Y_{\text{out}}(t)}} \tag{3.18}$$

where $C_{Y(t),Y_{\text{out}}(t)}$ is the covariance between clean EEG signal, $Y(t)$, and reconstructed EEG signal, $Y_{\text{out}}(t)$, while $\sigma_{Y(t)}$ and $\sigma_{Y_{\text{out}}(t)}$ are the standard deviations of these signals.

The correlation coefficient lies between 0 and 1, where a value approaching 1 denotes higher similarity or correlation. The SNR is used in this analysis to determine the scale of eyeblink artifact removed from the contaminated EEG signal via EMD. The SNR is calculated before and after eyeblink artifact removal, using Eq. (3.19) and (3.20).

$$SNR_{\text{before}} = 10 \log \left[\frac{\sigma_{Y(t)}}{\sigma_{(Y(t)-X(t))}} \right] \tag{3.19}$$

$$SNR_{\text{after}} = 10\log\left[\frac{\sigma_{Y(t)}}{\sigma_{(Y(t)-Y_{\text{out}}(t))}}\right] \tag{3.20}$$

where, Y is the original signal simulated through Eq. (3.13), $X(t)$ is the contaminated signal obtained by adding Eq. 3.13 and 3.14, and $Y_{\text{out}}(t)$ is the corrected EEG signal after decomposition. The standard deviations of these signals are represented with σ symbols.

3.4/ Overview of Canonical Correlation Analysis

Canonical Correlation Analysis (CCA) is a technique that is based on the blind source separation (BSS) concept. As suggested by the name, BBS separates out a set of source signals from a set of mixed signals without any priori knowledge about the source signals or the weighted mixing components. The linear relationship between two multidimensional variables is measured.

Conceptually, BSS assumes the contaminated or the set of mixed signals as the combination of clean EEG sources and artifacts, blended together with a mixing formula. Thus, BSS attempts to isolate EEG sources and artifacts apart with an unmixing formula, which can be useful for artifact elimination from EEG signals.

The observed EEG signal, $\mathbf{X(t)}$ is the first multidimensional variable, while the second multidimensional variable is obtained by taking a temporally delayed component of the observed EEG signal, $\mathbf{Y(t)} = \mathbf{X(t-1)}$. As BSS implies, the observed EEG signal $\mathbf{X(t)}$ is a combination of sources $\mathbf{S(t)}$, where $\mathbf{S(t)}$ consists of EEG sources and artifactual components, mixed through a weighted mixing matrix, $\mathbf{W}$:

$$\begin{aligned} \mathbf{X(t)} &= \mathbf{W_X S(t)} \\ \mathbf{Y(t)} &= \mathbf{W_Y S(t)} \end{aligned} \tag{3.21}$$

The source signals can be obtained by projecting the weighted de-mixing matrix onto the observed EEG signals as in Eq.(3.22) :

$$\begin{aligned} \mathbf{A} &= \mathbf{W_X}^{-1} \\ \mathbf{B} &= \mathbf{W_Y}^{-1} \\ \mathbf{S_X(t)} &= \mathbf{AX(t)} \\ \mathbf{S_Y(t)} &= \mathbf{BY(t)} \end{aligned} \tag{3.22}$$

Hence, sources of the two multidimensional variables, $\mathbf{S_X(t)}$ and $\mathbf{S_Y(t)}$ can be estimated if the weighted de-mixing matrices, $\mathbf{A}$ and $\mathbf{B}$ are known.

In CCA, the sources are named as canonical variates or canonical components, $\mathbf{U}$ and $\mathbf{V}$. Canonical variates for a multi-channel EEG signal can be represented through a linear combination between the de-mixing matrices with mean removed EEG variables, $\hat{\mathbf{X}}$ and $\hat{\mathbf{Y}}$, with n number of EEG sample points in one channel, and p are the number of channels

of $\mathbf{X(t)}$ and $\mathbf{Y(t)}$:

$$\begin{aligned} U_1 &= A_{11}\hat{x_1} + A_{12}\hat{x_2} + ... + A_{1p}\hat{x_p} \\ U_2 &= A_{21}\hat{x_1} + A_{22}\hat{x_2} + ... + A_{2p}\hat{x_p} \\ U_n &= A_{n1}\hat{x_1} + A_{n2}\hat{x_2} + ... + A_{np}\hat{x_p} \\ V_1 &= B_{11}\hat{y_1} + B_{12}\hat{y_2} + ... + B_{1p}\hat{y_p} \\ V_2 &= B_{21}\hat{y_1} + B_{22}\hat{y_2} + ... + B_{2p}\hat{y_p} \\ V_n &= B_{n1}\hat{y_1} + B_{n2}\hat{y_2} + ... + B_{np}\hat{y_p} \end{aligned} \tag{3.23}$$

The dimension of the two multidimensional variables $\mathbf{X}$ and $\mathbf{Y}$ is :

$$\begin{aligned} \mathbf{X} &= n \times p \\ \mathbf{Y} &= n \times p \end{aligned} \tag{3.24}$$

The dimension of the de-mixing matrices $\mathbf{A}$ and $\mathbf{B}$ is :

$$\begin{aligned} \mathbf{A} &= p \times p \\ \mathbf{B} &= p \times p \end{aligned} \tag{3.25}$$

The de-mixing matrices, $A_1 = [A_{11}, A_{12}, ..., A_{1p}]$ and $B_1 = [B_{11}, B_{12}, ..., B_{1p}]$ are p number of weight vectors with respect to $\hat{\mathbf{X}}$ and $\hat{\mathbf{Y}}$ respectively.

Eq. (3.23) can be generalized as below, similar to Eq. (3.22) :

$$\begin{aligned} \mathbf{U} &= \mathbf{A}\hat{\mathbf{X}} \\ \mathbf{V} &= \mathbf{B}\hat{\mathbf{Y}} \end{aligned} \tag{3.26}$$

The purpose of CCA is to find the de-mixing matrices $\mathbf{A}$ and $\mathbf{B}$ such that the correlation between canonical variates is maximized. The correlation between the canonical variates, $\mathbf{U}$ and $\mathbf{V}$ is called the canonical correlation, ρ. The ρ between $\mathbf{U}$ and $\mathbf{V}$ should be maximized, or as large as possible :

$$\begin{aligned} \rho_i &= \text{corr}(U_i, V_i) \\ \rho_i &= \frac{U_i^T V_i}{\sqrt{U_i^T U_i}\sqrt{V_i^T V_i}} \end{aligned} \tag{3.27}$$

where ρ_i is the i-th canonical correlation, U_i and V_i are the i-th canonical variates. From Eq. (3.27), canonical variate pairs are derived, where (U_1, V_1) is the first canonical variate pair ; similarly, (U_2, V_2) is the second canonical variate pair, so on and so forth. The de-mixing matrices $A_1 = [A_{11}, A_{12}, ..., A_{1p}]$ and $B_1 = [B_{11}, B_{12}, ..., B_{1p}]$ are computed such that the coefficient of canonical correlation between the first pair of canonical variates U_1 and V_1 is maximized. The canonical correlation of the second pair of canonical variates is computed in a similar way, provided that the second pair of canonical variates are uncorrelated or orthogonal with the first pair and other pairs of canonical variates in the subspace.

$$\text{corr}(U_1, U_2) = \text{corr}(V_1, V_2) = \text{corr}(U_1, V_2) = \text{corr}(U_2, V_1) = 0 \tag{3.28}$$

This procedure of finding de-mixing matrices is repeated until minimum dimension as in Eq. (3.25) is achieved and the canonical correlation for $n \times p$ canonical variate pairs are determined. Since every pair of canonical variates should be uncorrelated with each other, columns of $\mathbf{U}$ and $\mathbf{V}$ are cross orthogonal, with :

$$\mathbf{Diag} = \mathbf{U^T V} \tag{3.29}$$

where **Diag** is a diagonal matrix formed by a scalar multiplying an identity matrix.

3.5/ Eyeblink Artifact Correction with CCA

As discussed earlier, some rows of the canonical variates obtained through CCA represent the clean EEG sources and one canonical variates row represents the artifact. So, if the artifactual canonical variates are forced to become zero and the artifact-free canonical components are projected back, a clean EEG segment that is clean from artifacts can be reconstructed.

3.6/ Estimation of Weighted De-mixing Matrices in CCA

As stated in section 3.4, CCA maximizes the correlation between U and V through de-mixing matrices A and B. Subsection 3.6.1 illustrates how de-mixing matrices A and B are estimated conventionally through Eigen decomposition.

3.6.1/ Conventional Approach : Eigen Decomposition

In this subsection, the weighted de-mixing matrices are estimated through Eigen decomposition. Substituting the definition from Eq. (3.26) into Eq. (3.27) results in :

$$\rho = \frac{\mathbf{A^T \hat{X}^T \hat{Y} B}}{\sqrt{\mathbf{A^T \hat{X}^T \hat{X} A}}\sqrt{\mathbf{B^T \hat{Y}^T \hat{Y} B}}} \tag{3.30}$$

Let auto-covariance matrices of $\hat{\mathbf{X}}$ and $\hat{\mathbf{Y}}$ be $\mathbf{C_{XX}}$ and $\mathbf{C_{YY}}$, and the cross-covariance matrices between $\hat{\mathbf{X}}$ and $\hat{\mathbf{Y}}$ be $\mathbf{C_{XY}}$ and $\mathbf{C_{YX}}$. The auto-covariance and cross-covariance matrices are substituted into Eq. (3.30) :

$$\rho = \frac{\mathbf{A^T C_{XY} B}}{\sqrt{\mathbf{A^T C_{XX} A}}\sqrt{\mathbf{B^T C_{YY} B}}} \tag{3.31}$$

Now, to simplify Eq. (3.31), let's assume new variables $\mathbf{c}$ and $\mathbf{d}$ as representatives of auto-covariance matrices and de-mixing matrices :

$$\begin{aligned} \mathbf{c} &= \mathbf{C_{XX}^{1/2} A} \\ \mathbf{d} &= \mathbf{C_{YY}^{1/2} B} \\ \mathbf{A} &= \mathbf{c C_{XX}^{-1/2}} \\ \mathbf{B} &= \mathbf{d C_{YY}^{-1/2}} \end{aligned} \tag{3.32}$$

Next, substitute Eq. (3.32) into Eq. (3.31) :

$$\rho = \frac{\mathbf{c^T C_{XX}^{-1/2} C_{XY} C_{YY}^{-1/2} d}}{\sqrt{\mathbf{c^T C_{XX}^{-1/2} C_{XX} C_{XX}^{-1/2} c}}\sqrt{\mathbf{d^T C_{YY}^{-1/2} C_{YY} C_{YY}^{-1/2} d}}} \tag{3.33}$$

Eq. (3.33) can be simplified to Eq. (3.34) :

$$\rho = \frac{\mathbf{c^T C_{XX}^{-1/2} C_{XY} C_{YY}^{-1/2} d}}{\sqrt{\mathbf{c^T c}}\sqrt{\mathbf{d^T d}}} \tag{3.34}$$

Eq. (3.34) becomes :

$$\rho = \frac{\mathbf{e} \cdot \mathbf{d}}{\sqrt{\mathbf{c^T c}}\sqrt{\mathbf{d^T d}}} \tag{3.35}$$

where $\mathbf{e}$ is equal to $\mathbf{c^T C_{XX}^{-1/2} C_{XY} C_{YY}^{-1/2}}$. Now, applying Cauchy-Schwarz inequality on the numerator of Eq. (3.35), results in :

$$\begin{aligned} \mathbf{e, d} &\leq \|\mathbf{e}\| \cdot \|\mathbf{d}\| \\ \mathbf{e, d} &\leq \sqrt{\mathbf{e^T} \cdot \mathbf{e}}\sqrt{\mathbf{d^T} \cdot \mathbf{d}} \end{aligned} \tag{3.36}$$

replacing $\mathbf{e}$ back into (3.36), results in :

$$(\mathbf{c^T C_{XX}^{-1/2} C_{XY} C_{YY}^{-1/2}})(\mathbf{d}) \leq (\mathbf{c^T C_{XX}^{-1/2} C_{XY} C_{YY}^{-1/2} C_{YY}^{-1/2} C_{YX} C_{XX}^{-1/2} c})^{1/2} (\mathbf{d^T} \cdot \mathbf{d})^{1/2} \tag{3.37}$$

Eq. (3.35) is now re-written as :

$$\rho \leq \frac{(\mathbf{c^T C_{XX}^{-1/2} C_{XY} C_{YY}^{-1} C_{YX} C_{XX}^{-1/2} c})^{1/2} (\mathbf{d^T} \cdot \mathbf{d})^{1/2}}{(\mathbf{c^T c})^{1/2} (\mathbf{d^T d})^{1/2}} \tag{3.38}$$

Cancelling out $(\mathbf{d^T d})^{1/2}$ gives :

$$\rho \leq \frac{(\mathbf{c^T C_{XX}^{-1} C_{XY} C_{YY}^{-1} C_{YX} c})^{1/2}}{(\mathbf{c^T c})^{1/2}} \tag{3.39}$$

From Eq. (3.37), equality exists if vectors $\mathbf{d}$ and $\mathbf{C_{YY}^{-1/2} C_{YX} C_{XX}^{-1/2} c}$ are collinear. The maximum correlation can be achieved if $\mathbf{c}$ is the eigenvector for maximum eigenvalue matrix $\mathbf{C_{XX}^{-1} C_{XY} C_{YY}^{-1} C_{YX}}$. By reversing the coordinates, the maximum correlation can be attained if $\mathbf{A}$ is the eigenvector of $\mathbf{C_{XX}^{-1} C_{XY} C_{YY}^{-1} C_{YX}}$ and $\mathbf{B}$ is proportional to $\mathbf{C_{YY}^{-1} C_{YX} A}$, similarly if $\mathbf{B}$ is the eigenvector of $\mathbf{C_{YY}^{-1} C_{YX} C_{XX}^{-1} C_{XY}}$ and $\mathbf{A}$ is proportional to $\mathbf{C_{XX}^{-1} C_{XY} B}$. Eigen decomposition is then applied on matrix $\mathbf{C_{XX}^{-1} C_{XY} C_{YY}^{-1} C_{YX}}$ to solve the eigenvalue/eigenvector problem :

$$\begin{aligned} \mathbf{C_{XX}^{-1} C_{XY} C_{YY}^{-1} C_{YX} A} &= \lambda \mathbf{A} \\ \mathbf{C_{YY}^{-1} C_{YX} C_{XX}^{-1} C_{XY} B} &= \lambda \mathbf{B} \end{aligned} \tag{3.40}$$

where λ represents eigenvalues in descending order $(\lambda_1 > \lambda_2 >, ..., > \lambda_p)$ and $A = [a_{n1}, a_{n2}, ..., a_{np}]$ are the de-mixing matrices or the eigenvectors corresponding to the eigenvalues. Since both multidimensional variables $\mathbf{x(t)}$ and $\mathbf{y(t)}$ are related, either one of the weighted de-mixing matrix, $\mathbf{A}$ or $\mathbf{B}$, is solved.

3.6.2/ Alternative Approaches to Estimate Weighted De-mixing Matrices

The following subsections elaborate two alternative decomposition techniques that can be used to estimate the weighted de-mixing matrices.

3.6.2.1/ Singular Value Decomposition

This subsection will elaborate de-mixing matrices estimation through Singular Value Decomposition (SVD). Singular value decomposition factorizes a matrix $\mathbf{M}$ into :

$$\mathbf{M} = \mathbf{U}\mathbf{S}\mathbf{V}^{\mathbf{T}} \tag{3.41}$$

where $\mathbf{U}$ is an orthonormal eigenvector matrix of $\mathbf{M}\mathbf{M}^{\mathbf{T}}$, $\mathbf{V}$ is an orthonormal eigenvector of $\mathbf{M}^{\mathbf{T}}\mathbf{M}$ and $\mathbf{S}$ are diagonal non-negative square roots of the eigenvalues of $\mathbf{M}^{\mathbf{T}}\mathbf{M}$, which is called the singular values or principal values of $\mathbf{M}$.

In estimating the weighted de-mixing matrices of CCA, first SVD is applied separately on both multidimensional variables $\hat{\mathbf{x}}$ and $\hat{\mathbf{y}}$:

$$\begin{aligned} \hat{\mathbf{X}} &= \mathbf{u_1}\mathbf{s_1}{\mathbf{v_1}}^{\mathbf{T}} \\ \hat{\mathbf{Y}} &= \mathbf{u_2}\mathbf{s_2}{\mathbf{v_2}}^{\mathbf{T}} \end{aligned} \tag{3.42}$$

Next SVD is applied on the multiplied matrix of $\mathbf{u_1^T}$ and $\mathbf{u_2}$ to give :

$$\mathbf{u_1^T}\mathbf{u_2} = \mathbf{u_3}\mathbf{s_3}{\mathbf{v_3}}^{\mathbf{T}} \tag{3.43}$$

De-mixing matrices $\mathbf{A}$ and $\mathbf{B}$ are then computed as follows :

$$\mathbf{A} = \mathbf{v_1}\mathbf{s_1^{-1}}\mathbf{u_3} \tag{3.44}$$

$$\mathbf{B} = \mathbf{v_2}\mathbf{s_2^{-1}}\mathbf{v_3} \tag{3.45}$$

In order to check if the estimated weighted de-mixing matrices are correct, $\mathbf{A}$ and $\mathbf{B}$ are substituted back into Eq. (3.29) to verify if a diagonal matrix is obtained :

$$\begin{aligned} \mathbf{Diag} &= \mathbf{U^T}\mathbf{V} \\ &= \mathbf{A^T}\hat{\mathbf{X}}^{\mathbf{T}}\hat{\mathbf{Y}}\mathbf{B} \\ &= (\mathbf{v_1^T}\mathbf{s_1^{-1}}\mathbf{u_3^T})(\mathbf{u_1^T}\mathbf{s_1}\mathbf{v_1})(\mathbf{u_2}\mathbf{s_2}\mathbf{v_2^T})(\mathbf{v_2}\mathbf{s_2^{-1}}\mathbf{v_3}) \\ &= (\mathbf{u_3^T}\mathbf{s_1^{-1}}\mathbf{v_1^T})(\mathbf{v_1}\mathbf{s_1}\mathbf{u_1^T})(\mathbf{u_2}\mathbf{s_2}\mathbf{v_2^T})(\mathbf{v_2}\mathbf{s_2^{-1}}\mathbf{v_3}) \\ &= (\mathbf{u_3^T})(\mathbf{u_1^T}\mathbf{u_2})(\mathbf{v_3}) \\ &= \mathbf{u_3^T}(\mathbf{u_3}\mathbf{s_3}\mathbf{v_3^T})\mathbf{v_3} \\ \mathbf{Diag} &= \mathbf{s_3} \end{aligned} \tag{3.46}$$

where $\mathbf{s_3}$ are diagonal non-negative square roots of $\hat{\mathbf{x}}$ and $\hat{\mathbf{y}}$. This proves that the estimation of $\mathbf{A}$ and $\mathbf{B}$ through SVD is acceptable.

3.6.2.2/ QR Decomposition and Singular Value Decomposition

In this subsection, the QR decomposition is employed to estimate the de-mixing matrices instead of SVD alone. QR decomposition is a matrix decomposition that factorizes a given matrix into an orthogonal matrix Q, and a triangular matrix R.

First, the two multidimensional variables $\hat{\mathbf{X}}$ and $\hat{\mathbf{Y}}$ are decomposed with QR decomposition :

$$\hat{\mathbf{X}} = \mathbf{q_1}\mathbf{r_1} \tag{3.47}$$

$$\hat{\mathbf{Y}} = \mathbf{q_2}\mathbf{r_2} \tag{3.48}$$

where the $\mathbf{q_1}$ and $\mathbf{q_2}$ are orthogonal columns, while $\mathbf{r_1}$ and $\mathbf{r_2}$ are the upper triangular matrices. Secondly, singular value decomposition, SVD is applied onto the orthogonal columns from Eq. (3.47) and Eq. (3.48) to give :

$$\mathbf{q_1}^{\mathbf{T}}\mathbf{q_2} = \mathbf{u_3 s_3 v_3^T}. \tag{3.49}$$

De-mixing matrices $\mathbf{A}$ and $\mathbf{B}$ are then computed as follows :

$$\mathbf{A} = \mathbf{r_1^{-1}u_3} \tag{3.50}$$

$$\mathbf{B} = \mathbf{r_2^{-1}v_3} \tag{3.51}$$

In order to check if the estimated weighted de-mixing matrices are correct, $\mathbf{A}$ and $\mathbf{B}$ are substituted back into Eq. (3.29) to verify if a diagonal matrix is obtained :

$$\begin{aligned}
\mathbf{Diag} &= \mathbf{U^T V} \\
&= \mathbf{A^T \hat{X}^T \hat{Y} B} \\
&= (\mathbf{r_1^{-1T} u_3^T})(\mathbf{q_1^T r_1^T})(\mathbf{q_2 r_2})(\mathbf{r_2^{-1} v_3}) \\
&= (\mathbf{u_3^T r_1^{-1T}})(\mathbf{r_1^T q_1^T})(\mathbf{q_2 r_2})(\mathbf{r_2^{-1} v_3}) \\
&= (\mathbf{u_3^T})(\mathbf{q_1^T q_2})(\mathbf{v_3}) \\
&= \mathbf{u_3^T}(\mathbf{u_3 s_3 v_3^T})\mathbf{v_3} \\
\mathbf{Diag} &= \mathbf{s_3}
\end{aligned} \tag{3.52}$$

This proves that the estimation of $\mathbf{A}$ and $\mathbf{B}$ through QR and SVD is acceptable.

3.6.3/ Implementation of CCA in Artifact Removal

3.6.3.1/ Artifactual Component Elimination from EEG Signal

The implementation of eyeblink artifact removal from EEG using CCA is summarized below.

1. For elaboration purpose, a data set, $\mathbf{s(t)}$ with a length of 5 seconds is used.
2. Synthetic eyeblink artifacts are added to the EEG dataset to produce contaminated EEG signal. The synthetic eyeblink artifacts, $eb(t)$ can be simulated through exponential functions with different amplitudes, as in Eq. (3.53).

   $$\text{eb}(t) = 40e^{-(10t-10)^2} + 40e^{-(10t-30)^2} + 32e^{-(10t-45)^2} + 28e^{-(10t-70)^2} \tag{3.53}$$

   Contaminated EEG signal can be obtained by adding the EEG dataset $s(t)$ with synthetic eyeblink artifacts, as in Eq. (3.54).

   $$\mathbf{X(t)} = \mathbf{eb(t)} + \mathbf{s(t)} \tag{3.54}$$

3. The second multidimensional data set, $\mathbf{Y(t)}$ is taken, with $\mathbf{Y(t)} = \mathbf{X(t-1)}$.
4. Mean removed signals, $\hat{\mathbf{X}}(t)$ in Fig. 3.4 and $\hat{\mathbf{Y}}(t)$ in Fig. 3.5 are obtained by removing the respective mean from $\mathbf{X(t)}$ and $\mathbf{Y(t)}$.

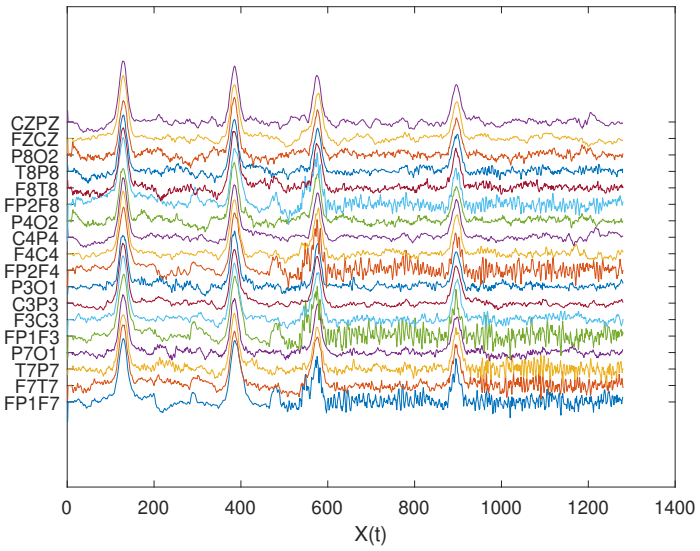

FIGURE 3.4 – First multidimensional data set, $\hat{\mathbf{X}}(t)$

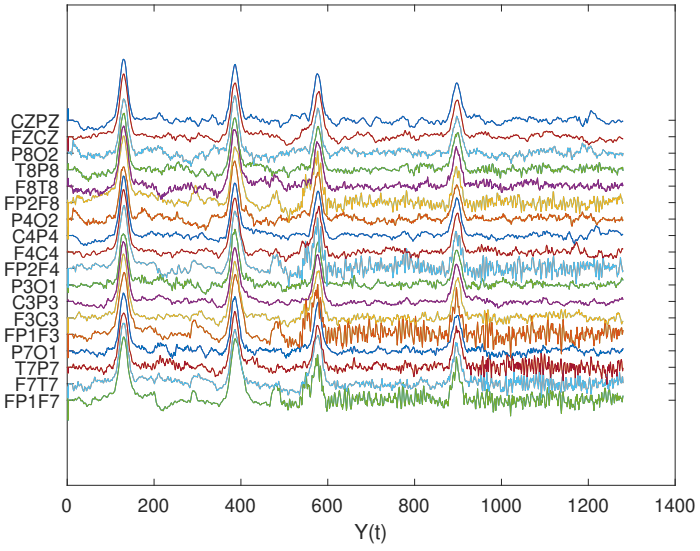

FIGURE 3.5 – Second multidimensional data set, $\hat{\mathbf{Y}}(t)$

5. Next, the weighted de-mixing matrices are estimated using approaches discussed in subsections 3.6.1, 3.6.2.1 and 3.6.2.2.

6. Canonical variates $\mathbf{U}$ are computed by projecting the estimated de-mixing weight matrix $\mathbf{A}$ onto the mean removed signal $\hat{\mathbf{X}}$ as in Eq. (3.26). The resulting canonical variate $\mathbf{U}$, is shown in Fig. 3.6.

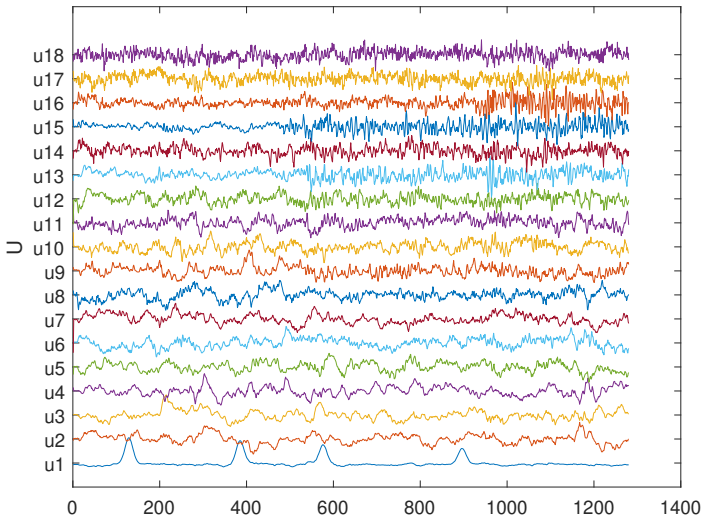

FIGURE 3.6 – Canonical components of $\hat{\mathbf{X}}$

7. The eyeblink artifact components are well distinguished from the neural components as they behave as the least cross-correlated components among the canonical variate vectors. This row of canonical components are excluded out by forcing it to become zero in order for it to behave non-artifactual, $\mathbf{U}_{\text{clean}}$ as shown in Fig. 3.7.

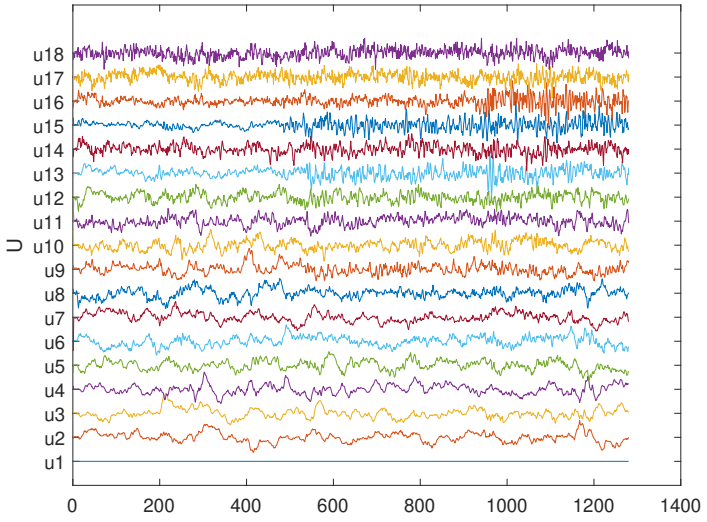

FIGURE 3.7 – Non-artifactual Canonical components

3.6.3.2/ RECONSTRUCTION OF CLEAN EEG SIGNAL

Clean EEG signal that is free from artifacts can be reconstructed by taking the inverse of de-mixing matrix, $\mathbf{A}^{-1}$, into the non-artifactual canonical components, $\mathbf{U}_{\text{clean}}$:

$$\mathbf{X}_{\text{clean}} = \mathbf{A}^{-1}\mathbf{U}_{\text{clean}} \tag{3.55}$$

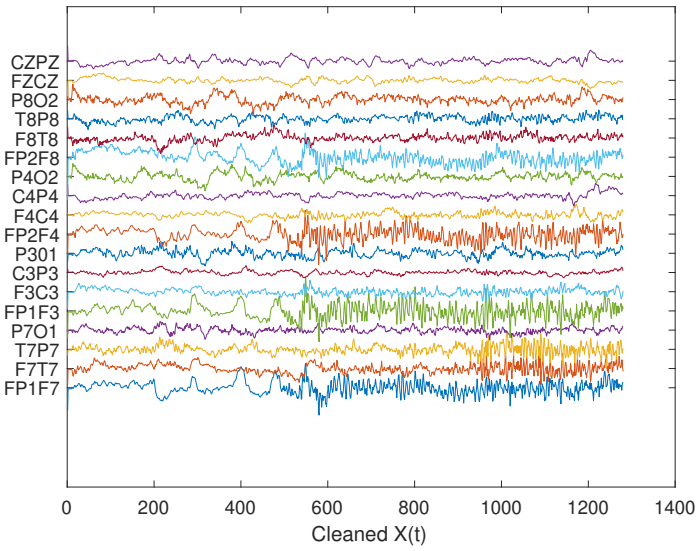

FIGURE 3.8 – Artifact-free EEG dataset

3.6.4/ PERFORMANCE ANALYSIS ON DECOMPOSITION TECHNIQUES IN CCA WITH REAL EEG SIGNALS

All three decomposition techniques, Eigen decomposition, QR-SVD and SVD in estimating the de-mixing matrices in CCA are evaluated on EEG signals before and after artifactual component elimination. This evaluation is necessary to determine which of these three decomposition techniques are most appropriate and effective in estimating weighted de-mixing matrices for CCA, thus making it reliable to be used in the proposed eyeblink artifact removal algorithm.

The evaluation is carried out on clean EEG signals of 5 randomly selected subjects, each with 5 seconds of length. These clean EEG signals are added with synthetically created eyeblink artifacts from Eq. (3.53) to obtain 5 seconds length of contaminated EEG signals. Contaminated EEG datasets are subjected to artifact elimination through CCA, with three matrix decomposition techniques discussed in subsections 3.6.1, 3.6.2.1 and 3.6.2.2. The performance of these matrix decomposition techniques within CCA in retaining the neural information of the EEG signals is verified through correlation coefficient (CC) and root mean square error (RMSE) values from Eq. (3.56) and (3.57) respectively :

$$\text{CC} = \frac{C_{X_{\text{in}},X_{\text{out}}}}{\sigma_{X_{\text{in}}} * \sigma_{X_{\text{out}}}} \tag{3.56}$$

$$\text{RMSE} = \sqrt{\frac{\sum_{t=1}^{n}(X_{\text{in}}(t) - X_{\text{out}}(t))^2}{n}} \tag{3.57}$$

where $C_{X_{\text{in}},X_{\text{out}}}$ is the covariance between clean EEG signal, X_{in}, and reconstructed EEG signal after eyeblink artifact elimination, X_{out}. $\sigma_{X_{\text{in}}}$ and $\sigma_{X_{\text{out}}}$ are the standard deviations of these signals, and n is the number of sample points of the EEG signal.

3.7/ Preliminary Results and Discussion

3.7.1/ Comparison of Envelope Interpolation Techniques in EMD for Eyeblink Aryifact Removal

The results obtained for EMD applied on 100 trials of synthetically contaminated EEG signals are tabulated in Table 3.1.

TABLE 3.1 – Performance metrics of CSI, CHSI and ASI on 100 Trials

Interpolation Technique	**CSI**	**CHSI**	**ASI**
RMSE (100 Trials)	5.6028	4.5503	**3.318**
PRD (%) (100 Trials)	82.0216	70.0675	**43.5816**
SNR-Before(dB) (100 Trials)	-9.8427	-9.8427	-9.8427
SNR-After (dB) (100 Trials)	3.1014	5.1581	**8.4794**
Correlation Coefficient (100 Trials)	0.7518	0.8077	**0.9063**
Computation Time (s) (100 Trials)	0.32	0.28	**0.24**

Fig. 3.9, 3.10 and 3.11 depict the recovered EEG signal and eyeblink artifact from EMD via CSI, CHSI and ASI respectively.

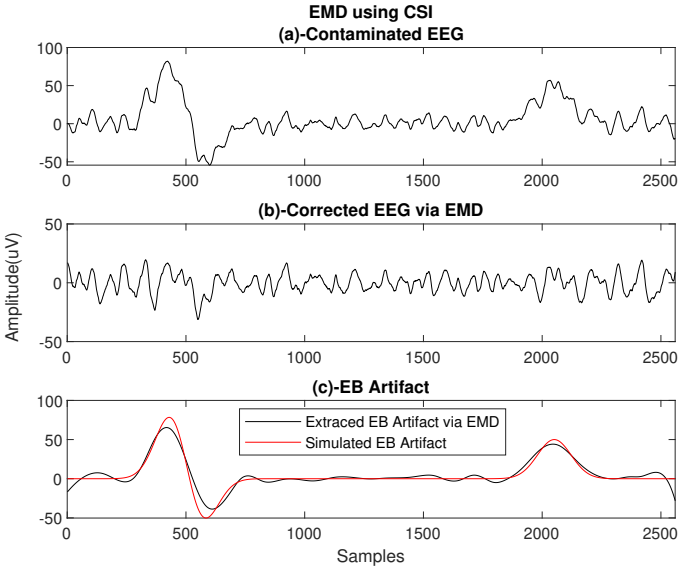

FIGURE 3.9 – (a) Mixed EEG and Eyeblink Signal, (b) Recovered EEG Signal from EMD, (c) Extracted Eyeblink Artifact from EMD-CSI

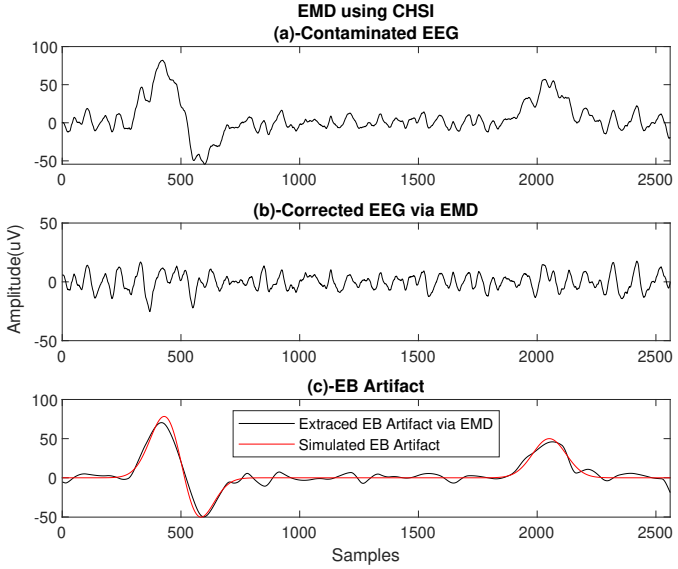

FIGURE 3.10 – (a) Mixed EEG and Eyeblink Signal, (b) Recovered EEG Signal from EMD, (c) Extracted Eyeblink Artifact from EMD-CHSI

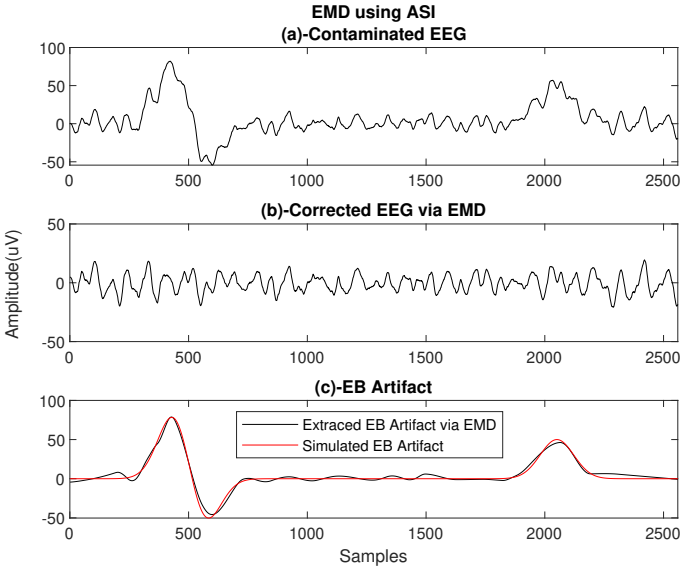

FIGURE 3.11 – (a) Mixed EEG and Eyeblink Signal, (b) Recovered EEG Signal from EMD, (c) Extracted Eyeblink Artifact from EMD-ASI

The RMSE obtained for these three interpolation techniques are tabulated in Table 3.1. In this analysis, the ASI has produced an average error of 27% lower than CHSI and 41% lower compared to the conventional CSI. As discussed earlier, a smaller RMSE value indicates higher accuracy between the original eyeblink artifact and the extracted eyeblink artifact via EMD. The PRD value when using ASI is 38% lower than the CHSI and 44% lower than the CSI. This result demonstrates that ASI produces the least distortion in reconstruction among the three interpolation techniques. The average correlation coefficient is obtained between the original EEG signal and the recovered EEG signal after eyeblink artifact removal through EMD for 100 trials. The use of ASI within the EMD algorithm has led to the highest correlation coefficient in comparison with the other two interpolation techniques. From Table 3.1, ASI for EMD yields 63% higher SNR on average compared to the CSI technique.

RMSE, PRD, SNR and correlation coefficient suggest that EMD algorithm with ASI will help to ensure higher decomposition accuracy and a better option for eyeblink artifact template extraction. These results justify that the ASI technique serves a lower computational burden to EMD algorithm with higher reconstruction accuracy in shorter computation time. Envelope construction through CSI fulfills second-order derivation at every extremum point to ensure continuity and spline curvature smoothness. Since envelope construction through CSI forces two adjacent splines to be continuous at first and second derivatives, the formed envelopes are susceptible to overshoots and undershoots. This produces an erroneous mean estimation during sifting and this error could eventually get transferred and added to the whole data set on every iteration of EMD's sifting process, resulting in an inaccurate and unreliable decomposition. Since the envelope construction of ASI is determined based only on the slopes of adjacent segments with continuity only up to the first-order derivative, ASI produces envelopes that are not as smooth as the CSI but results in better decomposition accuracy. This also reduces the necessity to solve large system equations which in turn, reduces the computation time as indicated by the results.

3.7.2/ Comparison of Decomposition Techniques in CCA for Eyeblink Aryifact Removal

The average CC , average RMSE and computation time of 5 EEG signals on all channels are tabulated in Table 3.2.

TABLE 3.2 – Average CC, RMSE and Time for Implementation of CCA through Eigendecomposition, QR-SVD and SVD

	Average CC			**Average RMSE**			**Average Time (s)**		
Channels	**Eigen**	**QR-SVD**	**SVD**	**Eigen**	**QR-SVD**	**SVD**	**Eigen**	**QR-SVD**	**SVD**
Fp1	0.9597	0.9597	**0.9609**	1.5284	1.5199	**1.4998**	**0.2265**	0.2384	0.3268
F3	0.9347	0.9347	**0.9353**	1.3800	1.3833	**1.3742**			
C3	0.9312	0.9312	**0.9329**	1.4278	1.4257	**1.4081**			
F7	0.9264	0.9264	**0.9269**	1.3856	1.3877	**1.3796**			
Fz	0.9564	0.9564	**0.9582**	1.5914	1.5772	**1.5508**			
Fp2	0.9634	0.9634	**0.9642**	1.4883	1.4796	**1.4629**			
F4	0.9528	0.9528	**0.9536**	1.4819	1.4817	**1.4661**			
C4	0.9315	0.9315	**0.9326**	1.3964	1.3952	**1.3865**			
F8	0.9515	0.9515	**0.9521**	1.4013	1.4002	**1.3872**			
Cz	0.9170	0.9170	**0.9177**	1.3514	1.3529	**1.3449**			
Pz	0.9293	0.9293	**0.9299**	1.3433	1.3449	**1.3348**			
A2A1	0.9258	0.9258	**0.9274**	1.4003	1.3969	**1.3848**			

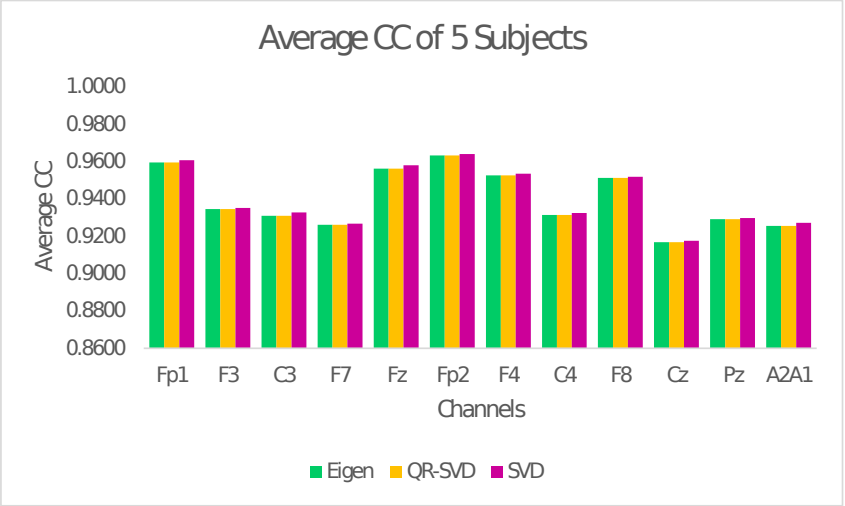

FIGURE 3.12 – Comparison of Average CC for Implementation of CCA through Eigendecomposition, QR-SVD and SVD

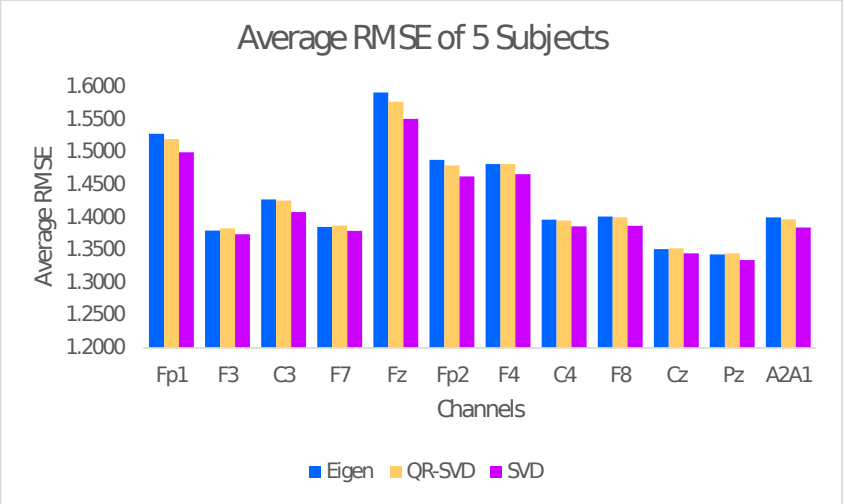

FIGURE 3.13 – Comparison of Average RMSE for Implementation of CCA through Eigen-decomposition, QR-SVD and SVD

The correlation coefficient (CC) is used to measure the resemblance of reconstructed EEG signal with the clean EEG signal after artifact elimination. The root mean square error (RMSE), on the other hand, measures the reconstruction error between clean and reconstructed EEG signals. The ideal expectation is to have the reconstructed EEG signals with zero distortion after artifactual components are eliminated, whereby CC should be 1 and RMSE should be 0. In reality, neural information loss during artifact correction is inevitable. However, the loss of neural information can be minimized through enhancements made to the artifact removal algorithms. The effectiveness of the three matrix decomposition techniques within CCA in preserving underlying EEG can be interpreted when CC value approaches 1 and RMSE value close to 0.

From Table 3.2, CCA implementation through Eigen decomposition and QR-SVD produces similar CC values on all channels, while SVD produces slightly better CC values than Eigen decomposition and QR-SVD, but the difference is not significant as depicted in Fig. 3.12. In the worst-case scenario, the maximum CC difference among the three matrix decomposition techniques is on the C3 channel, which is by 0.19%. In terms of RMSE, CCA through SVD produces the least reconstruction error among the three decomposition techniques, followed by either QR-SVD or the Eigen decomposition as shown in Fig. 3.13. The maximum RMSE difference among these techniques is 2.55% on Fz channel. In general, the CC values range from 0.9170 to 0.9642, and the RMSE values range from 1.3348 to 1.5914 for all three decomposition techniques. The minimum CC is 0.9170 and maximum RMSE is 1.5914, denoting apparent loss of neural information along with artifactual component elimination. This is due to the distribution of some EEG information into the artifactual canonical components, which is then forced to become zero and removed during artifact elimination. Hence it is imperative to minimize the loss of neural information during the reconstruction of a clean EEG signal. This can be achieved if CCA is used for artifact removal only on artifact occurring locations. Another way to minimize neural information loss is by incorporating a sliding window approach in CCA implementation.

3.8/ SUMMARY

In this chapter, three interpolation techniques in EMD and three matrix decomposition techniques in CCA are investigated to remove eyeblink artifacts from contaminated EEG signals. Based on the discussion above, it can be concluded that all three interpolation techniques in EMD are able to remove eyeblink artifacts reliably. The results have revealed that EMD with ASI performs better in removing eyeblink artifacts, but slow time. Therefore, further modification of the EMD algorithm is required to improve the computation time. This is to ensure the EMD algorithm can be used for real-time eyeblink artifact removal in EEG applications. On the other hand, matrix decomposition techniques in CCA has revealed that CCA implementation through SVD is better compared to Eigen and QR-SVD. However, the reconstruction differences among them are very less, which means they perform almost alike. Hence, any of these three techniques can be used as a reliable decomposition technique to estimate the weighted de-mixing matrices of CCA. The execution time of SVD is slightly longer, about 0.33s on average. Considering the the requirement of faster computation time for a real-time application, either eigen or QR-SVD technique can be used in CCA implementation for eyeblink artifact removal.

4

Proposed Techniques and Methodology

This chapter is divided into several sections. First, a new algorithm, (eADA), to automatically identify eyeblink artifacts with adaptable and varying threshold values, without any supervision on the EEG signal is proposed. The idea behind designing an eyeblink artifact detection algorithm is to assist the subsequent artifact removal algorithm. The eyeblink artifacts contaminate the EEG signal at random points of the EEG signal, which tantamount to a very short period in time compared to the entire length of the EEG signal. The artifact correction algorithm does not have to work on long EEG segments if accurate locations of the eyeblink artifacts are identified in advance. Consequently, distortion to the artifact-free segments of the EEG signal can be avoided.

Several modifications to the classical EMD algorithm are proposed to resolve the processing time inefficiency of the algorithm, which will be discussed in the second section. The combination of eADA, modified EMD and CCA is proposed, producing FastEMD-CCA^2 which can be used to remove eyeblink artifacts in online applications.

Thirdly, an algorithm that combines eADA and CCA, FastCCA, is proposed to remove eyeblink artifacts from EEG signals for online applications. In this algorithm, the need to use EMD is eliminated, so it is a viable solution as well for applications requiring online removal of eyeblink artifacts.

4.1/ EEG Recording/Simulation and Analysis

4.1.1/ Synthetic Signals

Synthetic eyeblink and EEG signals are simulated for validation purpose in MATLAB 2018b. Synthetic eyeblink artifacts, $Z(t)$ can be simulated through exponential functions with different amplitudes :

$$Z(t) = 15e^{-(10t-5)^2} + 15e^{-(10t-30)^2} + 10e^{-(10t-60)^2} + 12e^{-(10t-85)^2} \tag{4.1}$$

On the other hand, a synthetic EEG signal can be generated through pinknoise, $Y(t)$ for a duration of 10 seconds, 2560 sample points at a sampling frequency of 256 Hz. EEG and eyeblink artifact models simulated through pinknoise and exponential function are shown in Fig. 4.1(a) and 4.1(b) respectively. Both synthetic EEG signal and eyeblink artifact are

mixed together to acquire a set of synthetically contaminated EEG signal, $X(t)$ as in Fig. 4.1(c).

$$X(t) = Z(t) + Y(t) \tag{4.2}$$

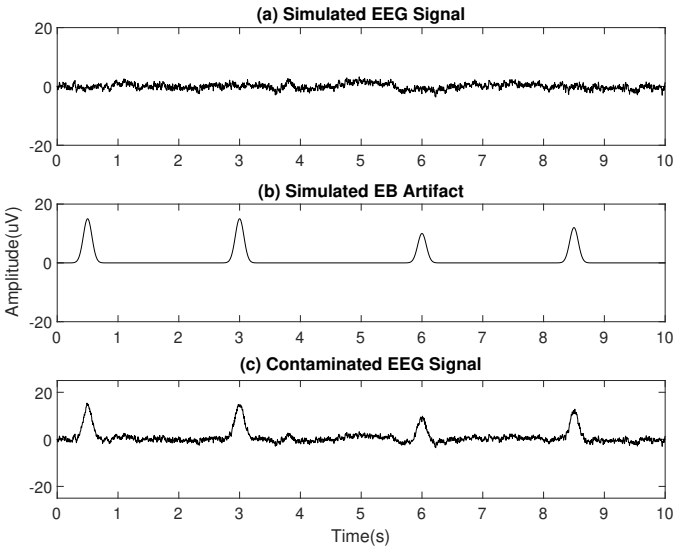

FIGURE 4.1 – (a) Synthetic EEG Signal, (b) Synthetic Eyeblink Artifact, (c) Contaminated EEG Signal

The synthetic EEG signals and the eyeblink artifact models differ from synthetic signals generated in section 3.3.3, Chapter 3. The parameters chosen in generating the synthetic signals differ as well, i.e., the amplitudes of the eyeblink artifacts generated through exponential functions. This difference is to indicate different means of generating synthetic signals, as well as to demonstrate that the algorithms will be able to remove artifacts from these synthetic signals regardless of the nature of their modelling.

4.1.2/ REAL SIGNALS

4.1.2.1/ HITACHI DATASET

The EEG dataset that is used for evaluation in this thesis were collected at Hitachi, Hatayoma site in Japan. EEG signals from volunteers were obtained according to the regulations of the internal review board on Central Research Laboratory, Hitachi, Ltd., following receipt of written informed consent. The approval number is 20131021-0138. These EEG signals have been primarily collected to conduct a study on mental stress. Since all recorded signals were contaminated by eyeblink artifacts, the dataset is appropriate for use in this research. These EEG signals are recorded using 14 free electrodes placed on the scalp following the 10-20 system. The EEG signals were collected from 10 participants with 6 recordings from each participant, resulting in 60 EEG signals. The participants are aged between 30 and 55 years. All recorded signals are of different durations, which were recorded at a sampling rate of 256 Hz. This EEG dataset is mainly used to verify various

techniques and algorithms discussed and proposed throughout the thesis. The total number of eyeblink artifacts found in this dataset are more than 5600, which were identified through manual inspection. The number of eyeblink artifacts contaminating each of the EEG signal varies, ranging from 20 to 172 occurrences.

4.1.2.2/ Public Dataset (INV-SK)

Apart from the Hitachi dataset collected, a publicly available EEG dataset which contains involuntary eyeblinks were used, which was collected through an experiment by Kanoga et al. [128]. These EEG signals are recorded using 14 electrodes, following the 10-20 system. This dataset consists of EEG signals from 20 participants, with 3 recordings from each participant, resulting in 60 EEG signals. The participation in the study was approved by the Research Ethics Committee of Keio University, Japan. All recorded signals are of different durations, which were recorded at a sampling rate of 256 Hz. This EEG dataset is used as an additional dataset for validation purpose. The total number of eyeblink artifacts found in this dataset are more than 4600, which were identified through manual inspection. The number of eyeblink artifacts contaminating each of the EEG signal varies, ranging from 5 to 200 occurrences.

4.2/ Proposed Eyeblink Artifact Detection Algorithm (eADA)

4.2.1/ Determination of EEG Segments with Eyeblink Artifacts

In an EEG signal, the eyeblink artifacts are primarily captured in the frontal electrodes, Fp1 and Fp2. This is because the frontal electrodes are in close proximity with the eyes. Another logical point to note here is, both eyes of any individual blink simultaneously. Hence, the correlation between the Fp1 channel and the Fp2 channel is expected to be high whenever eyes blink, which can be confirmed with correlation analysis. The correlation analysis is a method to statistically evaluate the relationship of two continuous variables. In EEG signal, the correlation between Fp1 and Fp2 signals are thus defined as a similarity index between these two signals, stated in Eq. (4.3) :

$$\text{Correlation Coefficient} = \frac{C_{Fp1,Fp2}}{\sigma_{\text{Fp1}} * \sigma_{\text{Fp2}}} \tag{4.3}$$

where $C_{Fp1,Fp2}$ is the covariance between segments of Fp1 and Fp2, σ_{Fp1} and σ_{Fp2} are the standard deviations of Fp1 and Fp2 respectively.

To validate the hypothesis, where the correlation of Fp1 and Fp2 channels will be high whenever eyes blink, the correlation between Fp1 and Fp2 channels of an EEG signal is computed in segments of 500 sample points ($\tilde{1}$.95 seconds) per segment, on 30 EEG signals. This window size is chosen so that at least one eyeblink artifact can be captured in this window. Fig. 4.2 shows an example of Fp1 and Fp2 recordings and their corresponding correlation coefficient values in each segment.

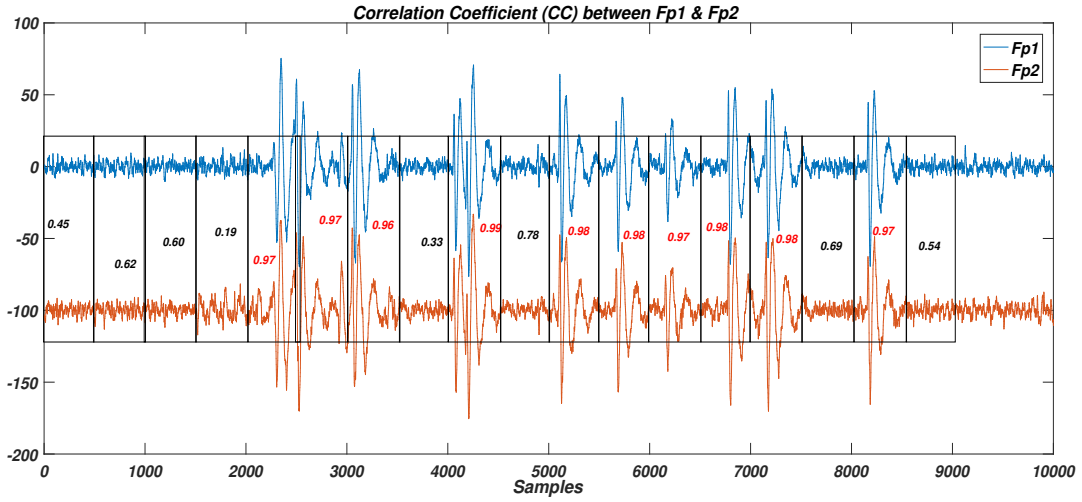

FIGURE 4.2 – Correlation Coefficient, CC, between Fp1 and Fp2 Electrodes

The test has revealed that segments of Fp1 and Fp2 without eyeblink artifact produce a correlation below than 0.7. This lower correlation may be due to the difference in neurological activity in the frontal region, which produces lesser similarity between Fp1 and Fp2 channels. Whereas segments containing eyeblink artifact results in higher correlation, usually more than 0.9. This is because, when the eyes blink, the electrical potentials generated around the eyes are very high, which can be easily captured by the Fp1 and Fp2 electrodes, hence producing a higher correlation between Fp1 and Fp2 channels during blinking. Thus, the existence of eyeblink artifact in a particular segment or window can be easily found, by the high correlation coefficient value of more than 0.9, which proves the hypothesis. So, the correlation coefficient value of 0.9 is set to indicate the presence of an eyeblink artifact in a particular window while designing the automatic eyeblink artifact detection algorithm.

Following this, segments of the EEG signal contaminated with eyeblink artifacts are identified. However, a threshold value is required to determine the eyeblink artifact potentials and the starting point of the eyeblink artifacts, for subsequent analysis or artifact removal. Subsection 4.2.2 will discuss on the automated calculation of the threshold level for every window identified to contain an eyeblink artifact.

4.2.2/ AUTOMATIC THRESHOLDING TO IDENTIFY EYEBLINK ARTIFACT COMPONENTS

The unsupervised and automatic artifact detection algorithm requires a threshold to determine the starting point of an eyeblink artifact. Displacement or deviation of amplitude from the mean is chosen as a threshold criterion to classify the onset of an eyeblink artifact. The displacement of amplitude is chosen as the threshold criterion because eyeblink artifacts are, in general, higher in amplitude relative to that of the EEG or brain signal. Therefore, the eyeblink artifact components are expected to produce higher amplitude displacement compared to uncontaminated EEG potentials. First, the amplitude displacement from the mean is calculated within an Fp1 window that exhibits a high correlation

with Fp2, as illustrated in subsection 4.2.1 using Eq. (4.4) :

$$\text{Displacement}[t] = |[X[t] - \mu]|. \tag{4.4}$$

$X[t]$ is the EEG signal's amplitude at time t, and for any given window starting at sample point n, $X[t]$ is evaluated from $t = n$ to $t = n + 500$, and μ is the mean of that particular window.

4.2.2.1/ Classification of EEG potentials and Eyeblink Artifact Components

An experiment is conducted to define the classification criterion to classify EEG potentials and eyeblink artifacts using varying threshold levels. From the displacement distribution, mean (μ) and standard deviation (σ) are acquired.

Fig. 4.3 shows an example of displacement distribution by setting the threshold value to be any displacement value beyond 1σ from the mean, while Fig. 4.4 shows the identified eyeblink artifacts (plotted in red) when the threshold is set beyond 1σ.

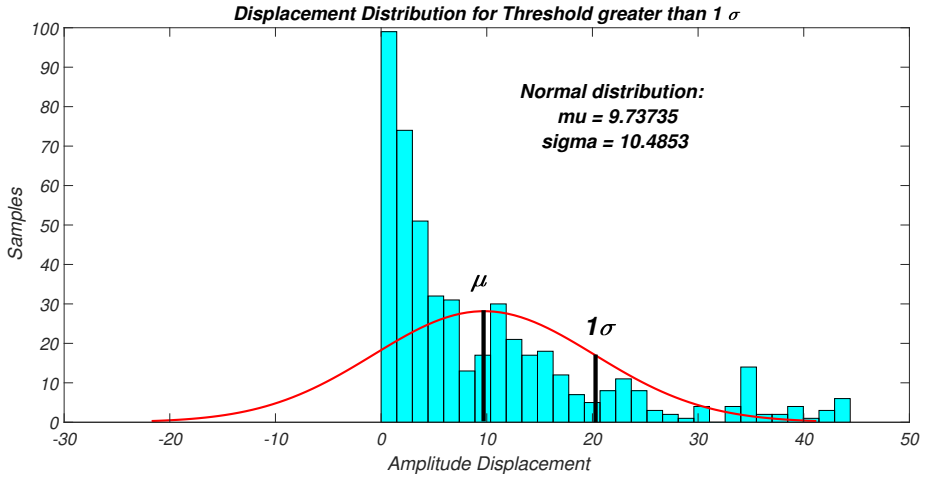

FIGURE 4.3 – Displacement Distribution for Threshold Greater Than 1σ

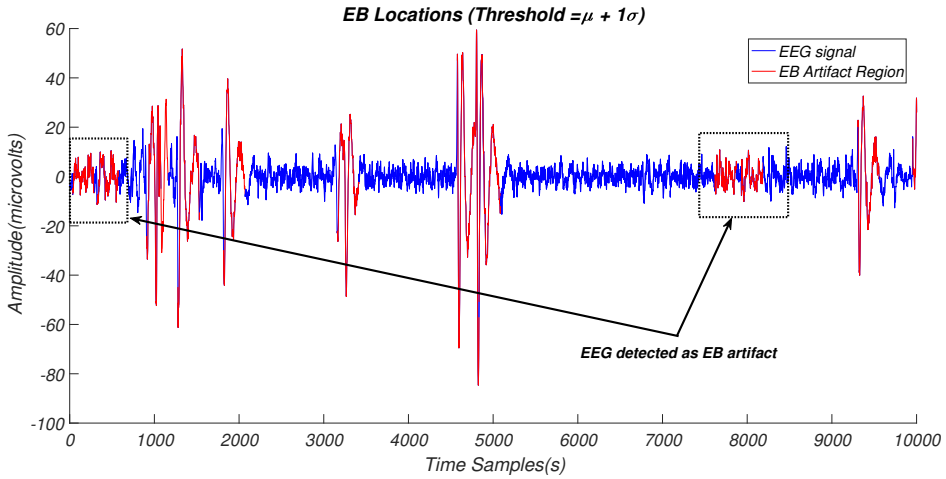

FIGURE 4.4 – Sample Points of Identified Eyeblink Artifacts for Threshold Greater Than 1σ

From Fig. 4.4, it can be seen that some of the EEG potentials are identified as eyeblink artifacts when the threshold is set beyond 1σ from the mean.

Fig. 4.5 shows the displacement distribution of the same segment by setting the threshold value to be any displacement value beyond 2σ from the mean, while Fig. 4.6 shows the identified eyeblink artifacts (plotted in red) when the threshold is set beyond 2σ.

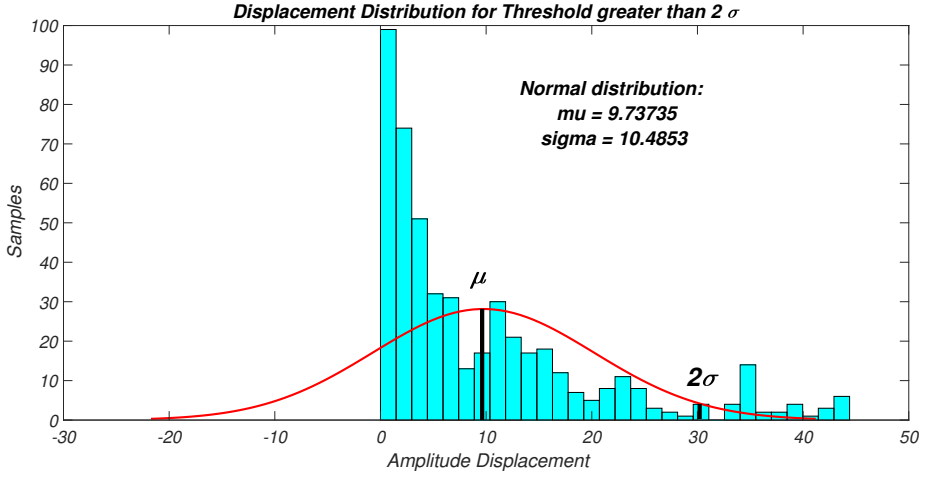

FIGURE 4.5 – Displacement Distribution for Threshold Greater Than 2σ

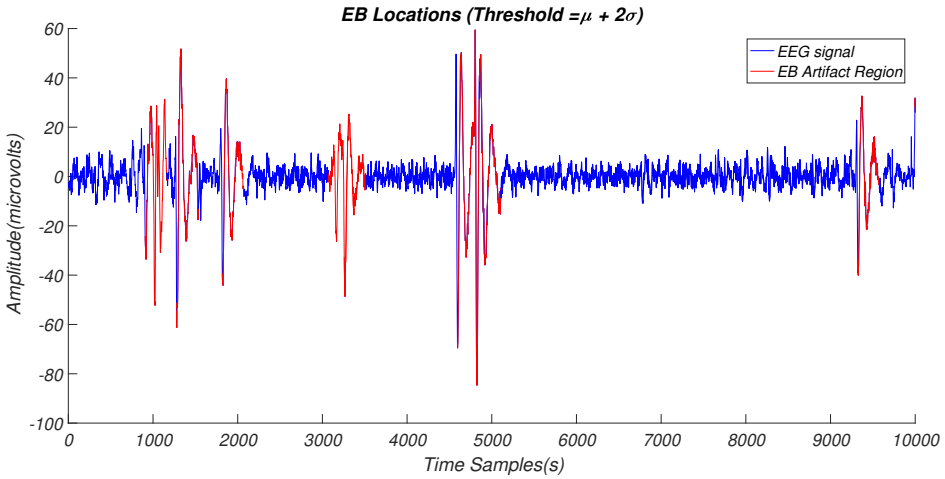

FIGURE 4.6 – Sample Points of Identified Eyeblink Artifacts for Threshold Greater Than 2σ

From Fig. 4.6, it can be seen that all eyeblink artifacts are identified as eyeblink artifacts when the threshold is set beyond 2σ from the mean, while no EEG potential is identified as eyeblink artifacts.

Fig. 4.7 shows the same displacement distribution by setting the threshold value to be any displacement value beyond 3σ from the mean, while Fig. 4.8 shows eyeblink artifacts plotted when threshold is set beyond 3σ.

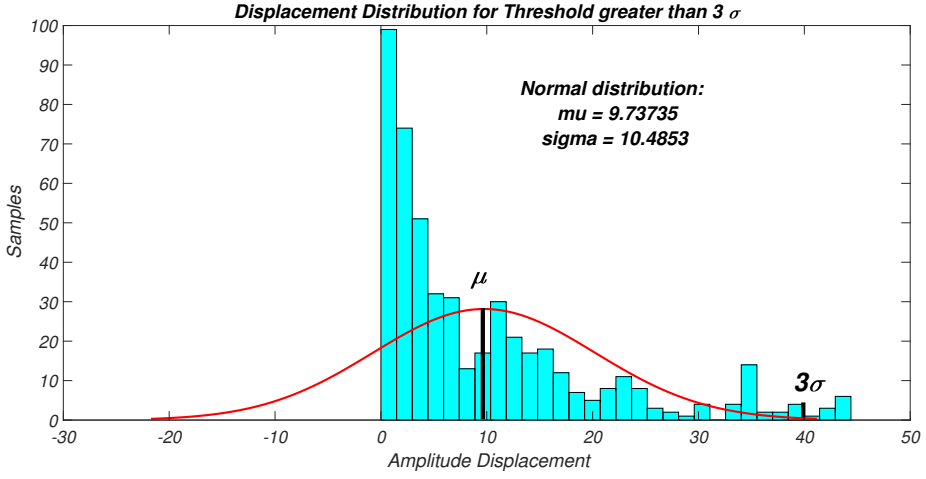

FIGURE 4.7 – Displacement Distribution for Threshold Greater Than 3σ

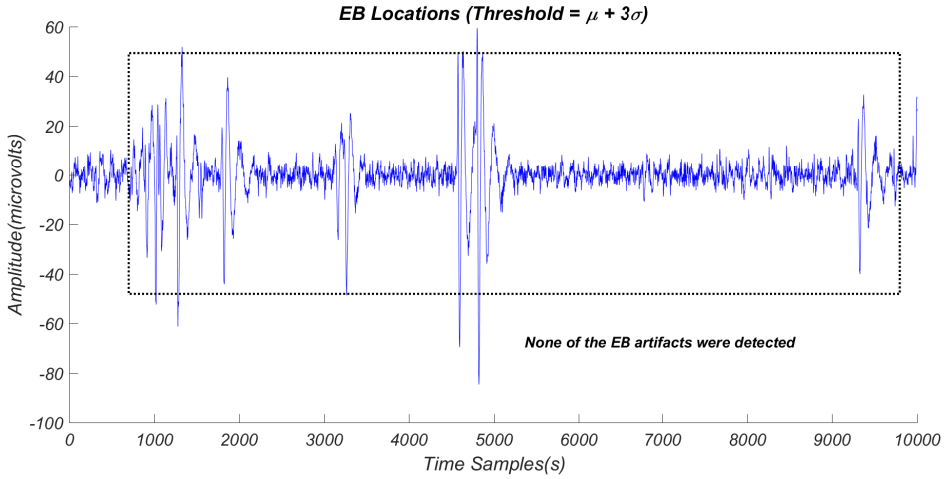

FIGURE 4.8 – Sample Points of Identified Eyeblink Artifacts for Threshold Greater Than 3σ

From Fig. 4.8, it can be seen that none of the eyeblink artifacts were identified as eyeblink artifacts when the threshold is set beyond 3σ from the mean.

The average accuracy level for 60 EEG signals from section 4.1.2.1, with thresholds greater than 1σ, 2σ and 3σ from the mean of the displacement distribution is tabulated in Table 4.1.

TABLE 4.1 – Average Accuracy in Eyeblink Artifact Detection with Different Thresholds

Average (60 EEG Signals)			
Threshold	μ **+ 1**σ	μ **+ 2**σ	μ **+ 3**σ
Accuracy	95.8%	**99.47%**	57.17%

From the experimental result, the onset point of an eyeblink artifact and eyeblink artifact potentials can be correctly determined by taking two standard deviations, 2σ width from the mean of the displacement distribution acquired, as in Eq. (4.5) :

$$\text{threshold} = \mu + 2\sigma. \tag{4.5}$$

Any absolute value beyond 2σ is classified as an eyeblink artifact potential and the first sample point that exceeds this threshold is considered as the eyeblink artifact's onset point.

In the algorithm, the starting point of the frame is moved 100 sample points (0.39 seconds) ahead from the onset of the eyeblink artifact. The reason for setting the starting point of the frame in advance of 100 sample points before the eyeblink artifact's onset is to provide a buffer for any subsequent analysis. The endpoint of the frame is then set to 256 sample points, or 1 second, after the onset of the eyeblink artifact. The eyeblink artifact frame is therefore taken to be from the starting point until the endpoint of the frame. Thus, an eyeblink that can last up to 0.8 seconds (205 sample points) in duration completely fit into this frame (100+256=356 sample points).

Fig. 4.9 summarizes the unsupervised eyeblink artifact detection (eADA) algorithm in a flowchart.

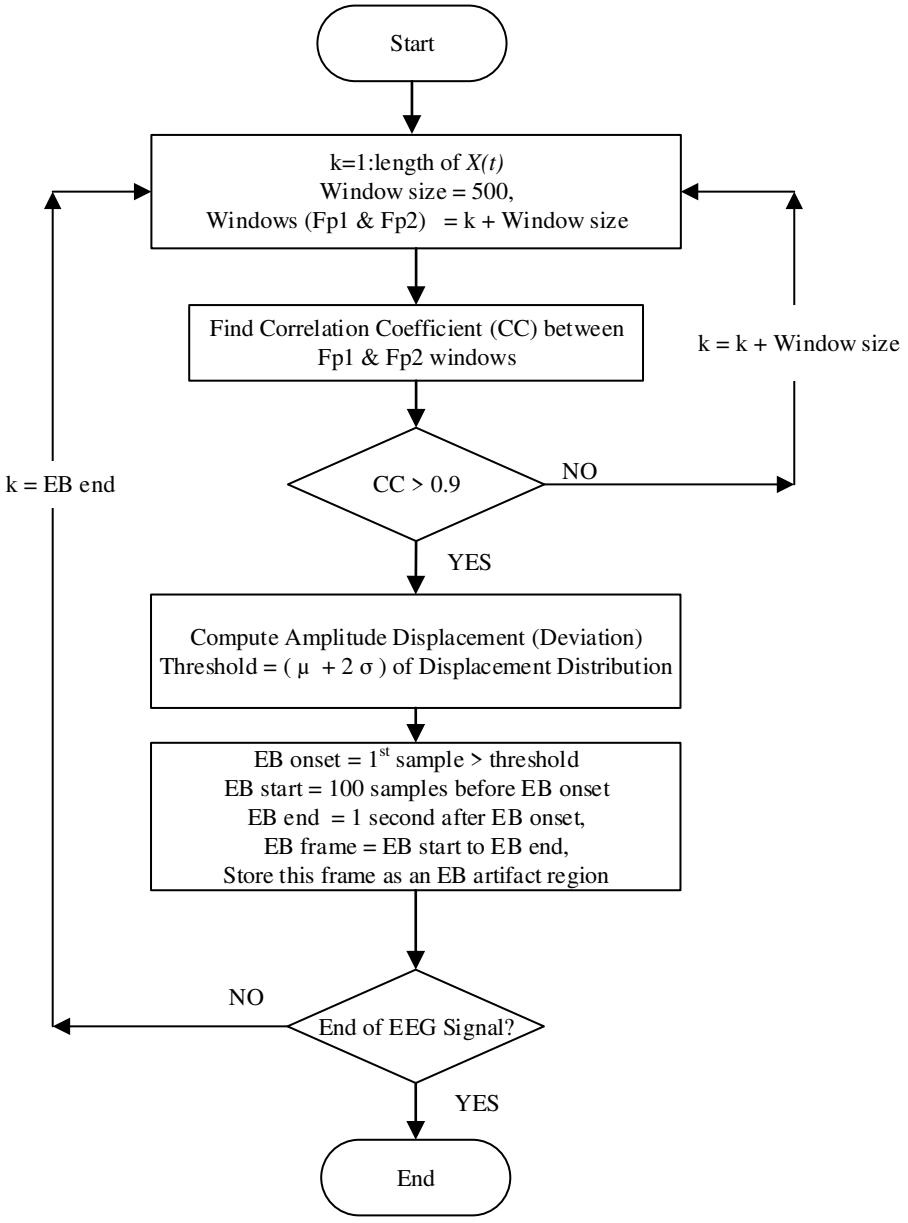

FIGURE 4.9 – Flowchart of the Unsupervised Eyeblink Artifact Detection Algorithm

4.3/ PROPOSED FASTEMD-CCA^2 FOR EYEBLINK ARTIFACT REMOVAL

4.3.1/ PROPOSED MODIFICATION TO CLASSICAL EMD : MODIFIED EMD (FASTEMD)

In online applications, classical EMD could cause the overall processing time to increase as the algorithm is iterative in nature. The existing classical EMD algorithm has to be

modified and its usage has to be reduced, such that it can be a feasible algorithm to be used in online applications. Some modifications to the classical EMD algorithm are proposed in this subsection to resolve the processing time inefficiency of the algorithm.

4.3.1.1/ Envelope Interpolation in FastEMD

A major concern in the sifting process of classical EMD is that it relies on how the upper and lower envelopes are being constructed through interpolation. In online applications, classical EMD could cause the overall processing time to increase as the algorithm is iterative and dependent on interpolating a large number of extrema. The interpolation within classical EMD would consume a lot of the computer resources, hence classical EMD can be inefficient when removing eyeblink artifacts from lengthy EEG signals, especially in applications requiring online processing.

The performance of classical EMD with other interpolation techniques were tested and evaluated as elaborated in Chapter 3. Among the alternative interpolation techniques investigated were the Cubic Hermite Spline Interpolation (CHSI), and the Akima Spline Interpolation (ASI). These two interpolation techniques were investigated in terms of their ability to retain the reconstruction accuracy after decomposition and their speed compared to Cubic spline interpolation (CSI), which is used in the classical EMD algorithm. The ASI has produced the highest correlation coefficient of 0.9063, lowest Root Mean Square Error (RMSE) of 3.3, and lowest percentage root means square difference (PRD) of 44%, better Signal to Noise Ratio (SNR) of 8.5dB and faster computation time of 0.24s, in decomposing an artificial EEG signal compared to CSI. These results justify that the ASI technique will serve a lower computational burden with shorter computation time within the FastEMD algorithm. Furthermore, its reconstruction accuracy is higher compared to the other two interpolation techniques.

4.3.1.2/ Stopping Criterion and Fixed Number of IMFs in FastEMD

Another factor that limits the usage of classical EMD in online applications is the repetitive sifting process required in obtaining the IMFs. Sifting in classical EMD algorithm can be classified as redundant in two aspects. First, the algorithm has to repeat sifting numerous times before any of the resulting trends satisfies the IMF criteria, and thus can be classified as an IMF. To overcome this issue, a stopping criterion for every IMF is used. The stopping criterion for IMFs is adopted from [156], which is based on a standard deviation computation. The standard deviation (SD) is defined as the normalized squared difference between two sifting iterations, which is assumed to indicate consistency between two sifting outputs and measures repetitiveness of the sifting outputs. The SD value is calculated from two consecutive sifting outputs, $y_j(t)$ and $y_{j-1}(t)$ as shown in Eq. (4.6) :

$$\mathrm{SD} = \sum_{t=0}^{k} \left[\frac{|y_{j-1}(t) - y_j(t)|^2}{y_{j-1}^2(t)} \right] \leq 0.2 \tag{4.6}$$

where k is the number of sample points in the original signal, $X(t)$. The SD value should be less than a pre-determined value, normally 0.2 or 0.3 to stop the sifting iteration in FastEMD.

Secondly, the algorithm has to reiterate itself multiple times to attain multiple numbers of such IMFs, because it can't terminate sifting until the residual signal becomes a monotonous function. Therefore, IMF extraction through repetitive sifting iterations causes the classical EMD algorithm to be computationally expensive. To overcome this issue, the number of IMFs extracted out through FastEMD is fixed to a constant number. The higher oscillations in the raw EEG signal will be isolated out in the first few IMFs, while the sum of remaining IMFs would by default produce an eyeblink artifact trend. Partially reconstructing the highly oscillating IMFs which are lower in amplitude would yield the EEG trend. Alternatively, low oscillating IMFs with high amplitudes are summed together to obtain the eyeblink artifact trend. Manual observation on IMFs produced by 30 EEG signals from the Hitachi dataset reveals that the clean EEG components are most often sifted out in the first two IMFs, while the remaining IMFs and the residual signal comprise the eyeblink artifact components. Therefore, the FastEMD algorithm is designed to decompose the raw EEG signal to up to 5 IMFs only, which is sufficient to segregate out the clean EEG signal and the eyeblink artifact trend. Consequently, this reduces the computation time, and the algorithm does not have to repeat itself to extract too many IMFs until a monotonic residue is acquired. However, IMFs corresponding to EEG and IMFs corresponding to eyeblink artifacts need to be selected for reconstruction purposes. This selection process can be automated with the help of CCA, which will be discussed in the following subsection.

4.3.1.3/ IMF Selection Through CCA for Eyeblink Template Extraction

Selection or classification of IMFs in FastEMD is required to categorize whether an IMF belongs to EEG or the eyeblink artifact, subsequently extracting out the eyeblink artifact template. This can be accomplished by subjecting the row vectors of IMFs to CCA. Fig. 4.10 shows the canonical variates obtained by applying CCA on the IMFs.

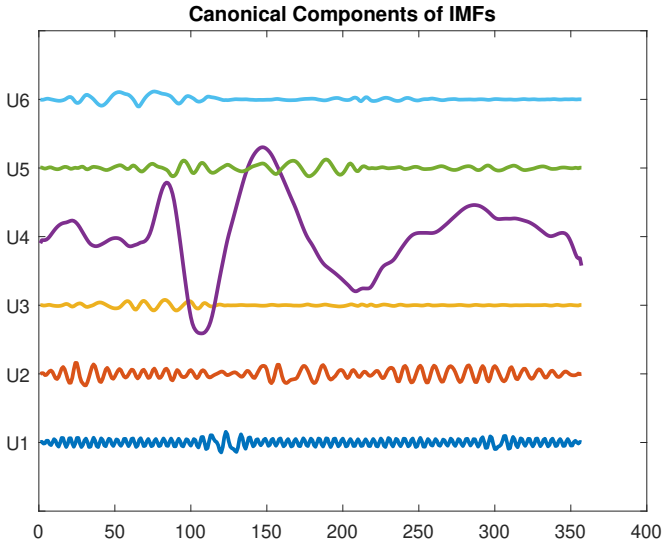

FIGURE 4.10 – Canonical Variates of the IMFs

The most pertinent artifactual canonical variate row is extracted out as the eyeblink artifact

template. The remaining canonical variates are non-artifactual sources, so they are used to reconstruct the clean EEG trend. The eyeblink artifact template and the clean EEG signal reconstructed using IMF's canonical components are shown in Fig. 4.11.

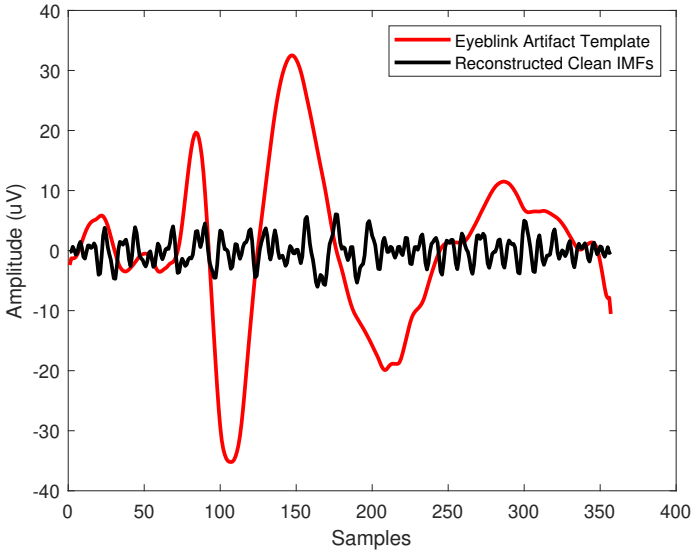

FIGURE 4.11 – Extracted Eyeblink Artifact Template and Reconstructed EEG Signal

An updated flowchart of FastEMD-CCA with modifications discussed above is shown in Fig. 4.12.

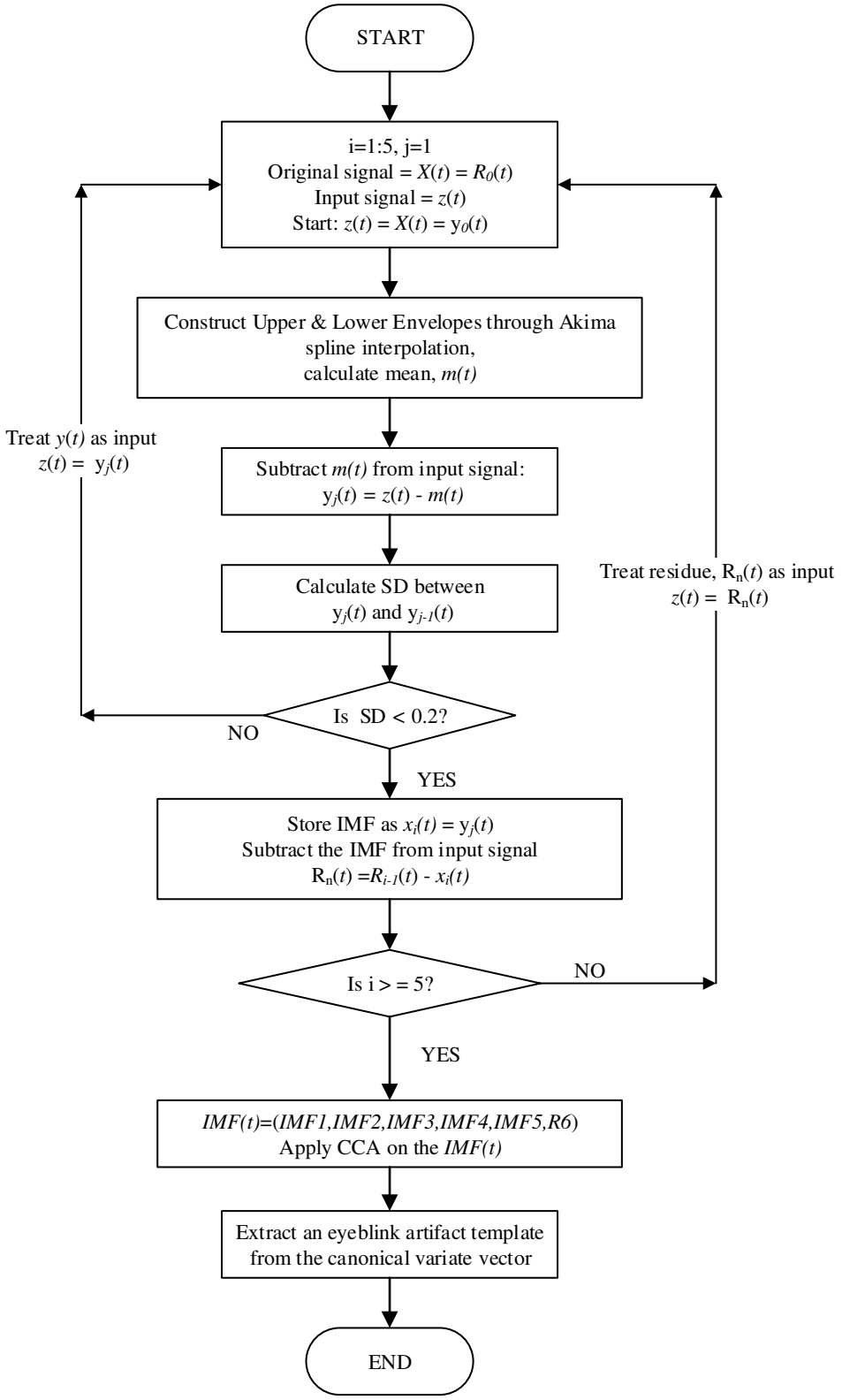

FIGURE 4.12 – Flowchart of FastEMD-CCA Algorithm

4.3.2/ Eyeblink Artifact Elimination

In the previous section, a general eyeblink artifact template is extracted. In this subsection, the extracted general eyeblink artifact template will be utilized further by CCA for eyeblink artifact elimination. So CCA is used, first in selecting the eyeblink artifact related IMFs after FastEMD application, and second in eliminating the remaining eyeblink artifacts that are present in an EEG signal. Thus the entire algorithm is named FastEMD-CCA^2 as CCA is used twice.

4.3.2.1/ Optimal Use of FastEMD with CCA for Online Applications

In applications that require online processing of EEG signals, the applications could not wait until the entire EEG signal is recorded for analysis, as it may take from a few hours to days for an EEG recording to be completed. Moreover, the eyeblink artifacts have to be removed as the EEG is being recorded. Generally, the classical EMD algorithm is not recommended to be used for artifact removal after the EEG recording is complete, as it may cause a delay in artifact correction and subsequent signal interpretation. Applying classical EMD on the entire EEG recording will also cause the desired application to get computationally heavy. As an option, classical EMD can be applied repetitively on short EEG segments to remove eyeblink artifacts, whenever eyeblink artifacts are captured, provided the occurrence of eyeblinks are known. Unfortunately, classical EMD gets computationally inefficient and slow on repetitive application to a huge EEG signal, especially during online recording and analysis, which may even cause disruption to the recording task.

To resolve this, the unsupervised eyeblink artifact detection algorithm (eADA) proposed in section 4.2 is utilized. Several eyeblink artifact regions are searched, identified and saved using eADA until two eyeblink artifact regions exhibit a correlation coefficient of more than 0.9. The correlation coefficient value of more than 0.9 is chosen assuming that a high correlation between the eyeblink artifact regions denotes repetitiveness or similarity in the blinking pattern of an individual, which can be assumed as a general eye blinking pattern for that particular EEG signal. The two eyeblink artifact regions with high cross-correlation are indicated with boxes in Fig. 4.13.

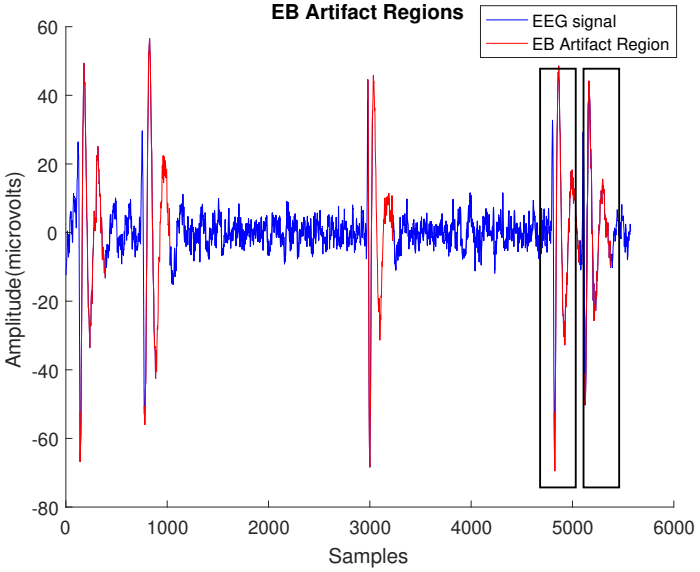

FIGURE 4.13 – Highly Correlating Eyeblink Artifact Regions Subjected to FastEMD

FastEMD is applied only on the latter eyeblink artifact region identified in Fig. 4.13 to extract out an eyeblink artifact template, thus keeping the number of FastEMD applications as low as possible. This prevents FastEMD to be used repetitively, especially when the EEG signal is processed in an online manner. This method is different compared to what is being practised in classical artifact removal technique through EMD, where classical EMD will be applied to remove the artifacts whenever an artifact event is identified. The IMFs obtained through FastEMD are subjected to CCA as illustrated in subsection 4.3.1.3 to extract out a general eyeblink artifact template. In this proposed technique, FastEMD and CCA serve just for an eyeblink pattern or template extraction to be utilized further by CCA again for artifact elimination. This eyeblink artifact template will serve as an artifact reference to remove every other eyeblink artifacts that contaminate the EEG signal.

4.3.2.2/ APPLICATION OF WINDOWED CCA FOR EYEBLINK ARTIFACT REMOVAL

Remaining eyeblink artifacts that are contaminating an EEG signal are removed with the help of the extracted eyeblink artifact template, assuming every other eyeblink artifacts within a subject exhibit consistent pattern with the template. A sliding window with the length of the extracted eyeblink artifact template is moved along the EEG signal and each EEG window is cross-correlated with the general eyeblink artifact template extracted, as in Eq. (4.7) :

$$\text{Cross-correlation} = \frac{C_{X(t),X_{\text{EB}}(t)}}{\sigma_{X(t)} * \sigma_{X_{\text{EB}}(t)}} \tag{4.7}$$

where $C_{X(t),X_{\text{EB}}(t)}$ is the covariance between the contaminated EEG signal, $X(t)$, and the eyeblink artifact template, $X_{\text{EB}}(t)$, while $\sigma_{X(t)}$ and $\sigma_{X_{\text{EB}}(t)}$ are the standard deviations of these signals.

Observations and validation on the real EEG signals illustrated in section 4.1.2.1 revealed that the correlation between the eyeblink artifact template and EEG windows contaminated with eyeblink artifacts often lies in the range of 0.4 to 0.6, so a correlation value of

more than 0.4 is used to indicate the presence of an eyeblink artifact. Hence, EEG windows that exhibit a similarity score of more than 0.4 with the eyeblink artifact template are confirmed as eyeblink artifacts, thus subjected to CCA for artifact removal. Removal of the eyeblink artifacts from the multichannel EEG signal relies on the elimination of the artifactual canonical components of CCA. First, CCA estimates the canonical components that maximize temporal correlation within the specified window. Then, the most pertinent artifactual canonical components, usually the the most cross-correlated canonical component (U_i, V_i), among the canonical variate vectors are forced to become zero in order for it to behave non-artifactual. The artifact-free canonical components are termed as U_{clean}. Finally, a clean EEG segment is reconstructed by projecting the inverse of the de-mixing matrix, A^{-1} into the non-artifactual source, U_{clean}, as explained in Chapter 3, section 3.6.3.2.

$$x(t)_{\text{clean}} = A^{-1} U_{\text{clean}}(t) \tag{4.8}$$

The flowchart of the proposed technique, FastEMD-CCA^2 is shown in Fig. 4.14.

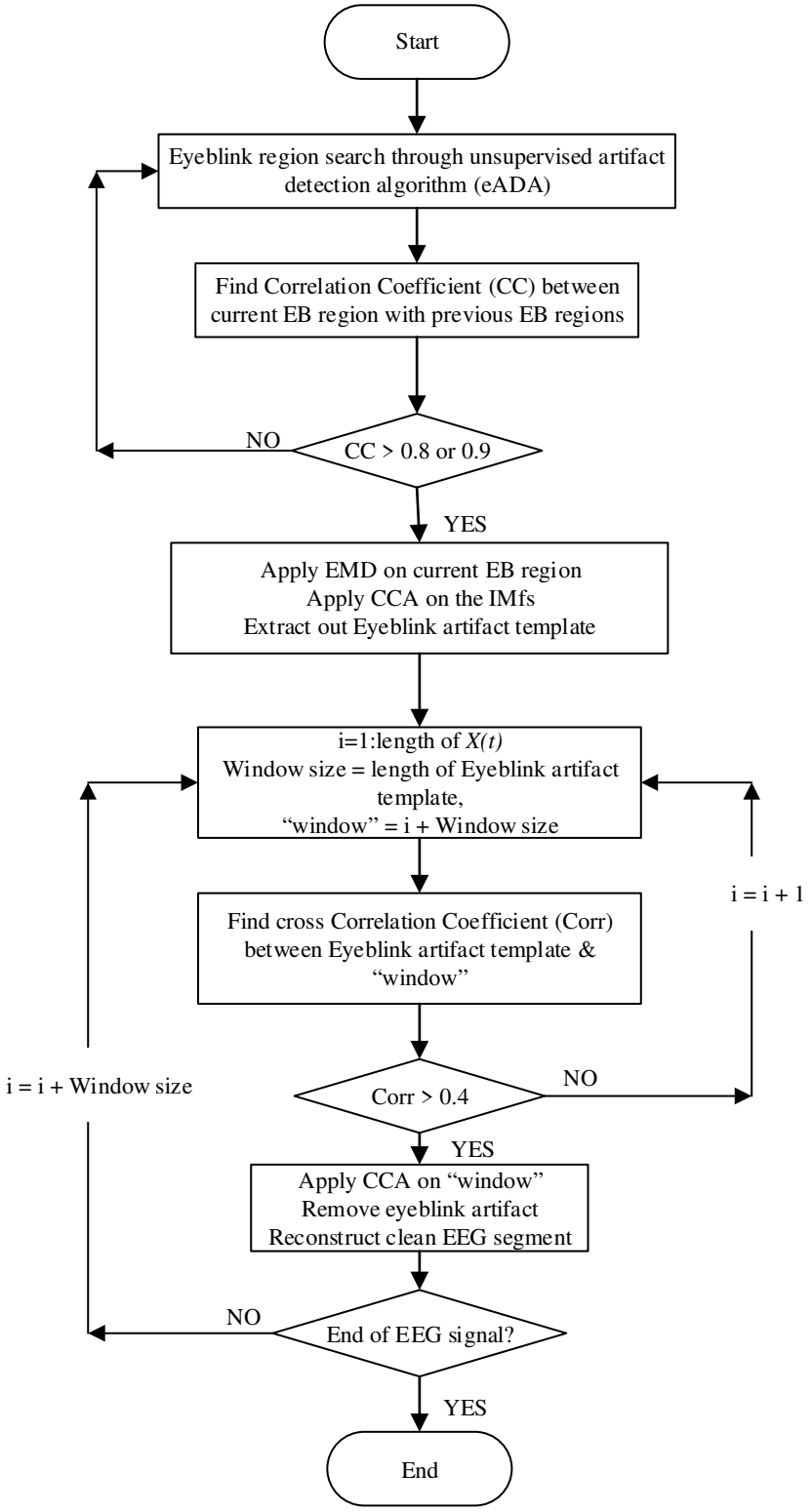

FIGURE 4.14 – Flowchart of the Proposed Technique FastEMD-CCA[2]

4.4/ PROPOSED FASTCCA FOR EYEBLINK ARTIFACT REMOVAL

FastEMD-CCA[2] is proposed and elaborated in section 4.3.1 for online removal of eyeblink artifacts from EEG signals. FastEMD-CCA[2] is a template matching approach, where the automated eyeblink artifact detection (eADA) mechanism is performed to identify relevant eyeblink artifact regions in Fp1 channel of an EEG signal, FastEMD with CCA is applied subsequently on the most relevant artifact region identified to extract out a general eyeblink template. Elimination of the remaining eyeblink artifacts from the entire multichannel EEG signal is then conducted through cross-correlation between EEG segments and the eyeblink artifact template, where EEG segments that are highly correlated with the eyeblink artifact template are subjected to CCA for artifact removal. Since an automatic eyeblink artifact detection (eADA) is already developed and it could accurately identify the eyeblink artifact locations, the performance of the proposed algorithm without dependency on the eyeblink artifact template to identify the eyeblink artifact locations is investigated.

Therefore, a second algorithm is proposed by combining eADA and CCA to develop FastCCA algorithm which is purely a correlation-based approach. In FastCCA, the unsupervised eyeblink artifact detection algorithm, eADA is performed in windows of about 1.95s on Fp1 and Fp2 EEG channels. Once an eyeblink artifact region is found on the Fp1 channel, the multichannel EEG signal of this region is subjected to CCA for artifact elimination. Then eADA is executed again to search for the next eyeblink artifact region on the Fp1 channel. Multichannel artifact elimination is performed on the newly found eyeblink artifact region via CCA. So, eADA and CCA are used repeatedly until all eyeblink artifacts contaminating the EEG signal are identified and removed. The flowchart of the proposed FastCCA algorithm is shown in Fig. 4.15. In this approach, CCA is directly applied to EEG segments identified with eyeblink artifacts with eADA. So this algorithm bypasses the requirement to have an eyeblink template extracted via FastEMD-CCA, which could reduce the computation time as well. This allows an adaptive detection and removal of eyeblink artifacts for every event of blink, without the need for a general template for artifact removal.

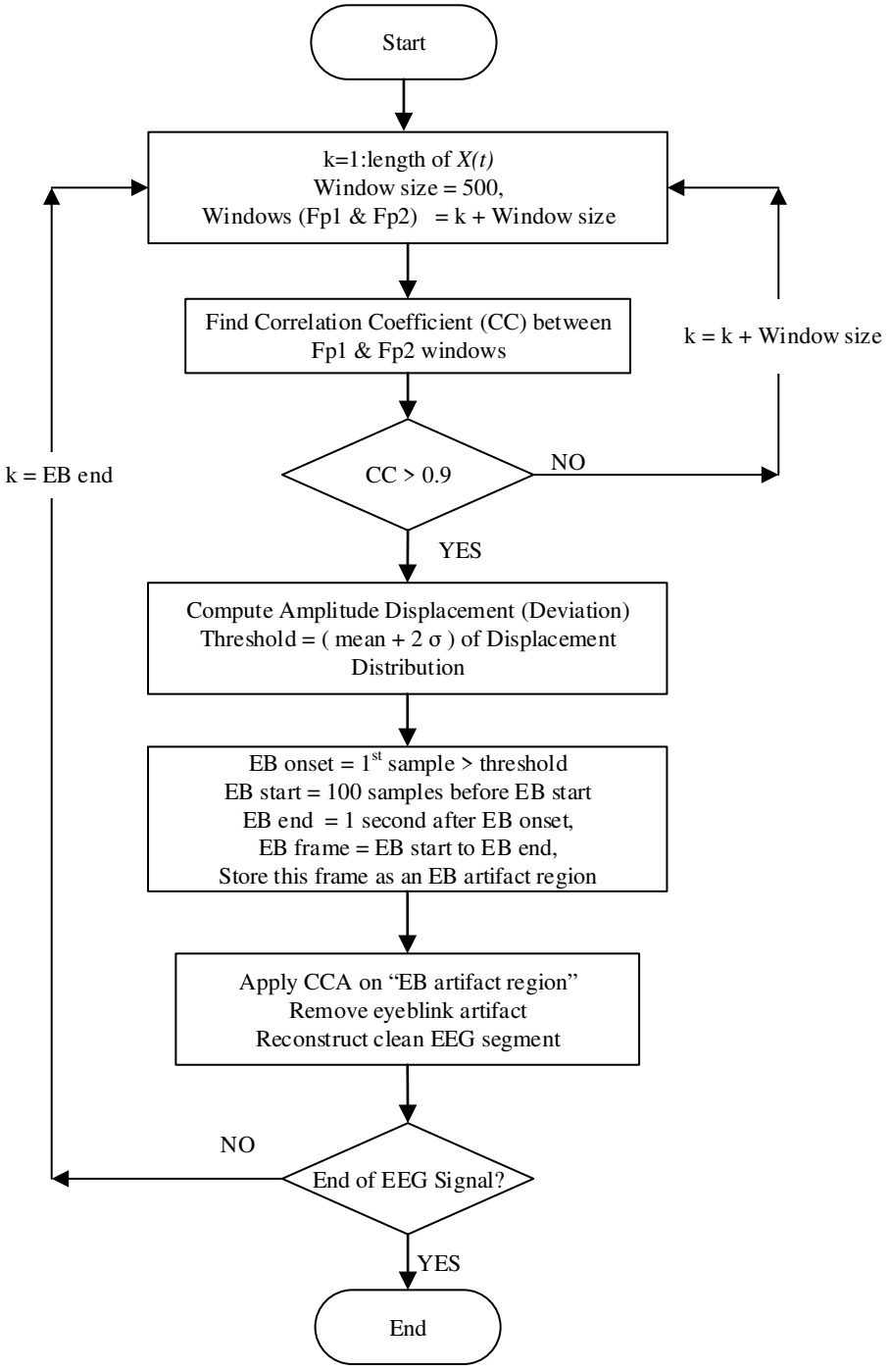

FIGURE 4.15 – Flowchart of the Proposed FastCCA Algorithm

The overall work flow of both algorithms are shown in Fig. 4.16.

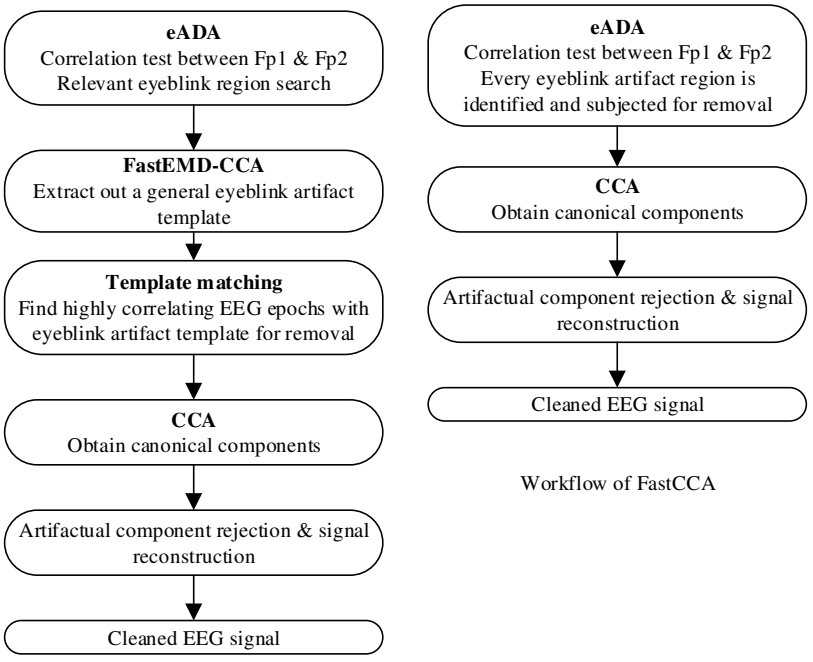

FIGURE 4.16 – Work flow of FastEMD-CCA[2] and FastCCA

4.5/ PERFORMANCE ANALYSIS

Every analysis of this research was performed using MATLAB R2018b in Windows 7 Professional (64 bit OS), with a 4GB RAM.

4.5.1/ EYEBLINK ARTIFACT DETECTION

4.5.1.1/ EADA VS FIXED THRESHOLDS

Sixty EEG signals from the Hitachi EEG dataset, from section 4.1.2.1 are used in this analysis. Eyeblink artifacts can be clearly captured in the frontal channels, Fp1-Fp2 electrodes of the EEG recordings. Hence, the proposed algorithm is evaluated on the frontal channel, Fp1, of these EEG signals. For comparison purpose, eADA is compared with the conventional constant threshold method. The constant threshold method is performed by fixing the threshold values, with different amplitude displacement, for example, thresholds of more than 10uV, 20uV, 30uV, 40uV and 50uV. Whichever amplitude displacement that exceeds these thresholds are considered to be eyeblink artifacts.

The performance of the proposed approach, eADA, is measured by validating if it is accurate in identifying eyeblink artifacts in comparison with the use of a fixed threshold value. Binary classification which produces the confusion matrix as in Table 4.2 is used to determine the accuracy level of eADA in detecting the eyeblink artifacts.

- True positive (TP) : correct Eyeblink artifact detection
- False positive (FP) : clean EEG identified as Eyeblink artifact

- True negative (TN) : correct clean EEG identification
- False negative (FN) : Eyeblink artifact identified as clean EEG

TABLE 4.2 – Confusion Matrix - Eyeblink Artifact Detection

		Detected	
		Eyeblink Artifact	Clean EEG
Observed	Eyeblink Artifact	TP	FN
	Clean EEG	FP	TN

The efficiency of the proposed algorithm compared to a constant threshold, is validated by manually inspecting the EEG signals after artifact detection, with accuracy, Eq.(4.9) derived from the confusion matrix. Accuracy is the ratio of correct eyeblink artifact and EEG detections by the total number of detections :

$$\text{ACC} = \frac{TP + TN}{TP + TN + FN + FP} \tag{4.9}$$

The best accuracy is 1.

4.5.2/ EYEBLINK ARTIFACT REMOVAL

Any artifact removal algorithm is considered effective and successful depending on two measures. The first and most important one is how well an algorithm is able to remove the artifacts, and the second one is how well an artifact removal algorithm is able to preserve neural information contained in an EEG signal after artifact elimination. On another note, the online eyeblink artifact removal capability can be interpreted through processing time taken by the algorithm. This is to evaluate whether the algorithm can achieve instantaneous artifact removal in online processing (real-time processing of a system is estimated between 6 to 20 milliseconds [164]), without loss of neural information.

However, evaluating the performance of any algorithm in identifying and discarding artifacts is challenging in the absence of ground truth. Hence, the eyeblink artifacts and EEG signals are artificially generated as discussed in subsection 4.1.1. These artificial signals serve as ground truth in carrying out the performance evaluation before applying the proposed algorithm to real EEG signals. The EOG signal is not recorded for convenience purpose. Additionally, there are no training data with blinking recorded so that the algorithm is fully automatic. Since EOG is not recorded, validation turns out to be difficult to confirm if the eyeblink artifacts are indeed removed. Thus, the algorithm's ability to remove eyeblink artifacts effectively is substantiated by an expert, through manual visual inspection (MVI).

4.5.2.1/ FASTEMD-CCA^2 VS FASTCCA VS WAVELET TRANSFORM

The developed algorithms, FastEMD-CCA^2 and FastCCA are compared with Wavelet Transform, to evaluate the performance exhibited by these algorithms on the synthetically contaminated EEG signal, in Eq. (4.2). The synthetic EEG signal and the eyeblink artifacts

are simulated for 100 trials for reliability purpose, and the results are averaged. Wavelet is chosen as it has been extensively used for eyeblink artifact removal in EEG [80–82]. FastEMD-CCA[2] and FastCCA work as discussed in sections 4.3 and 4.4 respectively. For Wavelet Transform, the sym9 mother wavelet from the Symlets family is chosen as it was suggested by Al-Qazzaz et al. in [165] as resembling EEG signals the most and would be the most compatible one for de-noising purposes. SWT is applied with soft thresholding on the entire contaminated EEG signal to obtain wavelet coefficients. Approximation coefficients are assumed to correspond to the eyeblink artifact and detail coefficients are assumed to correspond to EEG. The inverse of SWT, ISWT is then applied on the coefficients corresponding to EEG and the artifact to reconstruct the clean EEG signal and the eyeblink artifact respectively.

The performance of these algorithms in retaining the neural information in an EEG signal is quantitatively assessed. Reconstructed EEG signals after artifacts have been removed via these algorithms are validated against synthetically generated EEG signals as ground truths. Ideally, reconstructed EEG signals should remain intact after artifacts have been removed. The algorithms are evaluated in terms of correlations coefficient (CC), root means square error (RMSE) and signal to noise ratio (SNR), in the time domain. Each of the performance criteria is expressed as confidence intervals for 95% of confidence level. CC_{EEG} in Eq. (4.10) measures the similarity between synthetically generated EEG signals and reconstructed EEG signals after artifact correction, while CC_{EB} in Eq. (4.11) estimates the resemblance of removed eyeblink artifacts compared to synthetic eyeblink artifacts :

$$\text{CC}_{\text{EEG}} = \frac{C_{Y(t),Y_{\text{out}}(t)}}{\sigma_{Y(t)} * \sigma_{Y_{\text{out}}(t)}} \tag{4.10}$$

$$\text{CC}_{\text{EB}} = \frac{C_{Z(t),Z_{\text{out}}(t)}}{\sigma_{Z(t)} * \sigma_{Z_{\text{out}}(t)}} \tag{4.11}$$

.

RMSE measures the removal and reconstruction error for eyeblink and EEG signals respectively. The RMSE is calculated by finding the difference between synthetically generated eyeblink artifacts with removed eyeblink artifacts, as in Eq. (4.13) and synthetically generated EEG signals with reconstructed signals, as in Eq. (4.12) :

$$\text{RMSE}_{\text{EEG}} = \sqrt{\frac{\sum_{t=1}^{n}(Y(t) - Y_{\text{out}}(t))^2}{n}} \tag{4.12}$$

$$\text{RMSE}_{\text{EB}} = \sqrt{\frac{\sum_{t=1}^{n}(Z(t) - Z_{\text{out}}(t))^2}{n}} \tag{4.13}$$

.

The SNR is used in this analysis to determine the ratio of signal to artifact that remains after eyeblink artifacts are removed from the contaminated EEG signal. The SNR ratio is calculated before and after eyeblink artifact removal, using Eq. (4.14) and (4.15) :

$$\text{SNR}_{\text{before}} = 10 \log \left[\frac{\sigma_{Y(t)}}{\sigma_{(Y(t)-X(t))}} \right] \tag{4.14}$$

$$\text{SNR}_{\text{after}} = 10\log\left[\frac{\sigma_{Y(t)}}{\sigma_{(Y(t)-Y_{\text{out}}(t))}}\right] \tag{4.15}$$

where $X(t)$ represents the synthetically contaminated EEG signals, $Y(t)$ refers to the simulated/synthetic EEG signals generated using pinknoise, $Y_{\text{out}}(t)$ corresponds to the reconstructed EEG signals which are free from artifact, $Z(t)$ refers to the synthetic eyeblink artifact and $Z_{\text{out}}(t)$ correspond to the extracted eyeblink artifact. From the performance metrics, 95% of confidence interval has been estimated so that the probability of the performance is repetitive over 95% of the time if the evaluation to be repeated multiple times in another time frame.

4.5.2.2/ FastEMD-CCA^2 vs FastCCA vs Conventional EMD-CCA

This section aims to evaluate the total computation time taken by the conventional EMD-CCA compared to the proposed FastEMD-CCA^2 and FastCCA algorithms, evaluated on real EEG signals. In the conventional technique, EMD is applied to an eyeblink artifact region, followed by CCA on the IMFs obtained through classical EMD. Identified canonical components of the IMFs which are related to eyeblink artifact are excluded, thus clean EEG segment is reconstructed. This process of applying CCA within classical EMD for single-channel artifact removal will be repeated throughout the EEG signal whenever an eyeblink artifact region is identified.

The proposed FastEMD-CCA^2 is based on optimal usage of the FastEMD with CCA to extract an eyeblink artifact template, followed by eyeblink artifacts elimination from the entire EEG signal, as elaborated in section 4.3. FastCCA, on the other hand, performs eyeblink artifacts elimination through CCA on the locations identified by eADA. The overall workflow of these approaches is shown in Fig. 4.17.

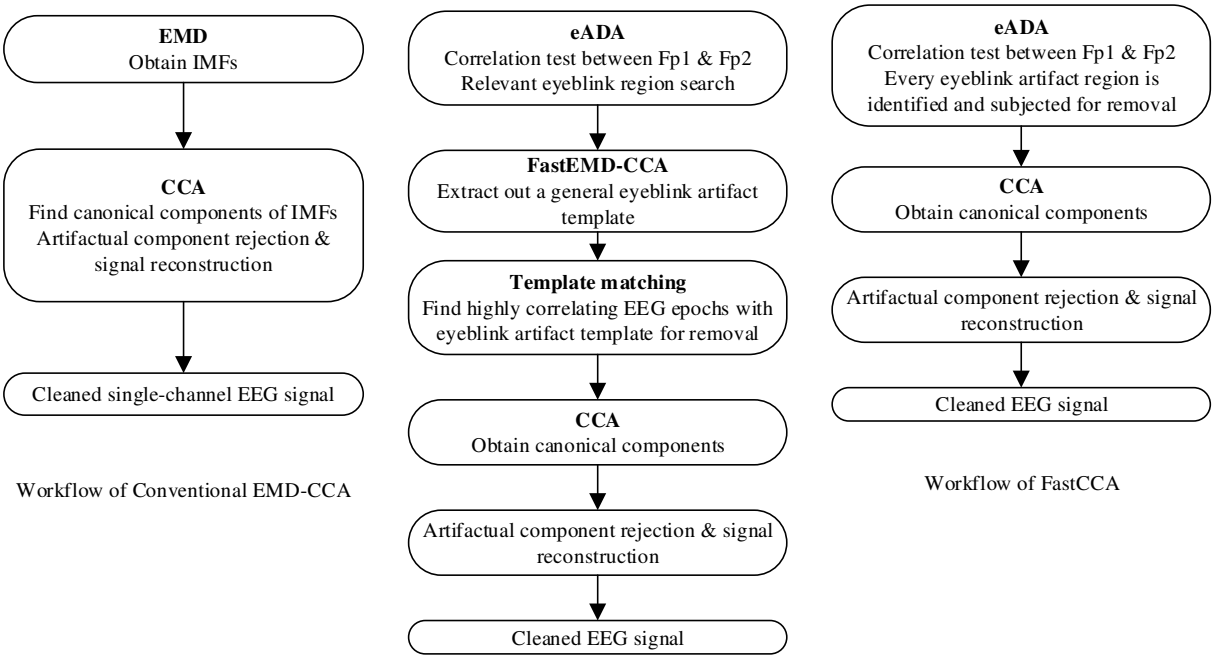

FIGURE 4.17 – Workflow of Conventional EMD-CCA, Proposed FastEMD-CCA^2 and FastCCA

4.5.2.3/ FASTEMD-CCA^2 VS FASTCCA VS FORCE

Real EEG signals illustrated in sections 4.1.2.1 and 4.1.2.2 were used to evaluate the proposed techniques, FastEMD-CCA^2 and FastCCA, compared to the state-of-the-art, FORCe algorithm. The outcomes are then averaged for each of the dataset. In MATLAB 2018b, the EEG recordings are imported into the workspace and processed automatically to remove the eyeblink artifacts in windows, with each window being at least 1-second in length for FastEMD-CCA^2, FastCCA and FORCe. The FastEMD-CCA^2 algorithm operates as discussed in sections 4.2, 4.3.1 and 4.3.2, while the FastCCA algorithm works as discussed in section 4.4. The FORCe algorithm first applies wavelet decomposition on each channel of an EEG signal. The resulting approximation coefficients obtained through wavelet are subjected to ICA to get independent components, ICs. Next, the artifactual ICs are identified through several threshold criteria, where ICs exceeding certain threshold values are classified as eyeblink and cardiac artifacts respectively, and thus removed. The inverse of ICA decomposition is performed to estimate a set of cleaned approximation coefficients. Then, soft thresholding is applied on resulting approximation coefficients from ICA and detail coefficients acquired from WT to suppress/remove muscle artifacts. Finally, a clean EEG signal is reconstructed.

Since the ground truths are not available for real EEG signals, the effectiveness of the compared algorithms in identifying and removing eyeblink artifacts, while preserving the artifact-free EEG segments are verified with the help of an expert, Neuroscientist Dr. Tahamina Begum, through MVI. The evaluation criteria are derived from various measures of the binary prediction [166, 167], thus determining the accuracy, sensitivity, specificity and error rate of the algorithms. The binary classification for eyeblink artifact detection

and removal produces the following outcomes and the confusion matrix as in Table 4.3 :

- True positive (TP) : correct eyeblink artifact detection and removal
- False positive (FP) : clean EEG identified as eyeblink artifact and removed
- True negative (TN) : correct clean EEG identification
- False negative (FN) : Eyeblink artifact identified as clean EEG, thus not removed

TABLE 4.3 – Confusion Matrix - Eyeblink Artifact Detection and Removal

		Detected	
		Eyeblink Artifact	**Clean EEG**
Observed	**Eyeblink Artifact**	TP	FN
	Clean EEG	FP	TN

Error : The error rate, ERR is computed by dividing the number of incorrect detection of both eyeblink artifact and non eyeblink artifact regions over the total number of detections. Values approaching zero denote better error rate.

$$\text{ERR} = \frac{FP + FN}{TP + TN + FN + FP} \tag{4.16}$$

Accuracy : ACC is the opposite of error rate, where it is the ratio of correct eyeblink artifacts and EEG segments detection by total number of detections. The best accuracy is 1.

$$\begin{aligned} \text{ACC} &= \frac{TP + TN}{TP + TN + FN + FP} \\ \text{ACC} &= 1 - ERR \end{aligned} \tag{4.17}$$

Sensitivity : SN is calculated by dividing correctly detected eyeblink artifacts with total number of actual eyeblink artifacts. 1 is considered to be the best sensitivity value.

$$\text{SN} = \frac{TP}{TP + FN} \tag{4.18}$$

Specificity : SP is estimated by dividing correctly identified clean EEG segments with actual clean EEG segments. 1 is considered to be the best specificity value.

$$\text{SP} = \frac{TN}{TN + FP} \tag{4.19}$$

4.6/ SUMMARY

The chapter mainly focused on proposing the eyeblink artifact detection algorithm and the eyeblink artifact removal algorithms. Conventional eyeblink artifact detection algorithms depend on constant thresholds or constant features to make a binary decision to recognize if an EEG segment contains eyeblink artifacts or not. In this chapter, an unsupervised eyeblink artifact detection, eADA algorithm, is proposed and evaluated. The algorithm determines the threshold for eyeblink artifacts based on the correlation between the signal from two EEG electrodes and the amplitude displacement range.

Next, the chapter has focused on incorporating the unsupervised eyeblink artifact detection algorithm, eADA with FastEMD and CCA. Various modification are made to EMD algorithm, so that it can serve a low computational burden to the entire proposed algorithm, FastEMD-CCA^2. Apart from FastEMD-CCA^2, another algorithm, FastCCA is proposed as well to remove eyeblink artifacts from EEG signals by combining eADA and CCA.

5

Results and Discussion

This chapter discusses the results obtained for the proposed eyeblink detection algorithm (eADA) and the proposed eyeblink artifact removal algorithms, FastEMD-CCA[2] and FastCCA. Also, comparisons of these proposed algorithms with one of the state-of-the-art algorithms are presented as well. Evaluation and analysis conducted on these algorithms are provided, mainly with performance scores such as computation time, error rate, accuracy, sensitivity and specificity of the algorithms in effectively detecting and removing the eyeblink artifacts.

5.1/ Eyeblink Artifact Detection Algorithm

The accuracy of the proposed approach, eADA, in detecting eyeblink artifacts compared to the use of a constant or fixed threshold is presented and discussed in this section. The average accuracy obtained from the proposed method in comparison with constant thresholds in detecting eyeblink artifacts correctly, applied on the Fp1 channel of 60 Hitachi EEG signals is tabulated in Table 5.1. The individual representation of accuracy for each EEG signal is provided in Table 5.2.

As elaborated in Section 4.2, an automated eyeblink artifact detection algorithm is designed. The proposed approach detects eyeblink artifacts without human supervision. First EEG segments containing eyeblink artifacts are recognized with the concept of correlation between EEG electrodes, Fp1 and Fp2 as in subsection 4.2.1. Secondly, to address the issues of a constant threshold, an automated and varying threshold level is calculated for every EEG segment containing eyeblink artifact using amplitude displacement. From Table 5.2, the accuracy achieved by the proposed technique in detecting eyeblink artifacts correctly is 99.47% on average. This average accuracy level is higher compared to the average accuracies achieved through fixed thresholds. Fixing the amplitude displacement thresholds of 10uV, 20uV, 30uV, 40uV and 50uV produced an average accuracy of 95.37%, 93.95%, 92.67%, 84.57.3% and 73.95% respectively.

TABLE 5.1 – Average Eyeblink Artifact Detection Accuracy

Average (60 EEG Signals)						
Threshold	**eADA**	**10uV**	**20uV**	**30uV**	**40uV**	**50uV**
Accuracy	99.47%	95.37%	95.34%	92.67%	84.57%	73.95%

The individual accuracy level on every EEG signal obtained using constant thresholds lies between 81% to 100% for 10uV, 72% to 100% for 20uV, 71% to 100% for 30uV, 46% to 100% for 40uV, and 22% to 100% for 50uV. The fixed thresholds achieved 100% detection accuracies on certain EEG signals, i.e. 10uV on(EEG 4, 43, 46, 47), 20uV on (EEG 4, 38, 39, 43, 46, 47), 30uV on (EEG 33, 35, 36, 38, 43, 46, 47), 40uV on (EEG 35, 38, 40) and 50uV on (EEG 38). It can be concluded that the detection accuracy of fixed thresholds is 100% perfect only on some of the EEG signals. The variation in accuracy shown by 40uV threshold is 54% (46% to 100% across all signals), whereas the accuracy of 50uV threshold varies by 78% (22% to 100% across all signals). This shows that the performance of the fixed threshold method is inconsistent across all the EEG signals; the method may sometimes achieve very high accuracy and sometimes may achieve very low accuracy in detecting the eyeblink artifacts. This is due to the unpredictable characteristics of the eyeblink artifacts, where the blinking duration, pattern and strength of eye blinks differ for every individual. For instance, the constant threshold of 30uV has achieved 100% accuracy in detecting eyeblink artifacts on EEG 33, 35, 36, 38, 43, 46, 47, which means this threshold level suits well for these EEG signals. However, the 30uV threshold has only achieved 71.6% of accuracy in eyeblink artifact detection for EEG 53. Similarly, the constant threshold of 50uV has achieved an accuracy of 100% in correctly detecting eyeblink artifacts of EEG 38, but this threshold value has only achieved 22.22% of detection accuracy for EEG 13. The analysis indicates that the performance of constant thresholds is purely dependent on the nature of the eyeblink artifacts and is not consistent across all EEG signals. Therefore, relying on fixed or constant thresholds in detecting eyeblink artifacts for subsequent artifact removal step is not desirable.

On the other hand, the least accuracy level achieved by the proposed method (eADA) in detecting eyeblink artifacts correctly is on EEG 5, about 94.34%. (eADA) achieved the best accuracy level, 100% on 36 EEG signals as can be seen from Table 5.2. This reveals that the performance of eADA is consistent in detecting the eyeblink artifacts in EEG signals, ranging between 94% to 100%. There is only a 6% accuracy variation among the EEG signals. Since the threshold level for every window is calculated individually, the calculated threshold thereby corresponds to the varying nature of the eyeblink artifact in that window. Hence, the threshold is automatically determined for every window without setting any specific value, producing high detection accuracy. This is the reason why the eyeblink artifact detection accuracy by eADA does not vary much across all the EEG signals. If eADA to be used in any other set of EEG signals to detect the eyeblink artifacts, the algorithm will be able to adjust itself to detect the eyeblink artifacts that are contaminating the EEG signal.

5.1.1/ Welch ANOVA Results

To check if the accuracies achieved by the proposed eADA algorithm are statistically significant compared to the fixed thresholds, an analysis of variance, ANOVA test is conducted. Before running the one way ANOVA test, the normality of the accuracies distribution by different techniques is checked. The Shapiro-Wilk is used for this purpose, and the results of the test are given in Table 5.3.

TABLE 5.3 – Test of Normality for the Accuracies

Parameter	Threshold	Statistic	df	Sig.
Accuracy	**Proposed eADA**	0.597	60	0.000
	10uV	0.900	60	0.000
	20uV	0.807	60	0.000
	30uV	0.870	60	0.000
	40uV	0.817	60	0.000
	50uV	0.873	60	0.000

From Table 5.3, statistically significant values ($P<0.05$) are observed for all accuracies of different threshold conditions, denoting the accuracy data is not normally distributed. A requirement for the ANOVA test is that the homogeneity of variance should be met, which means the variances of each of the compared groups, the threshold in this case, should be equal. Since the accuracies achieved by the different thresholds are not normally distributed, the assumption of homogeneity of variances is violated. So a Welch ANOVA test is conducted instead of the one-way ANOVA. This test is appropriate when the homogeneity of variance is violated. The accuracy of different threshold methods, i.e. the proposed and the fixed thresholds, were analyzed using the Welch ANOVA test using the SPSS software. The results of the Welch ANOVA test is provided in Table 5.4.

TABLE 5.4 – Welch ANOVA Test

Between Methods		Sig.
Proposed eADA	**10uV**	0.000
Proposed eADA	**20uV**	0.000
Proposed eADA	**30uV**	0.000
Proposed eADA	**40uV**	0.000
Proposed eADA	**50uV**	0.000

The Welch ANOVA test reveals that the accuracies achieved by the proposed eADA algorithm in comparison with the each of the fixed threshold in detecting the eyeblink artifacts in the EEG signals are statistically significant, with $P=0.000$ ($P<0.05$). Further analysis between the fixed thresholds reveals that there is no significant statistical difference observed between fixed thresholds of 10uV, 20uV and 30uV. The Welch ANOVA between 10uV and 20uV results in ($P=1.000$), between 10uV and 30uV results in ($P=0.114$), and between 20uV and 30uV results in ($P=0.164$).

5.2/ EYEBLINK ARTIFACT REMOVAL ALGORITHMS

5.2.1/ COMPARISON BETWEEN FASTEMD-CCA^2, FASTCCA AND WAVELET TRANSFORM

The proposed algorithms, FastEMD-CCA^2 and FastCCA are compared with WT as elaborated in section 4.5.2.1, to evaluate the performance exhibited by these algorithms on synthetically generated EEG signals. Fig. 5.1(a) - 5.1(c) show the reconstructed EEG signal and eyeblink artifact through FastEMD-CCA^2. Fig. 5.2(a) - 5.2(c) show the reconstructed EEG signal and eyeblink artifact through FastCCA. Fig. 5.3(a) - 5.3(c) show the reconstructed EEG signal and eyeblink artifact through SWT.

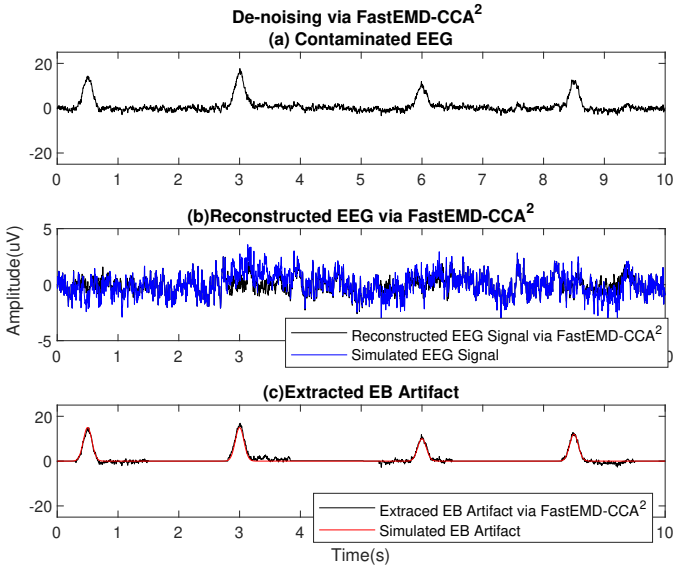

FIGURE 5.1 – (a) Mixed EEG and Eyeblink Signal, (b) Reconstructed EEG Signal, (c) Extracted Eyeblink Artifact

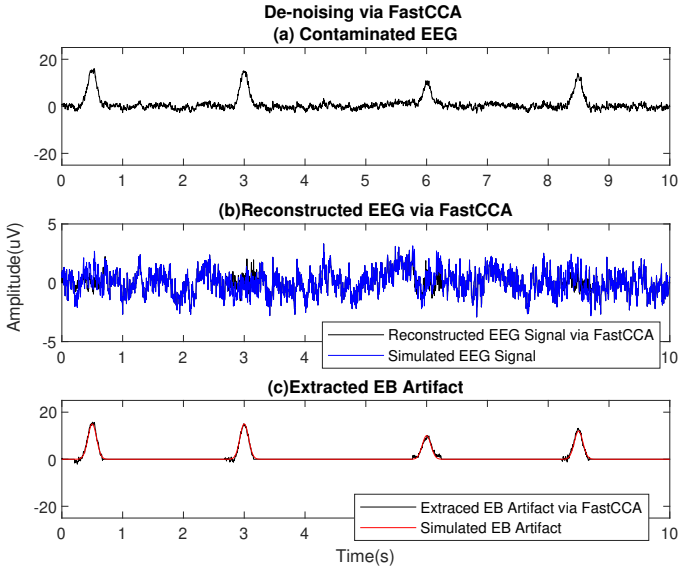

FIGURE 5.2 – (a) Mixed EEG and Eyeblink Signal, (b) Reconstructed EEG Signal, (c) Extracted Eyeblink Artifact

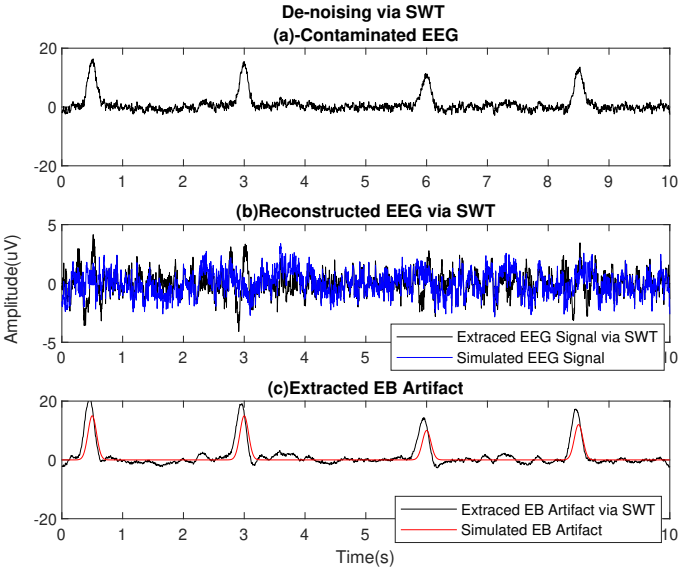

FIGURE 5.3 – (a) Mixed EEG and Eyeblink Signal, (b) Reconstructed EEG Signal, (c) Extracted Eyeblink Artifact

The performance metrics obtained for FastEMD-CCA[2], FastCCA and WT, applied on synthetically generated and contaminated EEG signals, are tabulated in Table 5.5.

TABLE 5.5 – Performance Metrics of FastEMD-CCA^2, FastCCA and WT

Techniques	FastEMD-CCA^2		FastCCA		Wavelet (SWT)	
	mean ± std ($\mu \pm \sigma$)	95% CI	mean ± std ($\mu \pm \sigma$)	95% CI	mean ± std ($\mu \pm \sigma$)	95% CI
CCeeg	0.8258 ± 0.0486	0.8162 to 0.8355	0.9257 ± 0.0202	0.9217 to 0.9297	0.5848 ± 0.0429	0.5763 to 0.5933
CCeb	0.9802 ± 0.0096	0.9783 to 0.9821	0.9913 ± 0.0022	0.9909 to 0.9918	0.8524 ± 0.0112	0.8502 to 0.8546
RMSEeeg	0.5665 ± 0.0888	0.5489 to 0.5841	0.3765 ± 0.0487	0.3669 to 0.3862	0.8969 ± 0.0344	0.8901 to 0.9038
RMSEeb	0.5665 ± 0.0888	0.5489 to 0.5841	0.3765 ± 0.0487	0.3669 to 0.3862	2.2612 ± 0.0932	2.2427 to 2.2797
SNRafter (dB)	5.8223 ± 1.2474	5.5748 to 6.3941	9.8988 ± 1.2976	9.6414 to 10.1563	1.0950 ± 0.3845	1.0187 to 1.1713
SNRbefore (dB)	-10.2999 ± 0.00	-10.2999	-10.2999 ± 0.00	-10.2999	-10.2999 ± 0.00	-10.2999
Time (s)	0.2651 ± 0.2980	0.2060 to 0.3242	0.1297 ± 0.0204	0.1256 to 0.1337	0.1111 ± 0.0294	0.1052 to 0.1169

The algorithms are evaluated on 100 trials of synthetically contaminated EEG signals to ensure the performance exhibited by the algorithms are reliable and repetitive. The confidence interval for 95% of confidence level is determined for each of the performance metrics. The 95% confidence level is chosen so that the estimation of results are statistically sound. CC value normally lies between -1 and 1, in which a value approaching 1 indicates a higher correlation or similarity. RMSE values that approach zero signifies a more precise and accurate signal reconstruction, relative to the synthetic signals. The SNR measures the scale of eyeblink artifacts that have been removed from the noisy EEG signal and the degree of neural signal preservation. The effectiveness of the evaluated algorithms in preserving the underlying neural information in an EEG signal can be deduced through CC value that approaches near 1, RMSE close to 0 and higher SNR value.

In this analysis, the proposed techniques, FastEMD-CCA^2 and FastCCA, produces higher CC values on average compared to SWT, 0.8258 and 0.9257 in reconstructing the EEG signal, 0.9802 and 0.9913 in extracting out the eyeblink artifact. The error produced by FastEMD-CCA^2 is 37% percent lower, and FastCCA is 58% lower than the error produced by SWT in reconstructing the EEG signal. While in extracting out the eyeblink artifact, FastEMD-CCA^2 has produced an error of 75% lower, and FastCCA has produced an error of 83% lower than SWT. This indicates that the FastEMD-CCA^2 and FastCCA algorithm is able to remove eyeblink artifact components from the contaminated EEG signals better in comparison with SWT. From Table 5.5, FastEMD-CCA^2 and FastCCA yield very high SNR values, close to 5 dB by FastEMD-CCA^2 and close to 9 dB by FastCCA on average from -10dB before artifact correction, which denotes a higher ratio of neural information has been preserved. Alternatively, SWT produced nearly 1 dB of SNR on average from -10dB before artifact elimination. This shows that the FastEMD-CCA^2 and FastCCA are a better choice in removing eyeblink artifacts, and at the same time, they are able to preserve underlying EEG components better, by not introducing much distortion to the neural signal. In terms of computation time, the SWT is 2.4 times faster than the FastEMD-CCA^2 and 1.1 times faster than the FastCCA. It has to be emphasized here that SWT removes artifacts only from a single-channel EEG signal, hence the faster computation time, while FastEMD-CCA^2 and FastCCA perform the artifact elimination from multichannel EEG signal. Moreover, SWT is applied to the entire signal for processing, which is not applicable for online applications, while FastEMD-CCA^2 and FastCCA algorithms process the EEG signals in windows, which is what required for online processing. SWT also relies on manual selection of appropriate mother wavelet, which comprises sine and cosine functions, which may not be suitable for non-stationary biomedical signals. Selecting an inappropriate mother wavelet could lead to inaccuracies in reconstructing artifact-free EEG si-

gnals. Furthermore, the accuracy of SWT is also sensitive to the selection of thresholding function which could have an effect on preserving or discarding the neural information in an EEG signal.

5.2.2/ Comparison between FastEMD-CCA^2, FastCCA and Conventional EMD-CCA

The time taken by the conventional EMD-CCA (repetitive usage of EMD with CCA for single-channel artifact removal)in comparison with the proposed FastEMD-CCA^2 and FastCCA (for multi-channel artifact removal), evaluated on 15 randomly selected real EEG signals section from 4.1.2.1 are tabulated in Table 5.6.

Table 5.6 – Comparison of Computation Time between Proposed FastEMD-CCA^2, FastCCA and Conventional EMD-CCA

		Total Computation Time (s)		
Artifact Elimination		Multi Channel		Single Channel
Signal	Duration per Channel (s)	Proposed FastEMD-CCA^2	Proposed FastCCA	Conventional EMD-CCA
EEG 1	389	15.17	27.12	251.87
EEG 2	329	5.66	16.73	275.13
EEG 3	294	5.77	14.67	144.08
EEG 4	369	6.84	15.17	506.84
EEG 5	337	7.65	9.18	434.79
EEG 6	312	6.75	9.03	344.00
EEG 7	330	8.17	6.58	436.61
EEG 8	308	7.00	10.07	327.63
EEG 9	306	5.12	11.33	419.05
EEG 10	346	7.79	8.75	683.36
EEG 11	321	6.65	10.67	478.37
EEG 12	272	4.52	9.09	223.50
EEG 13	345	7.50	6.01	363.46
EEG 14	310	4.39	0.99	969.84
EEG 15	271	4.36	0.71	976.72

Fig. 5.4-5.6 shows a portion of corrected EEG signal (EEG 2), through proposed FastEMD-CCA^2, FastCCA and the conventional EMD-CCA.

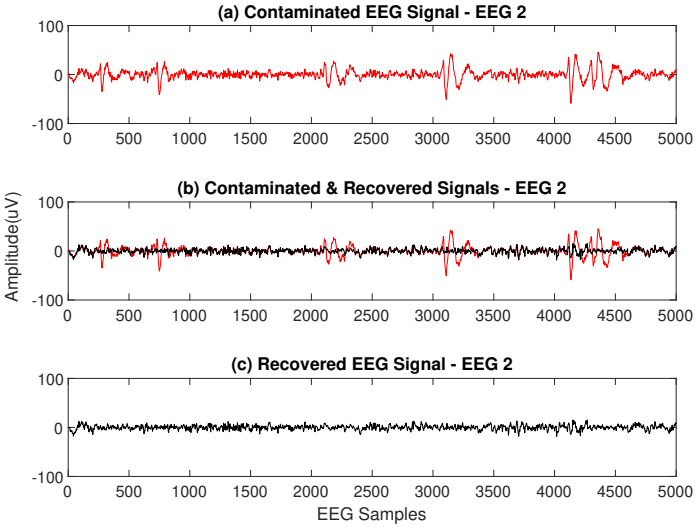

FIGURE 5.4 – Recovered EEG signal through proposed FastEMD-CCA[2]

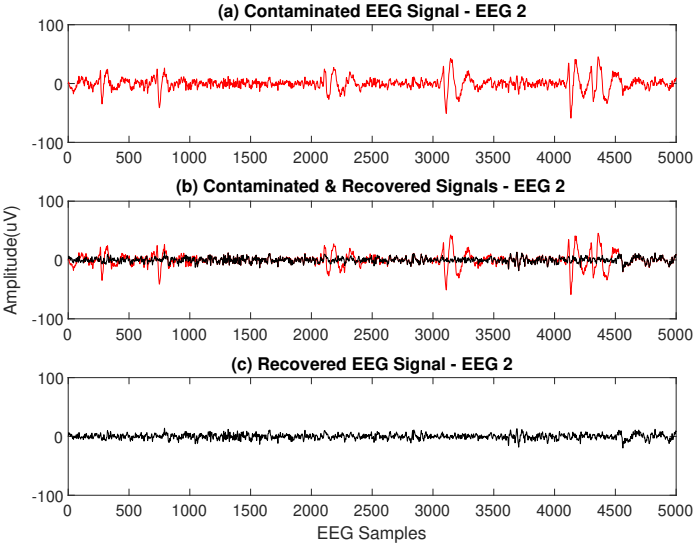

FIGURE 5.5 – Recovered EEG signal through proposed FastCCA

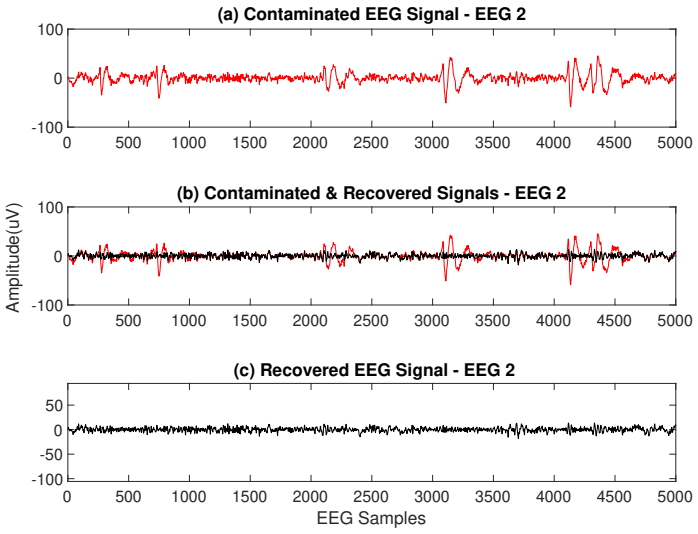

FIGURE 5.6 – Recovered EEG signal through conventional EMD-CCA

Comparing Figs. 5.4 - 5.6 by visual inspection, it can be clearly seen that all three techniques remove eyeblink artifacts reliably without distorting the neural signals. The computation time taken to remove eyeblink artifacts from the EEG signals individually is tabulated in Table 5.6. The proposed methods, FastEMD-CCA^2 and FastCCA evaluated on 15 multichannel EEG signals, are significantly faster and less computationally expensive than the conventional EMD-CCA. In the worst-case scenario, FastEMD-CCA^2 is at least 16 times faster compared to conventional EMD-CCA, FastCCA is 9 times faster compared to conventional EMD-CCA. While in extreme cases, the conventional EMD-CCA is roughly 224 times slower than FastEMD-CCA^2 and 1374 times slower than FastCCA. For instance in EEG 15, EMD-CCA's computation time is about 976.72s, whereas FastEMD-CCA^2's and FastCCA's computation time is 4.36s and 0.71s respectively. The resulting corrected EEG signal for EEG 15 through FastEMD-CCA^2, FastCCA and conventional EMD-CCA is presented in Fig. 5.7 - Fig. 5.9 for comparison purpose. As can be seen from these figures, EEG 15 is contaminated with too many eyeblink artifact events, justifying the time taken by conventional EMD-CCA to remove artifacts from this signal. The time conventional EMD-CCA took is primarily due to the repetitive application of classical EMD, where EMD has to be applied on every eyeblink artifact instance. Apart from this, the conventional EMD-CCA is also not able to completely remove the entire artifact region, whereby some peaks or potentials of the eyeblink artifacts remain in the corrected signal, as shown in Fig. 5.9. Such scenarios may happen when there are too many instances of eyeblink artifact in an EEG signal, which causes an error in aligning the EEG windows properly for artifact elimination. So applying EMD and CCA on the improperly aligned EEG windows can leave some of the artifact peaks uncorrected.

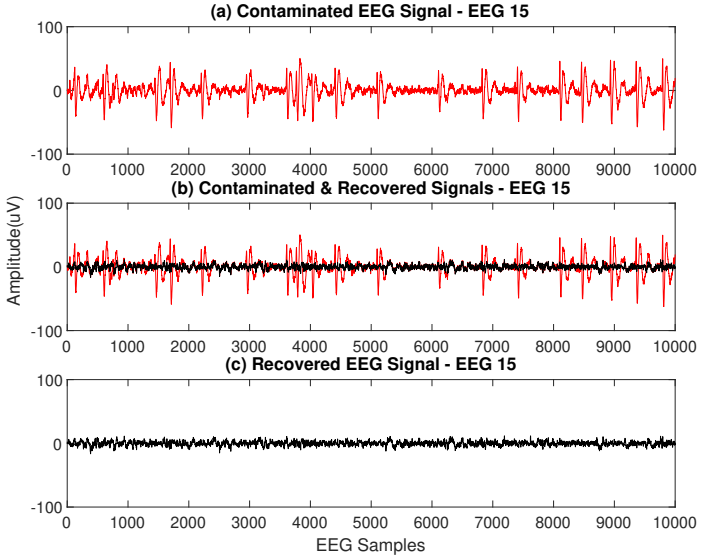

FIGURE 5.7 – Recovered EEG signal through proposed FastEMD-CCA[2]

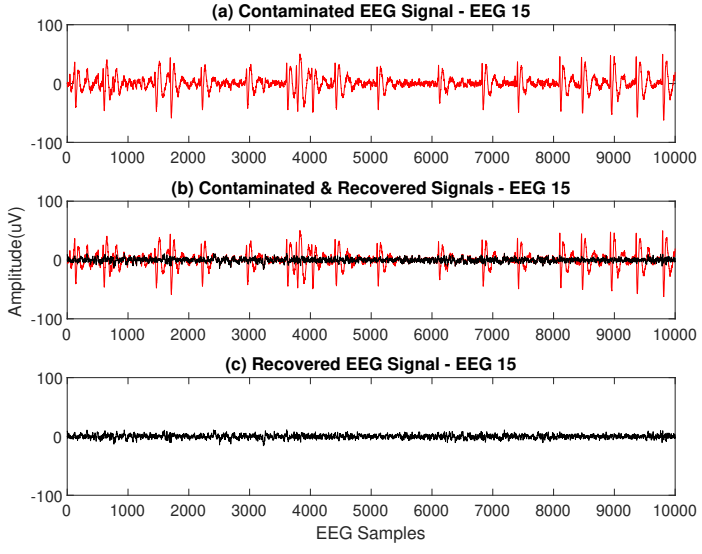

FIGURE 5.8 – Recovered EEG signal through proposed FastCCA

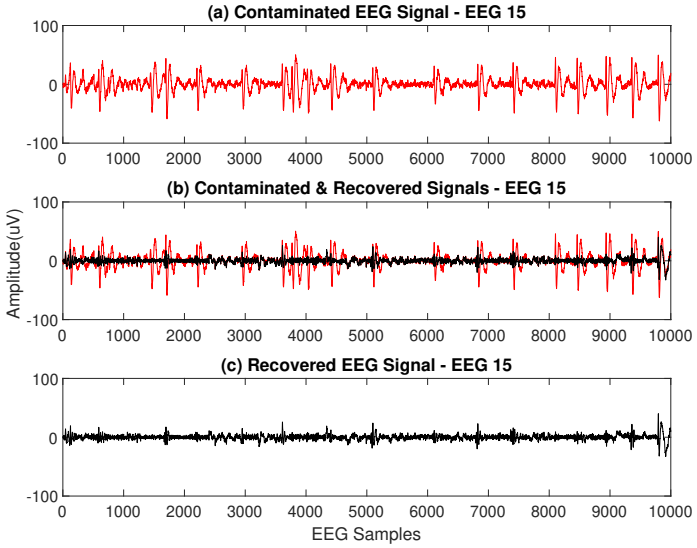

FIGURE 5.9 – Recovered EEG signal through conventional EMD-CCA

5.2.3/ COMPARISON BETWEEN FORCE, FASTEMD-CCA^2 AND FASTCCA

The average accuracy, sensitivity, specificity, error rate and computation time for FastEMD-CCA^2, FastCCA and FORCe on Hitachi and INV-SK datasets are tabulated in Tables 5.7 and 5.8.

TABLE 5.7 – Performance Metrics of FastEMD-CCA^2, FastCCA and FORCe on Hitachi Dataset

Techniques	**FORCe**	**FastEMD-CCA^2**	**FastCCA**
Accuracy	91.70%	97.90%	99.47%
Sensitivity	89.47%	97.65%	99.44%
Specificity	98.65%	99.22%	99.74%
Error Rate	8.30%	2.10%	0.53%
Computation Time	85.10s	6.78s	6.87s
Average Processing Time (to clean 1s of EEG)	272.5 ms	21.7 ms	22 ms

TABLE 5.8 – Performance Metrics of FastEMD-CCA^2, FastCCA and FORCe on INV-SK Dataset

Techniques	**FORCe**	**FastEMD-CCA^2**	**FastCCA**
Accuracy	96.60%	97.81%	98.33%
Sensitivity	95.32%	97.15%	97.60%
Specificity	100.00%	100.00%	100.00%
Error Rate	3.40%	2.19%	1.67%
Computation Time	85.94s	4.31s	7.20s
Average Processing Time (to clean 1s of EEG)	323 ms	16.2 ms	27 ms

Fig. 5.10 - 5.12 show an example of an entire EEG signal from Hitachi's dataset, reconstructed using FORCe algorithm and the proposed algorithms. Fig. 5.13 - 5.15 shows a short portion of the same EEG signal, reconstructed using FORCe algorithm and the proposed algorithms.

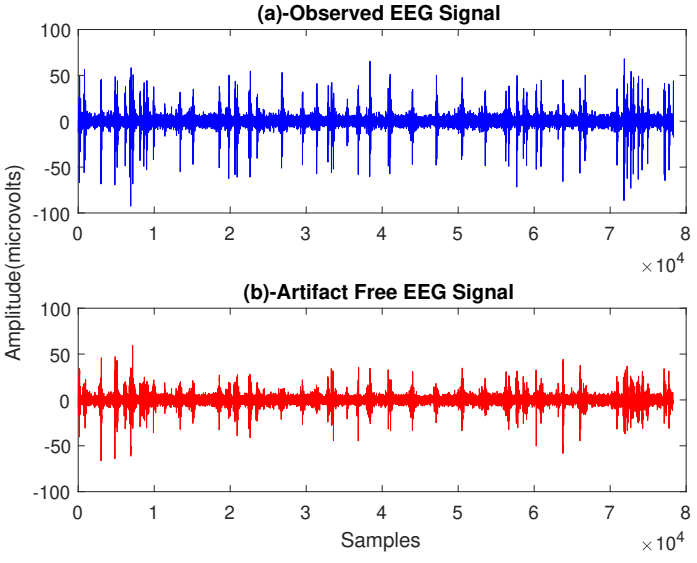

FIGURE 5.10 – Entire EEG Signal-Reconstructed through FORCe

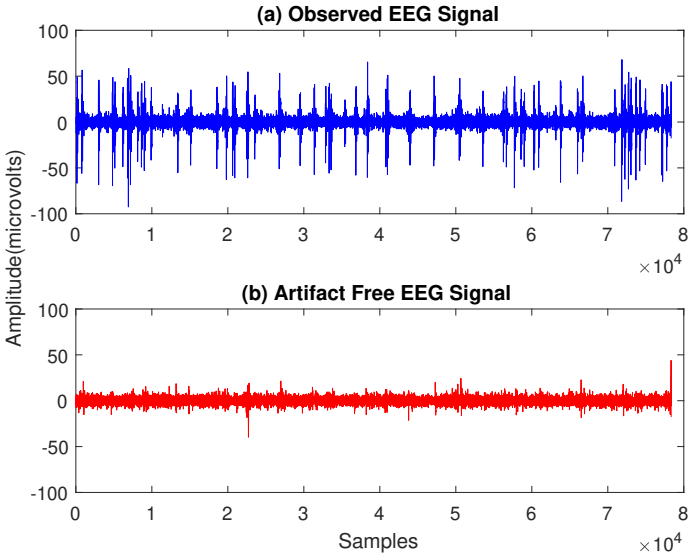

FIGURE 5.11 – Entire EEG Signal-Reconstructed through FastEMD-CCA[2]

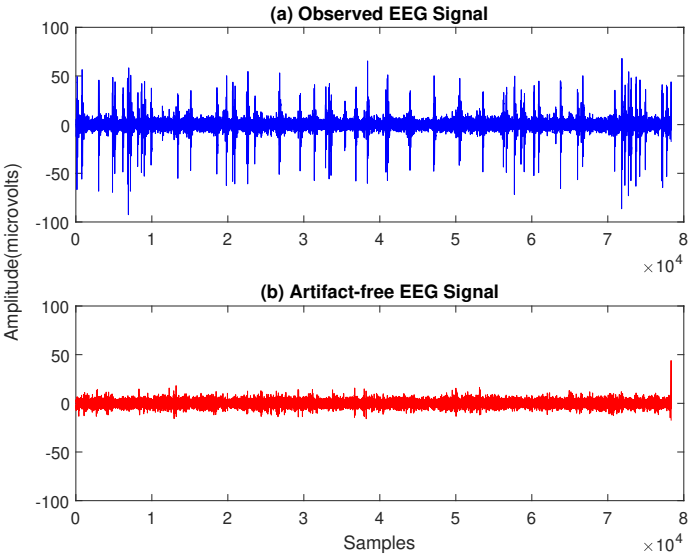

FIGURE 5.12 – Entire EEG Signal-Reconstructed through FastCCA

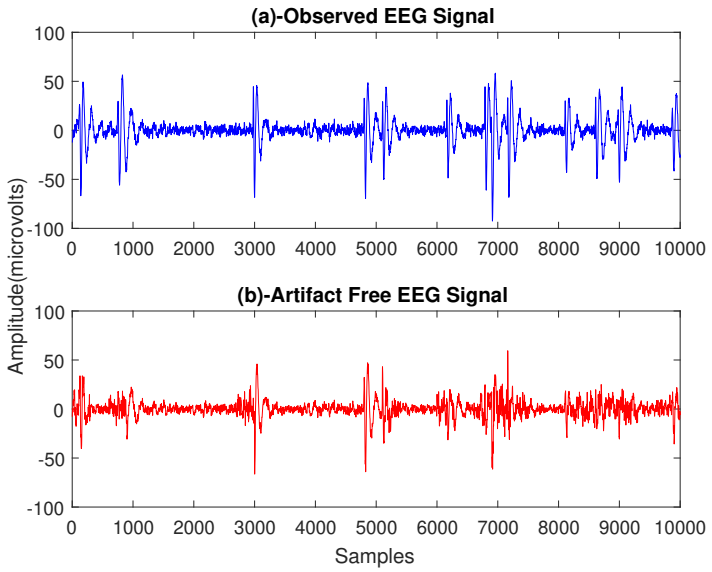

FIGURE 5.13 – A Portion of the EEG Signal-Reconstructed through FORCe

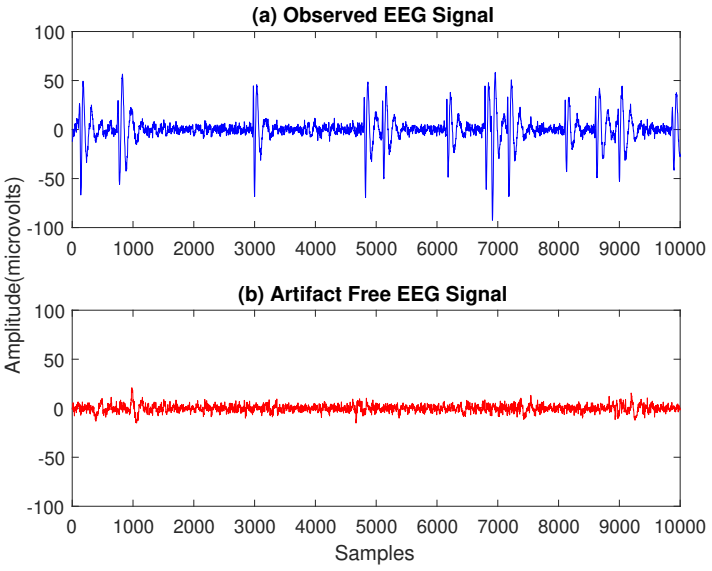

FIGURE 5.14 – A Portion of the EEG Signal-Reconstructed through FastEMD-CCA[2]

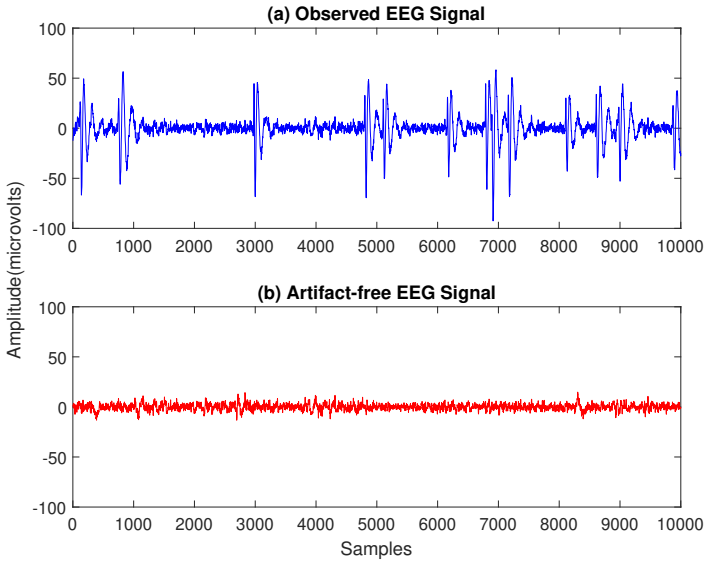

FIGURE 5.15 – A Portion of the EEG Signal-Reconstructed through FastCCA

Fig. 5.16 - 5.18 show an example of an entire EEG signal from INV-SK's dataset, reconstructed using FORCe algorithm and the proposed algorithms. Fig. 5.19 - 5.21 shows a short portion of the same EEG signal, reconstructed using FORCe algorithm and the proposed algorithms.

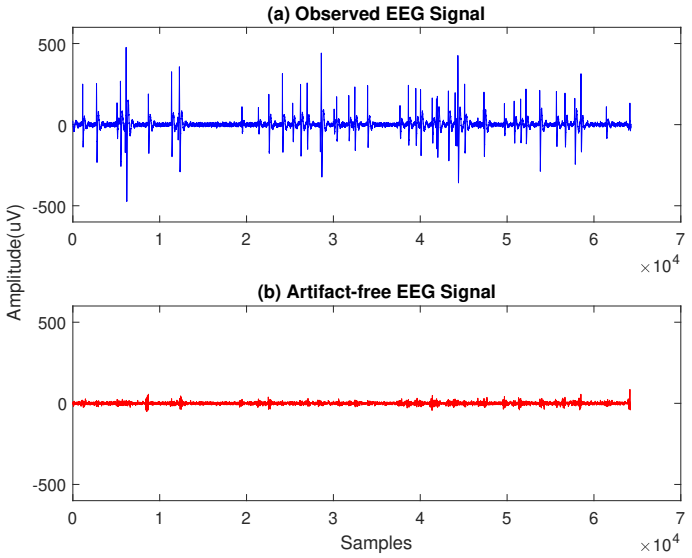

FIGURE 5.16 – Entire EEG Signal-Reconstructed through FORCe

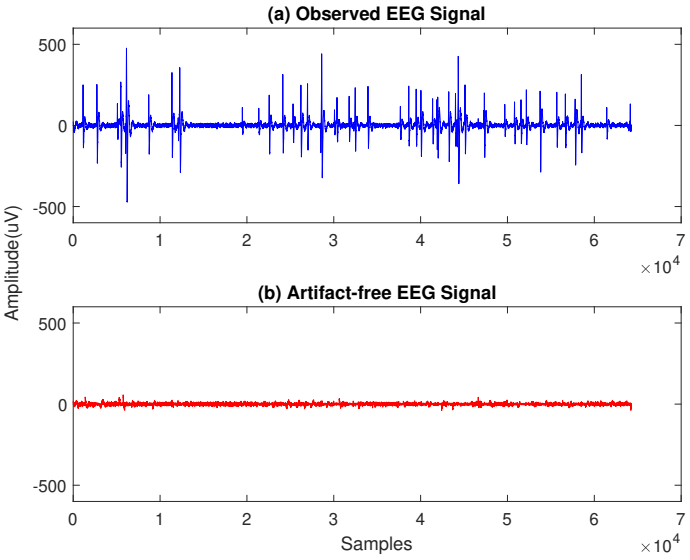

FIGURE 5.17 – Entire EEG Signal-Reconstructed through FastEMD-CCA[2]

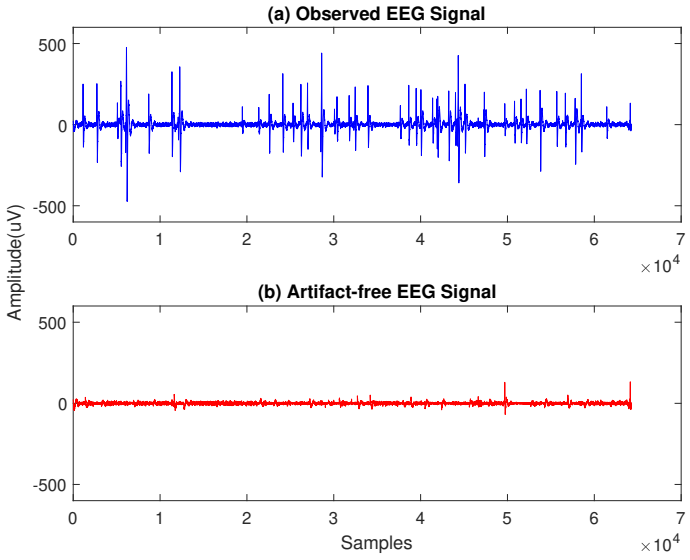

FIGURE 5.18 – Entire EEG Signal-Reconstructed through FastCCA

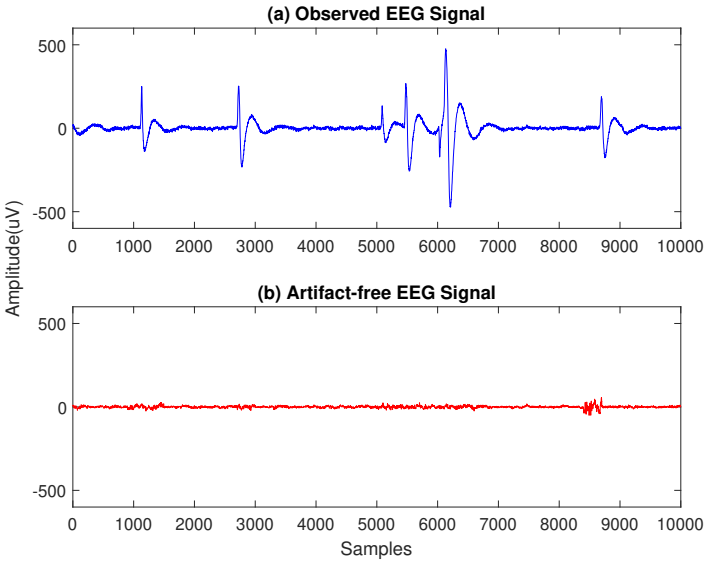

FIGURE 5.19 – A Portion of the EEG Signal-Reconstructed through FORCe

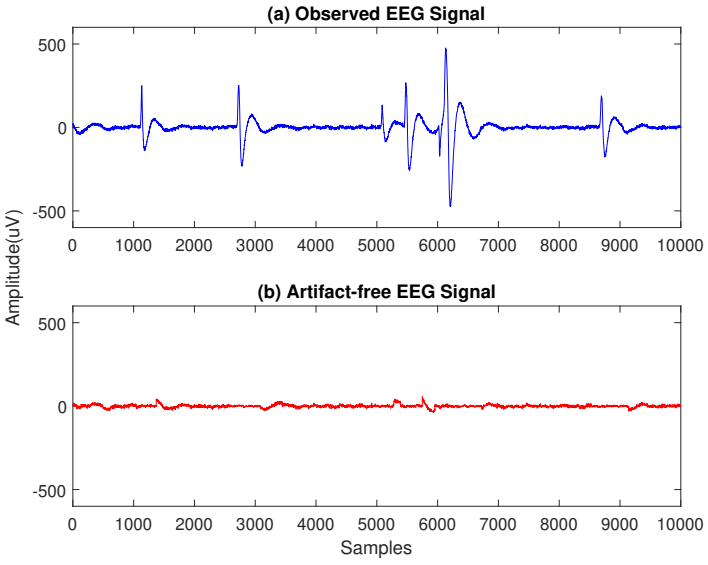

FIGURE 5.20 – A Portion of the EEG Signal-Reconstructed through FastEMD-CCA[2]

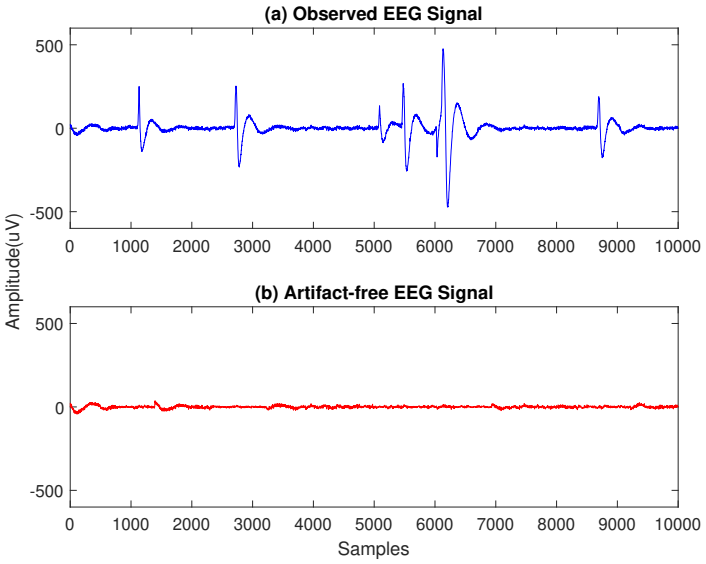

FIGURE 5.21 – A Portion of the EEG Signal-Reconstructed through FastCCA

The accuracy represents the ability of the proposed algorithms in accurately identifying the eyeblink artifacts and uncontaminated EEG segments, in order for it to remove the eyeblink artifacts. The proposed algorithms have achieved an average of 97.9% and 99.47% of accuracy compared to 91.7% by FORCe on the Hitachi dataset. While for the INV-SK dataset, FastEMD-CCA^2's average accuracy is 97.8%, FastCCA's is 98.3% and FORCe's is 96.6%. The proposed algorithms achieved a slightly higher accuracy level compared to the FORCe algorithm.

Failing to correctly identify the eyeblink artifacts and EEG segments are interpreted through the error rate produced by the algorithms, where it counts the chance of the algorithms to miss an eyeblink artifact. FastEMD-CCA^2 produced an average error rate of 2.10%, FastCCA with 0.53%, while FORCe yield 8.30% on the Hitachi dataset. For the INV-SK dataset, the average error rate of FastEMD-CCA^2, FastCCA and FORCe is 2.19%, 1.67% and 3.40% respectively. This denotes that these algorithms are still susceptible to miss out eyeblink artifacts, regardless of the EEG dataset. FORCe records the highest error rate and lowest accuracy level on average among the three algorithms for both datasets. The average eyeblink artifact detection and removal accuracy of FastCCA is 1.57% higher and the average error rate of FastCCA is 1.57% lower compared to FastEMD-CCA^2 with Hitachi's dataset. Similarly, with INV-SK's dataset, FastCCA's average accuracy is 0.52% higher than FastEMD-CCA^2. This shows that FastEMD-CCA^2 has a higher probability of identifying eyeblink artifacts or EEG segments erroneously.

Apart from error rate and accuracy, sensitivity is used as a measurement to measure how precise the algorithms are in correctly identifying and removing the eyeblink artifacts in comparison with the actual number of observed eyeblink artifacts. Similarly, specificity is used to measure the precision of the algorithms in properly recognizing EEG segments and retaining them. Again FORCe records the lowest sensitivity on average for both datasets, but not significantly low. The results indicate that the proposed algorithms, FastCCA and FastEMD-CCA^2 have achieved 99.44% and 97.65% of sensitivity respectively, which are 9.97% and 8.18% higher than that of FORCe algorithm for Hitachi's dataset. Evaluating the INV-SK dataset also reveals that FORCe is 2.28% and 1.83% lower in sensitivity

percentage than FastCCA and FastEMD-CCA^2 respectively. The sensitivity of FORCe in identifying and removing the artifacts is 89.47 %. This shows that FastCCA and FastEMD-CCA^2 could identify and remove eyeblink artifacts relatively better than FORCe could. The identification of artifact related ICs in FORCe during ICA application on the wavelet coefficients is dependent on manually adjusted threshold values, which classifies or make a binary decision whether an IC is artifactual. So, having manually adjusted thresholds may lead to detection errors, thereby some artifacts are not removed. Specificity is the ratio of undistorted artifact-free EEG segments before and after artifact elimination. The ideal expectation is to have these portions undistorted after artifacts have been removed. FastCCA, FastEMD-CCA^2 and FORCe records an average specificity of 99.74%, 99.22% and 98.65% respectively on the Hitachi dataset. Specificity of 100% is achieved by all three algorithms on the INV-SK dataset. This signifies that these algorithms do not introduce much distortion to the neural information of the EEG signals under evaluation. From the comparison, it is clear that FastCCA and FastEMD-CCA^2 have achieved better performance than FORCe on the same set of EEG signals.

The average computation time FastCCA and FastEMD-CCA^2 took to remove eyeblink artifacts from 14-channel EEG signals with an average signal length of 312s (Hitachi dataset) is 6.87 and 6.78 seconds respectively, while FORCe took 85.10 seconds. FastCCA, FastEMD-CCA^2 and FORCe took 7.20s, 4.31s and 85.94s respectively on the other dataset, INV-SK, with an average signal length of 266s. The computation time of FastEMD-CCA^2 and FastCCA is at least 12 times faster than that of FORCe for Hitachi's dataset. On INV-SK's dataset, FastEMD-CCA^2 is 19 times faster and FastCCA is 12 times faster than FORCe.

It has to be noted that although FastCCA is better than FastEMD-CCA^2 as demonstrated by accuracy, error rate and sensitivity measurement, it is slower than FastEMD-CCA^2 in terms of processing time. This can be due to the difference in the detection mechanism of the eyeblink artifact events in these algorithms. In FastEMD-CCA^2, eADA is used to locate a suitable eyeblink artifact frame, which is then extracted out as a general eyeblink artifact template using FastEMD with CCA. The extracted general eyeblink artifact template is used to identify the remaining eyeblink artifact events in that EEG signal. Whereas in FastCCA, every eyeblink artifact event is continuously searched by the eADA algorithm to be removed by CCA, so justifying the time difference between these algorithms. The average processing time of FastEMD-CCA^2 is about 21.7ms (Hitachi) and 16.20ms (INV-SK) to remove artifacts from a 1-second length of 14-channel EEG signal (256 sample points x 14 EEG channels). The next is FastCCA with an average processing time of 22ms (Hitachi) and 27.04ms (INV-SK) to remove eyeblink artifacts from a 1-second length of EEG signal. The slowest processing time is recorded by FORCe, with 272.5ms (Hitachi) and 323.01ms (INV-SK) to remove eyeblink artifacts from a 1-second length of EEG signal.

The results indicate that the proposed algorithm, FastCCA is highly accurate in removing eyeblink artifacts, as demonstrated by accuracy, error rate and sensitivity measurement. However, the results are not significantly better than FastEMD-CCA^2. Considering the average processing time, FastEMD-CCA^2 is a better choice for online applications compared to FastCCA, but again the processing time of FastEMD-CCA^2 is not significantly better than FastCCA. So, both proposed algorithms can be used for applications requiring online removal of eyeblink artifacts with high accuracy.

Despite the fact that the FastEMD-CCA^2 and FastCCA algorithms achieve attractive performance scores on both Hitachi and INV-SK datasets, these algorithms still fail to detect

and remove some of the eyeblink artifacts. FastEMD-CCA^2 was unable to detect and remove nearly 137 and 103 eyeblink artifact events on the Hitachi and INV-SK's dataset respectively, which accounts for about 2% of error rate. The undetected and unremoved eyeblink artifacts are analyzed to find out the root cause for the failure, although the error rate is quite low. The invalidity of the assumption mostly causes the failure cases, which assumes that every eyeblink artifact event within a subject exhibits a consistent pattern, similar to the eyeblink artifact template. In FastEMD-CCA^2, the general eyeblink template, is assumed closely correlates with all eyeblink artifact events in that EEG signal, so it is used as a reference template to locate the remaining eyeblink artifacts. Theoretically, the correlation between the general eyeblink artifact template and every EEG segment that is contaminated by eyeblink artifact is expected to be $\geq$0.9. In a practical scenario, this is not the case, whereby observations and validation on the real EEG signals, revealed that the correlation often lies in the range of 0.4 to 0.6. Hence, using an artifact template with a low correlation threshold of 0.4, as shown in the proposed flowchart in Fig. 4.14, to rule out if an EEG segment is contaminated by eyeblink artifact may fail occasionally. For instance, if an EEG segment contaminated with eyeblink artifact exhibits a correlation of lower than 0.4 with the eyeblink artifact template, this EEG segment will not be identified as containing an eyeblink artifact, producing a false negative scenario. So a correlation of 0.4 is considered strict for this eyeblink artifact event, and the algorithm could miss the occurrence of the eyeblink artifact. Similarly, if an uncontaminated EEG segment exhibits a correlation of more than 0.4 with the eyeblink artifact template, this EEG segment will be identified as containing an eyeblink artifact, although it does not, developing a false positive scenario. Subsequent application of CCA to this EEG segment to remove eyeblink artifact is irrelevant and may cause loss of neural information. Whereas in FastCCA, CCA is directly applied to EEG segments identified contaminated by eyeblink artifacts with the existing eADA algorithm. This allows an adaptive detection and removal of eyeblink artifacts for every event of blink. Thus the algorithm is not dependent on a general template for artifact detection.

This explains why the average accuracy, sensitivity and specificity of FastEMD-CCA^2 are lower than FastCCA by 1.57%, 1.79%, and 0.52%, respectively on the Hitachi dataset. In summary, it can be concluded that in FastEMD-CCA^2, eyeblink artifacts that are irregular in pattern compared with the eyeblink template extracted are not classified as eyeblink artifacts, thereby not getting removed. Similarly, when an artifact-free EEG segment exhibits an artifact-like pattern, this segment is misclassified as an eyeblink artifact and subjected to eyeblink artifact rejection, although it isn't contaminated by an eyeblink artifact. The high accuracy, sensitivity and specificity level of both algorithms suggest that these approaches are reliable in detecting and removing eyeblink artifacts in real-time ; however, FastCCA is a better choice because of its better performance over FastEMD-CCA^2.

5.2.3.1/ Welch ANOVA Results for Hitachi Dataset

The computation time, accuracy, sensitivity, specificity and error rate for FORCe and the proposed algorithms, FastEMD-CCA^2 and FastCCA for the Hitachi dataset are checked if statistically significant. Again, before conducting the ANOVA test, the normality of these parameters is tested with the Shapiro-Wilk. The distribution normality of these parameters is given in Table 5.9.

TABLE 5.9 – Test of Normality for the Hitachi Dataset

Performance Measure	Algorithm	Sig.
Time	**FORCe**	0.137
	FastEMD-CCA^2	0.000
	FastCCA	0.000
Error Rate	**FORCe**	0.893
	FastEMD-CCA^2	0.032
	FastCCA	0.000
Accuracy	**FORCe**	0.893
	FastEMD-CCA^2	0.032
	FastCCA	0.000
Sensitivity	**FORCe**	0.581
	FastEMD-CCA^2	0.077
	FastCCA	0.000
Specificity	**FORCe**	0.000
	FastEMD-CCA^2	0.000
	FastCCA	0.000

From Table 5.9, statistically significant values ($P<0.05$) are observed for all parameters except for FORCe on time, error rate, accuracy and sensitivity. In this case, it is concluded that not all the parameters are not normally distributed. Since the performance measures achieved by FORCe, FastEMD-CCA^2 and FastCCA are not normally distributed, the assumption of homogeneity of variances is violated. So a Welch ANOVA test is conducted instead of the one-way ANOVA. The results of the Welch ANOVA test are provided in Table 5.10.

TABLE 5.10 – Welch ANOVA Test for the Hitachi Dataset

Performance Measure	Between Algorithms		Sig.
Time	FORCe	FastEMD-CCA^2	0.000
		FastCCA	0.000
	FastEMD-CCA^2	FORCe	0.000
		FastCCA	0.992
	FastCCA	FORCe	0.000
		FastEMD-CCA^2	0.992
Error Rate	FORCe	FastEMD-CCA^2	0.000
		FastCCA	0.000
	FastEMD-CCA^2	FORCe	0.000
		FastCCA	0.000
	FastCCA	FORCe	0.000
		FastEMD-CCA^2	0.000
Accuracy	FORCe	FastEMD-CCA^2	0.000
		FastCCA	0.000
	FastEMD-CCA^2	FORCe	0.000
		FastCCA	0.000
	FastCCA	FORCe	0.000
		FastEMD-CCA^2	0.000
Sensitivity	FORCe	FastEMD-CCA2	0.000
		FastCCA	0.000
	FastEMD-CCA^2	FORCe	0.000
		FastCCA	0.000
	FastCCA	FORCe	0.000
		FastEMD-CCA^2	0.000
Specificity	FORCe	FastEMD-CCA2	0.364
		FastCCA	0.011
	FastEMD-CCA^2	FORCe	0.364
		FastCCA	0.288
	FastCCA	FORCe	0.011
		FastEMD-CCA^2	0.288

From the Welch ANOVA test, a significant difference for the time is observed between FastEMD-CCA^2, FastCCA and FORCe. Also between FastEMD-CCA^2 and FastCCA the P-value is 0.992, which means the computation time between FastEMD-CCA^2 and FastCCA is not statistically significant. Statistical significance observed on error rate, accuracy and sensitivity between all three algorithms, FORCe, FastEMD-CCA^2 and FastCCA too, with P=0.000. For specificity, significant results observed between FORCe and FastCCA, with P=0.011. In general, the proposed algorithms produce significant results compared to FORCe.

5.2.3.2/ WELCH ANOVA RESULTS FOR INV-SK DATASET

Similar to the Hitachi dataset, the Welch ANOVA is carried out on the INV-SK dataset. The test results are provided in Table 5.11.

TABLE 5.11 – Welch ANOVA Test for the INV-SK Dataset

Performance Measure	Between Algorithms		Sig.
Time	FORCe	FastEMD-CCA^2	0.000
		FastCCA	0.000
	FastEMD-CCA^2	FORCe	0.000
		FastCCA	0.000
	FastCCA	FORCe	0.000
		FastEMD-CCA^2	0.000
Error Rate	FORCe	FastEMD-CCA2	0.033
		FastCCA	0.002
	FastEMD-CCA^2	FORCe	0.033
		FastCCA	0.443
	FastCCA	FORCe	0.002
		FastEMD-CCA^2	0.443
Accuracy	FORCe	FastEMD-CCA2	0.033
		FastCCA	0.002
	FastEMD-CCA^2	FORCe	0.033
		FastCCA	0.443
	FastCCA	FORCe	0.002
		FastEMD-CCA^2	0.443
Sensitivity	FORCe	FastEMD-CCA^2	0.061
		FastCCA	0.018
	FastEMD-CCA^2	FORCe	0.061
		FastCCA	0.778
	FastCCA	FORCe	0.018
		FastEMD-CCA^2	0.778

A significant difference is observed between all three algorithms, FORCe, FastEMD-CCA^2 and FastCCA for time, with P=0.000 between them. For error rate and accuracy, no statistical significance observed between FastEMD-CCA^2 and FastCCA, with P=0.443, but these algorithms are significant compared to FORCe. The results are also not significant for sensitivity measurement, between FORCe and FastEMD-CCA^2 (P=0.061), and between FastEMD-CCA^2 and FastCCA (P=0.776). It can be concluded that the proposed algorithms produced significant computation time, error rate and accuracy in comparison to FORCe.

5.3/ SUMMARY

Based on the results and discussions, it is apparent that the automated and unsupervised eyeblink artifact detection algorithm proposed in this chapter is accurate in identifying eyeblink artifact events in an EEG signal. On the other hand, the algorithm is also consistent in detecting eyeblink artifacts across different EEG signals compared to the conventional algorithm, which uses a constant threshold to detect eyeblink artifacts. Thus, it can be concluded that the proposed algorithm is a reliable solution in detecting eyeblink artifacts across all types of EEG signals, which may have individual variance due to blinking duration, pattern and strength.

Next, the proposed eyeblink artifact removal algorithms proved to be effective in automatically identifying and eliminating eyeblink artifacts from multi-channel EEG signals without

the need to have an EOG channel as an artifact reference. Analysis proved that the proposed algorithms, FastEMD-CCA^2 and FastCCA are computationally fast and accurate. The algorithms appear promising to be used for online applications. The computation environment is crucial for any application that requires online processing. Currently, MATLAB is the most popular tool used for research purposes, but for online artifact removal applications, MATLAB alone may not be a feasible platform. Hence, the next chapter will discuss the implementation of eADA, FastEMD and CCA in an inexpensive computing environment, C++, to investigate the feasibility of the algorithms to support online applications.

TABLE 5.2 – Comparison of Eyeblink Artifact Detection Accuracy

Signal	Accuracy (%)					
	Proposed (Automated Varying Threshold, eADA)	Constant Thresholds				
		10uV	20uV	30uV	40uV	50uV
EEG 1	100.00	90.70	95.35	74.42	46.51	27.91
EEG 2	100.00	94.23	96.15	84.62	55.77	46.15
EEG 3	100.00	97.22	97.22	77.78	58.33	50.00
EEG 4	100.00	100.00	100.00	80.56	55.56	38.89
EEG 5	94.34	84.91	90.57	88.68	58.49	47.17
EEG 6	100.00	92.31	92.31	80.77	55.13	46.15
EEG 7	100.00	98.11	95.28	90.57	83.02	66.98
EEG 8	98.96	92.71	89.58	89.58	86.46	64.58
EEG 9	100.00	97.75	95.51	95.51	82.02	59.55
EEG 10	100.00	95.70	91.40	89.25	83.87	68.82
EEG 11	100.00	92.63	87.37	86.32	82.11	63.16
EEG 12	100.00	90.14	85.92	85.92	80.28	78.87
EEG 13	100.00	97.62	95.24	88.89	48.41	22.22
EEG 14	100.00	98.84	98.84	94.77	71.51	23.26
EEG 15	100.00	92.51	98.93	98.93	86.63	43.32
EEG 16	100.00	98.36	97.81	96.17	89.07	45.36
EEG 17	100.00	98.31	98.31	98.31	93.79	46.89
EEG 18	99.45	99.45	98.90	98.90	93.37	61.33
EEG 19	100.00	96.92	90.00	86.92	69.23	56.15
EEG 20	98.84	96.51	96.51	86.05	60.47	44.19
EEG 21	100.00	94.94	97.47	88.61	50.63	27.85
EEG 22	100.00	98.23	93.81	84.96	59.29	46.90
EEG 23	100.00	94.44	90.28	86.11	55.56	45.83
EEG 24	98.00	98.00	92.00	78.00	72.00	50.00
EEG 25	100.00	97.87	95.74	92.55	92.55	82.98
EEG 26	99.19	98.39	98.39	97.58	94.35	91.13
EEG 27	100.00	96.09	99.22	96.88	93.75	87.50
EEG 28	99.35	98.69	99.35	96.08	94.77	91.50
EEG 29	99.00	94.00	95.00	92.00	83.00	80.00
EEG 30	100.00	92.13	88.76	82.02	79.78	68.54

Table 5.2 continued from previous page

Signal	Accuracy (%)					
	Proposed (Automated Varying Threshold, eADA)	Constant Thresholds				
		10uV	20uV	30uV	40uV	50uV
EEG 31	99.44	93.26	94.38	97.19	97.19	97.75
EEG 32	99.26	99.26	99.26	98.52	98.52	94.81
EEG 33	97.47	94.30	94.30	100.00	99.37	97.47
EEG 34	97.31	92.47	93.01	97.31	94.09	93.55
EEG 35	97.47	94.30	96.20	100.00	100.00	98.73
EEG 36	98.16	93.25	94.48	100.00	98.16	96.93
EEG 37	100.00	94.00	97.00	99.00	98.00	95.00
EEG 38	100.00	99.01	100.00	100.00	100.00	100.00
EEG 39	100.00	94.74	100.00	98.95	98.95	98.95
EEG 40	100.00	89.87	97.47	98.73	100.00	98.73
EEG 41	100.00	97.56	97.56	98.78	98.78	98.78
EEG 42	100.00	98.85	98.85	98.85	98.85	96.55
EEG 43	100.00	100.00	100.00	100.00	94.57	88.37
EEG 44	100.00	97.66	98.44	98.44	97.66	95.31
EEG 45	97.76	96.27	94.78	94.03	94.03	88.06
EEG 46	99.40	100.00	100.00	100.00	98.80	95.81
EEG 47	100.00	100.00	100.00	100.00	99.43	95.43
EEG 48	100.00	93.98	98.80	98.80	98.19	87.35
EEG 49	100.00	95.83	93.33	90.83	89.17	84.17
EEG 50	100.00	99.19	98.39	96.77	95.97	87.90
EEG 51	100.00	89.57	95.65	94.78	92.17	82.61
EEG 52	100.00	92.59	87.96	86.11	84.26	79.63
EEG 53	100.00	81.48	72.84	71.60	70.37	62.96
EEG 54	99.05	95.24	93.33	93.33	90.48	80.95
EEG 55	99.14	97.41	95.69	95.69	95.69	92.24
EEG 56	100.00	95.20	98.40	97.60	96.00	95.20
EEG 57	98.73	93.67	95.57	95.57	94.94	92.41
EEG 58	100.00	97.37	96.49	95.61	94.74	94.74
EEG 59	99.44	91.53	99.44	96.61	96.05	95.48
EEG 60	98.36	96.72	97.81	99.45	93.99	97.81
AVERAGE	99.47	95.37	95.34	92.67	84.57	73.95

6

IMPLEMENTATION OF FASTEMD-CCA^2 AND FASTCCA IN C++

In this chapter, the proposed algorithms, FastEMD-CCA^2 and FastCCA are implemented in C++. As discussed earlier, an online artifact removal algorithm should be an unsupervised approach, fully automatic, and doesn't depend on reference electrodes for artifact identification. Apart from this, the online artifact removal algorithm should be able to process the EEG signals in windows or blocks to reduce computational cost. This will automatically improve the processing speed of the online algorithm, thus not introducing an unacceptable time delay to the entire application. The computational environment of which the eyeblink artifact removal algorithm is implemented plays a vital role in online applications. The proposed approaches are implemented and evaluated in an inexpensive computing environment, C++ programming language, to investigate the feasibility of the approaches in accommodating online applications. The reason the algorithms are implemented in C++ is to investigate the computation time or the processing speed the proposed algorithms, FastEMD-CCA^2 and FastCCA could achieve, in line to support an online application.

6.1/ IMPLEMENTATION STRATEGIES FOR ONLINE ARTIFACT REMOVAL

Sixty EEG signals that were used to evaluate the proposed approaches were collected at Hitachi, Hatayoma site in Japan, as stated in Chapter 4. These EEG signals are recorded following the 10-20 international standardization with free electrodes placed on the scalp. The EOG electrodes that capture eyeblink events are not used to record the EOG signals for convenience purpose. Validation whether the eyeblink artifacts are removed turns out to be difficult due to the unavailability of eyeblink ground truths. Thus, an expert's advice is required to substantiate if the approaches are able to remove eyeblink artifacts effectively.

In order to achieve an online implementation of the proposed approaches in removing eyeblink artifacts from EEG signals, two implementation procedures are proposed. First, the proposed algorithms are executed and processing is performed in small EEG windows, rather than applying the proposed algorithm to the entire EEG signal. Secondly, the proposed algorithms are implemented and evaluated with a compiled language, the C++ language on an Ubuntu Linux 14.04 (64-bit OS, 4GB RAM).

The proposed algorithms, FastEMD-CCA^2 and FastCCA are initially implemented in MAT-

LAB, then followed by C++. In MATLAB, the entire multichannel EEG signal is imported into MATLAB's workspace for processing. The algorithms are executed and artifact correction is performed on overlapping windows, with each window being about 1.95s in length. In the C++ language, the algorithms are executed in Ubuntu to process the EEG signals in a simulated online setting. The proposed algorithms are designed to stream EEG recording on a sample by sample basis to fill up a buffer. Once a 1.95s length of EEG epoch is buffered, the epoch will be subjected to unsupervised artifact detection and artifact removal.

6.2/ Performance Evaluation

The competency of an online eyeblink artifact removal algorithm relies on the processing speed of the algorithm, where the time taken for artifact elimination from EEG signals should be acceptable for an online application. The time taken for a system to be considered as real-time is still debatable, but estimated to be between 6 and 20 milliseconds [164]. As stated earlier, the reason for the proposed algorithms implemented in C++ is to investigate the processing speed the algorithms can achieve. So, the other performance measures should remain the same as they are the same algorithms, regardless of the implementation platform. This is feasible only if the algorithms are correctly implemented in C++. So, visual inspection and quantitative analysis in the time and frequency domains are performed on the EEG signals to verify whether the algorithms are correctly implemented in C++, compared to MATLAB. On the whole, the algorithm should achieve instantaneous artifact correction without loss of neural information, to be useful in online applications.

6.2.1/ Offline Evaluation

The proposed algorithms are evaluated through offline analysis performed on the online processed EEG signals after artifact correction, in MATLAB and C++. The analysis is conducted on 60 EEG signals, described in Chapter 4, section 4.1.2.1. The effectiveness of the proposed algorithms, FastEMD-CCA[2] and FastCCA in both MATLAB and C++ is evaluated through visual inspection on the EEG signals with measures such as error (Eq. (4.16)), accuracy(Eq. (4.17)), sensitivity(Eq. (4.18)) and specificity(Eq. (4.19)).

Supplementary to eyeblink artifact detection and rejection, the performance of the proposed algorithms in retaining the neural information were quantitatively assessed. Randomly selected artifact-free EEG segments from the above-mentioned 60 EEG recordings are used for this purpose. One randomly selected artifact-free EEG segment is assessed from each EEG signal. Ideally, it is expected that these segments remain undistorted, even after the artifacts have been removed. The evaluation is carried out in both time and frequency domains.

In the time domain, the correlation coefficient (CC), root mean square error (RMSE) and similarity index (η_{dB}) [108] are used to measure how well the proposed algorithms have preserved the artifact-free EEG segments after artifact correction. CC in Eq. (6.1) measures the similarity between the original artifact-free EEG segment, $X_{in}(t)$ with its corres-

ponding reconstructed EEG segment, $X_{out}(t)$ after artifact removal.

$$\text{CC} = \frac{C_{X_{\text{in}}(t),X_{\text{out}}(t)}}{\sigma_{X_{\text{in}}(t)} * \sigma_{X_{\text{out}}(t)}} \tag{6.1}$$

RMSE measures the reconstruction error between original artifact-free EEG segment and the reconstructed EEG segment. In Eq. (6.2), n is the number of sample points in the EEG segment :

$$\text{RMSE} = \sqrt{\frac{\sum_{t=1}^{n}(X_{\text{in}}(t) - X_{\text{out}}(t))^2}{n}} \tag{6.2}$$

Similarity index (η_{dB}) in Eq. (6.3), of the artifact-free EEG segment is computed to quantify the degree of neural information preservation.

$$\eta_{dB} = 10\log_{10}\left[\frac{\sum_{t=1}^{n}(1 - X_{\text{in}}(t) - X_{\text{out}}(t))}{n}\right] \tag{6.3}$$

In frequency domain, the mean absolute error (MAE) and mean absolute percentage error (MAPE) in Eq. (6.4) and (6.5) as suggested in [16] are calculated.

$$\text{MAE} = \left|P_{X_{\text{in}}(t)} - P_{X_{\text{out}}(t)}\right| \tag{6.4}$$

$$\text{MAPE} = \left|\frac{P_{X_{\text{in}}(t)} - P_{X_{\text{out}}(t)}}{P_{X_{\text{in}}(t)}}\right| \times 100 \tag{6.5}$$

MAE is used to measure any distortion in power spectral densities, $P_{X_{in}(t)}$ and $P_{X_{out}(t)}$ across different frequency bands of an artifact-free EEG segment. MAE is evaluated over five different frequency bands, including delta δ waves, theta θ waves, alpha α waves, beta β waves and gamma γ waves. It is expected that after artifact correction, the MAE has a value nearing 0, indicating minimal loss of neural information. MAPE is used to estimate the distortion percentage in every frequency band of the artifact-free EEG segment.

6.2.2/ Online Evaluation

The online performance of the proposed algorithms is evaluated in terms of the computation time taken by the algorithms in removing artifacts from EEG signals. The processing speed taken by both algorithms in two different platforms, MATLAB R2018b in Windows 7 Professional (64 bit OS, 4GB RAM) and C++ language on an Ubuntu Linux 14.04 (64-bit OS, 4GB RAM), are recorded for evaluation purpose. The computation time is interpreted as the computing efficiency of the algorithms in cleaning the eyeblink artifacts online. Hence, it is used to evaluate the feasibility of the algorithms for online processing, whether they can achieve instantaneous artifact removal. Whichever algorithm that achieves a shorter computation time denotes better computing efficiency, making it a more suitable candidate for online eyeblink artifact removal applications.

6.3/ Results and Discussion

6.3.1/ Offline Analysis Results through Visual Inspection

The EEG signals are subjected to online eyeblink artifact elimination via FastEMD-CCA[2] and FastCCA in MATLAB computing environment and C++ programming language. Visual comparison of Fp1 channel of EEG 3, before and after artifact correction using FastEMD-CCA[2] and FastCCA in MATLAB and C++ are presented in Figs. 6.1 and 6.2.

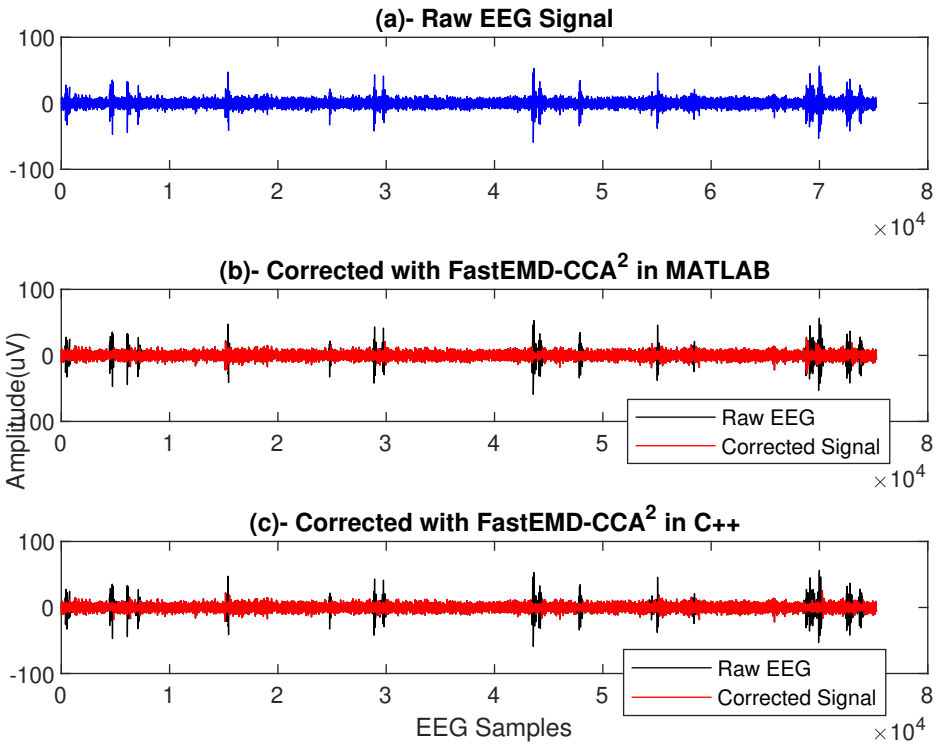

Figure 6.1 – Recovered EEG Signal from Fp1 Channel through FastEMD-CCA[2] in MATLAB and C++

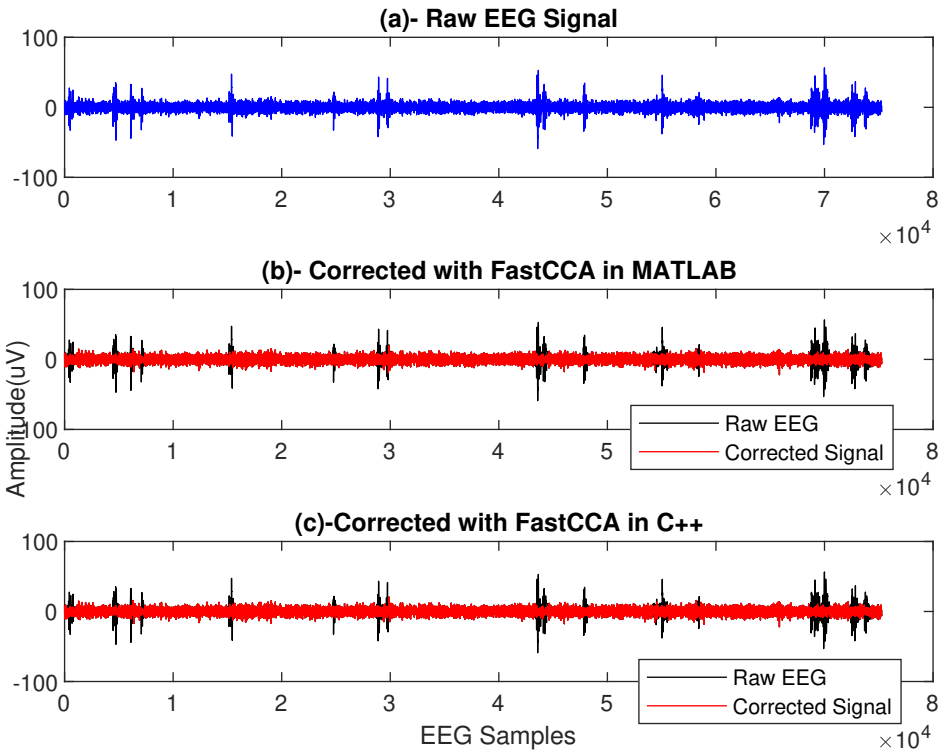

FIGURE 6.2 – Recovered EEG Signal from Fp1 Channel through FastCCA in MATLAB and C++

Screen-shots of EEG3's Fp1 channel display in the C++ programming language, after artifact correction through FastEMD-CCA[2] and FastCCA are shown in Figs. 6.3 and 6.4.

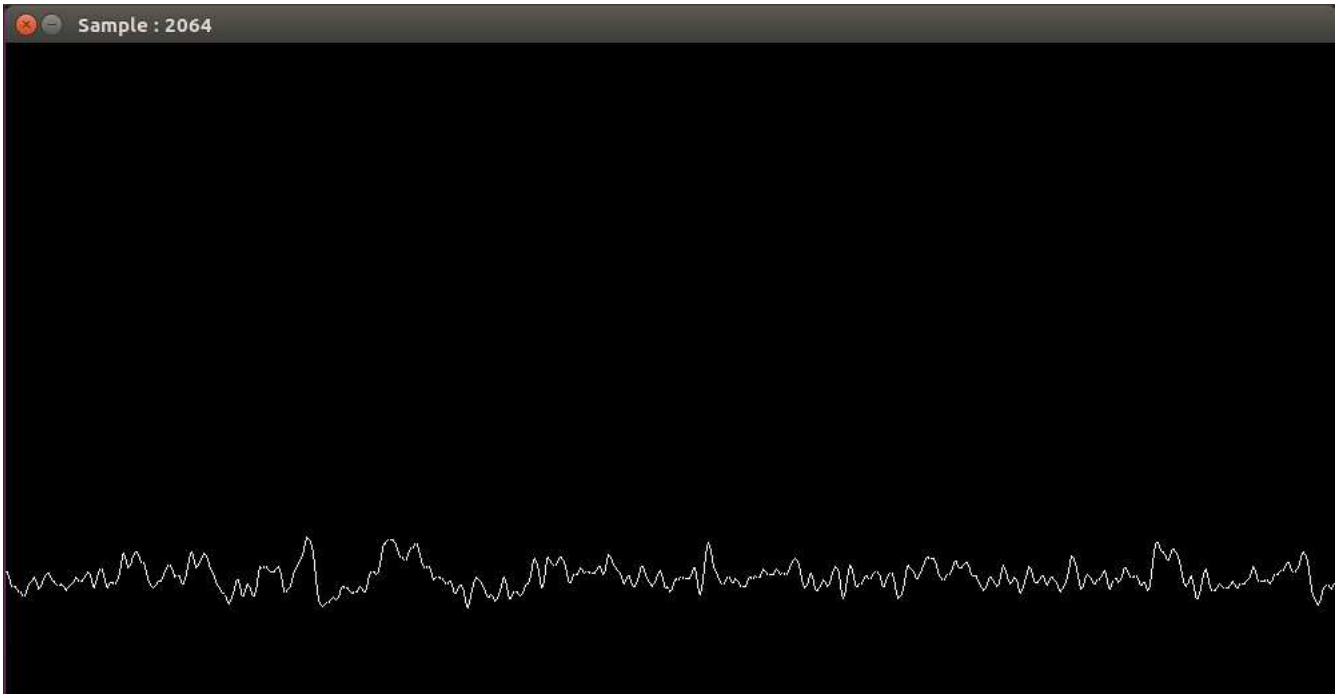

FIGURE 6.3 – Display of Recovered EEG Signal from Fp1 Channel through FastEMD-CCA^2 in C++

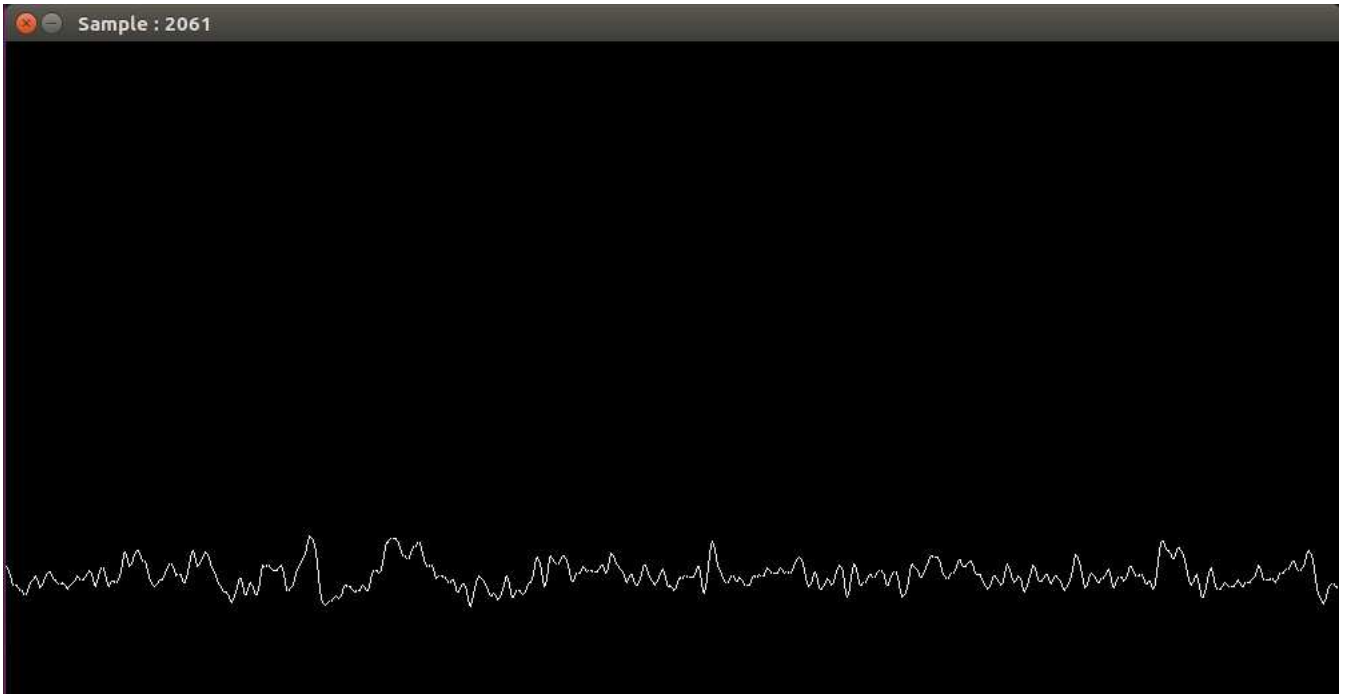

FIGURE 6.4 – Display of Recovered EEG Signal from Fp1 Channel through FastCCA in C++

Figs. 6.5, 6.6, 6.7 and 6.8 visualize multichannel EEG signal of EEG 3, before and after artifact correction using FastEMD-CCA^2 and FastCCA in MATLAB and C++.

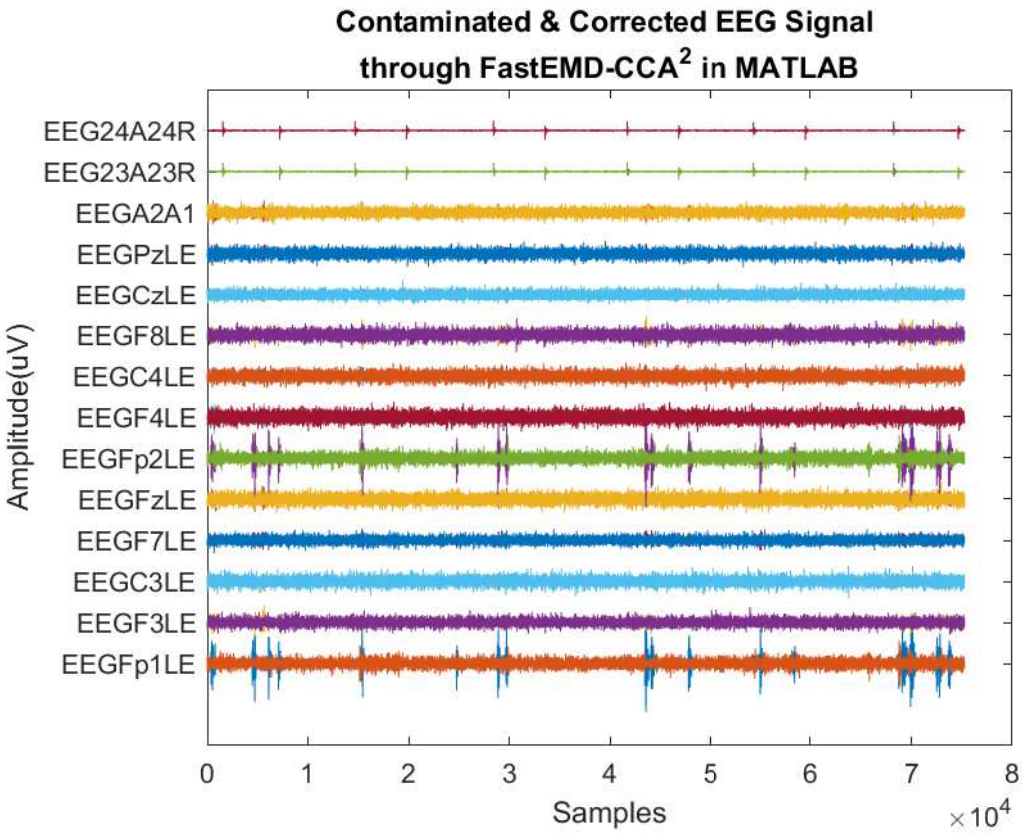

FIGURE 6.5 – Recovered Multichannel EEG Signal through FastEMD-CCA^2 in MATLAB

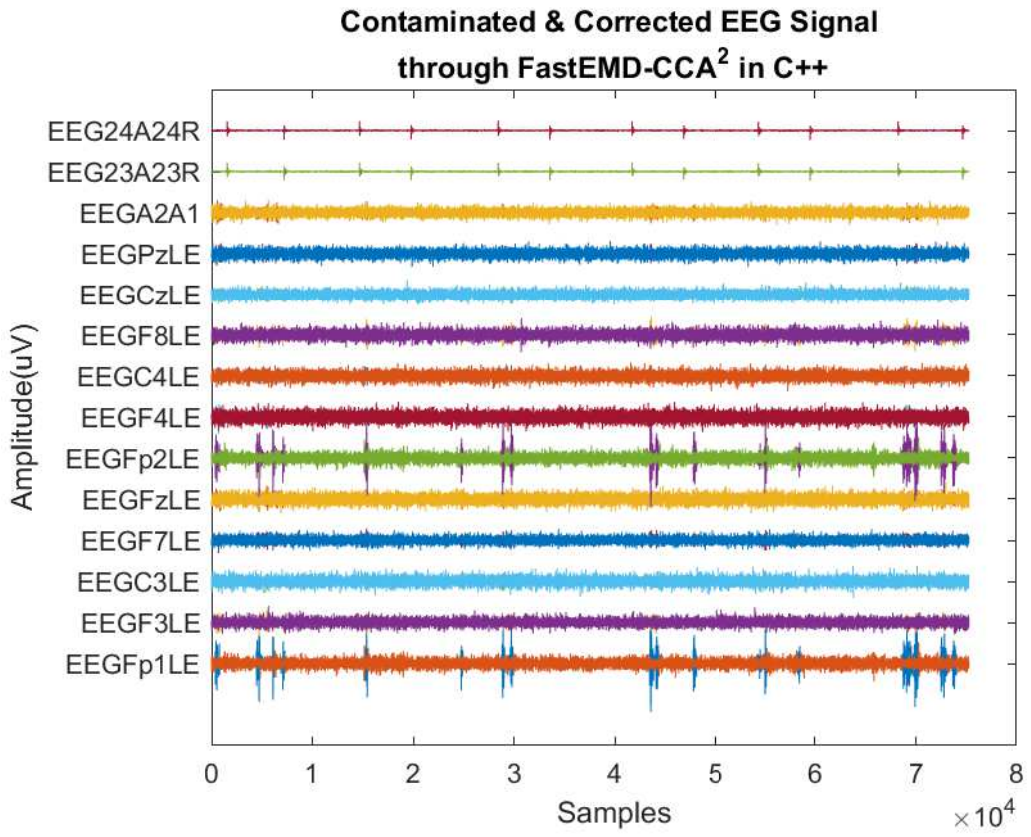

FIGURE 6.6 – Recovered Multichannel EEG Signal through FastEMD-CCA^2 in C++

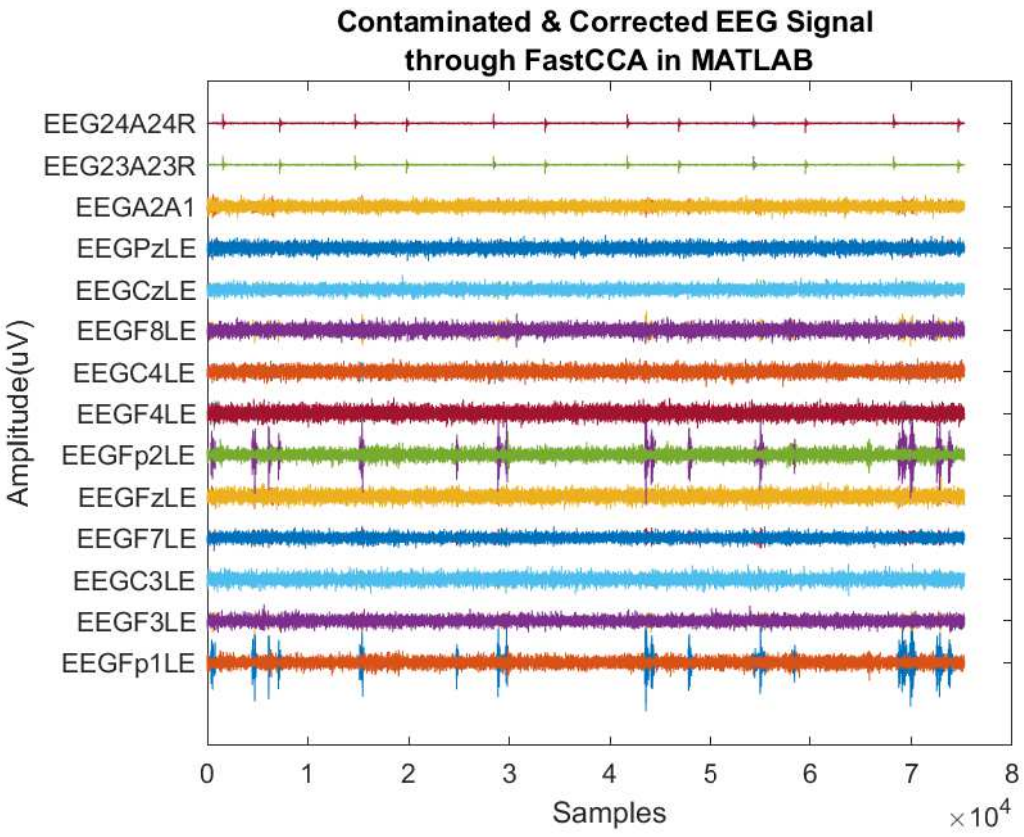

FIGURE 6.7 – Recovered Multichannel EEG Signal through FastCCA in MATLAB

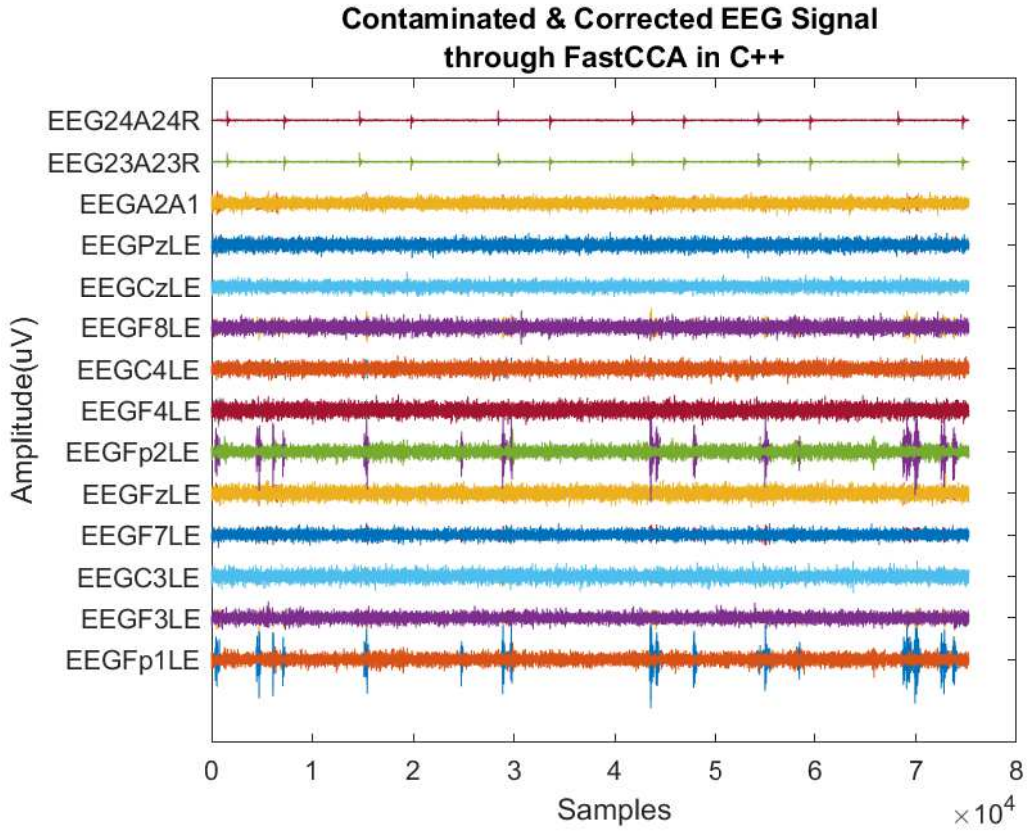

FIGURE 6.8 – Recovered Multichannel EEG Signal through FastCCA in C++

The average error rate, accuracy, sensitivity and specificity obtained through Eqs. (4.16), (4.17), (4.18) and (4.19), by offline visual inspection on the corrected EEG signals are presented in Table 6.1. The individual representation of error, accuracy, sensitivity and specificity are presented in **Appendix A**.

TABLE 6.1 – Average Performance Metrics of FastEMD-CCA^2 and FastCCA in MATLAB and C++

Average (%)				
Multichannel EEG Signal	**FastEMD-CCA^2**		**FastCCA**	
	MATLAB	**C++**	**MATLAB**	**C++**
Error Rate	2.10	2.10	0.53	0.53
Accuracy	97.9	97.9	99.47	99.47
Sensitivity	97.65	97.65	99.44	99.44
Specificity	99.22	99.22	99.74	99.74

6.3.1.1/ Discussion

Results in Tables A.1, A.2, A.3 and A.4 represent the individual error rate, accuracy, sensitivity and specificity obtained through offline manual visual inspection performed on the artifact-free EEG signals that have been processed online. FastEMD-CCA^2 has achieved similar performance measures in both MATLAB and C++, i.e error rate of 2.10%, accuracy of 97.9%, sensitivity of 97.65% and specificity of 99.22%. Similarly, FastCCA has achieved an error rate of 0.53%, accuracy of 99.47%, sensitivity of 99.44% and specificity of 99.74%, in both MATLAB and C++. Achieving similar performance measures in removing the eyeblink artifacts in both platforms is expected, proving that the algorithms are implemented correctly in C++.

6.3.2/ Offline Analysis Results through Quantitative Evaluation

6.3.2.1/ Time Domain Analysis

The performance of the proposed algorithms in preserving the underlying neural information of an EEG signal is evaluated on randomly selected artifact-free EEG segments, after artifact correction. One artifact-free Fp1 EEG segment is evaluated on every EEG signal. Some of the EEG signals are excluded from this analysis as they are contaminated by too many eyeblink artifacts, making it difficult to select a proper artifact-free EEG segment. The EEG signals that are excluded from the analysis are EEG 14-18, EEG 25-36, EEG 45-50 and EEG 57-60.

Figs. 6.9 and 6.10 show visual comparison of a short segment of EEG recording (EEG 3), corrected using FastEMD-CCA^2 and FastCCA in MATLAB and C++. From Fig. 6.9, it can be seen that the proposed algorithms are able to remove eyeblink artifacts effectively and Fig. 6.10 shows a portion of reconstructed artifact-free segment that overlaps well with the raw EEG segment. Visual inspection on the removed eyeblink artifacts and the reconstructed artifact-free EEG segment shows both algorithms are effective in eyeblink artifact removal and preserving the neural information.

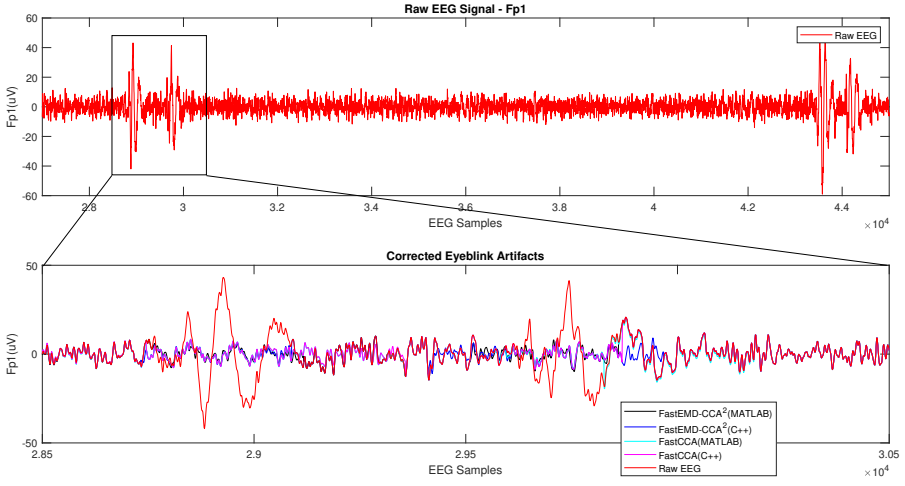

FIGURE 6.9 – Corrected Eyeblink Artifact Regions through FastEMD-CCA^2 and FastCCA in MATLAB and C++

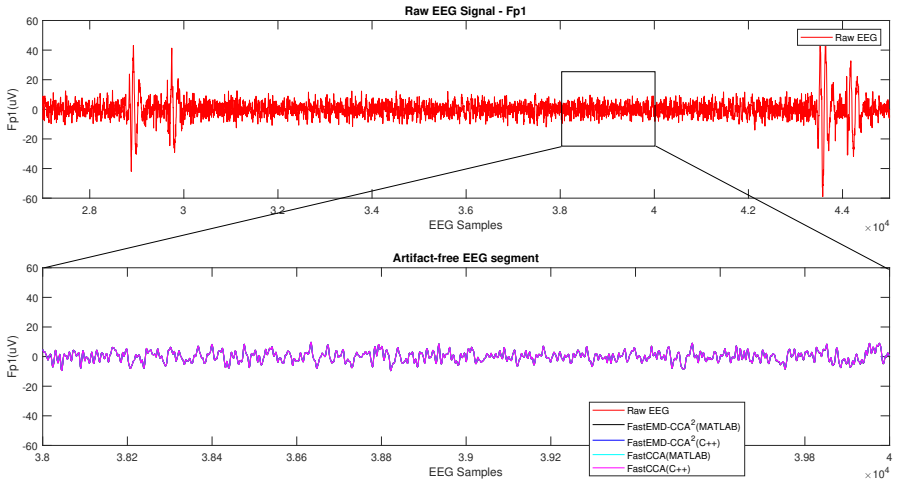

FIGURE 6.10 – Reconstructed Artifact-free EEG through FastEMD-CCA^2 and FastCCA in MATLAB and C++

The individual results obtained for CC, RMSE and Similarity Index (η_{dB}), of the artifact-free Fp1 EEG segments are presented in **Appendix A**. Table 6.2 presents the average CC, RMSE and Similarity Index (η_{dB}), of the artifact-free Fp1 EEG segments.

TABLE 6.2 – Average CC, RMSE and η_{dB} of FastEMD-CCA^2 and FastCCA in MATLAB and C++

Average				
Multichannel EEG Signal	**FastEMD-CCA^2**		**FastCCA**	
	MATLAB	**C++**	**MATLAB**	**C++**
Correlation Coefficient (CC)	0.9992	0.9999	0.9993	0.9998
Root Mean Square Error (RMSE)	0.1572	0.0154	0.1010	0.0227
Similarity Index (η_{dB})	-0.3132	0.0010	-0.1377	0.0009

6.3.2.2/ FREQUENCY DOMAIN ANALYSIS

In order to evaluate the proposed algorithms in the frequency domain, the mean absolute error (MAE) and mean absolute percentage error (MAPE) are calculated. The performance of the proposed algorithms in preserving the underlying neural information of an EEG signal is evaluated on randomly selected artifact-free EEG segments, after artifact correction. One artifact-free Fp1 EEG segment is evaluated on every EEG signal. Similar to time-domain analysis, some of the EEG signals are excluded from the analysis due to the presence of too many eyeblink artifacts. The results obtained for MAE and MAPE across five different frequency bands are given in **Appendix A**. The average MAE and MAPE across five different frequency bands of these EEG signals are tabulated in Tables 6.3 and 6.4.

TABLE 6.3 – Average MAE of FastEMD-CCA^2 and FastCCA in Different Frequency Bands

Average Mean Absolute Error		
Multichannel EEG Signal	**Delta**	
	FastEMD-CCA2	**FastCCA**
Delta	0.0059	0.0035
Theta	0.0004	0.0001
Alpha	0.0002	0.0004
Beta	0.0000	0.0001
Gamma	0.0000	0.0000

TABLE 6.4 – Average MAPE of FastEMD-CCA^2 and FastCCA in Different Frequency Bands

Average Mean Absolute Percentage Error (%)		
Multichannel EEG Signal	**Delta**	
	FastEMD-CCA2	**FastCCA**
Delta	0.0343	0.0201
Theta	0.0087	0.0044
Alpha	0.0044	0.0125
Beta	0.0096	0.0193
Gamma	0.0879	0.3777

6.3.2.3/ DISCUSSION

In the time domain, CC, RMSE and similarity index are used to evaluate the ability of the proposed algorithms in retaining neural information contained on artifact-free EEG segments. The proposed algorithms, FastEMD-CCA^2 and FastCCA are implemented in MATLAB and C++ to remove eyeblink artifacts from the EEG signals. Twenty-seven EEG signals designated with ”na” in Tables A.5, A.6 and A.7 are excluded from the analysis as they are contaminated by too many eyeblink artifacts, leading to difficulty in identifying proper artifact-free EEG segments. Hence, only 33 EEG signals out of 60 EEG signals are used for quantitative analysis. The artifact-free EEG segments in an EEG signal are expected to be unaffected, and the neural information in these segments should remain intact after artifact elimination is performed. The effectiveness of the proposed algorithms in preserving the underlying EEG information can be deduced through CC value that approaches 1, RMSE and η_{dB} that is close to 0.

The average RMSE and η_{dB} are very low, RMSE ranges between 0.0154 to 0.1572 and η_{dB} range between -0.3132 to 0.0010. The highest average RMSE was recorded

by FastEMD-CCA^2 in MATLAB, but it produced the least RMSE in C++. The average CC value for FastEMD-CCA^2 is 0.9992 and 0.9999 in MATLAB and C++ respectively. FastCCA has achieved average CC value of 0.9993 in MATLAB and 0.9998 in C++. In Section 6.2, it is stated that the performance measures should be similar in both MATLAB and C++, indicating correct implementation of the algorithms in C++. However, the quantitative analysis of the artifact-free EEG segments has shown a slight difference in results obtained in C++. This may be due to the QR decomposition and SVD that are used in MATLAB and C++ are from different toolboxes and libraries, producing decomposition difference. This difference in decomposition eventually causes a slight difference during EEG reconstruction. However, the average CC values for both algorithms in MATLAB and C++ are comparable and the difference among them is considered insignificant. In general, the individual CC values produced by FastEMD-CCA^2 and FastCCA in reconstructing artifact-free segments are more than 0.99, for all 33 analysed EEG signals, in both MATLAB and C++. This indicates that both algorithms do not introduce much distortion to the artifact-free EEG segments during reconstruction, thus reliable in preserving neural information of an EEG signal.

In the frequency domain, the MAE and MAPE are calculated to validate if the proposed algorithms introduce any distortion to the signal over different frequency bands after artifact elimination is performed. FastEMD-CCA^2 produces the highest average MAE in the delta band, which is 0.0059 compared to 0.0035 by FastCCA. The average MAE in every other frequency band is very close to zero, denoting negligible loss of neural information. The highest distortion percentage is observed in the gamma band with an average MAPE of 0.3777% and 0.0879%, produced by FastCCA and FastEMD-CCA^2 respectively. The least distortion percentage is 0.0044% by FastEMD-CCA^2 in the alpha band. It is clear that the average MAPE lies in the range of 0.0044% to 0.3777%. The percentage representation of MAPE is very low and can be considered very minimal. The MAE and MAPE have shown that the distortion caused by the proposed algorithms is very minimal, thus these algorithms are suitable to be used in any EEG-based applications for eyeblink artifact removal.

The time and frequency domain analysis were conducted to verify the performance of the proposed algorithms quantitatively, in retaining neural information of artifact-free EEG segments. The performance results of FastEMD-CCA^2 and FastCCA, in both time and frequency domains, suggest that they have caused insignificant loss of neural information to the EEG signals. In FastEMD-CCA^2, the eADA algorithm is first implemented to identify the first few eyeblink artifact locations, and an eyeblink artifact template is extracted out through FastEMD-CCA. The eyeblink artifact template is cross-correlated with sliding EEG windows, where highly correlated EEG windows are subjected to eyeblink artifact removal. CCA is applied to remove artifacts, only on EEG windows that were confirmed to be contaminated by eyeblink artifacts. Hence, this is the reason that the artifact-free EEG segments are unaffected in FastEMD-CCA^2, causing negligible loss of neural information during the reconstruction of the neural signal. In FastCCA, the eyeblink artifact locations are identified with the help of eADA algorithm, and then CCA is used for eyeblink artifact removal only on locations where eyeblink artifacts occur. Similar to FastEMD-CCA^2, the artifact-free EEG segments are unaffected, preventing loss of neural information during the reconstruction of a clean EEG signal.

6.3.3/ Online Analysis Results

The individual computation time taken by FastEMD-CCA^2 and FastCCA in MATLAB computing environment and C++ programming language to remove eyeblink artifacts from 14-channel EEG signals are provided in **Appendix A**, Table A.10. The average computation time taken by these algorithms in MATLAB computing environment and C++ programming language to remove eyeblink artifacts from 14-channel EEG signals are tabulated in Table 6.5.

TABLE 6.5 – Average Computation Time of FastEMD-CCA^2 and FastCCA in MATLAB and C++

Average					
Multichannel EEG Signal	**Average Duration per Channel (s)**	**FastEMD-CCA^2**		**FastCCA**	
		MATLAB	**C++**	**MATLAB**	**C++**
Computation Time (s)	312.33	6.78	3.35	6.87	3.96
Processing Time	1-second of EEG segment	0.0217	0.0107	0.0220	0.0127

The proposed algorithms are carried out on every 1.95s epoch of the recorded EEG signal to remove any eyeblink artifact that is present. The average computation time of FastEMD-CCA^2 is 6.78s in MATLAB and 3.35s in C++. It takes an average of 21.7 milliseconds in MATLAB and 10.7 milliseconds C++ to process and remove any eyeblink artifact from a 1-second length of 14-channel EEG signal (256 sample points x 14 EEG channels). The average computation time of FastCCA is 6.87s in MATLAB and 3.96s in C++. The average processing time to process and clean a 1-second length of 14-channel EEG signal by FastCCA is 22 milliseconds in MATLAB and 12.7 milliseconds in C++. Comparing FastEMD-CCA^2 and FastCCA, the shorter processing time of 10.7 milliseconds is achieved by FastEMD-CCA^2 in C++, followed by FastCCA in C++, with a processing time of 12.7 milliseconds. Results clearly show that the eyeblink artifact removal in C++ is well-suited for real-time implementation. Both algorithms took about 10 to 13 milliseconds on average to clean an EEG epoch of 1s length (256 x 14 EEG sample points) in C++ environment. This is because the proposed algorithms in C++ are designed to stream the EEG signal on a sample by sample basis into a buffer, before the eyeblink artifacts are located and removed. The streaming of EEG sample points into the buffer, and the cleaning process are performed in parallel. Therefore the processing speed of proposed algorithms in C++ is purely dependent on the speed of EEG sample point acquisition and instantaneous processing, hence the processing is considered as online.

6.4/ Summary

FastEMD-CCA^2 and FastCCA proposed in Chapter 4 are analysed and discussed after implementing the algorithms in C++. This chapter has evaluated the performance of these algorithms in removing eyeblink artifacts in real-time, and how well the algorithms are able to preserve artifact-free EEG segments, without distorting the neural signal. The algorithms are implemented in MATLAB and C++, both in a real-time setting. It appears that both algorithms have achieved instantaneous eyeblink artifact elimination, with very fast processing time in C++. From subsection 6.3.1, the artifact removal accuracy of FastCCA

is 1.57% higher than FastEMD-CCA^2 in both MATLAB and C++, indicating FastCCA is slightly better in artifact removal, regardless of the implementation medium, MATLAB or C++. On the other hand, quantitative analysis in time and frequency domains has pointed out that both FastEMD-CCA^2 and FastCCA are effective in retaining underlying neural information, with insignificant distortion to the artifact-free EEG segments. Thus, any of these two algorithms are suitable to be used in EEG-based applications requiring eyeblink artifact removal without loss of neural information in real-time, with FastCCA is slightly desirable in terms of artifact removal accuracy.

7

Conclusion and Future Directions

7.1/ Conclusion

The main intention of this research is to develop robust algorithms that are able to perform online detection and removal of eyeblink artifacts from EEG signals. In short, the developed algorithms are expected to perform online eyeblink artifact elimination from EEG signals without distorting the neural signal, with acceptable processing time delay. Online detection and removal of eyeblink artifacts from EEG signals are essential as contamination from eyeblink artifacts are inevitable in EEG based applications. BCI, neurofeedback, epileptic seizure detection and diagnosis of Alzheimer's disease are some of the EEG based applications that require multichannel EEG signals to be available online for further analysis and interpretation.

For an eyeblink artifact removal algorithm to be effective, the eyeblink artifact locations need to be correctly identified so that the algorithm doesn't have to perform artifact elimination on artifact-free EEG segments, preventing loss of neural information from the EEG signal. So, this work has first focused in developing a novel unsupervised eyeblink artifact detection algorithm (eADA), which locates eyeblink artifact frames effectively, assisting subsequent artifact elimination process. eADA is accurate in locating eyeblink artifacts that are contaminating an EEG signal. The performance of eADA is consistent as well, being able to identify and locate eyeblink artifacts across different EEG signals although there may be variance in the eyeblink characteristics, i.e. blinking duration, eyeblink pattern and eyeblink strength.

Secondly, the performance of Empirical Mode Decomposition (EMD) is improved with various modifications discussed in Chapters 3 and 4 to resolve the processing time inefficiency of the technique, resulting in FastEMD. FastEMD is then used with Canonical Correlation Analysis (CCA), for eyeblink artifact template extraction and removal of eyeblink artifacts from EEG signal, and the developed technique is called FastEMD-CCA^2. Additionally, another novel eyeblink artifact removal algorithm is proposed and developed, combining unsupervised eyeblink artifact detection algorithm (eADA) and CCA, and naming it as FastCCA. The proposed FastEMD-CCA^2 and FastCCA algorithms are compared with Wavelet Transform using simulated EEG signals and eyeblink artifacts, for its effectiveness in removing eyeblink artifacts from EEG signals. Moreover, the proposed FastEMD-CCA^2 and FastCCA are evaluated for their speed of computation using real EEG signals as shown in Chapter 5, and compared with conventional EMD-CCA

technique. FastEMD-CCA^2 and FastCCA proved to be very fast compared to the conventional EMD-CCA, at least 16 and 9 times faster respectively. To evaluate and analyze the ability of the proposed algorithms, FastEMD-CCA^2 and FastCCA in accurately removing eyeblink artifacts from EEG signals online, they are compared with one of the existing state-of-the-art methods, i.e. FORCe using two EEG datasets. These algorithms have outperformed FORCe in terms of artifact removal accuracy and processing speed, making them a feasible solution for applications requiring online removal of eyeblink artifacts.

Additionally, FastCCA and FastEMD-CCA^2 algorithms are developed and implemented in C++ programming language and compared with implementation in MATLAB. This is done to analyse the processing speed that can be achieved by the proposed algorithms in C++. The performance of the proposed algorithms in removing eyeblink artifacts online without distorting the neural signal is evaluated and quantitatively analysed. The artifact removal accuracy of FastCCA is slightly better than FastEMD-CCA^2 in both MATLAB and C++, indicating FastCCA is preferable. It appears that both algorithms have achieved instantaneous eyeblink artifact elimination, with FastEMD-CCA^2 slightly faster than FastCCA. These algorithms have also demonstrated impressive EEG signal reconstruction, with insignificant distortion to the artifact-free EEG segments.

To conclude, FastEMD-CCA^2 and FastCCA implemented in C++ programming language are reliable and suitable to be used to remove eyeblink artifacts from EEG signals in real-time applications, with FastCCA more preferable in terms of artifact removal accuracy.

7.2/ Limitations

FastEMD-CCA^2 and FastCCA have proven to be successful and reliable algorithms that can be used for online detection and removal of eyeblink artifacts from EEG signals. The implementation of the algorithms can be further enhanced if the following issues are addressed :

- The real EEG signals used in this thesis are recorded beforehand, thus the proposed algorithms are designed to process the EEG signals in a simulated online setting, i.e. EEG segments are processed in blocks in MATLAB and EEG sample points are streamed sample by sample basis to be processed in C++.
- Current work is done on a PC that operates with a central processing unit (CPU), for both MATLAB and C++. MATLAB is used on a Windows, while C++ is used on an Ubuntu Linux system. Although realization of the proposed algorithms in C++ programming language on a CPU achieve an online solution, it is not an application-centric solution. This is due to the fact that the algorithms rely on sequential execution on a CPU.

7.3/ Future Work

Future work is recommended for further improvement in the implementation of the proposed algorithms :

- An appropriate real-time EEG hardware system is required for real-time recording, acquisition and processing of the EEG signal. EEG signals can then be recorded

in real-time, allowing the proposed algorithms to grab the EEG sample points and remove eyeblink artifacts instantaneously.

- The real-time EEG system, incorporated with a high-performance computing system is required to support real-time implementation. A graphics processing unit (GPU) can be used for this purpose. GPU is capable of parallel computing and programming, with the help of CUDA (Compute Unified Device Architecture) created by NVIDIA. Using CUDA, the programmer can take advantage of the massive parallel computing power of an NVIDIA graphics card to perform general-purpose computation and multi-thread algorithm execution. Parallel processing and multi-thread execution methods are an efficient solution to decrease complexity in real-time implementations. Considering the parallel computational capabilities of a GPU compared to a CPU, it seems promising to use GPU in combination of an EEG system, for demanding EEG signal pre-processing tasks, particularly for real-time eyeblink artifact removal. The hardware-based implementation will not only be capable of removing eyeblink artifacts from EEG signals in real-time, but will also serve as an ideal device for ambulatory EEG applications.

BIBLIOGRAPHIE

[1] H. Sanei, Saeid and Hassani, Singular Spectrum Analysis of Biomedical Signals. CRC Press, 2015.

[2] G. H. Klem, H. O. Lüders, H. Jasper, C. Elger et al., "The ten-twenty electrode system of the international federation," Electroencephalogr Clinical Neurophysiology, vol. 52, no. 3, pp. 3–6, 1999.

[3] S. Sanei, Adaptive Processing of Brain Signals. John Wiley & Sons, 2013.

[4] K. Islam, A. Rastegarnia, and Z. Yang, "Methods for Artifact Detection and Removal from Scalp EEG : A Review," Neurophysiologie Clinique / Clinical Neurophysiology, no. November 2017, 2016. [Online]. Available : http://dx.doi.org/10.1016/j.neucli.2016.07.002

[5] V. Alvarez, "Therapeutic Coma for the Treatment of Status Epilepticus Timing , Choice of Drug , and Impact On," Springer Nature 2018, 2018.

[6] C. Braiman, E. A. Fridman, M. M. Conte, H. U. Voss, C. S. Reichenbach, T. Reichenbach, N. D. Schiff, C. Braiman, E. A. Fridman, M. M. Conte, H. U. Voss, and C. S. Reichenbach, "Cortical Response to the Natural Speech Envelope Correlates with Neuroimaging Evidence of Cognition in Severe Brain Injury Report Cortical Response to the Natural Speech Envelope Correlates with Neuroimaging Evidence of Cognition in Severe Brain Injury," Current Biology, pp. 1–7, 2018. [Online]. Available : https://doi.org/10.1016/j.cub.2018.10.057

[7] J. Claassen and F. S. Taccone, "Recommendations on the Use of EEG Monitoring in Critically Ill Patients : Consensus Statement from the Neurointensive Care Section of the ESICM," Intensive Care Medicine, pp. 1337–1351, 2013.

[8] U. R. Acharya, S. V. Sree, A. Peng, C. Alvin, and J. S. Suri, "Use of Principal Component Analysis for Automatic Classification of Epileptic EEG Activities in Wavelet Framework," Expert Systems With Applications, vol. 39, no. 10, pp. 9072–9078, 2012. [Online]. Available : http://dx.doi.org/10.1016/j.eswa.2012.02.040

[9] E. J. Stepanski and J. K. Wyatt, "Use of Sleep Hygiene in the Treatment of Insomnia," Sleep Medicine Reviews, vol. 7, no. 3, 2003.

[10] R. Flink, B. Pedersen, A. Guekht, K. Malmgren, R. Michelucci, B. Neville, F. Pinto, U. Stephani, and C. Ozkara, "Review article Guidelines for the use of EEG methodology in the diagnosis of epilepsy International League Against Epilepsy : Commission Report Commission on European Affairs : Subcommission on European Guidelines," pp. 1–7, 2002.

[11] B. Vivien, X. Paqueron, P. L. Cosquer, O. Langeron, P. Coriat, and B. Riou, "Detection of Brain Death Onset Using the Bispectral Index in Severely Comatose Patients," Intensive Care Medicine, pp. 419–425, 2002.

[12] G. B. Young, "The EEG in Coma," Journal of Clinical Neurophysiology, vol. 17, no. 5, pp. 473–485, 2000.

[13] R. I. Tivadar and M. M. Murray, "A Primer on Electroencephalography and Event-Related Potentials for Organizational Neuroscience," Organizational Research Methods, pp. 1–26, 2018.

[14] S. M. Peterson, E. Furuichi, and D. P. Ferris, "Effects of virtual reality high heights exposure during beam-walking on physiological stress and cognitive loading," PLOS ONE, pp. 1–17, 2018.

[15] C. Miniussi and Æ. G. Thut, "Combining TMS and EEG Offers New Prospects in Cognitive Neuroscience," Brain Topography, no. May 2014, 2009.

[16] M. M. Naeem Mannan, M. Ahmad Kamran, S. Kang, and M. Y. Jeong, "Effect of EOG signal filtering on the removal of ocular artifacts and EEG-based brain-computer interface : A comprehensive study," Complexity, vol. 2018, 2018.

[17] H. Adeli, S. Ghosh-dastidar, and N. Dadmehr, "A Spatio-Temporal Wavelet-Chaos Methodology for EEG-Based Diagnosis of Alzheimer's Disease," Neuroscience Letters, vol. 444, pp. 190–194, 2008.

[18] X. Jiang, G. B. Bian, and Z. Tian, "Removal of Artifacts from EEG signals : A review," Sensors (Switzerland), vol. 19, no. 5, pp. 1–18, 2019.

[19] M. M. N. Mannan, M. Y. Jeong, and M. A. Kamran, "Hybrid ICA-Regression : Automatic Identification and Removal of Ocular Artifacts from Electroencephalographic Signals," Frontiers in Human Neuroscience, vol. 10, no. 5, pp. 1–17, 2016.

[20] F. Minguillon, Jesus and Lopez-Gordo, M Angel and Pelayo, "Trends in EEG - BCI for Daily - Life : Requirements for Artifact Removal," Biomedical Signal Processing and Control, no. October, 2017.

[21] S. Kanoga and Y. Mitsukura, "Review of Artifact Rejection Methods for Electroencephalographic Systems," Electroencephalography, 2017.

[22] J. A. Uriguen and B. Garcia-Zapirain, "EEG Artifact Removal State of the Art and Guidelines," Journal of neural engineering, vol. 12, no. 3, p. 031001, 2015.

[23] H. Nolan, R. Whelan, and R. Reilly, "Faster : Fully automated statistical thresholding for EEG artifact rejection," Journal of neuroscience methods, vol. 192, no. 1, pp. 152–162, 2010.

[24] A. Aarabi, K. Kazemi, R. Grebe, H. A. Moghaddam, and F. Wallois, "Detection of EEG transients in neonates and older children using a system based on dynamic time-warping template matching and spatial dipole clustering," NeuroImage, vol. 48, no. 1, pp. 50–62, 2009. [Online]. Available : http://dx.doi.org/10.1016/j.neuroimage.2009.06.057

[25] A. Klein and W. Skrandies, "A reliable statistical method to detect eyeblink-artefacts from electroencephalogram data only," Brain topography, vol. 26, no. 4, pp. 558–568, 2013.

[26] S. Benedetto, M. Pedrotti, L. Minin, T. Baccino, A. Re, and R. Montanari, “Driver workload and eye blink duration,” Transportation Research Part F : Traffic Psychology and Behaviour, vol. 14, no. 3, pp. 199–208, 2011. [Online]. Available : http://dx.doi.org/10.1016/j.trf.2010.12.001

[27] G. Barbati, C. Porcaro, F. Zappasodi, P. M. Rossini, and F. Tecchio, “Optimization of an independent component analysis approach for artifact identification and removal in magnetoencephalographic signals,” Clinical Neurophysiology, vol. 115, no. 5, pp. 1220–1232, 2004.

[28] A. Mognon, J. Jovicich, L. Bruzzone, and M. Buiatti, “ADJUST : An Automatic EEG Artifact Detector Based on the Joint Use of Spatial and Temporal Features,” Psychophysiology, vol. 48, no. 2, pp. 229–240, 2011.

[29] W. D. Chang, H. S. Cha, K. Kim, and C. H. Im, “Detection of eye blink artifacts from single prefrontal channel electroencephalogram,” Computer Methods and Programs in Biomedicine, vol. 124, pp. 19–30, 2016. [Online]. Available : http://dx.doi.org/10.1016/j.cmpb.2015.10.011

[30] W. D. Chang, J. H. Lim, and C. H. Im, “An unsupervised eye blink artifact detection method for real-time electroencephalogram processing,” Physiological Measurement, vol. 37, no. 3, pp. 401–417, 2016. [Online]. Available : http://dx.doi.org/10.1088/0967-3334/37/3/401

[31] S. Kim and J. McNames, “Automatic spike detection based on adaptive template matching for extracellular neural recordings,” Journal of Neuroscience Methods, vol. 165, no. 2, pp. 165–174, 2007.

[32] G. Gratton, M. G. Coles, and E. Donchin, “A New Method for Off-line Removal of Ocular Artifact,” Electroencephalography and Clinical europhysiology, vol. 55, no. 4, pp. 468–484, 1983.

[33] J. L. Kenemans, P. Molenaar, M. N. Verbaten, and J. L. Slangen, “Removal of the Ocular Artifact from the EEG : A Comparison of Time and Frequency Domain Methods with Simulated and Real Data,” Psychophysiology, vol. 28, no. 1, pp. 114–121, 1991.

[34] J. Woestenburg, M. Verbaten, and J. Slangen, “The Removal of the Eye-movement Artifact from the EEG by Rgression Analysis in the Frequency Domain,” Biological Psychology, vol. 16, no. 1-2, pp. 127–147, 1983.

[35] N. Oosugi, K. Kitajo, N. Hasegawa, Y. Nagasaka, K. Okanoya, and N. Fujii, “A new method for quantifying the performance of EEG blind source separation algorithms by referencing a simultaneously recorded ECoG signal,” Neural Networks, vol. 93, pp. 1–6, 2017. [Online]. Available : http://dx.doi.org/10.1016/j.neunet.2017.01.005

[36] R. Romo Vázquez, H. Vélez-Pérez, R. Ranta, V. Louis Dorr, D. Maquin, and L. Maillard, “Blind source separation, wavelet denoising and discriminant analysis for EEG artefacts and noise cancelling,” Biomedical Signal Processing and Control, vol. 7, no. 4, pp. 389–400, 2012.

[37] H. Hallez, M. De Vos, B. Vanrumste, P. Van Hese, S. Assecondi, K. Van Laere, P. Dupont, W. Van Paesschen, S. Van Huffel, and I. Lemahieu, “Removing muscle

and eye artifacts using blind source separation techniques in ictal EEG source imaging," Clinical Neurophysiology, vol. 120, no. 7, pp. 1262–1272, 2009. [Online]. Available : http://dx.doi.org/10.1016/j.clinph.2009.05.010

[38] S. Makeig, S. D. Ca, A. J. Bell, and T. J. Sejnowski, "Independent Component Analysis of Electroencephalographic Data," Advances in neural information processing systems, no. 3, 1996.

[39] A. Delorme, J. Palmer, J. Onton, R. Oostenveld, and S. Makeig, "Independent EEG Sources are Dipolar," PLoS ONE, vol. 7, no. 2, 2012.

[40] M. Mennes, H. Wouters, B. Vanrumste, L. Lagae, and P. Stiers, "Validation of ICA As a Tool to Remove Eye Movement Artifacts from EEG/ERP," Psychophysiology, vol. 47, no. 6, pp. 1142–1150, 2010.

[41] S. Hoffmann and M. Falkenstein, "The Correction of Eye Blink Artefacts in the EEG : A Comparison of Two Prominent Methods," PLoS ONE, vol. 3, no. 8, 2008.

[42] A. Delorme, T. Sejnowski, and S. Makeig, "Enhanced Detection of Artifacts in EEG Data Using Higher-Order Statistics and Independent Component Analysis," NeuroImage, vol. 34, no. 4, pp. 1443–1449, 2007.

[43] R. Li and J. C. Principe, "Blinking Artifact Removal in Cognitive EEG Data Using ICA," in Annual International Conference of the IEEE Engineering in Medicine and Biology - Proceedings, no. 3, 2006, pp. 5273–5276.

[44] Y. Li, Z. Ma, W. Lu, and Y. Li, "Automatic Removal of the Eye blink Artifact from EEG Using an ICA-Based Template Matching Approach," Physiological Measurement, vol. 27, no. 4, pp. 425–436, 2006.

[45] T. Jung, S. Makeig, T. Lee, T. J. Sejnowski, and S. a. N. Diego, "Removing Electroencephalographic Artifacts by Blind Source Separation," Psychophysiology, vol. 37, no. 98, pp. 163–178, 2000.

[46] R. N. Vigário, "Extraction of Ocular Artefacts from EEG Using Independent Component Analysis," Electroencephalography and Clinical Neurophysiology, vol. 103, no. 3, pp. 395–404, 1997.

[47] M. Chaumon, D. V. Bishop, and N. A. Busch, "A Practical Guide to the Selection of Independent Components of the Electroencephalogram for Artifact Correction," Journal of Neuroscience Methods, vol. 250, pp. 47–63, 2015. [Online]. Available : http://dx.doi.org/10.1016/j.jneumeth.2015.02.025

[48] T. Radüntz, J. Scouten, O. Hochmuth, and B. Meffert, "EEG Artifact Elimination by Extraction of ICA-Component Features Using Image Processing Algorithms," Journal of Neuroscience Methods, vol. 243, pp. 84–93, 2015. [Online]. Available : http://dx.doi.org/10.1016/j.jneumeth.2015.01.030

[49] I. Winkler, S. Haufe, and M. Tangermann, "Automatic Classification of Artifactual ICA-Components for Artifact Removal in EEG Signals," Behavioral and Brain Functions, vol. 7, pp. 1–15, 2011.

[50] F. Campos Viola, J. Thorne, B. Edmonds, T. Schneider, T. Eichele, and S. Debener, "Semi-Automatic Identification of Independent Components Representing EEG Artifact," Clinical Neurophysiology, vol. 120, no. 5, pp. 868–877, 2009. [Online]. Available : http://dx.doi.org/10.1016/j.clinph.2009.01.015

[51] M. B. Pontifex, K. L. Gwizdala, A. C. Parks, M. Billinger, and C. Brunner, "Variability of ICA Decomposition May Impact EEG Signals When Used to Remove Eyeblink Artifacts," Psychophysiology, vol. 54, no. 3, pp. 386–398, 2017.

[52] F. Artoni, A. Delorme, and S. Makeig, "Applying Dimension Reduction to EEG Data by Principal Component Analysis Reduces the Quality of its Subsequent Independent Component Decomposition," NeuroImage, vol. 175, pp. 176–187, 2018. [Online]. Available : https://doi.org/10.1016/j.neuroimage.2018.03.016

[53] P. Berg and M. Scherg, "Dipole Modelling of Eye Activity and its Application to the Removal of Eye Artefacts from the EEG and MEG," Clinical Physics and Physiological Measurement, vol. 12, pp. 49–54, 1991.

[54] A. Turnip, D. E. Kusumandari, H. Fakhurroja, A. I. Simbolon, T. Hidayat, and P. Sihombing, "Artifacts Reduction of EEG-SSVEP Signals for Emotion Detection with Robust Principal Component Analysis," in Proceedings of the International Conference on Imaging, Signal Processing and Communication, 2017, pp. 94–99.

[55] E. M. Ter Braack, B. De Jonge, and M. J. A. M. Van Putten, "Reduction of TMS Induced Artifacts in EEG Using Principal Component Analysis," in IEEE Transactions on Neural Systems and Rehabilitation Engineering, vol. 21, no. 3, 2013, pp. 376–382.

[56] R. K. Niazy, C. F. Beckmann, G. D. Iannetti, J. M. Brady, and S. M. Smith, "Removal of FMRI Environment Artifacts from EEG Data Using Optimal Basis Sets," NeuroImage, vol. 28, no. 3, pp. 720–737, 2005.

[57] M. Negishi, M. Abildgaard, T. Nixon, and R. Todd Constable, "Removal of Time-Varying Gradient Artifacts from EEG Data Acquired During Continuous fMRI," Clinical Neurophysiology, vol. 115, no. 9, pp. 2181–2192, 2004.

[58] A. Turnip and E. Junaidi, "Removal Artifacts from EEG Signal Using Independent Component Analysis and Principal Component Analysis," in Proceedings of 2014 2nd International Conference on Technology, Informatics, Management, Engineering and Environment, TIME-E 2014, 2015, pp. 296–302.

[59] L. Vigon, M. Saatchi, J. Mayhew, and R. Fernandes, "Quantitative Evaluation of Techniques for Ocular Artefact Filtering of EEG Waveforms," in IEE Proceedings - Science, Measurement and Technology, vol. 147, no. 5, 2002, pp. 219–228.

[60] T. D. Lagerlund, F. W. Sharbrough, and N. E. Busacker, "Spatial Filtering of Multichannel Electroencephalographic Recordings Through Principal Component Analysis by Singular Value Decomposition." Journal of clinical neurophysiology : official publication of the American Electroencephalographic Society, vol. 14 1, pp. 73–82, 1997.

[61] H. Hotelling, "Relations Between Two Sets of Variates," Biometrika, vol. 28, no. 3, pp. 321–377, 1936.

[62] W. De Clercq, A. Vergult, B. Vanrumste, W. Van Paesschen, and S. Van Huffel, "Canonical Correlation Analysis Applied to Remove Muscle Artifacts from the Electroencephalogram," in IEEE Transactions on Biomedical Engineering, vol. 53, no. 12, 2006, pp. 2583–2587.

[63] H. Hallez, A. Vergult, R. Phlypo, P. Van Hese, W. De Clercq, Y. D'Asseler, R. Van De Walle, B. Vanrumste, W. Van Paesschen, S. Van Huffel, and I. Lemahieu, "Muscle and Eye Movement Artifact Removal Prior to EEG Source Localization," in Annual International Conference of the IEEE Engineering in Medicine and Biology - Proceedings. IEEE, 2006, pp. 1002–1005.

[64] D. M. Vos, S. Riès, K. Vanderperren, B. Vanrumste, F. X. Alario, V. S. Huffel, and B. Burle, "Removal of Muscle Artifacts from EEG Recordings of Spoken Language Production," Neuroinformatics, vol. 8, no. 2, pp. 135–150, 2010.

[65] J. Gao, Z. Chongxun, and W. Pei, "Online Removal of Muscle Artifact from Electroencephalogram Signals," CLINICAL EEG and NEUROSCIENCE, vol. 41, no. 1, 2010.

[66] W. De Clercq, A. Vergult, B. Vanrumste, J. Van Hees, A. Palmini, W. Van Paesschen, and S. Van Huffel, "A New Muscle Artifact Removal Technique to Improve the Interpretation of the Ictal Scalp Electroencephalogram," in IEEE Engineering in Medicine and Biology 27th Annual Conference, no. 3, 2006, pp. 944–947.

[67] T.-p. Jung and C. Humphries, "Extended ICA Removes Artifacts from Electroencephalographic Recordings," Advances in neural information processing systems, no. February 2013, 1998.

[68] T.-p. Jung, S. Makeig, M. Wester, J. Townsend, E. Courchesne, and T. J. Sejnowski, "Removal of eye activity artifacts from visual event-related potentials in normal and clinical subjects," Clinical Neurophysiology, vol. 111, pp. 1745–1758, 2000.

[69] S. Casarotto, A. M. Bianchi, S. Cerutti, and G. A. Chiarenza, "Principal component analysis for reduction of ocular artefacts in event-related potentials of normal and dyslexic children," Clinical Neurophysiology, vol. 115, pp. 609–619, 2004.

[70] C. A. Joyce, I. F. Gorodnitsky, and M. Kutas, "Automatic removal of eye movement and blink artifacts from EEG data using blind component separation," Psychophysiology, vol. 41, pp. 313–325, 2004.

[71] G. Dorffner, "Using ICA for removal of ocular artifacts in EEG recorded from blind subjects," Neural Networks, vol. 18, pp. 998–1005, 2005.

[72] T. Liu and D. Yao, "Removal of the ocular artifacts from EEG data using a cascaded spatio-temporal processing," computer methods and programs in biomedicine, vol. 3, pp. 95–103, 2006.

[73] A. Teixeiraa, A. Tome, P. Gruber, and A. Martins, "Automatic removal of high-amplitude artefacts from single-channel electroencephalograms," computer methods and programs in biomedicine, vol. 3, pp. 125–138, 2006.

[74] R. M. Frank and G. A. Frishkoff, "Automated protocol for evaluation of electromagnetic component separation (APECS) : Application of a framework for evaluating statistical methods of blink extraction from multichannel EEG," Clinical Neurophysiology, vol. 118, pp. 80–97, 2007.

[75] N. Mammone and F. C. Morabito, “Enhanced automatic artifact detection based on independent component analysis and Renyi ’ s entropy,” Neural Networks, vol. 21, pp. 1029–1040, 2008.

[76] J. Feng, G. Yong, and Y. Pan, “Automatic Removal of Eye-Movement and Blink Artifacts from EEG Signals,” Brain Topography, pp. 105–114, 2010.

[77] L. ZHANG, Y. WANG, and C. HE, “Online Removal of Eye Blink Artifact From Scalp Eeg Using Canonical Correlation Analysis Based Method,” Journal of Mechanics in Medicine and Biology, vol. 12, no. 05, p. 1250091, 2012.

[78] B. Somers and A. Bertrand, “Removal of eye blink artifacts in wireless EEG sensor networks using reduced-bandwidth canonical correlation analysis,” Journal of Neural Engineering, vol. 13, no. 6, pp. 1–13, 2016. [Online]. Available : http://dx.doi.org/10.1088/1741-2560/13/6/066008

[79] M. Chavez, F. Grosselin, A. Bussalb, F. De Vico Fallani, and N.-S. X, “Surrogate-Based Artifact Removal From Single-Channel EEG,” IEEE Transactions on Neural Systems and Rehabilitation Engineering, vol. 26, no. 3, pp. 540–550, 2018.

[80] S. Khatun, S. Member, R. Mahajan, and S. Member, “Comparative Study of Wavelet-Based Unsupervised Ocular Artifact Removal Techniques for Single-Channel EEG Data,” IEEE Journal of Translational Engineering in Health and Medicine, vol. 4, no. December 2015, pp. 1–8, 2016.

[81] P. S. Kumar, R. Arumuganathan, K. Sivakumar, and C. Vimal, “Removal of Ocular Artifacts in the EEG Through Wavelet Transform Without Using an EOG Reference Channel,” Int. J. Open Problems Compt. Math, vol. 1, no. 3, 2008.

[82] K. V.Krishnaveni, S.Jayaraman, S.Aravind, V.Hariharasudhan, “Automatic Identification and Removal of Ocular Artifacts from EEG Using Wavelet Transform,” MEASUREMENT SCIENCE REVIEW, vol. 6, no. 4, pp. 45–57, 2006.

[83] R. Patel, M. P. R. Janawadkar, S. Sengottuvel, K. Gireesan, and T. S. Radhakrishnan, “Suppression of Eye-Blink Associated Artifact Using Single Channel EEG Data by Combining Cross-Correlation with Empirical Mode Decomposition,” IEEE Sensors Journal, vol. 16, no. 18, pp. 6947–6954, 2016.

[84] D. Looney, V. Goverdovsky, P. Kidmose, and D. P. Mandic, “Subspace Denoising of EEG Artefacts via Multivariate EMD,” in ICASSP, IEEE International Conference on Acoustics, Speech and Signal Processing - Proceedings, 2014, pp. 4688–4692.

[85] M. K. I. Molla, M. Rabiul Islam, T. Tanaka, and T. M. Rutkowski, “Artifact Suppression from EEG Signals Using Data Adaptive Time Domain Filtering,” Neurocomputing, vol. 97, pp. 297–308, 2012. [Online]. Available : http://dx.doi.org/10.1016/j.neucom.2012.05.009

[86] D. Safieddine, A. Kachenoura, L. Albera, G. Birot, A. Karfoul, A. Pasnicu, A. Biraben, F. Wendling, L. Senhadji, and I. Merlet, “Removal of Muscle Artifact from EEG Data : Comparison Between Stochastic (ICA and CCA) and Deterministic (EMD and Wavelet-Based) Approaches,” Eurasip Journal on Advances in Signal Processing, vol. 2012, no. 1, pp. 1–15, 2012.

[87] M. Shahbakhti, V. Khalili, and G. Kamaee, “Removal of Blink from EEG by Empirical Mode Decomposition (EMD),” in The 5th 2012 Biomedical Engineering International Conference, 2012.

[88] K. I. Molla, T. Tanaka, T. M. Rutkowski, and A. Cichocki, “Separation of EOG Artifacts from EEG Signals Using Bivariate EMD,” in IEEE International Conference on Acoustics, Speech and Signal Processing, 2010, pp. 562–565.

[89] D. Looney, L. Li, T. M. Rutkowski, D. P. Mandic, and A. Cichocki, “Ocular Artifacts Removal from EEG Using EMD,” Advances in Cognitive Neurodynamics ICCN 2007, pp. 831–835, 2008.

[90] K. T. Sweeney, S. Member, F. Mcloone, S. Member, E. Ward, and S. Member, “The Use of Ensemble Empirical Mode Decomposition With Canonical Correlation Analysis as a Novel Artifact Removal Technique,” IEEE TRANSACTIONS ON BIOMEDICAL ENGINEERING, vol. 60, no. 1, pp. 97–105, 2013.

[91] C. Dora and P. K. Biswal, “An improved algorithm for efficient ocular artifact suppression from frontal EEG electrodes using VMD,” Integrative Medicine Research, pp. 1–14, 2019. [Online]. Available : https://doi.org/10.1016/j.bbe.2019.03.002

[92] T. Zikov, S. Bibian, G. A. Durnont, M. Huzmezan, and C. R. Ries, “A wavelet based de-noising technique,” in Conference and the Annual Fall Meeting of the Biomedical Engineering Society, 2002, pp. 98–105.

[93] D. Iyer and G. Zouridakis, “Single-trial evoked potential estimation : Comparison between independent component analysis and wavelet denoising,” Clinical Neurophysiology, vol. 118, pp. 495–504, 2007.

[94] X. Yong, M. Fatourechi, R. K. Ward, and G. E. Birch, “Automatic artefact removal in a self-paced hybrid brain- computer interface system,” JOURNAL OF NEUROENGINEERING AND REHABILITATION, pp. 1–20, 2012.

[95] M. Guarascio and S. Puthusserypady, “Biomedical Signal Processing and Control Automatic minimization of ocular artifacts from electroencephalogram : A novel approach by combining Complete EEMD with Adaptive Noise and Renyi ’ s Entropy,” Biomedical Signal Processing and Control, vol. 36, pp. 63–75, 2017. [Online]. Available : http://dx.doi.org/10.1016/j.bspc.2017.03.017

[96] M. A. Klados, C. Papadelis, C. Braun, and P. D. Bamidis, “REG-ICA : A Hybrid Methodology Combining Blind Source Separation and Regression Techniques for the Rejection of Ocular Artifacts,” Biomedical Signal Processing and Control, vol. 6, no. 3, pp. 291–300, 2011. [Online]. Available : http://dx.doi.org/10.1016/j.bspc.2011.02.001

[97] M. T. Akhtar, W. Mitsuhashi, and C. J. James, “Employing Spatially Constrained ICA and Wavelet Denoising for Automatic Removal of Artifacts from Multichannel EEG Data,” Signal Processing, vol. 92, no. 2, pp. 401–416, 2012. [Online]. Available : http://dx.doi.org/10.1016/j.sigpro.2011.08.005

[98] M. T. Akhtar and C. J. James, “Focal Artifact Removal from Ongoing EEG – A Hybrid Approach Based on Spatially-Constrained ICA and Wavelet De-noising,” in 31st Annual International Conference of the IEEE EMBS, 2009, pp. 4027–4030.

[99] M. Rakibul Mowla, S. C. Ng, M. S. Zilany, and R. Paramesran, "Artifacts-Matched Blind Source Separation and Wavelet Transform for Multichannel EEG Denoising," Biomedical Signal Processing and Control, vol. 22, pp. 111–118, 2015. [Online]. Available : http://dx.doi.org/10.1016/j.bspc.2015.06.009

[100] N. K. Al-Qazzaz, S. Hamid Bin Mohd Ali, S. A. Ahmad, M. S. Islam, and J. Escudero, "Automatic Artifact Removal in EEG of Normal and Demented Individuals Using ICA-WT during Working Memory Tasks," Sensors (Basel, Switzerland), vol. 17, no. 6, 2017.

[101] N. Mammone, F. La Foresta, and F. C. Morabito, "Automatic Artifact Rejection from Multichannel Scalp EEG by Wavelet ICA," IEEE Sensors Journal, vol. 12, no. 3, pp. 533–542, 2012.

[102] C. Zhao and T. Qiu, "An Ocular Artifacts Removal Method Based on Canonical Correlation Analysis," in IEEE EMBS, 2011, p. 2.

[103] V. Bono, S. Das, W. Jamal, and K. Maharatna, "Hybrid Wavelet and EMD/ICA Approach for Artifact Suppression in Pervasive EEG," Journal of Neuroscience Methods, vol. 267, pp. 89–107, 2016.

[104] V. Bono, W. Jamal, S. Das, and K. Maharatna, "Artifact Reduction in Multichannel Pervasive EEG Using Hybrid WPT-ICA and WPT-EMD Signal Decomposition Techniques," in 2014 IEEE International Conference on Acoustic, Speech and Signal Processing, 2014, pp. 6–7.

[105] R. Mahajan and B. I. Morshed, "Unsupervised Eye Blink Artifact Denoising of EEG Data With Modified Multiscale Sample Entropy, Kurtosis, and Wavelet-ICA," IEEE Journal of Biomedical and Health Informatics, vol. 19, no. 1, pp. 158–165, 2015.

[106] S. Çınar and N. Acır, "A Novel System for Automatic Removal of Ocular Artefacts in EEG by Using Outlier Detection Methods and Independent Component Analysis," Expert Systems with Applications, vol. 68, pp. 36–44, 2017.

[107] K. T. Sweeney, S. Member, H. Ayaz, T. E. Ward, S. Member, M. Izzetoglu, S. F. McLoone, and B. Onaral, "A Methodology for Validating Artifact Removal Techniques for Physiological Signals," in Ieee Transactions on Information Technology in Biomedicine, vol. 16, no. 5, 2012, pp. 918–926. [Online]. Available : http://ieeexplore.ieee.org.

[108] M. H. Soomro, N. Badruddin, M. Z. Yusoff, and M. A. Jatoi, "Automatic Eye-Blink Artifact Removal Method Based on EMD-CCA," in 2013 ICME International Conference on Complex Medical Engineering, CME 2013, no. April, 2013, pp. 186–190.

[109] R. Patel, S. Sengottuvel, M. P. Janawadkar, K. Gireesan, T. S. Radhakrishnan, and N. Mariyappa, "Ocular Artifact Suppression from EEG Using Ensemble Empirical Mode Decomposition with Principal Component Analysis," Computers and Electrical Engineering, vol. 54, pp. 78–86, 2016. [Online]. Available : http://dx.doi.org/10.1016/j.compeleceng.2015.08.019

[110] X. Chen, C. He, and H. Peng, "Removal of Muscle Artifacts from Single-Channel EEG Based on Ensemble Empirical Mode Decomposition and Multiset Canonical Correlation Analysis," Journal of Applied Mathematics, vol. 2014, pp. 1–10, 2014.

[111] X. Chen, X. Xu, A. Liu, M. J. McKeown, and Z. J. Wang, "The Use of Multivariate EMD and CCA for Denoising Muscle Artifacts from Few-Channel EEG Recordings," IEEE Transactions on Instrumentation and Measurement, vol. 67, no. 2, pp. 359–370, 2018.

[112] A. Jafarifarmand and M. A. Badamchizadeh, "Artifacts Removal in EEG Signal Using a New Neural Network Enhanced Adaptive Filter," Neurocomputing, vol. 103, pp. 222–231, 2013. [Online]. Available : http://dx.doi.org/10.1016/j.neucom.2012.09.024

[113] Q. Zhao, B. Hu, Y. Shi, Y. Li, P. Moore, M. Sun, and H. Peng, "Automatic Identification and Removal of Ocular Artifacts in EEG - Improved Adaptive Predictor Filtering for Portable Applications," IEEE Transactions on Nanobioscience, vol. 13, no. 2, pp. 109–117, 2014.

[114] L. Shoker, S. Sanei, and J. Chambers, "Artifact Removal from Electroencephalograms Using a Hybrid BSS-SVM Algorithm," IEEE Signal Processing Letters, vol. 12, no. 10, pp. 721–724, 2005.

[115] C. Y. Sai, N. Mokhtar, H. Arof, P. Cumming, and M. Iwahashi, "Automated Classification and Removal of EEG Artifacts with SVM and Wavelet-ICA," IEEE Journal of Biomedical and Health Informatics, vol. 22, no. 3, pp. 664–670, 2018.

[116] V. Lawhern, W. D. Hairston, K. McDowell, M. Westerfield, and K. Robbins, "Detection and Classification of Subject-generated Artifacts in EEG Signals Using Autoregressive Models," Journal of Neuroscience Methods, vol. 208, no. 2, pp. 181–189, 2012.

[117] S. Halder, M. Bensch, M. Bogdan, K. Andrea, N. Birbaumer, and W. Rosenstiel, "Online Artifact Removal for Brain-Computer Interfaces Using," Computational Intelligence and Neuroscience, vol. 2007, 2007.

[118] H. Ghandeharion and A. Erfanian, "A fully automatic ocular artifact suppression from EEG data using higher order statistics : Improved performance by wavelet analysis," Medical Engineering and Physics, vol. 32, no. 7, pp. 720–729, 2010. [Online]. Available : http://dx.doi.org/10.1016/j.medengphy.2010.04.010

[119] P. Lindsen and J. Bhattacharya, "Correction of blink artifacts using independent component analysis and empirical mode decomposition," Psychophysiology, vol. 47, pp. 955–960, 2010.

[120] H. L. Chan, Y. T. Tsai, L. Meng, and W. Tony, "The Removal of Ocular Artifacts from EEG Signals Using Adaptive Filters Based on Ocular Source Components," Annals of Biomedical Engineering, vol. 38, no. 11, pp. 3489–3499, 2010.

[121] B. S. Raghavendra and D. N. Dutt, "Wavelet Enhanced CCA for Minimization of Ocular and Muscle Artifacts in EEG," International Journal of Biomedical and Biological Engineering, vol. 5, no. 9, pp. 419–424, 2011.

[122] GuerreroMosquera and NaviaVazquez, "Automatic removal of ocular artefacts using adaptive filtering and independent component analysis for electroencephalogram data," IET Signal Processing, no. April 2011, 2012.

[123] H. Peng, B. Hu, Q. Shi, M. Ratcliffe, Q. Zhao, Y. Qi, and G. Gao, "Removal of Ocular Artifacts in EEG — An Improved Approach Combining DWT and ANC for Portable Applications," IEEE JOURNAL OF BIOMEDICAL AND HEALTH INFORMATICS, vol. 17, no. 3, pp. 600–607, 2013.

[124] L. Mingai, G. Shuoda, Z. Guoyu, S. Yanjun, and Y. Jinfu, "Removing ocular artifacts from mixed EEG signals with FastKICA and DWT," Journal of Intelligent & Fuzzy Systems, vol. 28, pp. 2851–2861, 2015.

[125] C. Gao and H. Li, "An ICA / HHT Hybrid Approach for Automatic," International Journal of Pattern Recognition, vol. 29, no. 2, pp. 1–19, 2015.

[126] K. Zeng, D. Chen, G. Ouyang, L. Wang, and S. Member, "An EEMD-ICA Approach to Enhancing Artifact Rejection for Noisy Multivariate Neural Data," IEEE Transactions on Neural Systems and Rehabilitation Engineering, vol. 4320, no. c, 2015.

[127] G. Wang, C. Teng, K. Li, Z. Zhang, and X. Yan, "The Removal of EOG Artifacts from EEG Signals Using Independent Component Analysis and Multivariate Empirical Mode Decomposition," IEEE Journal of Biomedical and Health Informatics, vol. 2194, no. c, pp. 1–7, 2015.

[128] S. Kanoga, M. Nakanishi, and Y. Mitsukura, "Assessing the effects of voluntary and involuntary eyeblinks in independent components of electroencephalogram," Neurocomputing, vol. 193, pp. 20–32, 2016. [Online]. Available : http://dx.doi.org/10.1016/j.neucom.2016.01.057

[129] A. Jafarifarmand, M.-a. Badamchizadeh, and S. Khanmohammadi, "Real-time ocular artifacts removal of EEG data using a hybrid ICA-ANC approach," Biomedical Signal Processing and Control, vol. 31, pp. 199–210, 2017. [Online]. Available : http://dx.doi.org/10.1016/j.bspc.2016.08.006

[130] R. Patel and K. G. S. Sengottuvel, "Common Methodology for Cardiac and Ocular Artifact Suppression from EEG Recordings by Combining Ensemble Empirical Mode Decomposition with Regression Approach," Journal of Medical and Biological Engineering, 2017.

[131] A. Vijayasankar, "Correction of Blink Artifacts from Single Channel EEG by EMD-IMF Thresholding," in Conference on Signal Processing And Communication Engineering Systems (SPACES), vol. 1, 2018, pp. 176–180.

[132] M. F. Issa and Z. Juhasz, "Improved EOG Artifact Removal Using Wavelet Enhanced Independent Component Analysis," Brain Sciences, 2019.

[133] H.-A. T. Nguyen, J. Musson, F. Li, W. Wang, G. Zhang, R. Xu, C. Richey, T. Schnell, F. D. McKenzie, and J. Li, "EOG Artifact Removal Using a Wavelet Neural Network," Neurocomputing, vol. 97, pp. 374–389, 2012.

[134] I. Daly, R. Scherer, M. Billinger, and G. Müller-Putz, "FORCe : Fully Online and Automated Artifact Removal for Brain Computer Interfacing," IEEE Transactions on Neural Systems and Rehabilitation Engineering, vol. 23, no. 5, pp. 725–736, 2015.

[135] L. Pion-Tonachini, S.-H. Hsu, C.-Y. Chang, T.-P. Jung, and S. Makeig, "Online Automatic Artifact Rejection Using the Real-time EEG Source-mapping Toolbox (REST)," in 2018 40th Annual International Conference of the IEEE Engineering in Medicine and Biology Society (EMBC). IEEE, 2018, pp. 106–109.

[136] Y. Paul, “Various epileptic seizure detection techniques using biomedical signals : a review,” Brain Informatics, 2018. [Online]. Available : https://doi.org/10.1186/s40708-018-0084-z

[137] S. A. Alshebeili, T. Alshawi, I. Ahmad, and F. E. A. El-samie, “EEG seizure detection and prediction algorithms : a survey,” EURASIP Journal on Advances in Signal Processing, 2014.

[138] M. Zhou, C. Tian, R. Cao, B. Wang, Y. Niu, T. Hu, H. Guo, and J. Xiang, “Epileptic Seizure Detection Based on EEG Signals and CNN,” Frontiers in Neuroinformatics, 2018.

[139] Q. Rincon, B. Bouaziz, L. Chaari, H. Batatia, and A. Quintero-rincón, “Epileptic Seizure Detection Using a Convolutional Neural Network,” Advances in Predictive, Preventive and Personalised Medicine, pp. 79–86, 2019.

[140] I. Ullah, M. Hussain, E.-u.-h. Qazi, and H. Aboalsamh, “An Automated System for Epilepsy Detection using EEG Brain Signals based on Deep Learning Approach,” Expert Systems with Applications, no. Ml, 2010.

[141] C. Sun and X. Wang, “Epileptic Seizure Detection with EEG Textural Features and Imbalanced Classification Based on EasyEnsemble Learning,” International Journal of Neural Systems, vol. 1950021, pp. 1–17, 2019.

[142] N. Mahmoodian, A. Boese, M. Friebe, and J. Haddadnia, “Seizure : European Journal of Epilepsy Epileptic seizure detection using cross-bispectrum of electroencephalogram signal,” Seizure : European Journal of Epilepsy, vol. 66, no. January, pp. 4–11, 2019. [Online]. Available : https://doi.org/10.1016/j.seizure.2019.02.001

[143] T. K. M.M. Hartmann, K. Schindler, T.A. Gebbink, G. Gritsch, “PureEEG : Automatic EEG Artifact Removal,” Neurophysiologie Clinique / Clinical Neurophysiology, vol. 44, no. 5, pp. 479–490, 2014. [Online]. Available : http://dx.doi.org/10.1016/j.neucli.2014.09.001

[144] E. Acar, C. Aykut-bingol, H. Bingol, and R. Bro, “Multiway Analysis of Epilepsy Tensors,” Bioinformatics, vol. 23, no. 2006, pp. 10–18, 2007.

[145] O. Hanosh, “Real-Time Epileptic Seizure Detection during Sleep using Passive Infrared (PIR) Sensors,” IEEE Sensors Journal, vol. PP, no. c, p. 1, 2019.

[146] F. Forooghifar, A. Aminifar, L. Cammoun, I. Wisniewski, C. Ciumas, P. Ryvlin, and D. Atienza, “A Self-Aware Epilepsy Monitoring System for Real-Time Epileptic Seizure Detection,” Mobile Networks and Applications, 2019.

[147] M.-p. Hosseini, A. Hajisami, and D. Pompili, “Real-time Epileptic Seizure Detection from EEG Signals via Random Subspace Ensemble Learning,” in IEEE International Conference on Autonomic Computing Real-time, 2016.

[148] L. S. Vidyaratne, K. M. Iftekharuddin, and S. Member, “Real-Time Epileptic Seizure Detection Using EEG,” Transactions on Neural Systems and Rehabilitation Engineering, vol. 4320, no. c, 2017.

[149] A. Mansouri, S. P. Singh, and K. Sayood, “Online EEG Seizure Detection and Localization,” Algorithms, 2019.

[150] M. Fatourechi, A. Bashashati, R. K. Ward, and G. E. Birch, “EMG and EOG artifacts in brain computer interface systems : A survey,” Clinical Neurophysiology, vol. 118, no. 3, pp. 480–494, 2007.

[151] A. Bashashati, B. Nouredin, R. K. Ward, P. Lawrence, and G. E. Birch, “Effect of eye-blinks on a self-paced brain interface design,” Clinical Neurophysiology, vol. 118, no. 7, pp. 1639–1647, 2007.

[152] I. I. Goncharova, D. J. Mcfarland, T. M. Vaughan, and J. R. Wolpaw, “EMG Contamination of EEG : Spectral and Topographical Characteristics,” Clinical Neurophysiology, vol. 114, pp. 1580–1593, 2003.

[153] R. J. Huster, Z. N. Mokom, S. Enriquez-geppert, and C. S. Herrmann, “Brain – Computer Interfaces for EEG Neurofeedback : Peculiarities and Solutions,” International Journal of Psychophysiology, 2013.

[154] L. H. Sherlin and C. Kerson, “Investigations in Neuromodulation , Neurofeedback and Applied Neuroscience Neurofeedback and Basic Learning Theory : Implications for Research and Practice,” Journal of Neurotherapy, no. December 2012, pp. 37–41, 2011.

[155] M. A. Bell and K. Cuevas, “Using EEG to Study Cognitive Development : Issues and Practices,” Journal of Cognition and Development, vol. 13, no. 3, pp. 281–294, 2012.

[156] S. R. L. Norden E. Huang, Zheng Shen, “The Empirical Mode Decomposition and the Hilbert Spectrum for Nonlinear and Non-Stationary Time Series Analysis,” Proceedings of the Royal Society of London, pp. 903–995, 1998. [Online]. Available : papers3://publication/uuid/B74763A9-34E1-446C-8677-521F1BEFF53A

[157] P. Flandrin, P. Gonc, and D. Lyon, “DETRENDING AND DENOISING WITH EMPIRICAL MODE DECOMPOSITIONS,” in 2004 12th European Signal Processing Conference, 2004, pp. 1581–1584.

[158] G. P. Rilling G, Flandrin P, “ON EMPIRICAL MODE DECOMPOSITION AND ITS ALGORITHMS,” in IEEE-EURASIP, vol. 3, no. 3, 2003, pp. 8–11.

[159] S. D. Hawley, L. E. Atlas, and H. J. Chizeck, “Some Properties of an Empirical Mode Type Signal Decomposition Algorithm,” in IEEE Signal Processing Letters, vol. 17, no. 1, 2010, pp. 24–27.

[160] Q. Chen, N. Huang, S. Riemenschneider, and Y. Xu, “A B-spline approach for empirical mode decompositions,” Advances in Computational Mathematics, vol. 24, no. 1-4, pp. 171–195, 2006.

[161] Y. Kopsinis and S. McLaughlin, “Investigation and performance enhancement of the empirical mode decomposition method based on a heuristic search optimization approach,” IEEE Transactions on Signal Processing, vol. 56, no. 1, pp. 1–13, 2008.

[162] D. Salomon, The computer graphics and Geometric Modeling. Springer Science & Business Media, 2011.

[163] M. H. Soomro, N. Badruddin, M. Z. Yusoff, and A. S. Malik, "A method for automatic removal of eye blink artifacts from EEG based on EMD-ICA," in Proceedings - 2013 IEEE 9th International Colloquium on Signal Processing and its Applications, CSPA 2013. IEEE, 2013, pp. 129–134.

[164] S. Kudrle, M. Proulx, P. Carrieres, and M. Lopez, "Fingerprinting for solving A/V synchronization issues within broadcast environments," SMPTE Motion Imaging Journal, pp. 279–296, 2010.

[165] N. K. Al-Qazzaz, S. Hamid Bin Mohd Ali, S. A. Ahmad, M. S. Islam, and J. Escudero, "Selection of Mother Wavelet Functions for Multi-channel EEG Signal Analysis During a Working Memory Task," Sensors, vol. 15, no. 11, pp. 29 015–29 035, 2015.

[166] D. B. Stone, G. Tamburro, P. Fiedler, J. Haueisen, and S. Comani, "Automatic Removal of Physiological Artifacts in EEG : The Optimized Fingerprint Method for Sports Science Applications," Frontiers in Human Neuroscience, vol. 12, p. 96, 2018.

[167] S. O'Regan, S. Faul, and W. Marnane, "Automatic Detection of EEG Artefacts Arising from Head Movements Using EEG and Gyroscope Signals," Medical Engineering & Physics, vol. 35, no. 7, pp. 867–874, 2013.

TABLE DES FIGURES

1.1 10-20 Electrodes Placement 1

3.1 Flowchart of Classical EMD Algorithm 27
3.2 Slope computation at point $[x_i, y_i]$ 29
3.3 (a) Synthetically Generated EEG Signal, (b) Synthetically Generated Eyeblink signal, (c) Mixed EEG and Eyeblink Signal 30
3.4 First multidimensional data set, $\hat{\mathbf{X}}(t)$ 38
3.5 Second multidimensional data set, $\hat{\mathbf{Y}}(t)$ 38
3.6 Canonical components of $\hat{\mathbf{X}}$ 39
3.7 Non-artifactual Canonical components 39
3.8 Artifact-free EEG dataset 40
3.9 (a) Mixed EEG and Eyeblink Signal, (b) Recovered EEG Signal from EMD, (c) Extracted Eyeblink Artifact from EMD-CSI 42
3.10 (a) Mixed EEG and Eyeblink Signal, (b) Recovered EEG Signal from EMD, (c) Extracted Eyeblink Artifact from EMD-CHSI 42
3.11 (a) Mixed EEG and Eyeblink Signal, (b) Recovered EEG Signal from EMD, (c) Extracted Eyeblink Artifact from EMD-ASI 43
3.12 Comparison of Average CC for Implementation of CCA through Eigendecomposition, QR-SVD and SVD 44
3.13 Comparison of Average RMSE for Implementation of CCA through Eigendecomposition, QR-SVD and SVD 45

4.1 (a) Synthetic EEG Signal, (b) Synthetic Eyeblink Artifact, (c) Contaminated EEG Signal 48
4.2 Correlation Coefficient, CC, between Fp1 and Fp2 Electrodes 50
4.3 Displacement Distribution for Threshold Greater Than 1σ 51
4.4 Sample Points of Identified Eyeblink Artifacts for Threshold Greater Than 1σ 52
4.5 Displacement Distribution for Threshold Greater Than 2σ 52
4.6 Sample Points of Identified Eyeblink Artifacts for Threshold Greater Than 2σ 53
4.7 Displacement Distribution for Threshold Greater Than 3σ 53
4.8 Sample Points of Identified Eyeblink Artifacts for Threshold Greater Than 3σ 54

4.9 Flowchart of the Unsupervised Eyeblink Artifact Detection Algorithm 55
4.10 Canonical Variates of the IMFs 57
4.11 Extracted Eyeblink Artifact Template and Reconstructed EEG Signal 58
4.12 Flowchart of FastEMD-CCA Algorithm 59
4.13 Highly Correlating Eyeblink Artifact Regions Subjected to FastEMD 61
4.14 Flowchart of the Proposed Technique FastEMD-CCA^2 63
4.15 Flowchart of the Proposed FastCCA Algorithm 65
4.16 Work flow of FastEMD-CCA^2 and FastCCA 66
4.17 Workflow of Conventional EMD-CCA, Proposed FastEMD-CCA^2 and FastCCA 70

5.1 (a) Mixed EEG and Eyeblink Signal, (b) Reconstructed EEG Signal, (c) Extracted Eyeblink Artifact 76
5.2 (a) Mixed EEG and Eyeblink Signal, (b) Reconstructed EEG Signal, (c) Extracted Eyeblink Artifact 77
5.3 (a) Mixed EEG and Eyeblink Signal, (b) Reconstructed EEG Signal, (c) Extracted Eyeblink Artifact 77
5.4 Recovered EEG signal through proposed FastEMD-CCA^2 80
5.5 Recovered EEG signal through proposed FastCCA 80
5.6 Recovered EEG signal through conventional EMD-CCA 81
5.7 Recovered EEG signal through proposed FastEMD-CCA^2 82
5.8 Recovered EEG signal through proposed FastCCA 82
5.9 Recovered EEG signal through conventional EMD-CCA 83
5.10 Entire EEG Signal-Reconstructed through FORCe 84
5.11 Entire EEG Signal-Reconstructed through FastEMD-CCA^2 85
5.12 Entire EEG Signal-Reconstructed through FastCCA 85
5.13 A Portion of the EEG Signal-Reconstructed through FORCe 86
5.14 A Portion of the EEG Signal-Reconstructed through FastEMD-CCA^2 86
5.15 A Portion of the EEG Signal-Reconstructed through FastCCA 87
5.16 Entire EEG Signal-Reconstructed through FORCe 87
5.17 Entire EEG Signal-Reconstructed through FastEMD-CCA^2 88
5.18 Entire EEG Signal-Reconstructed through FastCCA 88
5.19 A Portion of the EEG Signal-Reconstructed through FORCe 89
5.20 A Portion of the EEG Signal-Reconstructed through FastEMD-CCA^2 89
5.21 A Portion of the EEG Signal-Reconstructed through FastCCA 90

6.1 Recovered EEG Signal from Fp1 Channel through FastEMD-CCA^2 in MATLAB and C++ . . . 102
6.2 Recovered EEG Signal from Fp1 Channel through FastCCA in MATLAB and C++ . . . 103
6.3 Display of Recovered EEG Signal from Fp1 Channel through FastEMD-CCA^2 in C++ . . . 104
6.4 Display of Recovered EEG Signal from Fp1 Channel through FastCCA in C++ . . . 104
6.5 Recovered Multichannel EEG Signal through FastEMD-CCA^2 in MATLAB . 105
6.6 Recovered Multichannel EEG Signal through FastEMD-CCA^2 in C++ 106
6.7 Recovered Multichannel EEG Signal through FastCCA in MATLAB 107
6.8 Recovered Multichannel EEG Signal through FastCCA in C++ 108
6.9 Corrected Eyeblink Artifact Regions through FastEMD-CCA^2 and FastCCA in MATLAB and C++ . . . 109
6.10 Reconstructed Artifact-free EEG through FastEMD-CCA^2 and FastCCA in MATLAB and C++ . . . 110

LISTE DES TABLES

2.1 Studies on BSS Algorithms to Remove Artifacts . . . 11
2.2 Studies Based on WT and EMD to Remove Artifacts . . . 13
2.3 Studies Based on Hybrid Techniques to Remove Artifacts . . . 16
2.4 Related Work on Online Artifact Removal . . . 19
2.5 Criteria of Existing Techniques . . . 24

3.1 Performance metrics of CSI, CHSI and ASI on 100 Trials . . . 41
3.2 Average CC, RMSE and Time for Implementation of CCA through Eigen-decomposition, QR-SVD and SVD . . . 44

4.1 Average Accuracy in Eyeblink Artifact Detection with Different Thresholds . 54
4.2 Confusion Matrix - Eyeblink Artifact Detection . . . 67
4.3 Confusion Matrix - Eyeblink Artifact Detection and Removal . . . 71

5.1 Average Eyeblink Artifact Detection Accuracy . . . 73
5.3 Test of Normality for the Accuracies . . . 75
5.4 Welch ANOVA Test . . . 75
5.5 Performance Metrics of FastEMD-CCA^2, FastCCA and WT . . . 78
5.6 Comparison of Computation Time between Proposed FastEMD-CCA^2, FastCCA and Conventional EMD-CCA . . . 79
5.7 Performance Metrics of FastEMD-CCA^2, FastCCA and FORCe on Hitachi Dataset . . . 83
5.8 Performance Metrics of FastEMD-CCA^2, FastCCA and FORCe on INV-SK Dataset . . . 84
5.9 Test of Normality for the Hitachi Dataset . . . 93
5.10 Welch ANOVA Test for the Hitachi Dataset . . . 94
5.11 Welch ANOVA Test for the INV-SK Dataset . . . 95
5.2 Comparison of Eyeblink Artifact Detection Accuracy . . . 97

6.1 Average Performance Metrics of FastEMD-CCA^2 and FastCCA in MATLAB and C++ . . . 108
6.2 Average CC, RMSE and η_{dB} of FastEMD-CCA^2 and FastCCA in MATLAB and C++ . . . 110

6.3 Average MAE of FastEMD-CCA^2 and FastCCA in Different Frequency Bands111
6.4 Average MAPE of FastEMD-CCA^2 and FastCCA in Different Frequency Bands 111
6.5 Average Computation Time of FastEMD-CCA^2 and FastCCA in MATLAB and C++ 113

A.1 Comparison of Error Rate Between FastEMD-CCA^2 and FastCCA in MATLAB and C++ 142
A.2 Comparison of Accuracy Between FastEMD-CCA^2 and FastCCA in MATLAB and C++ 144
A.3 Comparison of Sensitivity Between FastEMD-CCA^2 and FastCCA in MATLAB and C++ 146
A.4 Comparison of Specificity Between FastEMD-CCA^2 and FastCCA in MATLAB and C++ 148
A.5 Comparison of Correlation Coefficient Between FastEMD-CCA^2 and FastCCA in MATLAB and C++ 150
A.6 Comparison of Root Mean Square Error Between FastEMD-CCA^2 and FastCCA in MATLAB and C++ 152
A.7 Comparison of Similarity Index Between FastEMD-CCA^2 and FastCCA in MATLAB and C++ 154
A.8 Comparison of MAE Between FastEMD-CCA^2 and FastCCA in Different Frequency Bands 156
A.9 Comparison of MAPE Between FastEMD-CCA^2 and FastCCA in Different Frequency Bands 157
A.10 Comparison of Computation Time Between FastEMD-CCA^2 and FastCCA in MATLAB and C++ 158

I

ANNEXES

A

Individual EEG Results of Chapter 6

TABLE A.1 – Comparison of Error Rate Between FastEMD-CCA^2 and FastCCA in MATLAB and C++

Error Rate (%)					
Multichannel EEG Signal	**Duration per Channel (s)**	**FastEMD-CCA^2**		**FastCCA**	
		MATLAB	**C++**	**MATLAB**	**C++**
EEG 1	389	4.65	4.65	0.00	0.00
EEG 2	329	1.92	1.92	0.00	0.00
EEG 3	294	2.78	2.78	0.00	0.00
EEG 4	369	2.78	2.78	0.00	0.00
EEG 5	337	5.66	5.66	5.66	5.66
EEG 6	312	2.56	2.56	0.00	0.00
EEG 7	330	0.00	0.00	0.00	0.00
EEG 8	308	1.04	1.04	1.04	1.04
EEG 9	306	1.12	1.12	0.00	0.00
EEG 10	346	4.30	4.30	0.00	0.00
EEG 11	321	2.11	2.11	0.00	0.00
EEG 12	272	1.41	1.41	0.00	0.00
EEG 13	345	2.38	2.38	0.00	0.00
EEG 14	310	1.16	1.16	0.00	0.00
EEG 15	271	0.53	0.53	0.00	0.00
EEG 16	345	1.09	1.09	0.00	0.00
EEG 17	316	1.13	1.13	0.00	0.00
EEG 18	280	1.66	1.66	0.55	0.55
EEG 19	335	0.77	0.77	0.00	0.00
EEG 20	302	2.33	2.33	1.16	1.16
EEG 21	289	1.27	1.27	0.00	0.00
EEG 22	346	0.00	0.00	0.00	0.00
EEG 23	304	0.00	0.00	0.00	0.00
EEG 24	269	2.00	2.00	2.00	2.00
EEG 25	359	1.06	1.06	0.00	0.00
EEG 26	265	3.23	3.23	0.81	0.81
EEG 27	334	2.34	2.34	0.00	0.00
EEG 28	326	1.31	1.31	0.65	0.65
EEG 29	272	4.00	4.00	1.00	1.00
EEG 30	264	1.12	1.12	0.00	0.00

Table A.1 continued from previous page

Error Rate (%)					
Multichannel EEG Signal	**Duration per Channel (s)**	**FastEMD-CCA**[2]		**FastCCA**	
		MATLAB	**C++**	**MATLAB**	**C++**
EEG 31	346	5.06	5.06	0.56	0.56
EEG 32	289	0.74	0.74	0.74	0.74
EEG 33	298	2.53	2.53	2.53	2.53
EEG 34	360	3.76	3.76	2.69	2.69
EEG 35	291	3.80	3.80	2.53	2.53
EEG 36	296	4.91	4.91	1.84	1.84
EEG 37	331	2.00	2.00	0.00	0.00
EEG 38	297	0.00	0.00	0.00	0.00
EEG 39	263	0.00	0.00	0.00	0.00
EEG 40	334	3.80	3.80	0.00	0.00
EEG 41	299	1.22	1.22	0.00	0.00
EEG 42	268	1.15	1.15	0.00	0.00
EEG 43	359	1.55	1.55	0.00	0.00
EEG 44	314	1.56	1.56	0.00	0.00
EEG 45	278	2.24	2.24	2.24	2.24
EEG 46	364	1.20	1.20	0.60	0.60
EEG 47	325	1.71	1.71	0.00	0.00
EEG 48	284	2.41	2.41	0.00	0.00
EEG 49	337	2.50	2.50	0.00	0.00
EEG 50	280	1.61	1.61	0.00	0.00
EEG 51	253	0.87	0.87	0.00	0.00
EEG 52	346	2.78	2.78	0.00	0.00
EEG 53	288	0.00	0.00	0.00	0.00
EEG 54	271	3.81	3.81	0.95	0.95
EEG 55	339	3.45	3.45	0.86	0.86
EEG 56	302	2.40	2.40	0.00	0.00
EEG 57	335	1.27	1.27	1.27	1.27
EEG 58	350	3.51	3.51	0.00	0.00
EEG 59	314	2.82	2.82	0.56	0.56
EEG 60	284	3.83	3.83	1.64	1.64
Average	**312.33**	**2.10**	**2.10**	**0.53**	**0.53**

TABLE A.2 – Comparison of Accuracy Between FastEMD-CCA^2 and FastCCA in MATLAB and C++

Accuracy (%)					
Multichannel EEG Signal	**Duration per Channel (s)**	**FastEMD-CCA^2**		**FastCCA**	
		MATLAB	**C++**	**MATLAB**	**C++**
EEG 1	389	95.35	95.35	100.00	100.00
EEG 2	329	98.08	98.08	100.00	100.00
EEG 3	294	97.22	97.22	100.00	100.00
EEG 4	369	97.22	97.22	100.00	100.00
EEG 5	337	94.34	94.34	94.34	94.34
EEG 6	312	97.44	97.44	100.00	100.00
EEG 7	330	100.00	100.00	100.00	100.00
EEG 8	308	98.96	98.96	98.96	98.96
EEG 9	306	98.88	98.88	100.00	100.00
EEG 10	346	95.70	95.70	100.00	100.00
EEG 11	321	97.89	97.89	100.00	100.00
EEG 12	272	98.59	98.59	100.00	100.00
EEG 13	345	97.62	97.62	100.00	100.00
EEG 14	310	98.84	98.84	100.00	100.00
EEG 15	271	99.47	99.47	100.00	100.00
EEG 16	345	98.91	98.91	100.00	100.00
EEG 17	316	98.87	98.87	100.00	100.00
EEG 18	280	98.34	98.34	99.45	99.45
EEG 19	335	99.23	99.23	100.00	100.00
EEG 20	302	97.67	97.67	98.84	98.84
EEG 21	289	98.73	98.73	100.00	100.00
EEG 22	346	100.00	100.00	100.00	100.00
EEG 23	304	100.00	100.00	100.00	100.00
EEG 24	269	98.00	98.00	98.00	98.00
EEG 25	359	98.94	98.94	100.00	100.00
EEG 26	265	96.77	96.77	99.19	99.19
EEG 27	334	97.66	97.66	100.00	100.00
EEG 28	326	98.69	98.69	99.35	99.35
EEG 29	272	96.00	96.00	99.00	99.00
EEG 30	264	98.88	98.88	100.00	100.00

Table A.2 continued from previous page

Accuracy (%)					
Multichannel EEG Signal	**Duration per Channel (s)**	**FastEMD-CCA**[2]		**FastCCA**	
		MATLAB	**C++**	**MATLAB**	**C++**
EEG 31	346	94.94	94.94	99.44	99.44
EEG 32	289	99.26	99.26	99.26	99.26
EEG 33	298	97.47	97.47	97.47	97.47
EEG 34	360	96.24	96.24	97.31	97.31
EEG 35	291	96.20	96.20	97.47	97.47
EEG 36	296	95.09	95.09	98.16	98.16
EEG 37	331	98.00	98.00	100.00	100.00
EEG 38	297	100.00	100.00	100.00	100.00
EEG 39	263	100.00	100.00	100.00	100.00
EEG 40	334	96.20	96.20	100.00	100.00
EEG 41	299	98.78	98.78	100.00	100.00
EEG 42	268	98.85	98.85	100.00	100.00
EEG 43	359	98.45	98.45	100.00	100.00
EEG 44	314	98.44	98.44	100.00	100.00
EEG 45	278	97.76	97.76	97.76	97.76
EEG 46	364	98.80	98.80	99.40	99.40
EEG 47	325	98.29	98.29	100.00	100.00
EEG 48	284	97.59	97.59	100.00	100.00
EEG 49	337	97.50	97.50	100.00	100.00
EEG 50	280	98.39	98.39	100.00	100.00
EEG 51	253	99.13	99.13	100.00	100.00
EEG 52	346	97.22	97.22	100.00	100.00
EEG 53	288	100.00	100.00	100.00	100.00
EEG 54	271	96.19	96.19	99.05	99.05
EEG 55	339	96.55	96.55	99.14	99.14
EEG 56	302	97.60	97.60	100.00	100.00
EEG 57	335	98.73	98.73	98.73	98.73
EEG 58	350	96.49	96.49	100.00	100.00
EEG 59	314	97.18	97.18	99.44	99.44
EEG 60	284	96.17	96.17	98.36	98.36
Average	**312.33**	**97.90**	**97.90**	**99.47**	**99.47**

TABLE A.3 – Comparison of Sensitivity Between FastEMD-CCA^2 and FastCCA in MATLAB and C++

Sensitivity (%)					
Multichannel EEG Signal	**Duration per Channel (s)**	**FastEMD-CCA^2**		**FastCCA**	
		MATLAB	**C++**	**MATLAB**	**C++**
EEG 1	389	93.94	93.94	100.00	100.00
EEG 2	329	96.97	96.97	100.00	100.00
EEG 3	294	100.00	100.00	100.00	100.00
EEG 4	369	96.00	96.00	100.00	100.00
EEG 5	337	97.14	97.14	97.14	97.14
EEG 6	312	96.36	96.36	100.00	100.00
EEG 7	330	100.00	100.00	100.00	100.00
EEG 8	308	100.00	100.00	98.46	98.46
EEG 9	306	98.25	98.25	100.00	100.00
EEG 10	346	96.05	96.05	100.00	100.00
EEG 11	321	97.06	97.06	100.00	100.00
EEG 12	272	97.92	97.92	100.00	100.00
EEG 13	345	97.06	97.06	100.00	100.00
EEG 14	310	98.77	98.77	100.00	100.00
EEG 15	271	99.38	99.38	100.00	100.00
EEG 16	345	98.69	98.69	100.00	100.00
EEG 17	316	98.73	98.73	100.00	100.00
EEG 18	280	98.17	98.17	99.39	99.39
EEG 19	335	100.00	100.00	100.00	100.00
EEG 20	302	96.43	96.43	98.21	98.21
EEG 21	289	98.33	98.33	100.00	100.00
EEG 22	346	100.00	100.00	100.00	100.00
EEG 23	304	100.00	100.00	100.00	100.00
EEG 24	269	96.55	96.55	96.55	96.55
EEG 25	359	98.41	98.41	100.00	100.00
EEG 26	265	96.08	96.08	99.02	99.02
EEG 27	334	96.88	96.88	100.00	100.00
EEG 28	326	98.26	98.26	99.13	99.13
EEG 29	272	94.81	94.81	100.00	100.00
EEG 30	264	98.59	98.59	100.00	100.00

Table A.3 continued from previous page

Sensitivity (%)					
Multichannel EEG Signal	**Duration per Channel (s)**	**FastEMD-CCA**[2]		**FastCCA**	
		MATLAB	**C++**	**MATLAB**	**C++**
EEG 31	346	94.55	94.55	99.39	99.39
EEG 32	289	99.15	99.15	99.15	99.15
EEG 33	298	97.28	97.28	97.28	97.28
EEG 34	360	95.93	95.93	97.09	97.09
EEG 35	291	95.92	95.92	97.28	97.28
EEG 36	296	94.70	94.70	98.01	98.01
EEG 37	331	97.37	97.37	100.00	100.00
EEG 38	297	100.00	100.00	100.00	100.00
EEG 39	263	100.00	100.00	100.00	100.00
EEG 40	334	98.15	98.15	100.00	100.00
EEG 41	299	98.48	98.48	100.00	100.00
EEG 42	268	98.51	98.51	100.00	100.00
EEG 43	359	98.08	98.08	100.00	100.00
EEG 44	314	98.02	98.02	100.00	100.00
EEG 45	278	97.52	97.52	97.52	97.52
EEG 46	364	98.71	98.71	99.35	99.35
EEG 47	325	98.01	98.01	100.00	100.00
EEG 48	284	97.33	97.33	100.00	100.00
EEG 49	337	96.94	96.94	100.00	100.00
EEG 50	280	97.73	97.73	100.00	100.00
EEG 51	253	98.92	98.92	100.00	100.00
EEG 52	346	96.70	96.70	100.00	100.00
EEG 53	288	100.00	100.00	100.00	100.00
EEG 54	271	96.51	96.51	98.84	98.84
EEG 55	339	96.39	96.39	98.80	98.80
EEG 56	302	96.77	96.77	100.00	100.00
EEG 57	335	98.31	98.31	98.31	98.31
EEG 58	350	95.45	95.45	100.00	100.00
EEG 59	314	96.97	96.97	99.24	99.24
EEG 60	284	95.57	95.57	98.10	98.10
Average	**312.33**	**97.65**	**97.65**	**99.44**	**99.44**

TABLE A.4 – Comparison of Specificity Between FastEMD-CCA^2 and FastCCA in MATLAB and C++

Specificity (%)					
Multichannel EEG Signal	**Duration per Channel (s)**	**FastEMD-CCA^2**		**FastCCA**	
		MATLAB	**C++**	**MATLAB**	**C++**
EEG 1	389	100.00	100.00	100.00	100.00
EEG 2	329	100.00	100.00	100.00	100.00
EEG 3	294	93.75	93.75	100.00	100.00
EEG 4	369	100.00	100.00	100.00	100.00
EEG 5	337	88.89	88.89	88.89	88.89
EEG 6	312	100.00	100.00	100.00	100.00
EEG 7	330	100.00	100.00	100.00	100.00
EEG 8	308	96.77	96.77	100.00	100.00
EEG 9	306	100.00	100.00	100.00	100.00
EEG 10	346	94.12	94.12	100.00	100.00
EEG 11	321	100.00	100.00	100.00	100.00
EEG 12	272	100.00	100.00	100.00	100.00
EEG 13	345	100.00	100.00	100.00	100.00
EEG 14	310	100.00	100.00	100.00	100.00
EEG 15	271	100.00	100.00	100.00	100.00
EEG 16	345	100.00	100.00	100.00	100.00
EEG 17	316	100.00	100.00	100.00	100.00
EEG 18	280	100.00	100.00	100.00	100.00
EEG 19	335	98.28	98.28	100.00	100.00
EEG 20	302	100.00	100.00	100.00	100.00
EEG 21	289	100.00	100.00	100.00	100.00
EEG 22	346	100.00	100.00	100.00	100.00
EEG 23	304	100.00	100.00	100.00	100.00
EEG 24	269	100.00	100.00	100.00	100.00
EEG 25	359	100.00	100.00	100.00	100.00
EEG 26	265	100.00	100.00	100.00	100.00
EEG 27	334	100.00	100.00	100.00	100.00
EEG 28	326	100.00	100.00	100.00	100.00
EEG 29	272	100.00	100.00	95.65	95.65
EEG 30	264	100.00	100.00	100.00	100.00

Table A.4 continued from previous page

Specificity (%)					
Multichannel EEG Signal	**Duration per Channel (s)**	**FastEMD-CCA**[2]		**FastCCA**	
		MATLAB	**C++**	**MATLAB**	**C++**
EEG 31	346	100.00	100.00	100.00	100.00
EEG 32	289	100.00	100.00	100.00	100.00
EEG 33	298	100.00	100.00	100.00	100.00
EEG 34	360	100.00	100.00	100.00	100.00
EEG 35	291	100.00	100.00	100.00	100.00
EEG 36	296	100.00	100.00	100.00	100.00
EEG 37	331	100.00	100.00	100.00	100.00
EEG 38	297	100.00	100.00	100.00	100.00
EEG 39	263	100.00	100.00	100.00	100.00
EEG 40	334	92.00	92.00	100.00	100.00
EEG 41	299	100.00	100.00	100.00	100.00
EEG 42	268	100.00	100.00	100.00	100.00
EEG 43	359	100.00	100.00	100.00	100.00
EEG 44	314	100.00	100.00	100.00	100.00
EEG 45	278	100.00	100.00	100.00	100.00
EEG 46	364	100.00	100.00	100.00	100.00
EEG 47	325	100.00	100.00	100.00	100.00
EEG 48	284	100.00	100.00	100.00	100.00
EEG 49	337	100.00	100.00	100.00	100.00
EEG 50	280	100.00	100.00	100.00	100.00
EEG 51	253	100.00	100.00	100.00	100.00
EEG 52	346	100.00	100.00	100.00	100.00
EEG 53	288	100.00	100.00	100.00	100.00
EEG 54	271	94.74	94.74	100.00	100.00
EEG 55	339	96.97	96.97	100.00	100.00
EEG 56	302	100.00	100.00	100.00	100.00
EEG 57	335	100.00	100.00	100.00	100.00
EEG 58	350	100.00	100.00	100.00	100.00
EEG 59	314	97.78	97.78	100.00	100.00
EEG 60	284	100.00	100.00	100.00	100.00
Average	**312.33**	**99.22**	**99.22**	**99.74**	**99.74**

TABLE A.5 – Comparison of Correlation Coefficient Between FastEMD-CCA^2 and FastCCA in MATLAB and C++

Correlation Coefficient (CC)					
Multichannel EEG Signal	**Evaluated Fp1 Segment (samples from - to)**	**FastEMD-CCA^2**		**FastCCA**	
		MATLAB	**C++**	**MATLAB**	**C++**
EEG 1	24000-33000	0.9989	0.9996	0.9999	1.0000
EEG 2	69000-78000	0.9991	1.0000	1.0000	1.0000
EEG 3	30000-43000	0.9980	1.0000	0.9994	1.0000
EEG 4	60000-70000	0.9986	1.0000	0.9989	0.9998
EEG 5	8000-18000	0.9964	0.9971	0.9971	0.9979
EEG 6	8000-14000	0.9989	1.0000	0.9995	1.0000
EEG 7	23000-24000	0.9999	1.0000	0.9943	0.9942
EEG 8	60000-61000	0.9998	1.0000	1.0000	1.0000
EEG 9	16000-18000	0.9992	1.0000	1.0000	1.0000
EEG 10	68000-69000	0.9999	1.0000	1.0000	1.0000
EEG 11	63000-66000	0.9993	1.0000	0.9991	1.0000
EEG 12	4500-8500	0.9996	1.0000	0.9998	1.0000
EEG 13	500-1500	1.0000	1.0000	1.0000	1.0000
EEG 14	na	na	na	na	na
EEG 15	na	na	na	na	na
EEG 16	na	na	na	na	na
EEG 17	na	na	na	na	na
EEG 18	na	na	na	na	na
EEG 19	65000-67000	0.9988	1.0000	0.9994	1.0000
EEG 20	44000-48000	0.9989	1.0000	0.9997	1.0000
EEG 21	56000-61000	0.9995	1.0000	0.9992	0.9999
EEG 22	51000-55000	0.9993	1.0000	0.9999	1.0000
EEG 23	5500-8500	0.9990	1.0000	0.9997	1.0000
EEG 24	18000-20000	0.9993	1.0000	0.9997	1.0000
EEG 25	na	na	na	na	na
EEG 26	na	na	na	na	na
EEG 27	na	na	na	na	na
EEG 28	na	na	na	na	na
EEG 29	na	na	na	na	na
EEG 30	na	na	na	na	na

Table A.5 continued from previous page

Correlation Coefficient (CC)					
Multichannel EEG Signal	**Evaluated Fp1 Segment (samples from - to)**	**FastEMD-CCA[2]**		**FastCCA**	
		MATLAB	**C++**	**MATLAB**	**C++**
EEG 31	na	na	na	na	na
EEG 32	na	na	na	na	na
EEG 33	na	na	na	na	na
EEG 34	na	na	na	na	na
EEG 35	na	na	na	na	na
EEG 36	na	na	na	na	na
EEG 37	10000-12000	0.9993	1.0000	1.0000	1.0000
EEG 38	26000-28000	0.9996	1.0000	1.0000	1.0000
EEG 39	21000-24000	1.0000	1.0000	0.9992	1.0000
EEG 40	39000-43000	0.9989	1.0000	0.9996	1.0000
EEG 41	13000-16000	0.9987	1.0000	0.9988	1.0000
EEG 42	35000-37000	0.9999	1.0000	0.9998	1.0000
EEG 43	40000-42000	0.9984	1.0000	0.9956	1.0000
EEG 44	5500-7500	0.9997	1.0000	0.9996	1.0000
EEG 45	na	na	na	na	na
EEG 46	na	na	na	na	na
EEG 47	na	na	na	na	na
EEG 48	na	na	na	na	na
EEG 49	na	na	na	na	na
EEG 50	na	na	na	na	na
EEG 51	59000-61000	0.9997	1.0000	1.0000	1.0000
EEG 52	54000-56000	0.9992	1.0000	1.0000	1.0000
EEG 53	55000-58000	0.9999	1.0000	1.0000	1.0000
EEG 54	41000-43000	0.9998	1.0000	1.0000	1.0000
EEG 55	42000-45000	0.9992	1.0000	1.0000	1.0000
EEG 56	12000-14000	0.9996	1.0000	1.0000	1.0000
EEG 57	na	na	na	na	na
EEG 58	na	na	na	na	na
EEG 59	na	na	na	na	na
EEG 60	na	na	na	na	na
Average		**0.9992**	**0.9999**	**0.9993**	**0.9998**

TABLE A.6 – Comparison of Root Mean Square Error Between FastEMD-CCA^2 and FastCCA in MATLAB and C++

Root Mean Square Error (RMSE)					
Multichannel EEG Signal	**Evaluated Fp1 Segment (samples from - to)**	**FastEMD-CCA^2**		**FastCCA**	
		MATLAB	**C++**	**MATLAB**	**C++**
EEG 1	24000-33000	0.1942	0.1180	0.0551	0.0000
EEG 2	69000-78000	0.1924	0.0000	0.0351	0.0000
EEG 3	30000-43000	0.2499	0.0000	0.1351	0.0000
EEG 4	60000-70000	0.2577	0.0444	0.2250	0.0923
EEG 5	8000-18000	0.3640	0.3202	0.3235	0.2764
EEG 6	8000-14000	0.2054	0.0247	0.1360	0.0000
EEG 7	23000-24000	0.0633	0.0000	0.3280	0.3300
EEG 8	60000-61000	0.0715	0.0000	0.0000	0.0000
EEG 9	16000-18000	0.1440	0.0000	0.0000	0.0000
EEG 10	68000-69000	0.0389	0.0000	0.0000	0.0000
EEG 11	63000-66000	0.1406	0.0000	0.1997	0.0000
EEG 12	4500-8500	0.0873	0.0000	0.0673	0.0000
EEG 13	500-1500	0.0658	0.0000	0.0000	0.0000
EEG 14	na	na	na	na	na
EEG 15	na	na	na	na	na
EEG 16	na	na	na	na	na
EEG 17	na	na	na	na	na
EEG 18	na	na	na	na	na
EEG 19	65000-67000	0.1535	0.0000	0.1178	0.0000
EEG 20	44000-48000	0.1377	0.0000	0.0751	0.0000
EEG 21	56000-61000	0.0952	0.0000	0.1230	0.0498
EEG 22	51000-55000	0.1131	0.0000	0.0421	0.0000
EEG 23	5500-8500	0.1711	0.0000	0.0772	0.0000
EEG 24	18000-20000	0.1327	0.0000	0.0679	0.0000
EEG 25	na	na	na	na	na
EEG 26	na	na	na	na	na
EEG 27	na	na	na	na	na
EEG 28	na	na	na	na	na
EEG 29	na	na	na	na	na
EEG 30	na	na	na	na	na

Table A.6 continued from previous page

Root Mean Square Error (RMSE)					
Multichannel EEG Signal	**Evaluated Fp1 Segment (samples from - to)**	**FastEMD-CCA[2]**		**FastCCA**	
		MATLAB	**C++**	**MATLAB**	**C++**
EEG 31	na	na	na	na	na
EEG 32	na	na	na	na	na
EEG 33	na	na	na	na	na
EEG 34	na	na	na	na	na
EEG 35	na	na	na	na	na
EEG 36	na	na	na	na	na
EEG 37	10000-12000	0.2843	0.0000	0.0000	0.0000
EEG 38	26000-28000	0.1608	0.0000	0.0000	0.0000
EEG 39	21000-24000	0.0592	0.0000	0.2417	0.0000
EEG 40	39000-43000	0.3169	0.0000	0.1805	0.0000
EEG 41	13000-16000	0.3282	0.0000	0.3012	0.0000
EEG 42	35000-37000	0.0753	0.0000	0.1192	0.0000
EEG 43	40000-42000	0.2011	0.0000	0.3606	0.0000
EEG 44	5500-7500	0.1167	0.0000	0.1214	0.0000
EEG 45	na	na	na	na	na
EEG 46	na	na	na	na	na
EEG 47	na	na	na	na	na
EEG 48	na	na	na	na	na
EEG 49	na	na	na	na	na
EEG 50	na	na	na	na	na
EEG 51	59000-61000	0.0983	0.0000	0.0000	0.0000
EEG 52	54000-56000	0.1445	0.0000	0.0000	0.0000
EEG 53	55000-58000	0.0477	0.0000	0.0000	0.0000
EEG 54	41000-43000	0.0698	0.0000	0.0000	0.0000
EEG 55	42000-45000	0.2424	0.0000	0.0000	0.0000
EEG 56	12000-14000	0.1624	0.0000	0.0000	0.0000
EEG 57	na	na	na	na	na
EEG 58	na	na	na	na	na
EEG 59	na	na	na	na	na
EEG 60	na	na	na	na	na
Average		**0.1572**	**0.0154**	**0.1010**	**0.0227**

TABLE A.7 – Comparison of Similarity Index Between FastEMD-CCA^2 and FastCCA in MATLAB and C++

Similarity Index (η_{dB})					
Multichannel EEG Signal	**Evaluated Fp1 Segment (samples from - to)**	**FastEMD-CCA^2**		**FastCCA**	
		MATLAB	**C++**	**MATLAB**	**C++**
EEG 1	24000-33000	-0.2278	0.0241	-0.1104	0.0000
EEG 2	69000-78000	-0.9123	0.0000	0.0671	0.0000
EEG 3	30000-43000	-0.6954	0.0000	-0.1620	0.0000
EEG 4	60000-70000	-0.3233	-0.0105	-0.2071	-0.0268
EEG 5	8000-18000	-0.6476	0.0159	-0.2416	-0.0687
EEG 6	8000-14000	-0.3959	0.0024	-0.0541	0.0000
EEG 7	23000-24000	0.4462	0.0000	0.1134	0.1191
EEG 8	60000-61000	-0.3118	0.0000	0.0000	0.0000
EEG 9	16000-18000	-0.4616	0.0000	0.0000	0.0000
EEG 10	68000-69000	-0.1050	0.0000	0.0000	0.0000
EEG 11	63000-66000	-0.3218	0.0000	-1.3111	0.0000
EEG 12	4500-8500	-0.0722	0.0000	0.1329	0.0000
EEG 13	500-1500	-0.5872	0.0000	0.0000	0.0000
EEG 14	na	na	na	na	na
EEG 15	na	na	na	na	na
EEG 16	na	na	na	na	na
EEG 17	na	na	na	na	na
EEG 18	na	na	na	na	na
EEG 19	65000-67000	0.1400	0.0000	0.5455	0.0000
EEG 20	44000-48000	-0.3239	0.0000	-0.3096	0.0000
EEG 21	56000-61000	0.2838	0.0000	-0.4595	0.0077
EEG 22	51000-55000	-0.3437	0.0000	-0.0289	0.0000
EEG 23	5500-8500	-1.2821	0.0000	-0.2697	0.0000
EEG 24	18000-20000	-0.8928	0.0000	-0.2965	0.0000
EEG 25	na	na	na	na	na
EEG 26	na	na	na	na	na
EEG 27	na	na	na	na	na
EEG 28	na	na	na	na	na
EEG 29	na	na	na	na	na
EEG 30	na	na	na	na	na

Table A.7 continued from previous page

Similarity Index (η_{dB})					
Multichannel EEG Signal	**Evaluated Fp1 Segment (samples from - to)**	**FastEMD-CCA**[2]		**FastCCA**	
		MATLAB	**C++**	**MATLAB**	**C++**
EEG 31	na	na	na	na	na
EEG 32	na	na	na	na	na
EEG 33	na	na	na	na	na
EEG 34	na	na	na	na	na
EEG 35	na	na	na	na	na
EEG 36	na	na	na	na	na
EEG 37	10000-12000	-2.0686	0.0000	0.0000	0.0000
EEG 38	26000-28000	-0.4610	0.0000	0.0000	0.0000
EEG 39	21000-24000	-0.2392	0.0000	-0.5537	0.0000
EEG 40	39000-43000	0.6426	0.0000	0.3529	0.0000
EEG 41	13000-16000	0.8944	0.0000	-0.2848	0.0000
EEG 42	35000-37000	-0.1956	0.0000	-0.5167	0.0000
EEG 43	40000-42000	0.2084	0.0000	-1.3070	0.0000
EEG 44	5500-7500	-0.4190	0.0000	0.3577	0.0000
EEG 45	na	na	na	na	na
EEG 46	na	na	na	na	na
EEG 47	na	na	na	na	na
EEG 48	na	na	na	na	na
EEG 49	na	na	na	na	na
EEG 50	na	na	na	na	na
EEG 51	59000-61000	-0.2224	0.0000	0.0000	0.0000
EEG 52	54000-56000	-0.0814	0.0000	0.0000	0.0000
EEG 53	55000-58000	-0.0061	0.0000	0.0000	0.0000
EEG 54	41000-43000	-0.0747	0.0000	0.0000	0.0000
EEG 55	42000-45000	-0.6005	0.0000	0.0000	0.0000
EEG 56	12000-14000	-0.6782	0.0000	0.0000	0.0000
EEG 57	na	na	na	na	na
EEG 58	na	na	na	na	na
EEG 59	na	na	na	na	na
EEG 60	na	na	na	na	na
Average		**-0.3132**	**0.0010**	**-0.1377**	**0.0009**

TABLE A.8 – Comparison of MAE Between FastEMD-CCA^2 and FastCCA in Different Frequency Bands

Mean Absolute Error											
Multichannel	Evaluated Fp1 Segment	δ		θ		α		β		γ	
EEG Signal	(samples from - to)	FastEMD-CCA^2	FastCCA	FastEMD-CCA^2	FastCCA	FastEMD-CCA^2	FastCCA	FastEMD-CCA^2	FastCCA	FastEMD-CCA^2	FastCCA
EEG 1	24000-33000	0.0188	0.0000	0.0085	0.0000	0.0024	0.0000	0.0003	0.0000	0.0000	0.0000
EEG 2	69000-78000	0.0000	0.0000	0.0000	0.0000	0.0000	0.0000	0.0000	0.0000	0.0000	0.0000
EEG 3	30000-43000	0.0000	0.0000	0.0000	0.0000	0.0000	0.0000	0.0000	0.0000	0.0000	0.0000
EEG 4	60000-70000	0.0112	0.0448	0.0012	0.0001	0.0007	0.0001	0.0000	0.0000	0.0000	0.0000
EEG 5	8000-18000	0.1614	0.0612	0.0041	0.0022	0.0007	0.0093	0.0003	0.0010	0.0000	0.0000
EEG 6	8000-14000	0.0016	0.0000	0.0010	0.0000	0.0014	0.0000	0.0001	0.0000	0.0000	0.0000
EEG 7	23000-24000	0.0000	0.0030	0.0000	0.0002	0.0000	0.0010	0.0000	0.0003	0.0000	0.0001
EEG 8	60000-61000	0.0000	0.0000	0.0000	0.0000	0.0000	0.0000	0.0000	0.0000	0.0000	0.0000
EEG 9	16000-18000	0.0000	0.0000	0.0000	0.0000	0.0000	0.0000	0.0000	0.0000	0.0000	0.0000
EEG 10	68000-69000	0.0000	0.0000	0.0000	0.0000	0.0000	0.0000	0.0000	0.0000	0.0000	0.0000
EEG 11	63000-66000	0.0000	0.0000	0.0000	0.0000	0.0000	0.0000	0.0000	0.0000	0.0000	0.0000
EEG 12	4500-8500	0.0000	0.0000	0.0000	0.0000	0.0000	0.0000	0.0000	0.0000	0.0000	0.0000
EEG 13	500-1500	0.0000	0.0000	0.0000	0.0000	0.0000	0.0000	0.0000	0.0000	0.0000	0.0000
EEG 14	na	na	na	na	na	na	na	na	na	na	na
EEG 15	na	na	na	na	na	na	na	na	na	na	na
EEG 16	na	na	na	na	na	na	na	na	na	na	na
EEG 17	na	na	na	na	na	na	na	na	na	na	na
EEG 18	na	na	na	na	na	na	na	na	na	na	na
EEG 19	65000-67000	0.0000	0.0000	0.0000	0.0000	0.0000	0.0000	0.0000	0.0000	0.0000	0.0000
EEG 20	44000-48000	0.0000	0.0000	0.0000	0.0000	0.0000	0.0000	0.0000	0.0000	0.0000	0.0000
EEG 21	56000-61000	0.0000	0.0060	0.0000	0.0019	0.0000	0.0015	0.0000	0.0010	0.0000	0.0000
EEG 22	51000-55000	0.0000	0.0000	0.0000	0.0000	0.0000	0.0000	0.0000	0.0000	0.0000	0.0000
EEG 23	5500-8500	0.0000	0.0000	0.0000	0.0000	0.0000	0.0000	0.0000	0.0000	0.0000	0.0000
EEG 24	18000-20000	0.0000	0.0000	0.0000	0.0000	0.0000	0.0000	0.0000	0.0000	0.0000	0.0000
EEG 25	na	na	na	na	na	na	na	na	na	na	na
EEG 26	na	na	na	na	na	na	na	na	na	na	na
EEG 27	na	na	na	na	na	na	na	na	na	na	na
EEG 28	na	na	na	na	na	na	na	na	na	na	na
EEG 29	na	na	na	na	na	na	na	na	na	na	na
EEG 30	na	na	na	na	na	na	na	na	na	na	na
EEG 31	na	na	na	na	na	na	na	na	na	na	na
EEG 32	na	na	na	na	na	na	na	na	na	na	na
EEG 33	na	na	na	na	na	na	na	na	na	na	na
EEG 34	na	na	na	na	na	na	na	na	na	na	na
EEG 35	na	na	na	na	na	na	na	na	na	na	na
EEG 36	na	na	na	na	na	na	na	na	na	na	na
EEG 37	10000-12000	0.0000	0.0000	0.0000	0.0000	0.0000	0.0000	0.0000	0.0000	0.0000	0.0000
EEG 38	26000-28000	0.0000	0.0000	0.0000	0.0000	0.0000	0.0000	0.0000	0.0000	0.0000	0.0000
EEG 39	21000-24000	0.0000	0.0000	0.0000	0.0000	0.0000	0.0000	0.0000	0.0000	0.0000	0.0000
EEG 40	39000-43000	0.0000	0.0000	0.0000	0.0000	0.0000	0.0000	0.0000	0.0000	0.0000	0.0000
EEG 41	13000-16000	0.0000	0.0000	0.0000	0.0000	0.0000	0.0000	0.0000	0.0000	0.0000	0.0000
EEG 42	35000-37000	0.0000	0.0000	0.0000	0.0000	0.0000	0.0000	0.0000	0.0000	0.0000	0.0000
EEG 43	40000-42000	0.0000	0.0000	0.0000	0.0000	0.0000	0.0000	0.0000	0.0000	0.0000	0.0000
EEG 44	5500-7500	0.0000	0.0000	0.0000	0.0000	0.0000	0.0000	0.0000	0.0000	0.0000	0.0000
EEG 45	na	na	na	na	na	na	na	na	na	na	na
EEG 46	na	na	na	na	na	na	na	na	na	na	na
EEG 47	na	na	na	na	na	na	na	na	na	na	na
EEG 48	na	na	na	na	na	na	na	na	na	na	na
EEG 49	na	na	na	na	na	na	na	na	na	na	na
EEG 50	na	na	na	na	na	na	na	na	na	na	na
EEG 51	59000-61000	0.0000	0.0000	0.0000	0.0000	0.0000	0.0000	0.0000	0.0000	0.0000	0.0000
EEG 52	54000-56000	0.0000	0.0000	0.0000	0.0000	0.0000	0.0000	0.0000	0.0000	0.0000	0.0000
EEG 53	55000-58000	0.0000	0.0000	0.0000	0.0000	0.0000	0.0000	0.0000	0.0000	0.0000	0.0000
EEG 54	41000-43000	0.0000	0.0000	0.0000	0.0000	0.0000	0.0000	0.0000	0.0000	0.0000	0.0000
EEG 55	42000-45000	0.0000	0.0000	0.0000	0.0000	0.0000	0.0000	0.0000	0.0000	0.0000	0.0000
EEG 56	12000-14000	0.0000	0.0000	0.0000	0.0000	0.0000	0.0000	0.0000	0.0000	0.0000	0.0000
EEG 57	na	na	na	na	na	na	na	na	na	na	na
EEG 58	na	na	na	na	na	na	na	na	na	na	na
EEG 59	na	na	na	na	na	na	na	na	na	na	na
EEG 60	na	na	na	na	na	na	na	na	na	na	na
Average		**0.0059**	**0.0035**	**0.0004**	**0.0001**	**0.0002**	**0.0004**	**0.0000**	**0.0001**	**0.0000**	**0.0000**

TABLE A.9 – Comparison of MAPE Between FastEMD-CCA^2 and FastCCA in Different Frequency Bands

Mean Absolute Percentage Error (%)											
Multichannel	Evaluated Fp1 Segment	delta		theta		alpha		beta		gamma	
EEG Signal	(samples from - to)	FastEMD-CCA^2	FastCCA	FastEMD-CCA^2	FastCCA	FastEMD-CCA^2	FastCCA	FastEMD-CCA^2	FastCCA	FastEMD-CCA^2	FastCCA
EEG 1	24000-33000	0.1197	0.0000	0.1624	0.0000	0.0730	0.0000	0.1433	0.0000	2.6894	0.0000
EEG 2	69000-78000	0.0000	0.0000	0.0000	0.0000	0.0000	0.0000	0.0000	0.0000	0.0000	0.0000
EEG 3	30000-43000	0.0000	0.0000	0.0000	0.0000	0.0000	0.0000	0.0000	0.0000	0.0000	0.0000
EEG 4	60000-70000	0.0440	0.1763	0.0220	0.0014	0.0236	0.0034	0.0144	0.0067	0.0900	0.4504
EEG 5	8000-18000	0.9571	0.3630	0.0880	0.0477	0.0219	0.2922	0.1187	0.3523	0.0723	2.3148
EEG 6	8000-14000	0.0100	0.0000	0.0151	0.0000	0.0277	0.0000	0.0400	0.0000	0.0492	0.0000
EEG 7	23000-24000	0.0000	0.0398	0.0000	0.0069	0.0001	0.0522	0.0000	0.0288	0.0001	5.4902
EEG 8	60000-61000	0.0000	0.0000	0.0000	0.0000	0.0000	0.0000	0.0000	0.0000	0.0000	0.0000
EEG 9	16000-18000	0.0000	0.0000	0.0000	0.0000	0.0000	0.0000	0.0000	0.0000	0.0000	0.0000
EEG 10	68000-69000	0.0000	0.0000	0.0000	0.0000	0.0000	0.0000	0.0000	0.0000	0.0000	0.0000
EEG 11	63000-66000	0.0000	0.0000	0.0000	0.0000	0.0000	0.0000	0.0000	0.0000	0.0000	0.0000
EEG 12	4500-8500	0.0000	0.0000	0.0000	0.0000	0.0000	0.0000	0.0000	0.0000	0.0000	0.0000
EEG 13	500-1500	0.0000	0.0000	0.0000	0.0000	0.0000	0.0000	0.0000	0.0000	0.0001	0.0000
EEG 14	na	na	na	na	na	na	na	na	na	na	na
EEG 15	na	na	na	na	na	na	na	na	na	na	na
EEG 16	na	na	na	na	na	na	na	na	na	na	na
EEG 17	na	na	na	na	na	na	na	na	na	na	na
EEG 18	na	na	na	na	na	na	na	na	na	na	na
EEG 19	65000-67000	0.0000	0.0000	0.0000	0.0000	0.0000	0.0000	0.0000	0.0000	0.0000	0.0000
EEG 20	44000-48000	0.0000	0.0000	0.0000	0.0000	0.0000	0.0000	0.0000	0.0000	0.0000	0.0000
EEG 21	56000-61000	0.0000	0.0827	0.0000	0.0881	0.0000	0.0640	0.0000	0.2476	0.0000	4.2071
EEG 22	51000-55000	0.0000	0.0000	0.0000	0.0000	0.0000	0.0000	0.0000	0.0000	0.0000	0.0000
EEG 23	5500-8500	0.0000	0.0000	0.0000	0.0000	0.0000	0.0000	0.0000	0.0000	0.0000	0.0000
EEG 24	18000-20000	0.0000	0.0000	0.0000	0.0000	0.0000	0.0000	0.0000	0.0000	0.0000	0.0000
EEG 25	na	na	na	na	na	na	na	na	na	na	na
EEG 26	na	na	na	na	na	na	na	na	na	na	na
EEG 27	na	na	na	na	na	na	na	na	na	na	na
EEG 28	na	na	na	na	na	na	na	na	na	na	na
EEG 29	na	na	na	na	na	na	na	na	na	na	na
EEG 30	na	na	na	na	na	na	na	na	na	na	na
EEG 31	na	na	na	na	na	na	na	na	na	na	na
EEG 32	na	na	na	na	na	na	na	na	na	na	na
EEG 33	na	na	na	na	na	na	na	na	na	na	na
EEG 34	na	na	na	na	na	na	na	na	na	na	na
EEG 35	na	na	na	na	na	na	na	na	na	na	na
EEG 36	na	na	na	na	na	na	na	na	na	na	na
EEG 37	10000-12000	0.0000	0.0000	0.0000	0.0000	0.0000	0.0000	0.0000	0.0000	0.0000	0.0000
EEG 38	26000-28000	0.0000	0.0000	0.0000	0.0000	0.0000	0.0000	0.0000	0.0000	0.0000	0.0000
EEG 39	21000-24000	0.0000	0.0000	0.0000	0.0000	0.0000	0.0000	0.0000	0.0000	0.0000	0.0000
EEG 40	39000-43000	0.0000	0.0000	0.0000	0.0000	0.0000	0.0000	0.0000	0.0000	0.0000	0.0000
EEG 41	13000-16000	0.0000	0.0000	0.0000	0.0000	0.0000	0.0000	0.0000	0.0000	0.0000	0.0000
EEG 42	35000-37000	0.0000	0.0000	0.0000	0.0000	0.0000	0.0000	0.0000	0.0000	0.0000	0.0000
EEG 43	40000-42000	0.0000	0.0000	0.0000	0.0000	0.0000	0.0000	0.0000	0.0000	0.0000	0.0000
EEG 44	5500-7500	0.0000	0.0000	0.0000	0.0000	0.0000	0.0000	0.0000	0.0000	0.0000	0.0000
EEG 45	na	na	na	na	na	na	na	na	na	na	na
EEG 46	na	na	na	na	na	na	na	na	na	na	na
EEG 47	na	na	na	na	na	na	na	na	na	na	na
EEG 48	na	na	na	na	na	na	na	na	na	na	na
EEG 49	na	na	na	na	na	na	na	na	na	na	na
EEG 50	na	na	na	na	na	na	na	na	na	na	na
EEG 51	59000-61000	0.0000	0.0000	0.0000	0.0000	0.0000	0.0000	0.0000	0.0000	0.0000	0.0000
EEG 52	54000-56000	0.0000	0.0000	0.0000	0.0000	0.0000	0.0000	0.0000	0.0000	0.0000	0.0000
EEG 53	55000-58000	0.0000	0.0000	0.0000	0.0000	0.0000	0.0000	0.0000	0.0000	0.0000	0.0000
EEG 54	41000-43000	0.0000	0.0000	0.0000	0.0000	0.0000	0.0000	0.0000	0.0000	0.0000	0.0000
EEG 55	42000-45000	0.0000	0.0000	0.0000	0.0000	0.0000	0.0000	0.0000	0.0000	0.0001	0.0000
EEG 56	12000-14000	0.0000	0.0000	0.0000	0.0000	0.0000	0.0000	0.0000	0.0000	0.0000	0.0000
EEG 57	na	na	na	na	na	na	na	na	na	na	na
EEG 58	na	na	na	na	na	na	na	na	na	na	na
EEG 59	na	na	na	na	na	na	na	na	na	na	na
EEG 60	na	na	na	na	na	na	na	na	na	na	na
Average		**0.0343**	**0.0201**	**0.0087**	**0.0044**	**0.0044**	**0.0125**	**0.0096**	**0.0193**	**0.0879**	**0.3777**

TABLE A.10 – Comparison of Computation Time Between FastEMD-CCA^2 and FastCCA in MATLAB and C++

Computation Time (s)					
Multichannel EEG Signal	**Duration per Channel (s)**	**FastEMD-CCA^2**		**FastCCA**	
		MATLAB	**C++**	**MATLAB**	**C++**
EEG 1	389	15.17	4.04	27.12	3.92
EEG 2	329	5.66	3.32	16.73	3.22
EEG 3	294	5.77	3.18	14.67	2.86
EEG 4	369	6.84	3.72	15.17	4.10
EEG 5	337	7.65	3.72	9.18	4.03
EEG 6	312	6.75	3.22	9.03	3.65
EEG 7	330	8.17	3.32	6.58	4.06
EEG 8	308	7.00	3.20	10.07	3.45
EEG 9	306	5.12	3.19	11.33	3.33
EEG 10	346	7.79	3.61	8.75	4.16
EEG 11	321	6.65	3.64	10.67	3.63
EEG 12	272	4.52	2.97	9.09	2.96
EEG 13	345	7.50	3.78	6.01	4.22
EEG 14	310	4.39	3.21	0.99	4.53
EEG 15	271	4.36	2.92	0.71	4.04
EEG 16	345	7.64	3.83	2.45	4.82
EEG 17	316	6.22	3.32	1.83	4.53
EEG 18	280	3.17	3.05	0.80	4.14
EEG 19	335	5.94	3.55	5.01	4.62
EEG 20	302	4.09	3.21	4.88	3.94
EEG 21	289	4.17	3.21	7.61	3.57
EEG 22	346	5.45	3.98	4.56	4.81
EEG 23	304	6.07	3.29	5.98	3.90
EEG 24	269	3.78	2.86	5.40	3.46
EEG 25	359	15.29	3.60	na	4.78
EEG 26	265	3.15	2.89	2.88	3.67
EEG 27	334	6.54	3.59	4.25	4.48
EEG 28	326	7.36	3.90	1.50	4.76
EEG 29	272	2.48	3.27	3.80	3.51
EEG 30	264	2.74	3.02	3.97	3.46

Table A.10 continued from previous page

Computation Time (s)					
Multichannel EEG Signal	**Duration per Channel (s)**	**FastEMD-CCA**[2]		**FastCCA**	
		MATLAB	**C++**	**MATLAB**	**C++**
EEG 31	346	7.63	3.77	0.92	5.26
EEG 32	289	2.79	3.16	0.69	4.32
EEG 33	298	6.39	3.43	0.67	4.48
EEG 34	360	6.22	4.50	1.07	5.40
EEG 35	291	5.80	3.70	0.62	4.43
EEG 36	296	4.84	3.32	0.71	4.46
EEG 37	331	6.27	3.45	7.39	4.10
EEG 38	297	7.25	3.06	7.40	3.52
EEG 39	263	8.45	2.67	6.06	3.13
EEG 40	334	8.28	3.44	7.87	4.10
EEG 41	299	6.74	3.21	7.07	3.64
EEG 42	268	7.04	2.79	5.99	3.25
EEG 43	359	9.51	3.62	8.29	4.64
EEG 44	314	7.93	3.27	4.55	4.12
EEG 45	278	4.75	3.00	1.63	3.85
EEG 46	364	8.62	3.72	2.91	5.13
EEG 47	325	9.03	3.34	2.74	4.47
EEG 48	284	5.50	3.16	1.86	4.07
EEG 49	337	9.41	3.52	10.73	3.98
EEG 50	280	6.44	2.99	5.29	3.52
EEG 51	253	5.40	2.69	5.34	3.23
EEG 52	346	9.34	3.78	13.19	3.97
EEG 53	288	9.27	2.89	13.78	2.80
EEG 54	271	6.70	2.91	8.49	3.16
EEG 55	339	9.48	3.43	18.18	3.55
EEG 56	302	6.25	3.21	9.72	3.49
EEG 57	335	13.61	3.44	12.92	3.49
EEG 58	350	7.25	3.61	17.57	3.81
EEG 59	314	6.82	3.38	6.92	3.95
EEG 60	284	6.20	3.20	3.69	3.76
Average	**312.33**	**6.78**	**3.35**	**6.87**	**3.96**
Processing Time	**1s EEG**	**0.0217**	**0.0107**	**0.0220**	**0.0127**

B

List of Publications

1. A. Egambaram, N. Badruddin, V. S. Asirvadam, and T. Begum, “Comparison of envelope interpolation techniques in Empirical Mode Decomposition (EMD) for eye-blink artifact removal from EEG,” in IECBES 2016 - IEEE-EMBS Conference on Biomedical Engineering and Sciences, 2016, pp. 590–595.
2. A. Egambaram, N. Badruddin, V. S. Asirvadam, T. Begum, E. Fauvet, and C. Stolz, “Variance thresholded EMD-CCA technique for fast eye blink artifacts removal in EEG,” in IEEE Region 10 Annual International Conference, Proceedings/TENCON, 2017.
3. A. Egambaram, N. Badruddin, V. S. Asirvadam, E. Fauvet, C. Stolz, and T. Begum, “Unsupervised Eye Blink Artifact Identification in Electroencephalogram,” IEEE Reg. 10 Annu. Int. Conf. Proceedings/TENCON, vol. 2018-October, no. October, pp. 2148–2152, 2019.
4. A. Egambaram, N. Badruddin, E. Fauvet, and C. Stolz, “Automated and Online Eye Blink Artifact Removal from Electroencephalogram,” Conf. Signal Image Process. Appl., pp. 159–163, 2019.
5. A. Egambaram, N. Badruddin, V. S. Asirvadam, T. Begum, E. Fauvet, and C. Stolz, “FastEMD–CCA algorithm for unsupervised and fast removal of eyeblink artifacts from electroencephalogram,” Biomed. Signal Process. Control, vol. 57, p. 101692, 2020.

Document réalisé avec LaTeX et :
le style LaTeX pour Thèse de Doctorat créé par S. Galland — http://www.multiagent.fr/ThesisStyle
la collection de paquets `tex-upmethodology` — http://www.arakhne.org/tex-upmethodology/